Design of Active and Versatile Iron(II) Catalysts for Living Radical Polymerization

Muneki Ishio

2010

Design of Active and Versatile Iron(II) Catalysts for Living Radical Polymerization

Muneki Ishio

2010

CONTENTS

GENERAL INTRODUCTION

Background

Transition Metal-Complexes as Catalysts. *"Transition Metal Complex"* is now a leading performer in organic and polymer syntheses to accomplish advanced and/or demanding reactions.[1] The landmark discovery on transition metal catalysis goes back to "Ziegler-Natta catalysts" for olefin polymerization, typically consisting of titanium chloride and an alkyl aluminum [e.g., $(C_2H_5)_3Al$; as a cocatalyst]. These catalysts provided the potential of transition metal complexes for more feasible and/or stereospecific reactions, e.g., ethylene polymerization under conditions milder than the free-radical processes[2] and isospecific propylene polymerization of propylene.[3] In the wake of these milestones, a number of transition metal complexes have been developed as catalysts to control reactions with some selectivity not only for polymerizations but also for organic reactions.

An important character of transition metals is that, different from representative elements, they possess a *d*-orbital, receptive to electrons of ligands. Compounds carrying σ- or π-electrons are eligible as the ligands to form coordination bonds with a central transition metal by donating their electrons to a vacant *d*-orbital of a transition metal (Figure 1). Accordingly, the electronic and the steric states of the central metal are governed by the ligands, meaning that they serve as "modifiers" of their host elements by their electronic

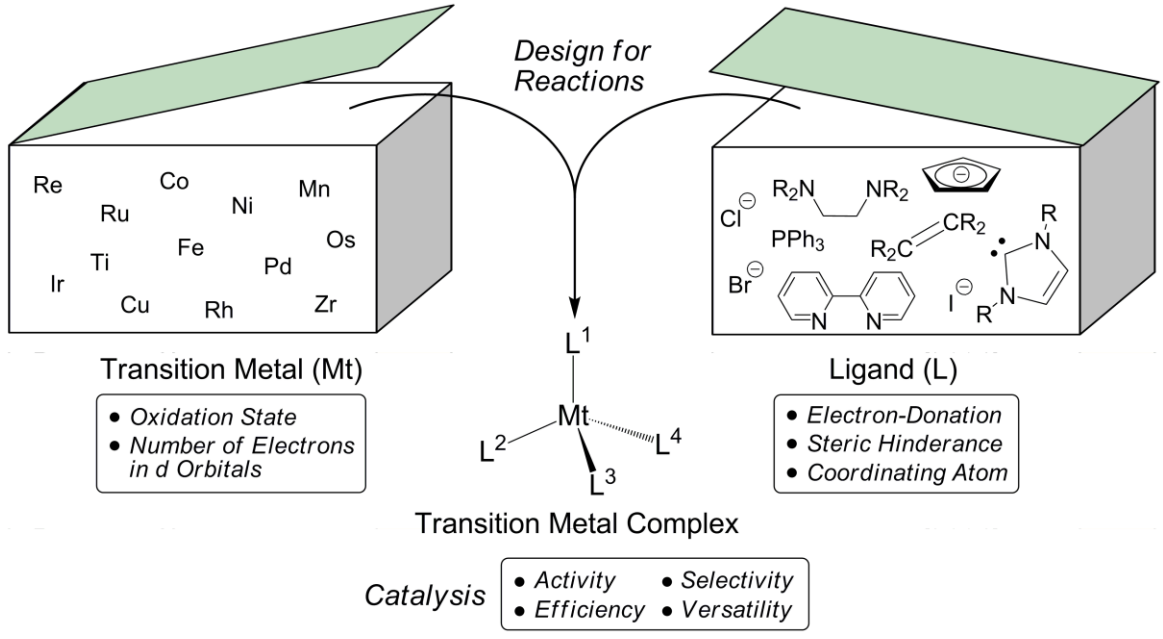

Figure 1. Building blocks of transition metal complexes for catalysts

(donating and withdrawing) and structural (bulkiness, symmetry, and chirality) characters. Importantly, some ligands can dynamically or reversibly detach from the metal and can thereby be replaced with a substrate or to provide a reaction (coordination) site. Such a "ligand exchange" or a vacant-site formation, respectively, in turn leads to the activation of the coordinating substrate by the metal or to a specific environment around the metal. Thus, catalysis is accomplished by the corporative functions of transition metals and their ligands, and the catalytic features (i.e., efficiency, selectivity, versatility, etc.) thus strongly depend on metal-ligand combinations. In other words, *one can dictate and control chemical reactions via the design of transition metal catalysts*.

Iron Complexes toward Sustainable Catalysts. Thus, the development of transition metal catalysts has been attractive for chemists. However, some of transition metals are toxic or precious on the earth, and the use of such metals is less favorable for practical applications, even though their complexes are active as catalysts. Therefore, ubiquitous and less toxic metals have started to garner attention in developing sustainable or environmentally benign catalytic systems.[4]

In view of such sustainable aspects, "*Iron"* would be one of the most promising among transition metals (Figure 2) because of the following features:[5] iron abundantly exists in the earth crust (4.7 wt% in igneous rocks);[6] iron can be easily obtained in a large scale at a low price; the toxicity is potentially low, as iron is a vital component of biological systems including human body, serving, for example, as a cofactor for metalloproteins [i.e., hydrogenase, reductase, and cytochrome (heme)].

Iron belongs to group-8 in the periodic table, with the electronic configuration $[Ar](3d)^6(4s)^2$. It assumes a wide range of oxidation states from -2 to 6, and the reactivity

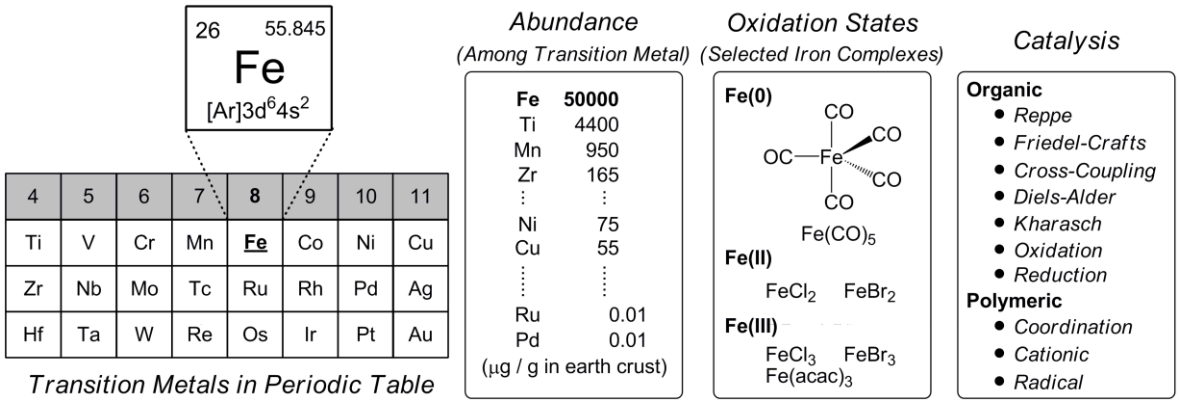

Figure 2. Characters of iron and its complexes

(e.g., Lewis acidity and oxidation/reduction) is depending on the oxidation state. Such versatility is suited to a catalyst, and indeed a variety of complexes have been studied for various reactions. For example, in the early period of iron-catalyst development, the pentacarbonyl form [$Fe(CO)_5$] and its salts (halides, acetylacetone, etc.) were applied for Reppe[7] and Friedel-Crafts[8] reactions, respectively. In the subsequent decades, other iron-based complexes have been employed for numerous organic reactions[9] [e.g., oxidation,[10] reduction,[11] Kharasch,[12] Diels-Alder,[13] and cross-coupling[14]] and polymerizations [e.g. coordination,[15] cationic,[16] and radical (see below)].

In these catalyses, however, iron complexes are often a "supporting performer" in terms of activity and selectivity relative to other metal counterparts; namely, iron catalysts do work well but usually not the best. Nowadays, in contrast, a development of an iron catalyst to be a "leading performer" has been gathering momentum, as sustainability and eco-friendliness are now being more important than simple activity and effectiveness in catalytic systems .[17]

Transition-Metal Catalyzed Living Radical Polymerization. Living polymerization by definition consists of an initiation and a propagation reaction (or no side reactions other than these), and then allows precise syntheses of desired polymeric architectures. Originally, living polymerization was limited to ionic systems (anionic,[18] cationic,[19] ring-opening,[20] etc.), whereas fine control of radical polymerization had been considered difficult, primarily due to the high reactivity of the "free" radical intermediates therein.[21] Recently, however, a universalized concept for living polymerization, i.e., the introduction of a "dormant" species and its reversible activation, has been extended to radical systems, and a variety of living radical polymerization are available. Now, a living radical polymerization is an essential method to design well-defined polymeric materials, since variety of monomers are applicable, including "functional" monomers without protection of their polar functionality, in sharp contrast to the ionic vanguards, which are often disturbed by functional groups.

Transition metal-catalyzed living radical polymerization is one of such living/controlled radical polymerizations, and, as the name implies, a transition metal complex serves as a catalyst to control the radical polymerization.[22] The first system was discovered by the author's group in 1995 with a ruthenium catalyst [$RuCl_2(PPh_3)_3$] and an aluminum cocatalyst [e.g., $MeAl(ODBP)_2$ (ODBP = 2,6-di-*tert*-butylphenoxy) or $Al(O\textit{i}\text{-}Pr)_3$]

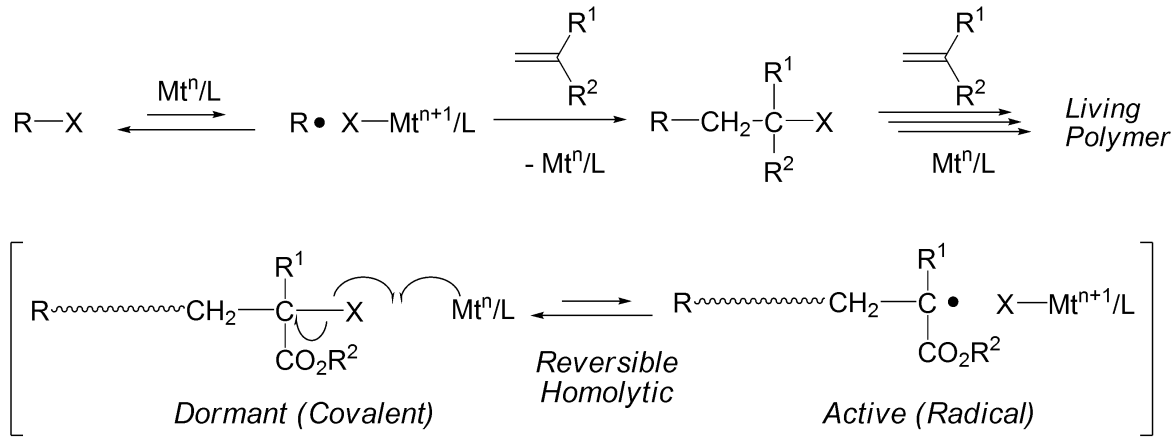

Scheme 1. Transition Metal-Catalyzed Living Radical Polymerization

in conjunction with a halogen compound (CCl_4) as an initiator.[23] In this system, a transition-metal catalyst (Mt^n/L; n = valence number; L = ligands) activates the carbon-halogen bond in an initiator (R-X) or in a "dormant" polymer terminal (~~~C-X) so as to trigger its homolysis into a carbon-centered growth-active radical (R• or ~~~C•) via one-electron oxidation from Mt^n to Mt^{n+1} (Scheme 1). These growing species propagate with monomers, and the oxidized catalyst sooner or later donates its halogen (X) back to the radical, to regenerate the dormant terminal while returning to the original lower valance state via one-electron reduction from Mt^{n+1} to Mt^n. The polymerization thus proceeds by repeating the reversible activation-deactivation process or a one-electron oxidation-reduction cycle and, with the dormant species thermodynamically much more favored than the radical species, the instantaneous radical concentration is kept so low as to practically suppress undesirable bimolecular terminations and chain-transfer reactions.

Thus, the transition metal-catalysts are necessary for a precise control of the "active-dormant equilibrium" and many late transition metals have been applied for the catalysts combined with ligands [e.g. Ru,[24] Fe,[25-55] Ni,[56] Cu,[57] Mo,[58] Mn,[59] Os,[60] Re,[61] Co,[62] Rh,[63] and Pd[64]]. As already pointed out, the catalytic properties of these metal complexes strongly depend on the combination of a transition metal and coordinating ligands.

Iron-Catalyzed Living Radical Polymerization. In 1997, the author's group first presented an iron-catalyzed living radical polymerization with a divalent iron complex $FeCl_2(PPh_3)_2$ (**1**).[25] The complex induced a living radical polymerization of methyl methacrylate (MMA) in conjunction with a halide initiator [i.e., CCl_4, $CHCl_2COPh$, $(CH_3)_2CBrCO_2C_2H_5$, and $CH_3CBr(CO_2C_2H_5)_2$] to give controlled polymers with narrow

molecular weight distributions (MWDs) [M_w/M_n ~ 1.2; with $CH_3CBr(CO_2C_2H_5)_2$]. Since then, some iron complexes have been reported for living radical polymerizations. Isolated and well-defined examples include (Figure 3): cyclopentadiene (Cp = η-C_5H_5) (**2**,**4**),[26] pentamethylcyclopentadiene (Cp* = η-C_5Me_5) (**3**,**5**),[27] imidazolidene (*N*-heterocyclic carbene) (**6**),[28] alkyl phosphine (**7**),[29] phosphine-nitrogen chelate (**8**),[30] diimine (**9**),[31] diiminopyridine (**10**),[32] diaminopyridine (**11**),[32] salicylaldiminato (**12**),[33] tridentate amine (**13-15**),[34] bis(oxazoline) (**16**),[35] and triazacyclononane (**17**).[36] Ligands for iron halides have been also reported for *in-situ* complexation (Figure 4): alkylphosphine (**L1**),[37,38] alkylamine (**L2**),[37] bipyridine (**L3**),[37] *N*-(*n*-hexyl)-2-pyridylmethanimine (**L4**),[39] monodentate amine (**L5**),[40] diiminopyridine (**L6**),[41] ethylenediaminetetraacetic acid (EDTA, **L7**),[42] tetradentate amine (**L8**),[43] bispyrazole (**L9**),[44] bisoxazoline (**L10**),[44] hexamethylphosphorictriamide (**L11**),[45] pyridylphosphine (**L12**, **L13**),[46] onium salt (**L14-L17**),[47,48] acetic acid (**L18**),[49,50] iminodiacetic acid (**L19**),[49,51] succinic acid (**L20**),[49,52] isophthalic acid (**L21**),[49,53] pyromellitic acid (**L22**),[54] and (di)picolinic acid (**L23-L30**).[55]

These complexes certainly catalyze living radical polymerizations, but the catalytic activities are mostly inferior to ruthenium and copper counterparts, especially in regard to activity (minimum amount required for the catalysis), tolerance to functional monomers, and efficiency of block copolymerization.

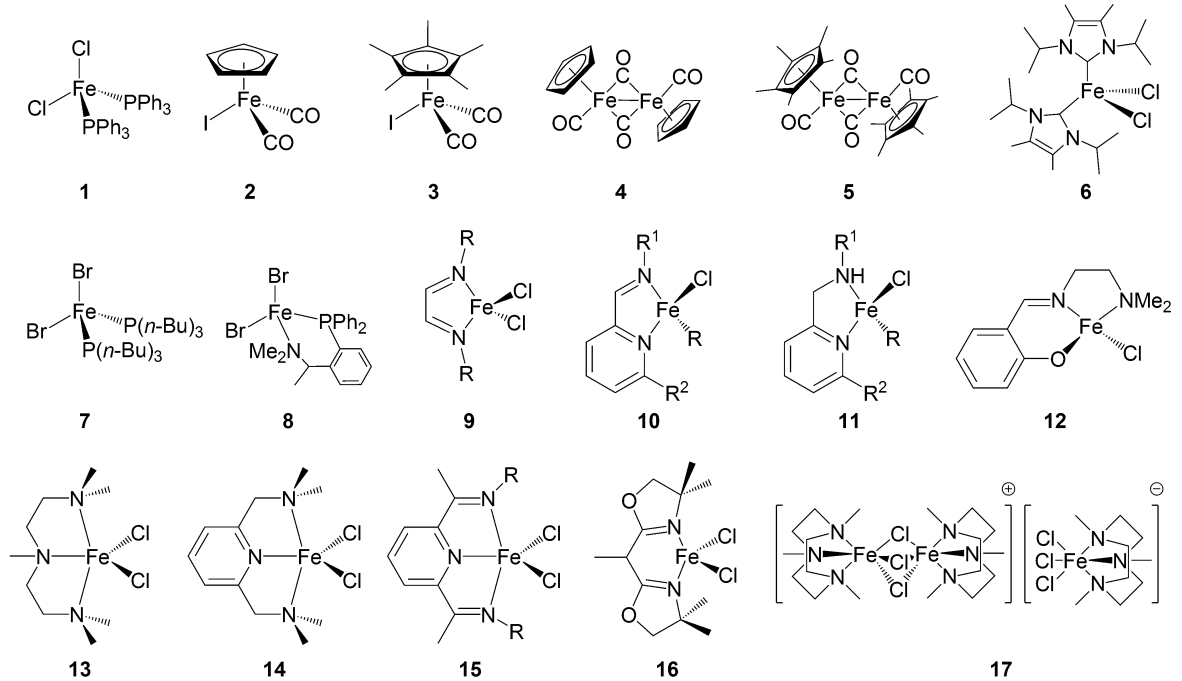

Figure 3. Iron complexes for living radical polymerization

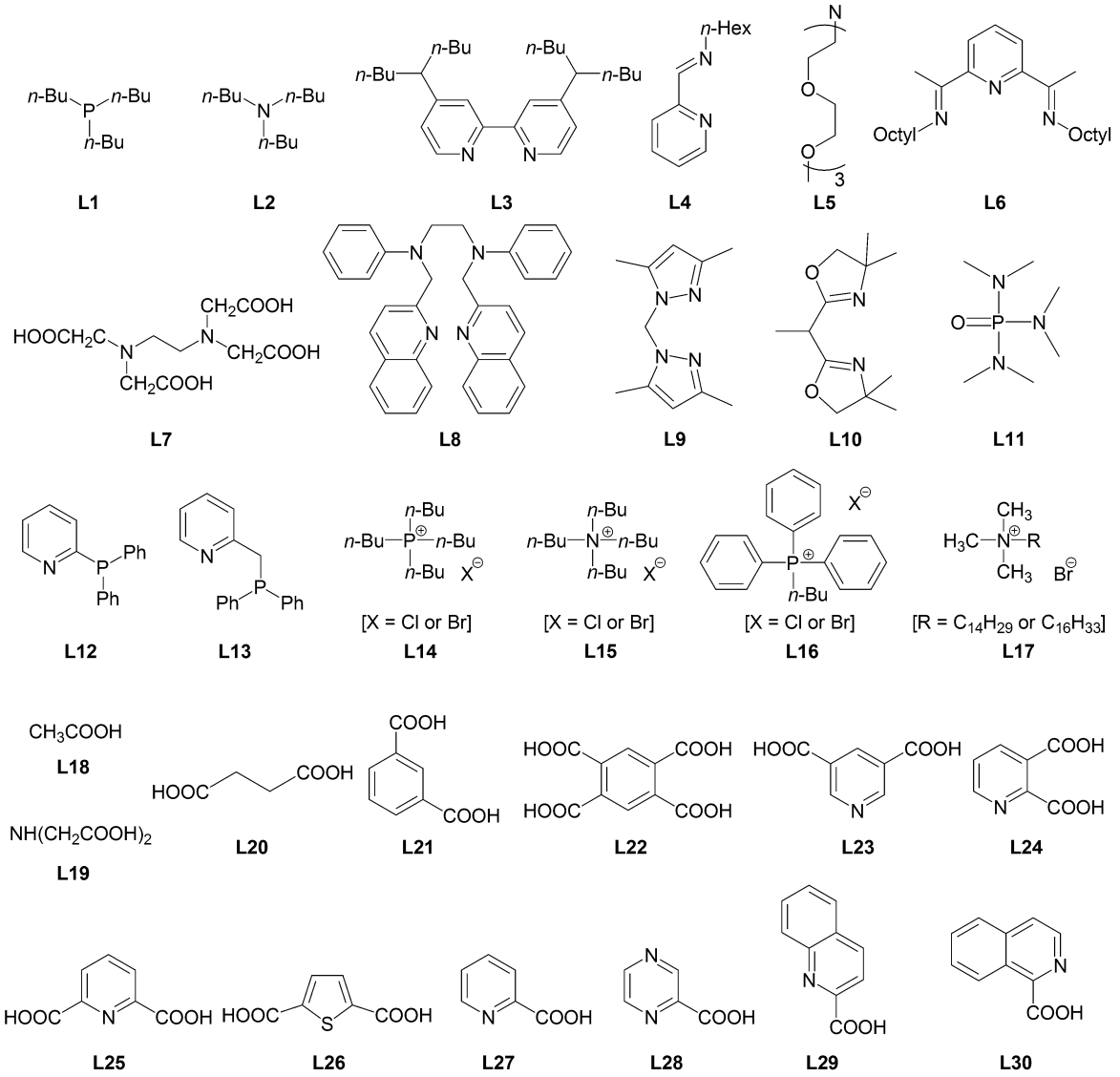

Figure 4. Ligands of iron halides for living radical polymerization

Objectives

From these backgrounds, the author decided to develop novel iron catalysts for living radical polymerization via an interrelated and mutually feed-backing three-stage procedure, "Synthesis"-"Polymerization"-"Analysis", as shown in Figure 5. First, iron complexes were synthesized focusing on the electronic modulation and the steric bulkiness around a central iron via ligand design (Synthesis). The prepared complexes were then employed for living radical polymerizations to see the catalytic functions such as activity, controllability, monomer versatility, and tolerance to functional groups (Polymerization). Importantly, the redox behaviors and the reaction mechanisms (e.g., *in-situ* structural transformation) were

analyzed for further advancement of the catalysts (Analysis). In this thesis, the author targeted two design principles for evolution of iron catalysts:

(1) "Anionization" of Iron Complexes by Bulky and Conjugated Phosphazenium Salts
(2) Ligand Design in Half-Metallocene Iron Complexes

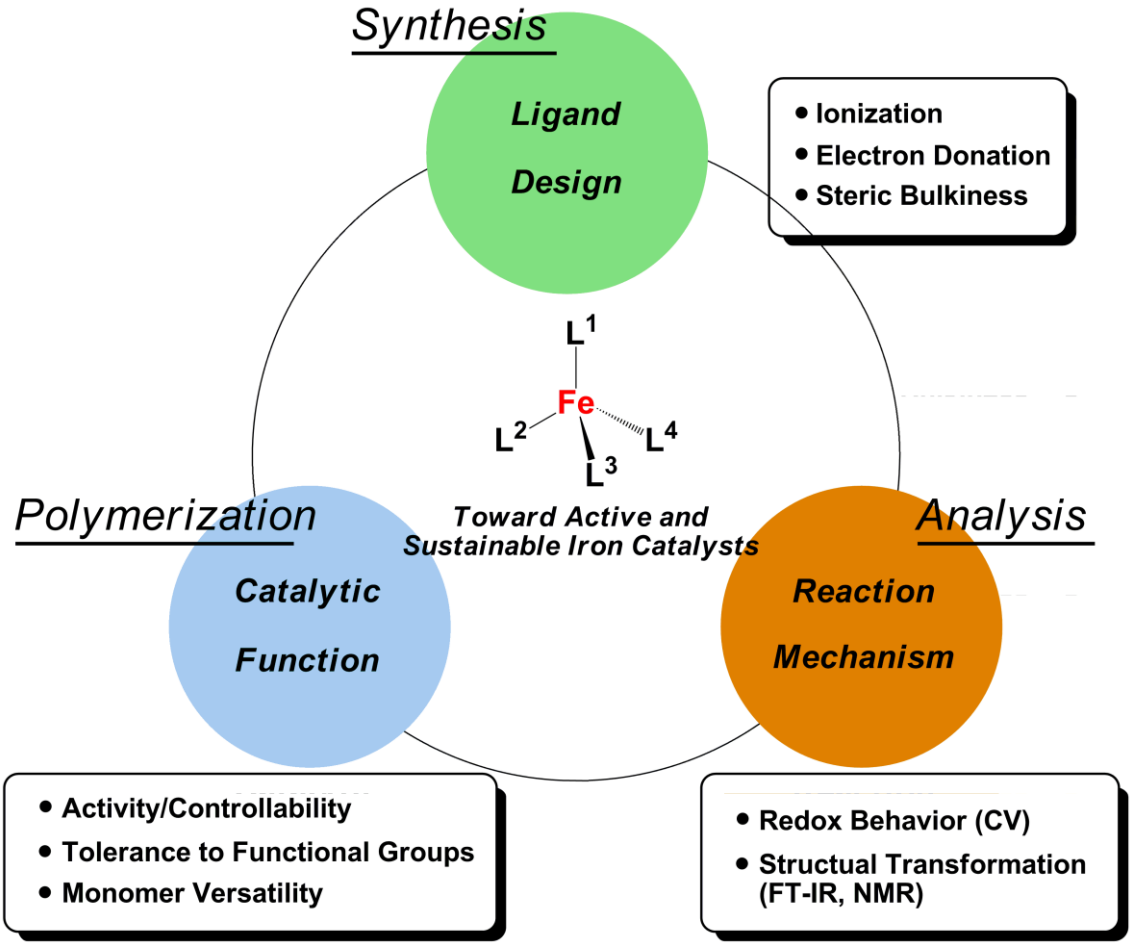

Figure 5. Three steps for development of active and sustainable iron catalysts

(1) "Anionization" of Iron Complexes by Bulky and Conjugated Phosphazenium Salts. In metal catalyzed living radical polymerization, one-electron transfer from the catalyst triggers the activation of an initiator. Thus, introduction of an electron-donating group into ligands is one of the key strategies for an improvement in catalytic activity. The author focused on this "*anionization*" to increase the electron density of an iron center, as well

as the bulkiness around the catalyst core to enhance tolerance to functional monomers.

In the first part of this thesis work, bulky and conjugated phosphazenium salts (PZN-X; X = Cl, Br, I; Figure 6) were employed as anion sources for iron(II) halides ($FeCl_2$ or $FeBr_2$). The phosphazenium salts were originally developed by Mitsui Chemical[65] as nonmetallic molecular catalysts for nucleophilic substitution reactions or ring-opening reactions of oxiranes with aryl carboxylates.[66] Structurally, they are considered as bulky, dendritic, and conjugated cations (ca. 12 Å in diameter) where the positive charge is highly delocalized, effectively rendering it non-nucleophilic and well separated from the halide counteranion, both spatially and electronically. Such a unique structure would effectively increase the electron density of the central iron and protect the complex from unfavorable interactions with functional monomers.

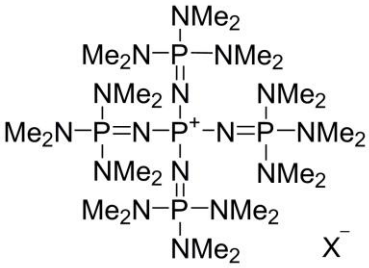

Phosphazene
[PZN-X; X=Cl, Br, I]

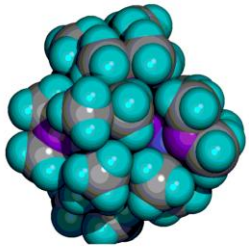

Structure Model

Figure 6. Phosphazenium salts

(2) Ligand Design in Half-Metallocene Iron Complexes. The author's group has already reported that cyclopentadienyl (Cp; η-C_5H_5) iron dicarbonyl complexes [$CpFe(CO)_2X$; X = Br or I] catalyze living radical polymerizations of acrylates and styrenes in conjunction with a metal alkoxide as a cocatalyst [e.g., Ti(O*i*-Pr)$_4$ and Al(O*i*-Pr)$_3$].[26] However, the catalytic activities of the CpFe complexes were not so high, and a large amount was necessary for catalysis ($[catalyst]_0/[initiator]_0 \sim 1$). More seriously, they were less capable to catalyze living polymerizations of methacrylates.

Thus, the author further designed and modified the cyclopentadiene-based iron complexes [$CpFe(CO)_2X$; X = Br or I] to enhance their catalytic functions, especially toward a higher activity to reduce catalyst amount and toward a higher functionality tolerance or robustness to various monomers including methacrylates (Figure 7). Note that $CpFe(CO)_2X$ complexes are of the 18e structure, and such electrically saturated complexes should turn into unsaturated 16e forms via ligand release, in order to trigger the activation for a halide initiator. This catalytic mechanism encouraged the author to examine "hetero ligation", since it might be prospective for the efficient structural conversion if one ligand is more labile than the other. Also, because of their diversity, introduction of phosphine ligands would be advantageous to

examine the electronic and the steric effects in catalysis. Thus, the author embarked on the "hetero ligation" with one carbonyl and one phosphine [CpFe(CO)(L^{phos})Br].[67] *N*-heterocyclic carbene (NHC) was also examined as a ligand in place of the phosphine, to possibly enhance electron donation and bulkiness.[68] Furthermore, design was directed to the substituents on the Cp ring. Thus, pentamethyl- (Cp*; η-C_5Me_5)[69] and pentaphenyl (Cp^{Ph}; η-C_5Ph_5) cyclopentadienes[70] were employed in place of Cp: Cp* would increase bulkiness, solubility, stability, and electron density of the complex; Cp^{Ph} would give the unique reactivity for ligand exchange[71] and redox behavior.[72]

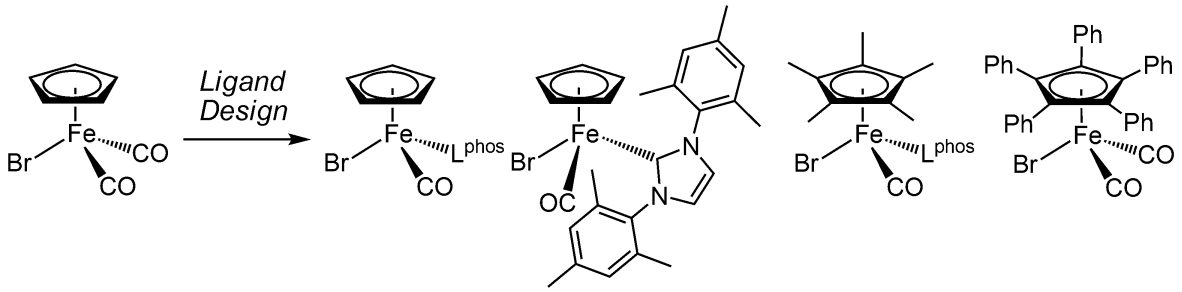

Figure 7. Design of half-metallocene iron catalysts

Outline of This Study

This thesis consists of two parts to deal with developments of novel iron catalysts for living radical polymerizations (Scheme 2). **Part I** (Chapters 1-2) presents bulky and conjugated ionic phosphazenium salts combined with iron halides, especially focusing on differences with conventional onium salts. **Part II** (Chapters 3-6) discusses

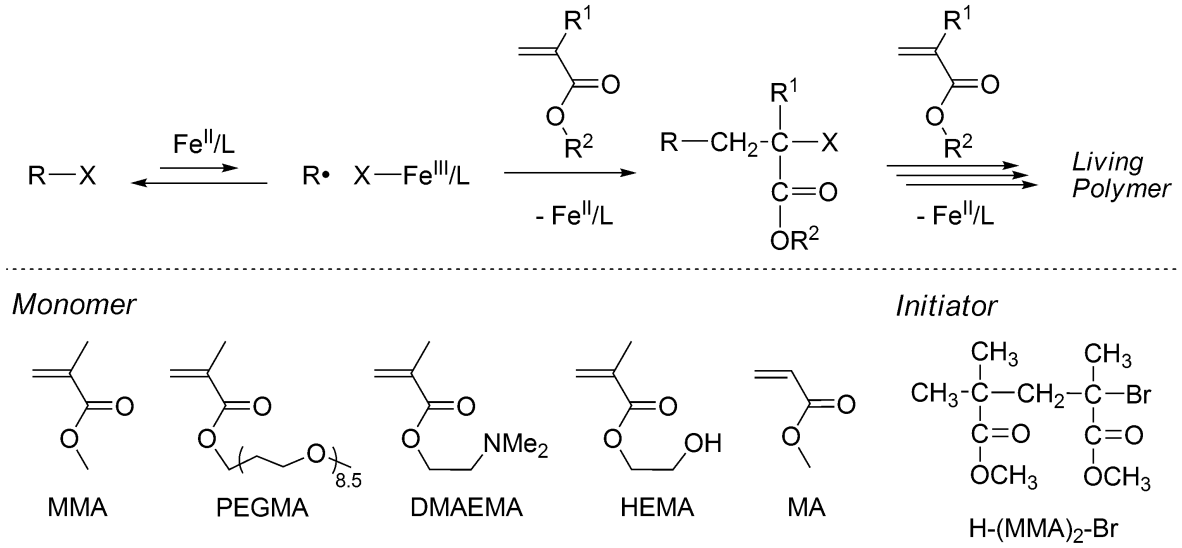

Scheme 2. Initiating Systems of Iron-Catalyzed Living Radical Polymerization

half-metallocene iron catalysts, where the structural transformation during polymerization is important for efficient catalysis.

Chapter 1 deals with iron halide (FeX_2; X = Cl, Br) combined with bulky, conjugated, and ionic phosphazenium salts (PZN-X; X = Cl, Br, I) for living radical polymerization of MMA (Figure 8). With equimolar combinations of $FeBr_2$/PZN-Br in conjunction with a bromide initiator [H-$(MMA)_2$-Br], the molecular weights were precisely controlled by the feed ratio of the monomer to the initiator and the molecular weight distributions (MWDs) were quite narrow (M_w/M_n < 1.2). In terms of activity and controllability, $FeBr_2$/PZN-Br was distinguished from not only a conventional iron complex [$FeBr_2(PPh_3)_2$] but also other hitherto known combinations of $FeBr_2$ with onium salts such as tetrabutylammonium bromide (TBA-Br) or tetrabutylphosphonium bromide (TBP-Br).

In **Chapter 2**, the $FeBr_2$/PZN-Br catalytic system was applied for functional monomers. It efficiently catalyzed living radical polymerization of functional methacrylate carrying poly(ethylene glycol) pendent group (PEGMA) to give narrow MWDs (M_w/M_n ~ 1.2), and the tolerance to PEG groups was supported by cyclicvoltammetry (CV) measurements in the presence of the monomer. This catalysis was distinguished from not only a conventional iron catalyst [$FeBr_2(PPh_3)_2$] but also combinations of simple onium salts (i.e., TBA-Br and TBP-Br) with $FeBr_2$, where the polymerizations were retarded likely due to deactivation of the catalysts by PEG moiety. Also, such combinations were found to give controlled polymers for block copolymerization of MMA and PEGMA, random compolymerizations of *N*,*N'*-dimethylaminoethyl methacrylate (DMAEMA) with MMA and a homopolymerization of methyl acrylate (MA).

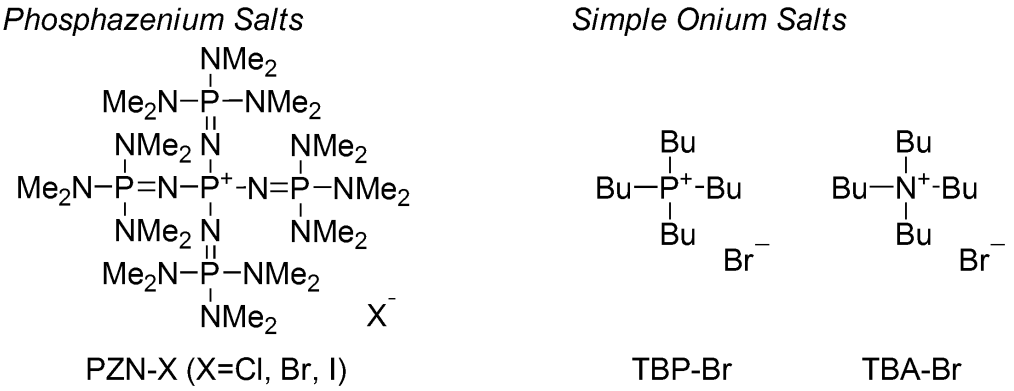

Figure 8. Structures of phosphazenium salts and conventional onium salts

Chapter 3 deals with "hetero-ligated" cyclopentadienyl (Cp) iron catalysts coordinated with one carbonyl and one phosphine, [CpFe(CO)(L^{phos})Br; Cp = η-C_5H_5; L^{phos} = PPh_3, $P(OPh)_3$, $PMePh_2$, PMe_2Ph, $P(n\text{-}Bu)_3$] (Figure 9). They induced living radical polymerization of MMA in conjunction with a bromide-initiator [H-$(MMA)_2$-Br] and gave controlled PMMAs, while the dicarbonyl (i.e., starting complex) resulted in less control/activity. Among the phosphine, $PMePh_2$ showed the best results for both activity and controllability (> 90% conversion within 24 h; M_w/M_n = 1.29). Compared with a diphosphine complex [CpFe($PMePh_2$)$_2$Br, homo ligated], these hetero-ligated catalysts are superior on catalytic activity, molecular weight control and tolerance to air-oxidation. The concomitant high activity and high stability were attributed to the *in-situ* generation of a real active catalyst with a 16-electron configuration via the irreversible release of the carbonyl group from CpFe(CO)(L^{phos})Br upon the activation of a terminal C-Br bond, as confirmed by FT-IR monitoring of model reactions with the initiator as a dormant-end model compound.

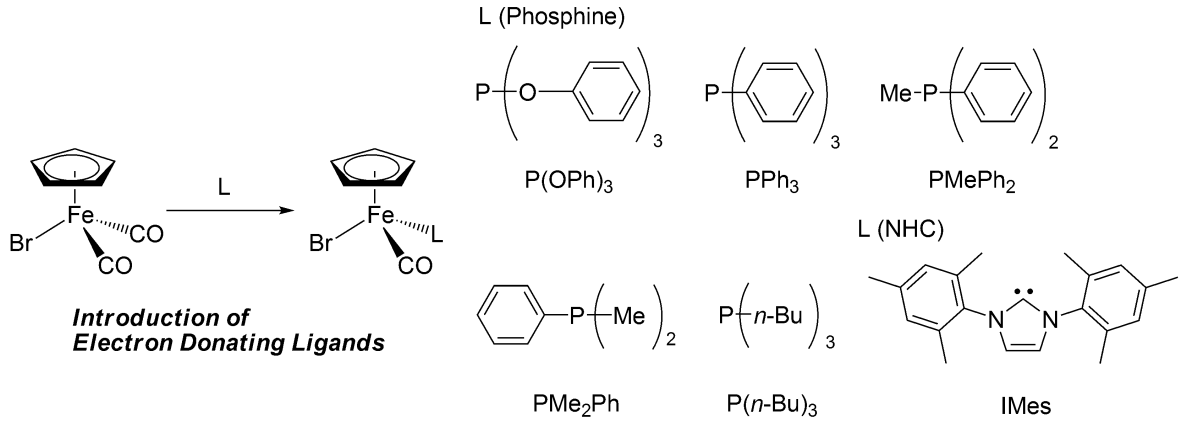

Figure 9. Ligand design of CpFe(CO)(L)Br for living radical polymerization

In **Chapter 4**, a cyclopentadienyl iron (II) complex coordinated with 1,3-bis(2,4,6-trimethylphenyl)imidazol-2-ylidene [IMes: CpFe(CO)(IMes)Br] was employed for living radical polymerization to see effects of the "*N*-heterocyclic carbene (NHC)" ligand on the catalysis (Figure 9). The complex allowed "controlled" polymerization of methyl acrylate (MA) to give fairly narrow MWDs (M_w/M_n ~1.3), while the phosphine derivative [CpFe(CO)($PMePh_2$)Br] resulted in less controlled polymers with much broader MWDs. The NHC ligand is more electron-donating ligand than any phosphine, and the redox potential of the complex was lower than phosphine-coordinated ones analyzed by FT-IR and CV.

Chapter 5 focuses on a series of pentamethylcyclopentadienyl (Cp*; η-C_5Me_5) iron complexes, ligated by one carbonyl and one phosphine [Cp*Fe(CO)(L^{phos})Br; L^{phos} = PPh_3,

$PMePh_2$, PMe_2Ph, P(*m*-tol)$_3$, and P(*p*-tol)$_3$] (Figure 10). These Cp*Fe complexes catalyzed living radical polymerization of MMA and gave better controlled polymers than the corresponding CpFe complexes [CpFe(CO)(L^{phos})Br]. Their superiority was demonstrated by successful monomer-addition experiments, a wider range of controllable molecular weight (M_n = 10^4-10^5), and narrower MWDs (M_w/M_n ~ 1.2). FT-IR analysis of initiator-catalyst model reactions showed that an efficient carbonyl release from the original coordinatively saturated 18e complex [CpFe(CO)(L^{phos})Br] into the unsaturated 16e form [CpFe(L^{phos})Br] is important in the catalysis to generate a growing radical from the initiator. The higher catalytic activity allowed controlled polymerizations of other monomers that are not available for CpFe catalysts, such as MA and PEGMA.

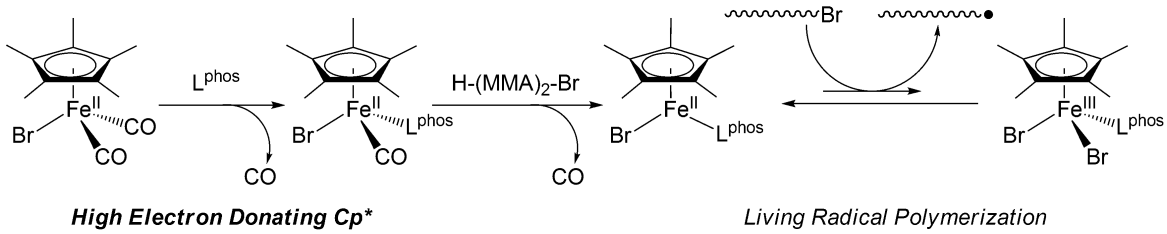

Figure 10. Living radical polymerization with $Cp^*Fe(CO)(L^{phos})Br$

Chapter 6 presents pentaphenylcyclopentadienyl (η-C_5Ph_5; Cp^{Ph}) dicarbonyl iron complex [$(Cp^{Ph})Fe(CO)_2Br$] (Figure 11). The complex itself was stable and inactive for the polymerization of MMA, however, in the presence of triphenylphosphine (PPh_3), it smoothly polymerized MMA to give controlled polymers with narrow MWDs in conjunction with a bromide-initiator [H-(MMA)$_2$-Br] (~ 90% conversion within 24 h; M_w/M_n = 1.2). Analyses of the model reaction with FT-IR and ^{31}P-NMR clarified that the carbonyl ligands were

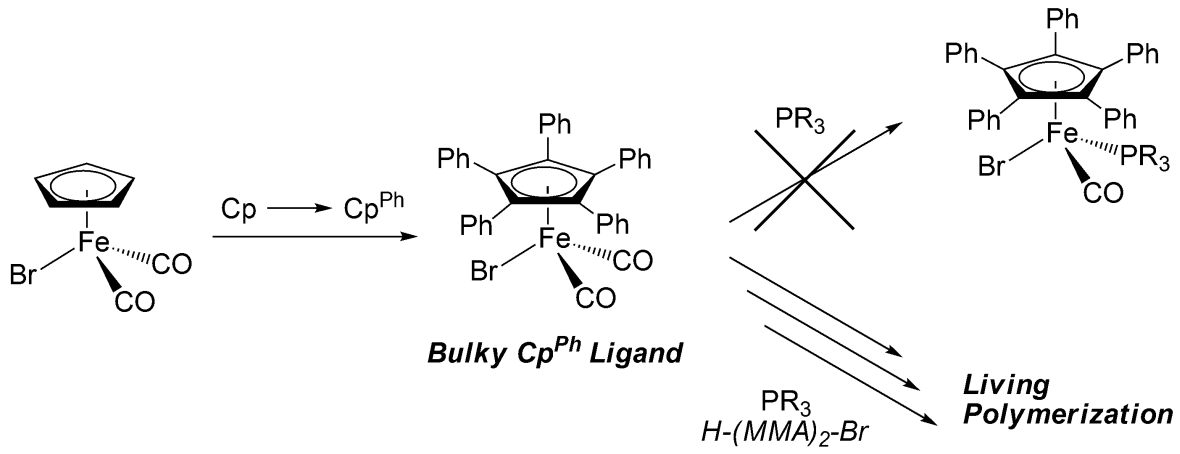

Figure 11. Living radical polymerization with $(Cp^{Ph})Fe(CO)_2Br$

efficiently exchanged with the phosphine for the complex to transform into real active catalyst. The high catalytic activity was proved by the monomer addition experiment, fine control even for higher molecular weight polymer ($M_n \sim 10^5$; $M_w/M_n < 1.2$), and control for MA. Such an *in-situ* transformation from a stable complex to an active catalyst would be advantageous to practical applications.

References

(1) Crabtree, R. H., Ed.; *The Organometallic Chemistry of the Transition Metals*; John Wiley & Sons, Inc.: New York, 2001.

(2) Ziegler, K.; Holzkamp, E.; Breil, H.; Martin, H. *Angew. Chem., Int. Ed.* **1955**, *67*, 541-547.

(3) Natta, G.; Pino, P.; Corradini, P.; Danusso, F.; Mantica, E.; Mazzanti, G.; Moraglio, G. *J. Am. Chem. Soc.* **1955**, *77*, 1708-1710.

(4) Plietker, B. Ed.; *Iron Catalysis in Organic Chemistry*; Wiley-VCH Verlag GmbH & Co. KGaA: Weinheim, 2008.

(5) Hawker, P.; Twigg, M. V. *Comprehensive Coordination Chemistry;* Wilkinson, G., Eds.; Pergamon Press.: Oxford, 1987; vol. 4, p 1179-1288.

(6) *KAGAKU BINRAN, 4th ed*.; Maruzen: Tokyo, 1978, vol. 1; p 51.

(7) Reppe, W.; Vetter, H. *Justus Liebigs Ann. Chem.* **1953**, *582*, 133-161.

(8) (a) Olah, G. A.; Kobayashi, S.; Tashiro, M. *J. Am. Chem. Soc.*, **1972**, *94*, 7448-7461. (b) Pearsons, D. E.; Buehler, C. A. *Synthesis* **1972**, 533-542.

(9) Bolm, C.; Legros, J.; Paih, J. L.; Zani, L. *Chem. Rev.* **2004**, *104*, 6217-6254.

(10) (a) Barton, D. H. R.; Doller, D. *Acc. Chem. Res.* **1992**, *25*, 504-512. (b) Barton, D. H. R. *Chem. Soc. Rev.* **1996**, *25*, 237-239. (c) Barton, D. H. R. *Tetrahedron* **1998**, *54*, 5805-5817. (d) White, M. C.; Doyle, A. G.; Jacobsen, E. *J. Am. Chem. Soc.* **2001**, *123*, 7194-7195. (e) Pillai, U. R.; Sahle-Demessie, E.; Namboodiri, V. V.; Varma, R. S. *Green Chem.* **2002**, *4*, 495-497. (f) Cotas, M; Mehn, M. P. Jensen, M. P.; Que, L., Jr. *Chem. Rev.* **2004**, *104*, 939-986. (g) Mas-Ballesté, R.; Costas, M.; van den Berg, T.; Que, L.; *Chem. Eur.* **2006**, *12*, 7489-7500. (h) Taktak, S.; Ye, W.; Herrera, A. M.; Rybak-Akimova, E. V. *Inorg. Chem.* **2007**, *46*, 2929-2942.

(11) (a) Frankel, E. N.; Emken, E. A.; Peters, H. M.; Davison, V. L.; Butterfield, R. O. *J. Org. Chem.* **1964**, *29*, 3292-3297. (b) Markó, L.; Radhi, M. A.; Ötvös, I. *J. Organomet. Chem.* **1981**, *218*, 369-376. (c) Inoue, H.; Sato, M. *J. Chem. Soc., Chem. Commun.*

1983, 983-984. (d) Miller, M. E.; Grant, E. R. *J. Am. Chem. Soc.* **1984**, *106*, 4635-4636. (e) Lynch, T. J.; Banah, M.; Kaesz, H. D.; Porter, C. R. *J. Org. Chem.* **1984**, *49*, 1266-1270. (f) Bart, S. C.; Hawrelak, E. J.; Lobkovsky, E. *Organometallics* **2005**, *24*, 5518-5527. (g) Trovitch, R. J.; Lobkovsky, E.; Chirik, P. J. *Inorg. Chem.* **2006**, *45*, 7252-7260. (h) Enthaler, S.; Hagemann, B.; Erre, G.; Junge, K.; Beller, M. *Chem, Asian J.* **2006**, *1*, 598-604.

(12) (a) Susuki, T.; Tsuji, J. *J. Org. Chem.* **1970**, *35*, 2982-2986. (b) Elzinga, J.; Hogeveen, H. *J. Org. Chem.* **1980**, *45*, 3957-3969. (c) Hayes, T. K.; Freyer, A. J.; Parvez, M.; Weinreb, S. M. *J. Org. Chem.* **1986**, *51*, 5501-5503. (d) Hayes, T. K.; Villani, R.; Weinreb, S. M. *J. Am. Chem. Soc.* **1988**, *110*, 5533-5543. (e) Lee, G. M.; Parvez, M.; Weinreb, S. M. *Tetrahedron* **1988**, *44*, 4671-4678. (f) Lee, G. M.; Weinreb, S. M. *J. Org. Chem.* **1990**, *55*, 1281-1285. (g) de Campo, F.; Lastécouères, D.; Verlhac, J. -B.; *Chem. Commun.* **1998**, 2117-2118.

(13) (a) Bonnsen, P. V.; Puckett, C. L.; Honeychuck, R. V.; Hersh, W. H. *J. Am. Chem. Soc.* **1989**, *111*, 6070-6081. (b) Olson, A. S.; Seitz, W. J.; Hossain, M. M. *Tetrahedron Lett.* **1991**, *32*, 5299-5302. (c) Corey, E. J.; Ishihara, K. *Tetrahedron Lett.* **1992**, *33*, 6807-6810. (d) Kanemasa, S.; Oderaotoshi, Y.; Yamamoto, H,; Tanaka, J.; Wada, E.; Curran, D. P. *J. Org. Chem.* **1997**, *62*, 6454-6455. (e) Kanemasa, S.; Oderaotoshi, Y.; Sakaguchi, S. -i.; Yamamoto, H,; Tanaka, J.; Wada, E. J.; Curran, D. P. *J. Am. Chem. Soc.* **1998**, *120*, 3074-3088. (f) Kündig, E. P.; Bourdin, B.; Bernardinelli, G. *Angew. Chem., Int. Ed.* **1994**, *33*, 1856-1858. (g) Bruin, M. E.; Kündig, E. P. *Chem. Commun.* **1998**, 2635-2636. (h) Kündig, E. P.; Saudan, C. M.; Viton, F. *Adv. Synth. Catal.* **2001**, *343*, 51-56. (i) Gorman, D. B.; Tomlinson, I. A. *Chem. Commun.* **1998**, 25-26. (j) Usuda, H.; Kuramochi, M.; Kanai, M.; Shibasaki, M. *Org, Lett.* **2004**, *6*, 4387-4390.

(14) (a) Tamura, M.; Kochi, J. K. *J. Am. Chem. Soc.* **1971**, *93*, 1487-1489. (b) Kochi, J. K. *Acc. Chem. Res.* **1974**, *7*, 351-360. (c) Fürstner, A; Leitner, A. *Angew. Chem., Int. Ed.* **2002**, *41*, 609-1612. (d) Sherry, B. D.; Fürstner, A; *Acc. Chem. Res.* **2008**, *41*, 1500-1511. (e) Nakamura, M.; Matsuo, K.; Ito, S.; Nakamura, E. *J. Am. Chem. Soc.* **2004**, *126*, 3686-3687. (f) Sapountzis, I.; Lin, W.; Kofink, C. C.; Despotopoulou, C.; Knochel, P. *Angew. Chem., Int. Ed.* **2005**, *44*, 1654-1658. (g) Cahiez, G.; Habiak, V.; Duplais, C.; Moyeux, A. *Angew. Chem., Int. Ed.* **2007**, *46*, 4364-4366. (h) Correa, A.; Bolm, C. *Angew. Chem., Int. Ed.* **2007**, *46*, 8862-8865. (i) Czaplik, W. M.; Mayer, M.; Cvengroš, J.; Wangelin, A. J. V. *ChemSusChem* **2009**, *2*, 396-417. (j) Czaplik, W. M.;

Mayer, M.; Wangelin, J. A. V. *Angew. Chem., Int. Ed.* **2009**, *48*, 607-610.

(15) (a) Small, B. L.; Brookhart, M.; Bennett, A. M. A. *J. Am. Chem. Soc.* **1998**, *120*, 4049-4050. (b) Britovsek, G. J. P.; Gibson, V. C.; Kimberley, B. S.; Maddox, P. J.; McTavish, S. J.; Solan, G. A.; White, A. J. P.; Williams, D. J.; *Chem. Commun.* **1998**, 849-850. (c) Britovsek, G. J. P.; Bruce, M.; Gibson, V. C.; Kimberley, B. S.; Maddox, P. J.; Mastroianni, S.; McTavish, S. J.; Redshaw, C.; Solan, G. A.; Stromberg, S.; White, A. J. P.; Williams, D. J. *J. Am. Chem. Soc.* **1999**, *121*, 8728-8740. (d) Bianchini, C.; Giambastiani, G.; Rios, I. G.; Mantovani, G.; Meli, A.; Segarra, A. M. *Coord. Chem. Rev.* **2006**, *250*, 1391-1418.

(16) (a) Kanazawa, A.; Hirabaru, Y.; Kanaoka, S.; Aoshima, S. *J. Polym. Sci., Part A: Polym. Chem.* **2006**, *44*, 5795-5800. (b) Aoshima, S.; Yoshida, T.; Kanazawa, A.; Kanaoka, S. *J. Polym. Sci., Part A: Polym. Chem.* **2007**, *45*, 1801-1813.

(17) (a) Fürstner, A; Martin, R. *Chem. Lett.* **2005**, *34*, 624-629. (b) Enthaler, S.; Junge, K.; Beller, M. *Angew. Chem. Int. Ed.* **2008**, *47*, 3317-3321. (c) Correa, A.; Mancheño, O. G.; Bolm, C. *Chem. Soc. Rev.* **2008**, *37*, 1108-1117. (d) Gaillard, S.; Renaud, J. -C. *ChemSusChem* **2008**, *1*, 505-509.

(18) (a) Szwarc, M. *Nature* **1956**, *178*, 1168-1169. (b) Szwarc, M.; Levy, M. Milkovich, R. *J. Am. Chem. Soc.* **1956**, *78*, 2656-2657.

(19) (a) Higashimura, T.; Sawamoto, M. *Adv. Polym. Sci.* **1984**, *62*, 49-94. (b) Sawamoto, M. *Prog. Polym. Sci.* **1991**, *16*, 111-172. (c) Kennedy, J. P.; Iva´n, B. *Designed Polymers by Carbocationic Macromolecular Engineering: Theory and Practice*; Hanser: Munich, Germany, 1992. (d) *Cationic Polymerizations*; Matyjaszewski, K., Ed.; Marcel Dekker: New York, 1996.

(20) Mecerreyes, D.; Je´roˆme, R.; Dubois, Ph. *Adv. Polym. Sci.* **1999**, *147*, 1-59.

(21) Moad, G.; Solomon, D. H. *The Chemistry of Radical Polymerization: Second fully revised editon*; Elsevier: Oxford, U. K., 2006.

(22) (a) Kamigaito, M.; Ando, T.; Sawamoto, M. *Chem. Rev.* **2001**, *101*, 3689-3745. (b) Kamigaito, M.; Ando, T.; Sawamoto, M. *Chem. Rec.* **2004**, *4*, 159-175. (c) Ouchi, M.; Terashima, T.; Sawamoto, M. *Acc. Chem. Res.* **2008**, *41*, 1120-1132. (d) Ouchi, M.; Terashima, T.; Sawamoto, M. *Chem. Rev.* **2009**, *109*, 4963-5050. (e) Matyjaszewski, K.; Xja, J. *Chem. Rev.* **2001**, *101*, 2921-2990. (f) Tsarevsky, N, V.; Matyjaszewski, K. *Chem. Rev.* **2007**, *107*, 2270-2299. (g) Matyjaszewski K., Ed.; *Controlled/Living Radical Polymerization From Synthesis to Materials*; ACS Symposium Series 944;

American Chemical Society: Washington, DC, 2006.

(23) Kato, M.; Kamigaito, M.; Sawamoto, M.; Higashimura, T. *Macromolecules* **1995**, *28*, 1721-1723.

(24) (a) Takahashi, H.; Ando, T.; Kamigaito, M.; Sawamoto, M. *Macromolecules* **1999**, *32*, 3820-3823. (b) Watanabe, T.; Ando, T.; Kamigaito, M.; Sawamoto, M. *Macromolecules* **2001**, *34*, 4370-4374.

(25) Ando, T.; Kamigaito, M.; Sawamoto, M. *Macromolecules* **1997**, *30*, 4507-4510.

(26) (a) Kotani, Y.; Kamigaito, M.; Sawamoto, M. *Macromolecules* **1999**, *32*, 6877-6880. (b) Kotani, Y.; Kamigaito, M.; Sawamoto, M. *Macromolecules* **2000**, *33*, 6746-6751. (c) Onishi, I.; Baek, K. -Y.; Kotani, Y.; Kamigaito, M.; Sawamoto, M. *J. Polym. Sci., Part A: Polym. Chem.* **2002**, *40*, 2033-2043.

(27) Kotani, Y.; Kamigaito, M.; Sawamoto, M. *Macromolecules* **2000**, *33*, 3543-3549.

(28) Louie, Y.; Grubbs, R. H. *Chem. Commun.* **2000**, 1479-1480.

(29) Uchiike, C.; Terashima, T.; Ouchi, M.; Ando, T.; Kamigaito, M.; Sawamoto, M. *Macromolecules* **2007**, *40*, 8658-8662.

(30) Uchiike, C.; Ouchi, M.; Ando, T.; Kamigaito, M.; Sawamoto, M. *J. Polym. Sci., Part A: Polym. Chem.* **2008**, *46*, 6819-6827.

(31) (a) Gibson, V. C.; O'Reilly, R. K.; Reed, W.; Wass, D. F.; White, A. J. P.; Williams, D. J. *Chem. Commun.* **2002**, 1850-1851. (b) Gibson, V. C.; O'Reilly, R. K.; Wass, D. F.; White, A. J. P.; Williams, D. J. *Macromolecules* **2003**, *36*, 2591-2593. (c) O'Reilly, R. K.; Shaver, M. P.; Gibson, V. C.; White, A. J. P.; *Macromolecules* **2007**, *40*, 7441-7452.

(32) Gibson, V. C.; O'Reilly, R. K.; Wass, D. F.; White, A. J. P.; Williams, D. J. *Dalton Trans.* **2003**, 2824-2830.

(33) O'Reilly, R. K.; Gibson, V. C.; White, A. J. P.; Williams, D. J. *J. Am. Chem. Soc.* **2003**, *125*, 8450-8451.

(34) O'Reilly, R. K.; Gibson, V. C.; White, A. J. P.; Williams, D. J. *Polyhedron* **2004**, *23*, 2921-2928.

(35) Ferro, R.; Milione, S.; Bertolasi, V.; Capacchione, C.; Grassi, A. *Macromolecules* **2007**, *40*, 8544-8546.

(36) (a) Niibayashi, S.; Hayakawa, H.; Jin, R-H.; Nagashima, H. *Chem. Commun.* **2007**, 1855-1857. (b) Kawamura, M.; Sunada, Y.; Kai, H.; Koike, N.; Hamada, A.; Hayakawa, H.; Jin, R. -H.; Nagashima, H. *Adv. Synth. Catal.* **2009**, *351*, 2086-2090.

(37) Matyjaszewski, K.; Wei, M.; Xia, J.; McDermott, N. E. *Macromolecules* **1997**, *30*,

8161-8164.

(38) Satoh, K.; Aoshima, H.; Kamigaito, M. *J. Polym. Sci., Part A: Polym. Chem.* **2008**, *46*, 6358-6363.

(39) (a) Zhang, H.; Schubert, U. S. *Chem. Commun.* **2004**, 858-859. (b) Zhang, H.; Schubert, U. S. *J. Polym. Sci., Part A: Polym. Chem.* **2004**, *42*, 4882-4894.

(40) Wang, G.; Zhu, X.; Zhu, J.; Cheng, Z. *J. Polym. Sci., Part A: Polym. Chem.* **2006**, *44*, 483-489.

(41) Göbelt, B.; Matyjaszewski, K. *Macromol. Chem. Phys.* **2000**, *201*, 1619-1624.

(42) Bergenudda, H.; Jonssona, M.; Nyströmb, D.; Malmströmb, E. *J. Mol. Catal. A: Chem.* **2009**, *306*, 69-76.

(43) Ibrahim, K.; Yliheikkilä, K.; Abu-Surrah, A.; Löfgren, B.; Lappalainen, K.; Markku Leskelä, M.; Repo, T.; Seppälä, *J. Eur. Polym. J.* **2004**, *40*, 1095-1104.

(44) Ferro, R.; Milione, S.; Caruso, T.; Grassi, A. *J. Mol. Catal. A: Chem.* **2009**, *307*, 128-133.

(45) Cao, J.; Chen, J.; Zhang, K.; Shen, Q.; Zhang, Y. *Appl. Catal., A* **2006**, *311*, 76-78.

(46) (a) Xue, Z.; Lee, B. W.; Noh, S. K.; Lyoo, W. S. *Polymer* **2007**, *48*, 4704-4714. (b) Xue, Z.; Noh, S. K.; Lyoo, W. S. *J. Polym. Sci., Part A: Polym. Chem.* **2008**, *46*, 2922-2935. (c) Xue, Z.; Linh, T. B.; Noh, S. K.; Lyoo, W. S. *Angew. Chem., Int. Ed.* **2008**, *47*, 6426-6429.

(47) Teodorescu, M.; Gaynor, S. G.; Matyjaszewski, K.; *Macromolecules* **2000**, *33*, 2335-2339.

(48) Wang, G.; Zhu, X.; Cheng, Z.; Zhu, J. *J. Macromol. Sci., Pure Appl. Chem.* **2004**, *41*, 487-499.

(49) Zhu, S.; Yan, D. *Macromol. Rapid Commun.* **2000**, *21*, 1209-1213.

(50) Zhu, S.; Yan, D.; Zhang, G. *Polym. Bull.* **2001**, *45*, 457-464.

(51) (a) Zhu, S.; Yan, D. *J. Polym. Sci., Part A: Polym. Chem.* **2000**, *38*, 4308-4314. (b) Hou, C.; Qu, R.; Liu, J.; Guo, Z.; Wang, C.; Ji, C.; Sun, C.; Wang, C. *Polymer* **2006**, *47*, 1505-1510.

(52) Zhu, S.; Yan, D.; Zhang, G.; Li, M. *Macromol. Chem. Phys.* **2000**, *201*, 2666-2669.

(53) Zhu, S.; Yan, D. *Macromolecules* **2000**, *33*, 8233-8238.

(54) Wang, G.; Zhu, X.; Cheng, Z.; Zhu, J. *Eur. Polym. J.* **2003**, *39*, 2161-2165.

(55) Wang, G.; Zhu, X.; Cheng, Z.; Zhu, J. *J. Polym. Sci., Part A: Polym. Chem.* **2006**, *44*, 2912-2921.

(56) (a) Granel, C.; Dubois, Ph.; Jérôme, R.; Teyssié, Ph. *Macromolecules* **1996**, *29*, 8576-8582. (b) Uegaki, H.; Kotani, Y.; Kamigaito, M.; Sawamoto, M. *Macromolecules* **1997**, *30*, 2249-2253. (c) Uegaki, H.; Kotani, Y.; Kamigaito, M.; Sawamoto, M. *Macromolecules* **1998**, *31*, 6756-6761. (d) Uegaki, H.; Kotani, Y.; Kamigaito, M.; Sawamoto, M. *J. Polym. Sci., Part A: Polym. Chem.* **1999**, *37*, 3003-3009.

(57) (a) Wang, J. S.; Matyjaszewski, K. *J. Am. Chem. Soc.* **1995**, *117*, 5614-5615. (b) Percec, V.; Barboiu, B. *Macromolecules* **1995**, *28*, 7970-7972.

(58) (a) Bandts, J. A. M.; van de Geijn, P.; van Faassen, E. E.; Boersma, J.; van Koten, *G. J. Organomet. Chem.* **1999**, *584*, 246-253. (b) Grognec, E. L.; Claverie, J.; Poli, R. *J. Am. Chem. Soc.* **2001**, *123*, 9513-9524. (c) Stoffelbach, F.; Haddleton, D. M.; Poli, R. *Eur. Polym. J.* **2003**, *39*, 2099-2105. (d) Matta, J. A.; Maria, S.; Daran, J -C.; Poli, R. *Eur. J. Inorg. Chem.* **2006**, 2624-2633.

(59) (a) Endo, K.; Yachi, A.; *Polym. Bull.* **2001**, *46*, 363-369. (b) Koumura, K.; Satoh, K.; Kamigaito, M. *Macromolecules* **2008**, *41*, 7359-7367.

(60) (a) Braunecker, W. A.; Itami, Y.; Matyjaszewski, K. *Macromolecules* **2005**, *38*, 9402-9404. (b) Braunecker, W. A.; Brown, W. C.; Morelli, B. C.; Tang, W.; Poli, R.; Matyjaszewski, K. *Macromolecules* **2007**, *40*, 8576-8585.

(61) (a) Kotani, Y.; Kamigaito, M.; Sawamoto, M. *Macromolecules* **1999**, *32*, 2420-2424. (b) Komiya, S.; Chigira, T.; Suzuki, T.; Hirano, M.; *Chem. Lett.* **1999**, 347-348.

(62) (a) Wang, B.; Zhuang, Y.; Luo, X.; Xu, S.; Zhou, X. *Macromolecules* **2003**, *36*, 9684-9686. (b) Matsubara, K.; Matsumoto, M. *J. Polym. Sci., Part A: Polym. Chem.* **2006**, *44*, 4222-4228.

(63) (a) Percec, V.; Barboiu, B.; Neumann, A.; Ronda, J. C.; Zhao, M. *Macromolecules* **1996**, *29*, 3665-3668. (b) Moineau, G.; Granel, C.; Dubois, Ph.; Jérôme, R.; Teyssié, Ph. *Macromolecules* **1998**, *31*, 542-544. (c) Petrucci, M. G. L.; Lebuis, A. -M.; Kakkar, A. K. *Organometallics* **1998**, *17*, 4966-4975.

(64) Lecomte, Ph.; Drapier, I.; Dubois, Ph.; Jérôme, R.; Teyssié, Ph. *Macromolecules* **1997**, *30*, 7631-7633.

(65) Nobori, T.; Kouno, M.; Suzuki, T.; Mizutani, K.; Kiyono, S.; Sonobe, Y.; Takaki, U. Phosphazenium salt and preparation process thereof, and process for producing poly(alkylene oxide), U.S. 5,990,352 (1999).

(66) Furuyama, R.; Fujita, T.; Funaki, S. F.; Nobori, T.; Nagata, T.; Fujiwara, K. *Catalysis*

Surveys from Asia **2004**, *8*, 61-71.

(67) Treichel, P. H.; Shubkin, R. L.; Barnett, K. W.; Reichard, D. *Inorg. Chem.* **1966**, *5*, 1177-1181.

(68) (a) Herrmann, W. A.; Köcher, C. *Angew. Chem., Int. Ed. Engl.* **1997**. *36*, 2162-2187. (b) Herrmann, W. A. *Angew. Chem., Int. Ed.* **2002**. *41*, 1290-1309. (c) Herrmann, W. A.; Weskamp, T.; Böhm, V. P. W. *Adv. Organomet. Chem.* **2002**, *48*, 1-69.

(69) King, R. B. *Coord. Chem. Rev.* **1976**, *20*, 155-169.

(70) Janiak, C.; Schumann, H. *Adv. Organomet. Chem.* **1991**, *33*, 291-393.

(71) Adams, H.; Bailey, N. A.; Browning, A. F.; Ramsden, J. A.; White, C. *J. Organomet. Chem.* **1990**, *387*, 305-314.

(72) Broadley, K.; Lane, G. A.; Connelly, N. G.; Geiger, W. E. *J. Am. Chem. Soc.*, **1983**, *105*, 2486-2487.

PART I

Phosphazenium Salts Combined with Iron Halides

Chapter 1

Well-Controlled Polymerization of Methyl Methacrylate: Optimization of Catalytic System

Abstract

Phosphazenium halides (PZN-X; X = Cl, Br, I), highly delocalized bulky salts, turned out to be excellent co-catalysts to be combined with iron halides (FeX_2) to form in situ active anionic Fe(II) complexes that effectively catalyze living radical polymerization of alkyl and functionalized methacrylates with improved catalytic activity and tolerance to polar functionalities. For example, equimolar combinations of $FeBr_2$/PZN-Br efficiently induced a living radical polymerization of methyl methacrylate (MMA) with a bromide initiator [H-$(MMA)_2$-Br], to give polymers with controlled molecular weights and narrow molecular weight distributions (M_w/M_n < 1.2). Polymer molecular weight could be extended upon addition of second feeds of monomer or at lower initiator dose, while retaining narrow distributions. In terms of activity and controllability, the PZN-based catalysts were thus predominantly distinguished from not only a conventional iron complex [$FeBr_2(PPh_3)_2$; Ph = C_6H_5] but also other hitherto known combinations of $FeBr_2$ with such an onium salt as tetrabutylammonium or -phosphonium bromide, as further demonstrated by their reversible and hysteresis-free redox cycles with lower oxidation and reduction potentials (cyclic voltammetry). The new iron catalysts could be readily removed from as-prepared polymer solutions by simple washing with water to give virtually colorless products with the metal residue below 5 ppm.

Introduction

Design criteria for transition metal complex catalysts in organic and polymerization reactions often involve conflicting factors of primary importance starting with feasibility, activity, selectivity, substrate-versatility, and functionality-tolerance, along with those particularly important upon actual applications, removability, recyclability, durability, and cost. Additional considerations currently prevailing include environmental friendliness, safety (toxicity), and global abundance (availability). From these multi-faceted viewpoints, iron (Fe) would be a promising central metal for catalysts, potentially active, highly abundant, readily recoverable, and relatively nontoxic.[1]

"Transition metal-catalyzed living radical polymerization"[2] is one of such catalyzed reactions where metal catalysts critically contribute to the precision control of radical polymerization to give polymers of well-defined molecular weight, architecture, and functionality (Scheme 1).[2,3] Therein a metal catalyst activates an initiator (R-X) bearing a carbon−halogen bond for homolysis cleavage, where the metal center itself is one-electron oxidized. The primary radical species (R·) thus generated initiates radical propagation with some monomers to grow into a polymer chain, and afterwards the oxidized catalyst returns the halogen to the growing radical to regenerate a terminal carbon-halogen (dormant species), while it is one-electron reduced to return to the original lower-valence state complex. To achieve living polymerization, the activation-deactivation process should be reversible and far favored to the dormant species so as to retain an extremely low radical concentration, and to

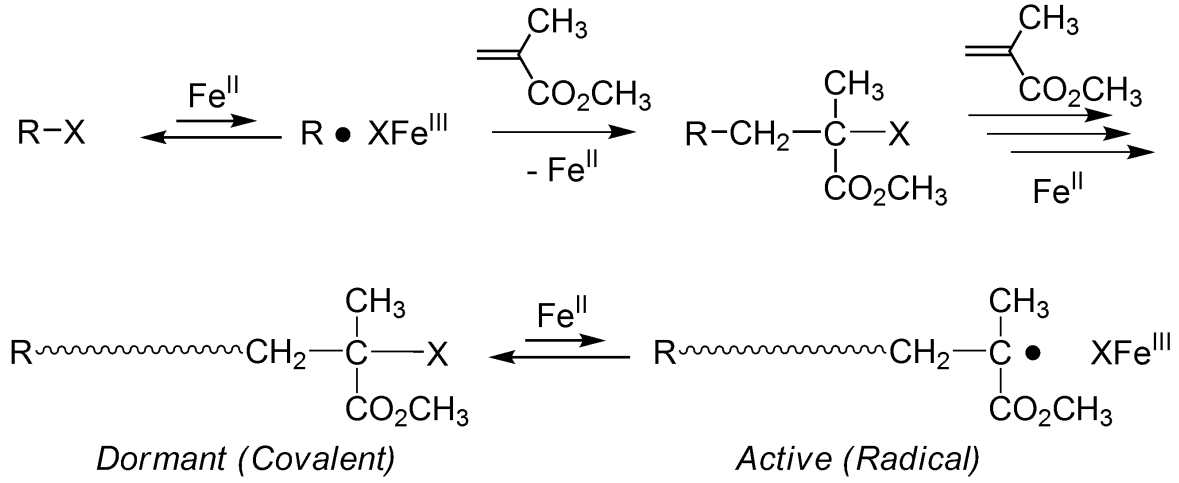

Scheme 1. Living Radical Polymerization of MMA with Fe(II) Complex

suppress bimolecular radical termination, relative to radical propagation. Obviously, the efficiency depends on the metal catalyst, which is modified by the combination of a central metal and ligands, in accordance with the structure of dormant species derived from monomer and leaving halogen. So far, a large variety of catalysts have been developed worldwide, where the central metals are primarily confined to ruthenium[2] and copper,[4] with nickel,[5] iron,[6-18] and other late transition metals acquiring renewed attention.

Iron complexes, undergoing oxidation/reduction cycle by one electron, have already been demonstrated to catalyze living radical polymerization, since the first example with a divalent iron chloride coordinated by triphenylphosphine [$FeCl_2(PPh_3)_2$].[6] As with other metal complexes, their catalytic performance such as activity and controllability clearly depends on ligands, which now also include bipyridine,[7] cyclopentadiene,[8] pentamethylcyclopentadiene,[9] isophthalic acid,[10] imidazolidene,[11] diimine,[12] diiminopyridine,[13] salicylaldiminato,[14] pyridylphosphine,[15] triazacyclononane,[16] alkyl phosphine,[17] bis(oxazoline),[18] among many others. In addition to their inherent advantages of abundance and benignity, some iron catalysts are readily removed from the products by simply washing with water.

However, as polymerization catalysts iron complexes seem generally inferior to the ruthenium or copper counterparts. For example, some iron-complexes show lower activity for polymerization of methacrylates, even though they effectively work for acrylates and styrenes. It is more serious that most of them are unable to catalyze living polymerizations of functional monomers directly, because they readily interact with polar groups to lose their catalytic activity. Actually, few iron catalysts have been reported active for polar monomers.

Herein the author therefore directed attention to "anionic" iron complexes as catalysts from the viewpoint that the higher electron density of the metal center would possibly enhance catalytic activity as well as tolerance to electron-rich polar functional monomers. For this the author have employed phosphazenium salts[19] (PZN-X; X = Cl, Br, I; Figure 1) as anion resources for iron(II) halides (FeX_2), to achieve living radical polymerization of methyl methacrylate (MMA) or functional monomers with higher controllability and activity. PZN-X salts were originally designed as nonmetallic molecular catalysts for nucleophilic substitution reactions or ring-opening reactions of oxiranes with aryl carboxylates, and structurally they are characterized by the bulky, dendritic, conjugated cation (ca. 12Å in diameter) where the positive charge is highly delocalized, effectively rendering it

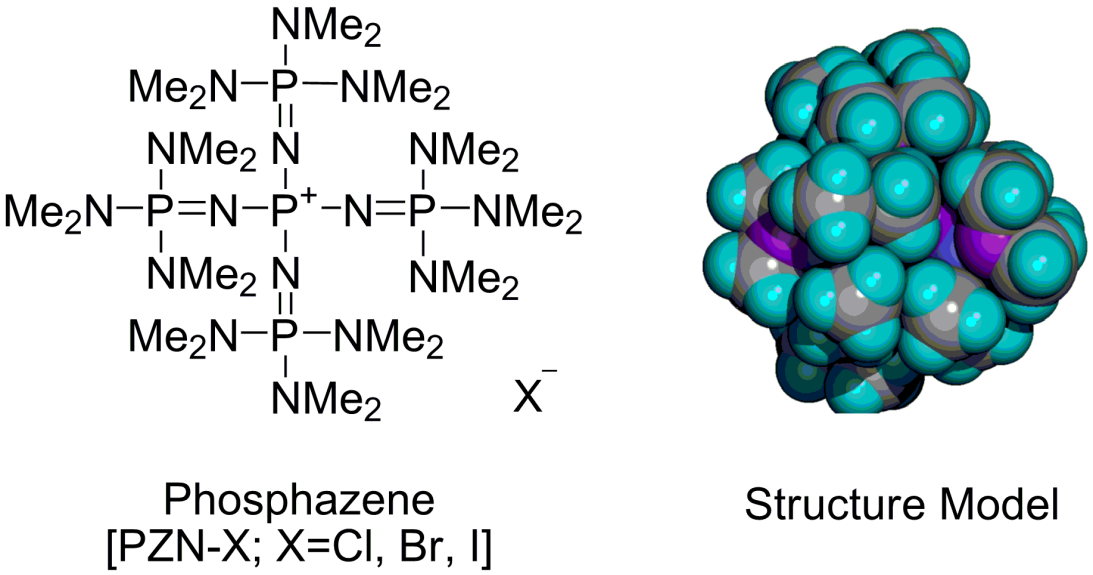

Figure 1. Structures of phosphazenium salts. Colors in atom labeling: green (hydrogen), gray (carbon), purple (nitrogen) and blue (phosphorus).

non-nucleophilic and well separated from the halide anion, both spatially and electronically.

Similar salt-based Fe(II) catalysts have in fact been reported for living radical polymerization,[20] in which tetraalkyl-ammonium and -phosphonium salts are combined with $FeBr_2$, but their overall activity appears not so high (incomplete monomer conversion), most likely because of the heterogeneity in polymerization media.

In this chapter, the author examined the suitable conditions of iron-halide/phosphazene (FeX_2/PZN-X) catalyst systems for living radical polymerization of MMA. Equimolar combinations of bromide derivatives, in conjunction with a bromide initiator [e.g., H-$(MMA)_2$-Br], induced living polymerization where the catalytic activity is clearly superior to conventional neutral phosphine complexes [e.g., $FeBr_2(PPh_3)_2$] or the anionic ammonium and phosphonium $FeBr_2$ salts.

Results and Discussion

1. Effects of Polymerization Conditions: $FeBr_2$/Phosphazene Ratio and Polymerization Temperature

First, the author examined effects of $FeBr_2$/phosphazenium-bromide (PZN-Br) ratio on the polymerization of MMA coupled with bromide-initiator [H-$(MMA)_2$-Br] in THF at 60 °C, where the $[FeBr_2]_0/[PZN\text{-}Br]_0$ was changed to be 10/5, 10/10 and 10/20 mM for $[MMA]_0/[H\text{-}(MMA)_2\text{-}Br]_0$ = 2000/20 mM (Figure 2). Polymerization proceeded in

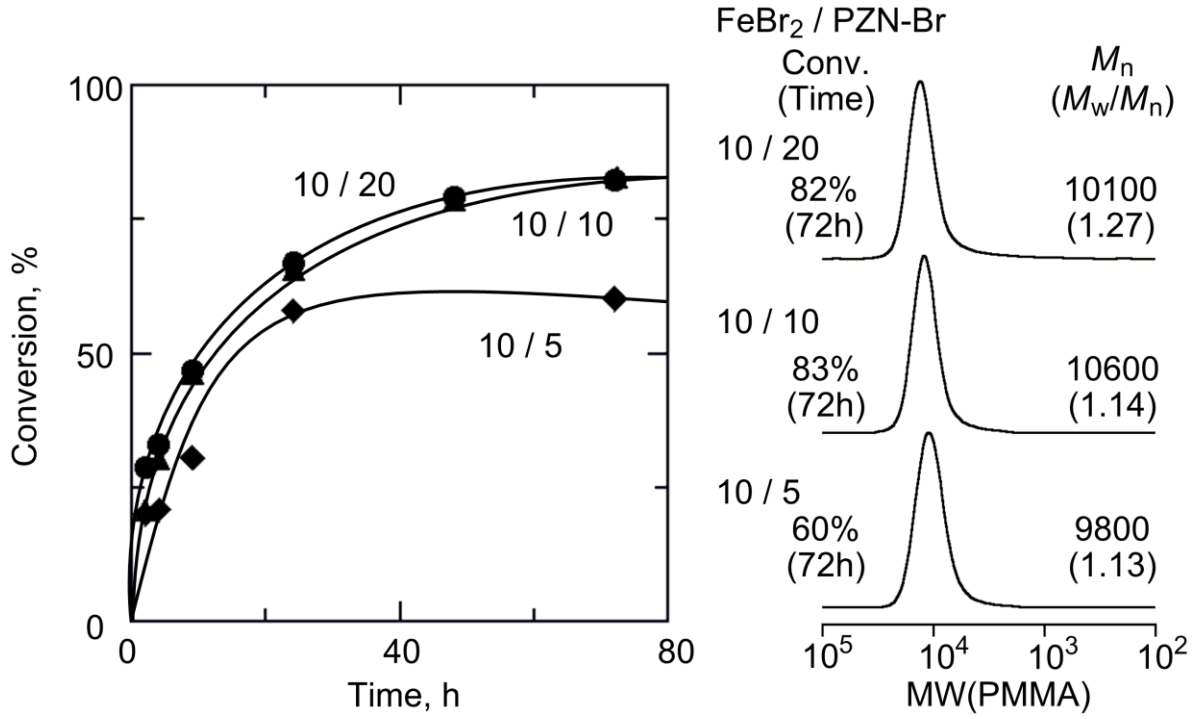

Figure 2. Effects of phosphazene/iron(II) bromide ratio on living radical polymerization of MMA with H-$(MMA)_2$-Br/$FeBr_2$/PZN-Br in THF at 60 °C: $[MMA]_0$ = 2000 mM; $[H\text{-}(MMA)_2\text{-}Br]_0$ = 20 mM; $[FeBr_2]_0$ = 10 mM; $[PZN\text{-}Br]_0$ = 5.0 (◆), 10 (▲), 20 (●) mM.

homogeneous system under every condition and the rate was dependent on the ratio: the less feed of phosphazene than $FeBr_2$ ($[FeBr_2]_0/[PZN\text{-}Br]_0$ = 10/5 mM) resulted in relatively slow polymerization and retardation at the latter stage, while the equimolar and twice feed induced smooth polymerization without such deactivation. Interestingly, the molecular weights were fairly controlled regardless of the conditions, although the molecular weight distributions became slightly broader with more feed of phosphazene (M_w/M_n > 1.25). These results would suggest that the equimolar ratio is suitable for control in this system and possibly $FeBr_2$ forms an ionic complex, $[FeBr_2X]^-$,[21] with equimolar phosphazene to catalyze the controlled polymerization.

Then, the author also investigated effects of polymerization temperature (Table 1). Increasing temperature from 60 °C to 80 °C resulted in worse control giving broader molecular weight distributions [M_w/M_n = 1.14 (60 °C) vs 1.55 (80 °C)], which would be caused by the low thermal stability of the catalyst or the oxidized form. Interestingly, even at 40 °C, the polymerization proceeded to give controlled PMMA, suggesting the catalyst generated from $FeBr_2$/PZN-Br is potentially active.

Table 1. Effects of Temperature on Living Radical Polymerization of MMA with H-(MMA)$_2$-Br/FeBr$_2$/PZN-Br[a]

Entry	Temp (°C)	Time (h)	Conv. (%)	M_n	M_w/M_n
1	80	72	73	6700	1.55
2	60	72	83	10600	1.14
3	40	72	81	7600	1.17

[a] $[MMA]_0$ = 2000 mM, $[H\text{-}(MMA)_2\text{-}Br]_0$ = 20 mM, $[FeBr_2]_0$ = 10 mM, $[PZN\text{-}Br]_0$ = 10 mM in THF.

2. Effects of Halogen: Initiator, Iron Halide, and Phosphazenium salt

In transition metal catalyzed living radical polymerization, the halogen in growing terminal is likely exchanged with that of catalyst during the repeating activation process, as already confirmed by ^{1}H-NMR analyses.[22,23] Different halogen-combination in initiator/catalyst gives rise to multiple growing terminals and catalysts because of the halogen exchange between them, which is sometimes caused by worse control due to the irregularity. Additionally, in this system, the phosphazenium salt also possesses a halogen, which might make the halogen-exchange further complicated. Thus, the author examined effects of the halogen-combination in the three components; initiator, iron halide, and phosphazene, on polymerization behaviors to clarify contribution of the phosphazene.

Table 2. Comparisons of Initiator, Iron halide and Phosphazene on Living Radical Polymerization of MMA[a]

Entry	Initiator	Iron halide	Phosphazene	Conv. (%)	M_n	M_w/M_n
1	H-(MMA)$_2$-Br	$FeBr_2$	PZN-I	84	14200	1.20
2	H-(MMA)$_2$-Br	$FeBr_2$	PZN-Br	83	10600	1.14
3	H-(MMA)$_2$-Br	$FeBr_2$	PZN-Cl	74	9300	1.38
4	H-(MMA)$_2$-Cl	$FeBr_2$	PZN-Br	92	12000	1.92
5	H-(MMA)$_2$-Br	$FeCl_2$	PZN-Br	77	12400	1.53
6	H-(MMA)$_2$-Cl	$FeCl_2$	PZN-Cl	83	14200	1.73

[a] $[MMA]_0$ = 2000 mM, $[Initiator]_0$ = 20 mM, $[Iron\ halide]_0$ = 10 mM, $[Phosphazene]_0$ = 10 mM in THF at 60 °C; Polymerization time = 72 h.

Table 2 shows polymerization-results obtained with various combinations. The polymerization rate was not so sensitive for the combination, while the M_w/M_n of the prepared polymer got broader as the halogen of phosphazene was changed from Br to Cl and I for H-$(MMA)_2$-Br/$FeBr_2$ system (Entry 1-3). Although each solution of the three phosphazene-halogen show colorless, the color of polymerization solution, presumably based on the in situ formed catalyst, was clearly dependent on the phosphazene-halogen: black (PZN-I), orange (PZN-Br) and yellow (PZN-Cl), which would support the formation of anionic catalyst $[FeBr_2X]^-$ from the mixture of phosphazene (PZN-X). Thus, the oxidized $[FeBr_3X]^-$, generated after activation of C-Br in the initiator, might sometimes return the X to growing radical, consequently giving different dormant species carrying halogen derived from the phosphazene.[20] The worse control would be caused by such irregularity. Additionally, Cl-based species seems to be less suitable for the iron catalyst (Entry 4-6), which is similar to our $FeX_2(PR_3)_2$-catalyzed systems.[17]

3. Comparison with Conventional Iron Catalyst: $FeBr_2(PPh_3)_2$

The author compared the catalytic performance of $FeBr_2$/PZN-Br with the conventional iron catalyst $[FeBr_2(PPh_3)_2]$ under the same condition. Although there was little difference in the polymerization rate, the controllability for molecular weight and its distribution was quite different (Figure 3). With the $FeBr_2(PPh_3)_2$, the molecular weight

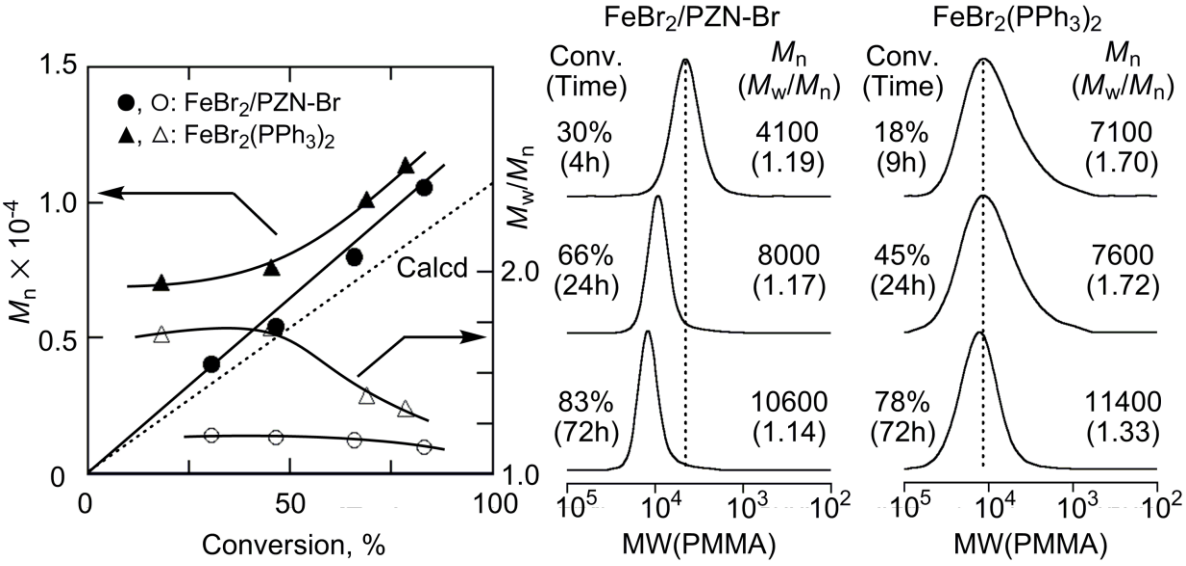

Figure 3. Comparison of $FeBr_2$/PZN-Br with $FeBr_2(PPh_3)_2$ on living radical polymerization of MMA in THF at 60 °C: $[MMA]_0$ = 2000 mM; $[H\text{-}(MMA)_2\text{-}Br]_0$ = 20 mM; $[Iron\ catalyst]_0$ = 10 mM. Iron catalyst: $FeBr_2$/PZN-Br (●, ○); $FeBr_2(PPh_3)_2$ (▲, △).

distributions (MWDs) were rather broad (M_w/M_n ~ 1.70) especially at the initial stage, and the number-average molecular weights (M_n) were larger than the theoretical values, assuming that one initiator molecule generates one polymer chain. In contrast, the $FeBr_2$/PZN-Br system gave well-controlled polymers where the M_n almost follows the theoretical line and the MWDs were narrow (M_w/M_n < 1.20) regardless of the monomer-conversion or polymerization-degree. These results show the better controllability of the $FeBr_2$/PZN-Br.

4. Comparison with $FeBr_2$/Conventional Onium Salts

The phosphazene derivatives are categorized in onium salts. Therefore, the author employed conventional onium salts such as ammonium and phosphonium derivatives in conjunction with $FeBr_2$ to examine the difference with phosphazenium salt. Figure 4 shows the time-conversion curves of the polymerization and the SEC curves of the obtained PMMAs for a series of onium salts under the same condition; tetrabutylammonium bromide (TBA-Br), tetrabutylphosphonium bromide (TBP-Br) and tetraphenylphosphonium bromide (TPP-Br), in addition to PZN-Br. As reported in a previous article,[20] the combination of iron halide with onium salt is likely effective as a catalyst for living radical polymerization to give controlled polymers. However, the activity with PZN-Br was apparently higher than with the others as seen in time-conversion curve.

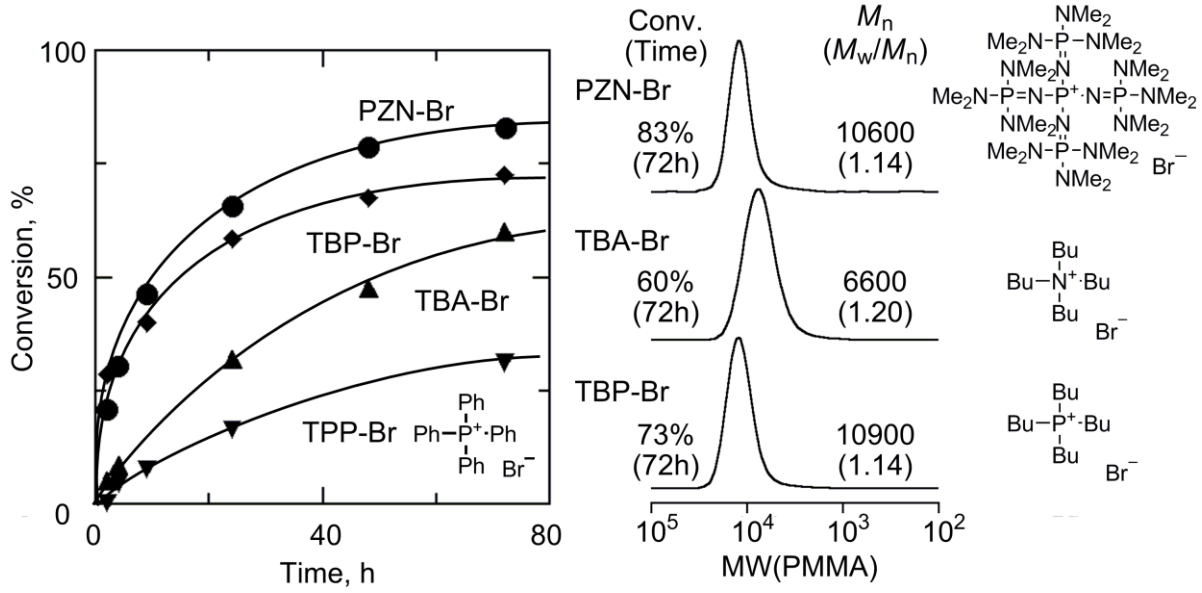

Figure 4. Comparison of onium salts for ligands of $FeBr_2$ on living radical polymerization of MMA in THF at 60 °C: $[MMA]_0$ = 2000 mM; $[H\text{-}(MMA)_2\text{-}Br]_0$ = 20 mM; $[FeBr_2]_0$ = 10 mM; $[Onium\ salt]_0$ = 10 mM. Onium salt: PZN-Br (●), TBA-Br (▲), TBP-Br (◆), TPP-Br (▼).

5. Cyclic Voltammetry of $FeBr_2$/PZN-Br

Observation of the redox behavior of catalysts has often supported the catalytic ability in living radical polymerization because it undergoes one-electron redox by reversibly activating carbon-halogen bond. Thus, we measured cyclic voltammetry (CV) for the $FeBr_2$/PZN-Br complex and compared the behavior with the comparable catalysts.

For the $FeBr_2$/PZN-Br complex, clear oxidation/reduction waves, which was likely to be assigned to one electron redox between Fe^{II} and Fe^{III}, were seen at E_{pa} = 0.30 V and E_{pc} = 0.16 V, respectively (solid line, Figure 5). In addition to these, there were ambiguous peaks at from 1.0 V to 1.4 V, which would be due to PZN-Br itself because they were quite similar to those observed with only PZN-Br. Importantly, the redox cycles were recurrent after several scans in the range of 0 to 1.4 V, indicating the trivalent species was not decomposed and can be reversibly converted into divalent one without assistance of an additive, in contrast to half-metallocene-type carbonyl iron complex [$FeCpI(CO)_2$] and ruthenium dichloride phosphine complex [$RuCl_2(PPh_3)_3$], requiring Ti(O*i*-Pr)$_4$ and Al(O*i*-Pr)$_3$ for such recurrent

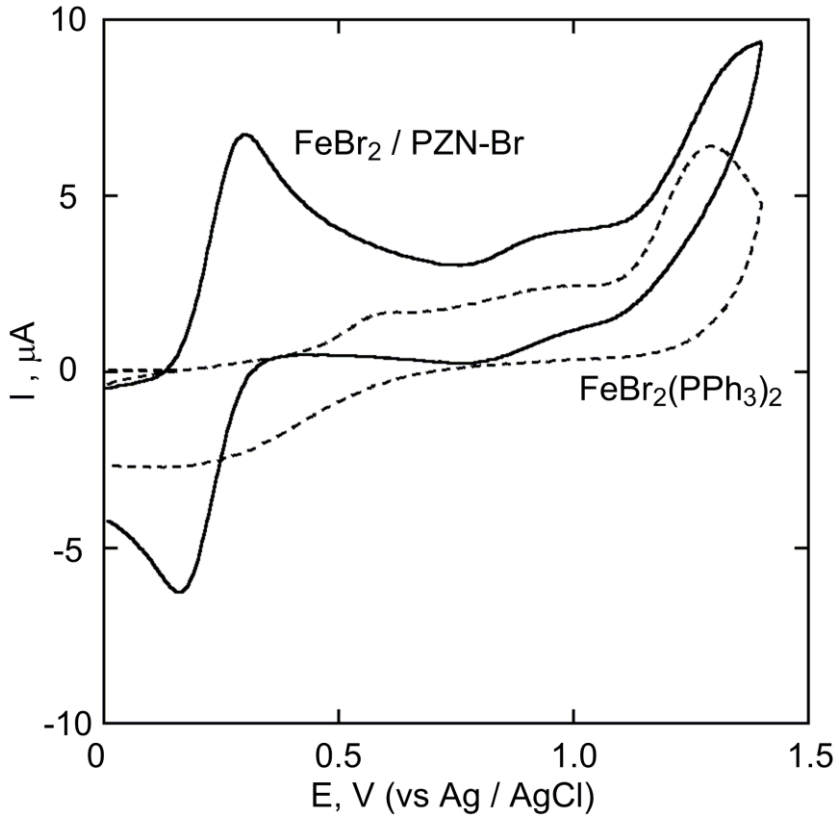

Figure 5. Cyclic voltammograms of iron catalysts in $ClCH_2CH_2Cl$ at 25 °C: [Iron Complex]$_0$ = 5.0 mM; [*n*-Bu_4NPF_6]$_0$ = 100 mM. Iron complex: $FeBr_2$/PZN-Br (solid line); $FeBr_2(PPh_3)_2$ (dashed line).

redox cycle as well as polymerization-control.[9,24] Interestingly, the redox potential of the $FeBr_2$/PZN-Br complex [$E_{1/2} = (E_{pa} + E_{pc})/2 = 0.23$ V] was lower than those of conventional active catalysts such as Cp*(η-C_5Me_5)-based half-metallocene iron[9] or ruthenium[25] catalysts. The dibromide phosphine catalyst [$FeBr_2(PPh_3)_2$] showed an unclear cycle (dashed line, Figure 5), and the behavior gradually changed as the measure was repeated, indicating the less stability under the redox process.

The previous researches have indicated the trend that an enhancement of the electron density of a central metal contributes to a decrease in a redox potential and an increase in the catalytic activity.[26,27] The mixture of $FeBr_2$ with PZN-Br would form an ionic catalyst $[FeBr_3]^-(PZN)^+$ and therefore the electron density of a central iron might be richer than the neutral iron catalyst $FeBr_2(PPh_3)_2$. Thus, the $FeBr_2$/PZN-Br complex would show better catalytic performances than the neutral form for the living radical polymerization. However, the superiority of the phosphazenium salt to the conventional onium salts was not clear: there was little difference of the redox behavior between them, coupled with $FeBr_2$. Such ionization by an onium salt certainly seems to be effective to promote the efficiency of the redox cycle.

6. High Controllability of $FeBr_2$/PZN-Br System: Monomer Addition and Synthesis of High Molecular Weight Polymer

To investigate the living nature for the $FeBr_2$/PZN-Br catalyzed system, the author added a fresh MMA to the polymerization solution when the MMA-conversion reached over 80%. In the second phase, MMA was smoothly consumed to give additional 84% conversion (totally 167%) (Figure 6). The SEC analysis of the obtained polymers showed the high controllability even after the addition, where the M_n increased in direct proportion with the conversion and the peak top was shifted to higher molecular weight keeping narrow MWD, although just a slight tailing was detected.

The high controllability of $FeBr_2$/PZN-Br system encouraged the author to synthesize higher molecular weight polymers with narrow MWDs. We varied the monomer/initiator ratio from 100 to 200, 400, 1000 targeting 20,000, 40,000, 100,000 (for 100% conversion) of M_n (Figure 7). Under every condition, the MWDs of the obtained PMMAs were kept narrow ($M_w/M_n < 1.20$) and the molecular weights agreed well with the theoretical values, calculated from the feed ratio and the conversion, even for nearly 100,000 of M_n. These results indicate that the $FeBr_2$/PZN-Br was highly active for living radical polymerization of

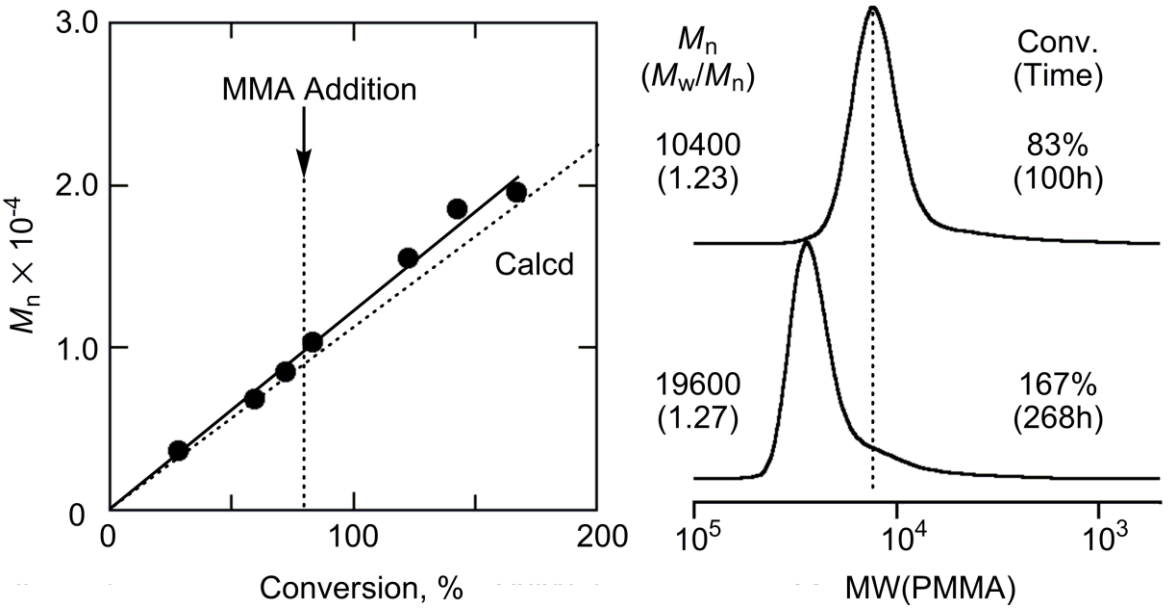

Figure 6. Monomer-addition experiments in the polymerization of MMA with H-$(MMA)_2$-Br/$FeBr_2$/PZN-Br in THF at 60 °C: $[MMA]_0$ = $[MMA]_{add}$ = 2000 mM; $[H\text{-}(MMA)_2\text{-}Br]_0$ = 20 mM; $[FeBr_2]_0$ = 10 mM; $[PZN\text{-}Br]_0$ =10 mM.

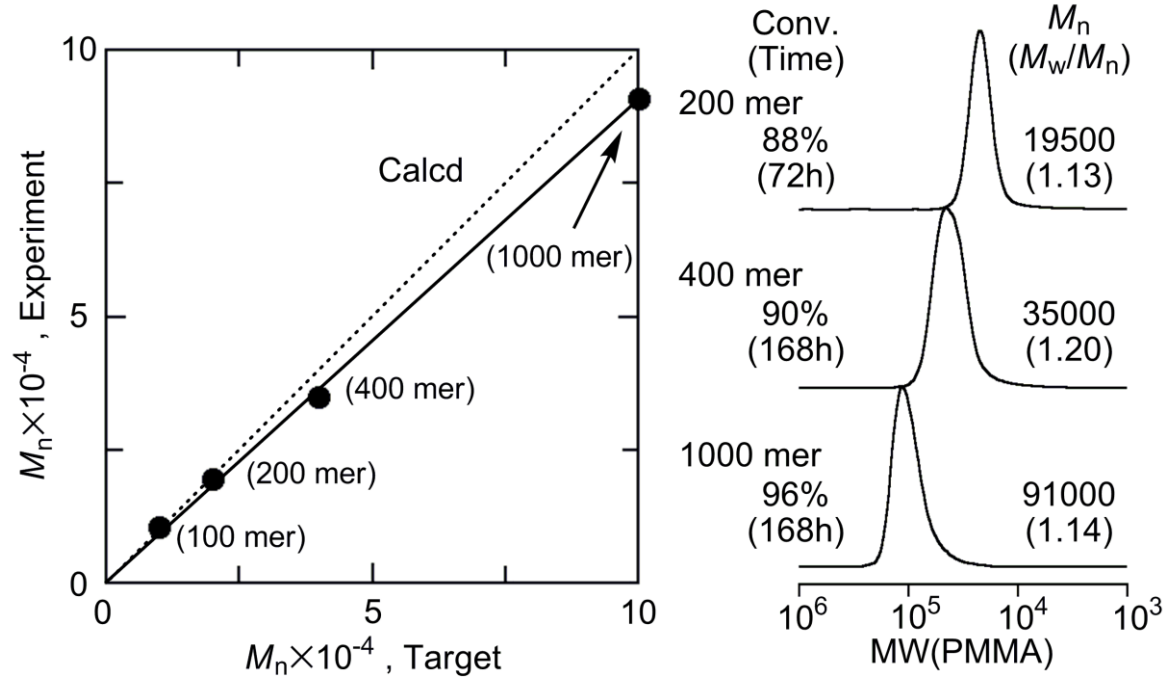

Figure 7. Synthesis of high molecular weight PMMA targeted 100 mer (A), 200 mer (B), 400 mer (C), 1000 mer (D) with H-$(MMA)_2$-Br/$FeBr_2$/PZN-Br in THF at 60 °C: (A) $[MMA]_0$ = 2000 mM; $[H\text{-}(MMA)_2\text{-}Br]_0$ = 20 mM; $[FeBr_2]_0$ = 10 mM; [PZN-Br] =10 mM, (B) $[MMA]_0$ = 4000 mM; $[H\text{-}(MMA)_2\text{-}Br]_0$ = 20 mM; $[FeBr_2]_0$ = 10 mM; $[PZN\text{-}Br]_0$ =10 mM, (C) $[MMA]_0$ = 4000 mM; $[H\text{-}(MMA)_2\text{-}Br]_0$ = 10 mM; $[FeBr_2]_0$ = 5.0 mM; $[PZN\text{-}Br]_0$ =5.0 mM, (D) $[MMA]_0$ = 5000 mM; $[H\text{-}(MMA)_2\text{-}Br]_0$ = 5.0 mM; $[FeBr_2]_0$ = 5.0 mM; $[PZN\text{-}Br]_0$ =5.0 mM.

MMA and effective for wide range of molecular weight control.

7. Polymerization of Functional Monomer

Most conventional iron-catalysts interact with functional groups (e.g., ethylene glycol, hydroxyl, amino, and carboxyl groups, etc.), and thus they unfavorably turn into "deactivation" to lose the catalysis for monomers bearing such functional groups, although such functional monomers are essential for preparation of advanced polymeric materials. Here, the author applied the ionic catalyst, generated from $FeBr_2$ and PZN-Br, to polymerization of one of functional methacrylates, PEGMA, carrying a poly(ethylene glycol) pendant group, coupled with H-$(MMA)_2$-Br as an initiator in toluene at 60 °C.

In sharp contrast to little activity of the conventional iron catalyst [$FeBr_2(PPh_3)_2$], as seen in the time-conversion curve in Figure 8, the $FeBr_2$/PZN-Br catalyst showed higher activity even for such functional monomer, where PEGMA was smoothly polymerized in high conversion (> 90%) for 40 h without retardation. The SEC curves of the obtained poly(PEGMA) was shifted to higher molecular weight with the monomer conversion and the molecular weight distributions were relatively narrow regardless of the conversion (M_w/M_n < 1.25). The bulky and conjugated structure of phosphazene ligand would contribute to the

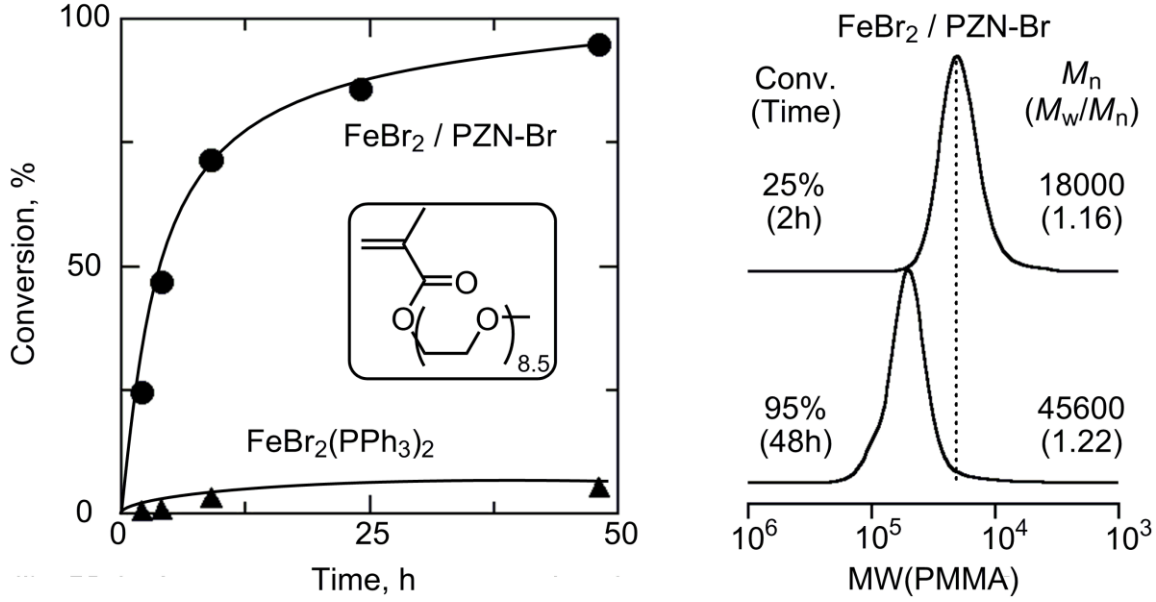

Figure 8. Comparison of $FeBr_2$/PZN-Br with $FeBr_2(PPh_3)_2$ on living radical polymerization of PEGMA in toluene at 60 °C: $[PEGMA]_0$ = 500 mM; $[H\text{-}(MMA)_2\text{-}Br]_0$ = 5.0 mM; $[Iron\ catalyst]_0$ = 5.0 mM. Iron catalyst: $FeBr_2$/PZN-Br (●); $FeBr_2(PPh_3)_2$ (▲).

protection of the iron center against polar functional groups. In Chapter 2, the tolerance to functional groups of phosphazene was discussed in detail.

8. Removal of Catalyst

Finally, the author examined the removability of the $FeBr_2$/PZN-Br catalyst from the products after the polymerization of MMA. The polymerization solution expressed rust-color derived from the catalyst, but only water washing, followed by dilution with toluene, made the solution colorless. The ICP-AES (Inductively Coupled Plasma-Atomic Emission Spectrometry) analysis of the obtained polymer after three-times washing showed that it contained less than 5 ppm iron, namely nearly perfect removability of the catalyst.

Conclusion

Phosphazenium bromide (PZN-Br) with $FeBr_2$ was effective as a catalyst for living radical polymerization of MMA. The catalytic performance was maximized with an equimolar mixture of the both, indicating they would form an equimolar anionic complex. The $FeBr_2$/PZN-Br catalyst possessed higher activity/controllability than a conventional iron-catalyst [$FeBr_2(PPh_3)_2$] or the combinations with other conventional onium-halogen salts, demonstrated by the successful chain-extension by monomer addition and fine control even for high molecular weight polymer (M_n ~ 90,000; M_w/M_n < 1.20). More importantly, the catalyst showed high activity even for living polymerization of PEGMA, one of the functional methacrylates, which is quite distinguished from previous iron catalysts. Despite of such tolerance to functional groups, the catalyst was almost quantitatively removed by just water-washing. Therefore, the catalyst would open the door to new development for actual application of iron-catalyzed living radical polymerization.

Experimental Section

Materials

MMA (TCI; purity >99%) was dried overnight over calcium chloride and purified by double distillation from calcium hydride before use. Poly(ethyleneglycol) methacrylate

[PEGMA; CH_2=$CMeCO_2(CH_2CH_2O)_nMe$; Me = CH_3; n = 8.5 on average] (Aldrich) was purified by passing through an inhibitor removal column (Aldrich) and was subsequently degassed by three-time vacuum-argon bubbling cycles before use. The MMA-dimeric initiators [H-$(MMA)_2$-X; X = Cl,[22] Br[23]] were prepared according to literature. Iron bromide (Aldrich; purity >98%), iron chloride (Kanto Kagaku >97%), tetrabutylammonium bromide (TCI, >98%), tetrabutylphosphonium bromide (TCI >99%), and tetraphenylphosphonium bromide (TCI >98%), were used as received and handled in a glove box (M. Braun Labmaster 130) under a moisture- and oxygen-free argon atmosphere (H_2O <1 ppm; O_2 <1 ppm). The phosphazenium salts were received form Mitsui Chemical, Inc.[28] and handled in a glove box. THF was passed through purification columns (Solvent Dispensing System) and bubbled with dry nitrogen for more than 15 min immediately before use. *n*-Octane (internal standard for gas chromatography) and 1,2,3,4-tetrahydronaphthalene (tetralin; internal standard for ^{1}H NMR) were dried over calcium chloride and distilled twice from calcium hydride.

Polymerization Procedures

Polymerization was carried out by the syringe technique under dry argon in baked glass tubes equipped with a three-way stopcock or in sealed glass vials. A typical procedure for MMA polymerization with H-$(MMA)_2$-Br/$FeBr_2$/PZN-Br was as follows. In a 50-mL round-bottom flask, $FeBr_2$ (9.7 mg, 0.045 mmol), PZN-Br (36.9 mg, 0.045 mmol) and THF (3.23 mL) were added under dry argon and stirred at 60 °C in 5 minutes. After cooling to room temperature, *n*-octane (0.12 mL), MMA (0.96 mL, 9 mmol), and H-$(MMA)_2$-Br (0.19 mL of 480 mM in toluene, 0.09 mmol) were added sequentially under dry argon. The total volume of reaction mixture was thus 4.5 mL. Immediately after mixing, aliquots (0.60 mL each) of the solution were injected into glass tubes which were then sealed (except when a stopcock was used) and placed in an oil bath kept at desired temperature. In predetermined intervals, the polymerization was terminated by cooling the reaction mixtures to -78 ºC. Monomer conversion was determined from the concentration of residual monomer measured by gas chromatography with *n*-octane as an internal standard. The quenched reaction solutions were diluted with toluene (ca. 20 mL), washed with water three times, and evaporated to dryness to give the products that were subsequently dried overnight under vacuum at room temperature.

For PEGMA, the same procedures as described above were applied except that monomer conversion was determined by ^{1}H NMR from the integrated peak area of the

olefinic protons of the monomers with tetralin as internal standard. The products were similarly isolated but without washing with water because of their hydrophilicity

Measurements

The molecular weight distribution, M_n, and M_w/M_n values of polymers measured in chloroform at 40 ºC on three polystyrene gel columns [Shodex K-805L (pore size: 20-1000Å; 8.0 mm i.d.×30 cm) ×3; flow rate 1.0 mL/min] connected to a Jasco PU-980 precision pump and a Jasco 930-RI refractive-index detector, and 970-UV ultraviolet detector. The columns were calibrated against 13 standard PMMA samples (Polymer Laboratories; M_n = 630-1,200,000; M_w/M_n = 1.06-1.22) as well as the monomer. For poly(PEGMA), DMF containing 10 mM LiBr was applied as an eluent. ^{1}H-NMR spectra of the obtained polymers were recorded in $CDCl_3$ at 25 °C on a JEOL JNM-LA500 spectrometer operating at 500.16 MHz. Polymers for ^{1}H-NMR analysis were fractionated by preparative SEC (column: Shodex K-2002).

Cyclic voltammograms were recorded by using a Hokuto Denko HZ-3000 apparatus. The sample-preparation for $FeBr_2$/PZN-Br catalyst is described. $FeBr_2$ (8.6 mg, 0.040 mmol), PZN-Br (32.8 mg, 0.040 mmol) and THF (8 mL) were added sequentially in a baked glass tube equipped with a three-way stopcock under argon and stirred at 60 °C for 3 h. After heating, solvent was evaporated and a solution of *n*-Bu_4NPF_6 (supporting electrolyte) in CH_2ClCH_2Cl solution (100 mM, 8 mL) was added into the tube under argon. Measurements were carried out at 0.1 Vs^{-1} under argon. A three-electrode cell was used which was equipped with a platinum disk as a working electrode, a platinum wire as a counter electrode, and an Ag/AgCl electrode as a reference.

References and Notes

(1) Bolm, C.; Legros, J.; Paih, J. L.; Zani, L. *Chem. Rev.* **2004**, *104*, 6217-6254.

(2) (a) Kato, M.; Kamigaito, M.; Sawamoto, M.; Higashimura, T. *Macromolecules* **1995**, *28*, 1721-1723. (b) Ando, T.; Kato, M.; Kamigaito, M.; Sawamoto, M. *Macromolecules* **1996**, *29*, 1070-1072.

(3) For recent reviews on transition metal catalyzed living radical polymerization, see: (a) Kamigaito, M.; Ando, T.; Sawamoto, M. *Chem. Rev.* **2001**, *101*, 3689-3745. (b) Kamigaito, M.; Ando, T.; Sawamoto, M. *Chem. Rec.* **2004**, *4*, 159-175. (c) Ouchi, M.;

Terashima, T.; Sawamoto, M. *Acc. Chem. Res.* **2008**, *41*, 1120-1132. (d) Matyjaszewski, K.; Xja, J. *Chem. Rev.* **2001**, *101*, 2921-2990. (e) Matyjaszewski K., Ed.; *Controlled/Living Radical Polymerization From Synthesis to Materials*; ACS Symposium Series 944; American Chemical Society: Washington, DC, 2006.

(4) Wang, J. S.; Matyjaszewski, K. *J. Am. Chem. Soc.* **1995**, *117*, 5614-5615.

(5) Granel, C.; Dubois, P.; Jerome, R.; Teyssie, P. *Macromolecules* **1996**, *29*, 8576-8582.

(6) Ando, T.; Kamigaito, M.; Sawamoto, M. *Macromolecules* **1997**, *30*, 4507-4510.

(7) Matyjaszewski, K.; Wei, M.; Xia, J.; McDermott, N. E. *Macromolecules* **1997**, *30*, 8161-8164.

(8) Kotani, Y.; Kamigaito, M.; Sawamoto, M. *Macromolecules* **1999**, *32*, 6877-6880.

(9) Kotani, Y.; Kamigaito, M.; Sawamoto, M. *Macromolecules* **2000**, *33*, 3543-3549.

(10) Zhu, S.; Yan, D. *Macromolecules* **2000**, *33*, 8233-8238.

(11) Louie, Y.; Grubbs, R. H. *Chem. Commun.* **2000**, 1479-1480.

(12) Gibson, V. C.; O'Reilly, R. K.; Reed, W.; Wass, D. F.; White, A. J. P.; Williams, D. J. *Chem. Commun.* **2002**, 1850-1851.

(13) Göbelt, B.; Matyjaszewski, K. *Macromol. Chem. Phys.* **2000**, *201*, 1619-1624.

(14) O'Reilly, R. K.; Gibson, V. C.; White, A. J. P.; Williams, D. J. *J. Am. Chem. Soc.* **2003**, *125*, 8450-8451.

(15) Xue, Z.; Lee, B. W.; Noh, S. K.; Lyoo, W. S. *Polymer* **2007**, *48*, 4704-4714.

(16) Niibayashi, S.; Hayakawa, H.; Jin, R-H.; Nagashima, H. *Chem. Commun.* **2007**, 1855-1857.

(17) Uchiike, C.; Terashima, T.; Ouchi, M.; Ando, T.; Kamigaito, M.; Sawamoto, M. *Macromolecules* **2007**, *40*, 8658-8662.

(18) Ferro, R.; Milione, S.; Bertolasi, V.; Capacchione, C.; Grassi, A. *Macromolecules* **2007***, 40,* 8544-8546.

(19) Furuyama, R.; Fujita, T.; Funaki, S. F.; Nobori, T.; Nagata, T.; Fujiwara, K. *Catalysis Surveys from Asia* **2004**, *8*, 61-71.

(20) Teodorescu, M.; Gaynor, S. G.; Matyjaszewski, K. *Macromolecules* **2000**, *33*, 2335-2339.

(21) Iron dichloride ($FeCl_2$) is known to form a dinuclear anionic compound $(Fe_2Cl_6)^{2-}$ with 1 equivalence of onium chloride salt: Sun, J. S.; Zhao, H.; Ouyang, X.; Clérac, R.; Smith, J. A.; Clemente-Juan, J. M.; Gómez-Garcia, C.; Coronado, E.; Dunbar, K. R. *Inorg. Chem.* **1999**, *38*, 5841-5855. Based on this paper, the author supposes that the

equimolar mixture of $FeBr_2$ and phosphazenium salt (PZN-X) also generates similar anionic complex. However, the author has never examined the detailed structure or whether it exists with monomeric or dimeric form. Thus, the author just describes the forming complex as $[FeBr_2X]^-$ in this paper.

(22) Ando, T.; Kamigaito, M.; Sawamoto, M. *Macromolecules* **2000**, *33*, 2819-2824.

(23) Ando, T.; Kamigaito, M.; Sawamoto, M. *Tetrahedron* **1997**, *53*, 15445-15457.

(24) Ando, T.; Kamigaito, M.; Sawamoto, M. *Macromolecules* **2000**, *33*, 6732-6737.

(25) Ando, T.; Kamigaito, M.; Sawamoto, M. *Macromolecules* **2000**, *33*, 5825-5829.

(26) Takahashi, H.; Ando, T.; Kamigaito, M.; Sawamoto, M. *Macromolecules* **1999**, *32*, 3820-3823.

(27) Kamigaito, M.; Watanabe, Y.; Ando, T.; Sawamoto, M. *J. Am. Chem. Soc.* **2002**, *124*, 9994-9995.

(28) Nobori, T.; Kouno, M.; Suzuki, T.; Mizutani, K.; Kiyono, S.; Sonobe, Y.; Takaki, U. Phosphazenium salt and preparation process thereof, and process for producing poly(alkylene oxide), U.S. 5,990,352 (1999).

Chapter 2

Versatility and Tolerance to Monomer Functionalities: Functional Methacrylates and Methyl Acrylate

Abstract

The combination of phosphazenium halides (PZN-X; X = Cl, Br, I), with iron bromide ($FeBr_2$) turned to be active catalysts for living radical polymerization of various monomers including functional ones. For example, the equimolar combination of $FeBr_2$ and PZN-Br efficiently catalyzed living radical polymerization of a functional methacrylate carrying poly(ethylene glycol) pendent group (PEGMA) to give narrow molecular weight distributions (MWDs; M_w/M_n ~ 1.2). This catalysis was distinguished from not only a conventional iron catalyst [$FeBr_2(PPh_3)_2$] but also combinations of simple onium salts (i.e., ammonium and phosphonium) with $FeBr_2$, where the polymerizations were retarded or likely due to deactivation of the catalysts by ethylene glycol moiety. The system also allowed quantitative block copolymerizations of methyl methacrylate (MMA) and PEGMA regardless of the addition order. Also, such combinations were found to give controlled polymers for random compolymerizations of *N*,*N'*-dimethylaminoethyl methacrylate (DMAEMA) with MMA and a homopolymerization of methyl acrylate (MA).

Introduction

Precise structural control of functional polymers would lead to advanced materials with renewed functionalities. Living radical polymerization is one of the essential methods to produce such well-defined functional polymers, because it essentially allows direct polymerizations of functional monomers without the protection of their pendent groups due to the neutral species, distinguished from ionic polymerizations.

"Transition metal-catalyzed living radical polymerization" is one of systems for living radical polymerization.[1] In this polymerization, a transition-metal catalyst (Mt^n n = valence number) activates an initiator (R-X) bearing a carbon-halogen bond for homolysis cleavage, where the metal center itself is one-electron oxidized (from Mt^n to Mt^{n+1}), as shown in Scheme 1. The radical species (R・) thus generated initiates radical propagation with some monomers to grow into a polymer chain, and afterwards the oxidized catalyst returns the halogen to the growing radical to regenerate a terminal carbon-halogen (dormant species), while it is one-electron reduced to return to the original lower-valence state complex (from Mt^{n+1} to Mt^n). Among the components, the catalyst is most essential to control the system, and so far ruthenium (Ru)[2] and copper (Cu)[3] complexes has been centrally developed as the catalyst toward higher catalytic activity and better control for a variety of monomers.

On the other hand, the practical utilities have been also required for the catalysts along with the catalytic functions. In this regard, iron complexes should be potential candidates because the metal, i.e., "Fe" is environmentally benign, safe, less toxic, biocompatible, and abundant.[4] Since the first successful report with $FeCl_2(PPh_3)_2$,[5] Fe(II) complexes

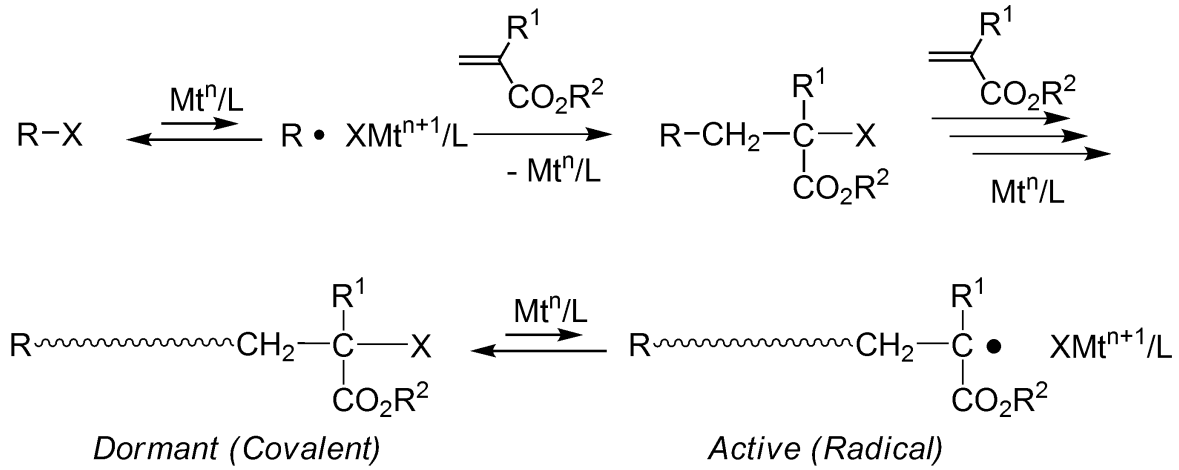

Scheme 1. Transition Metal-Catalyzed Living Radical Polymerization

coordinated with various ligands in living radical polymerization has been developed.[6-17] However, these iron complexes were inferior to the ruthenium- and copper-based vanguards in terms of activity for functional monomers because of the unfavorable interaction with their polar pendant groups resulting in deactivation of their catalysts.

In Chapter 1, the author presented that the combination of phosphazenium halides (PZN-X; X = Cl. Br, I) with iron bromide ($FeBr_2$) was active catalysts for living radical polymerization of methyl methacrylate (MMA) (Figure 1). The catalytic activity was higher than a conventional iron catalyst [$FeBr_2(PPh_3)_2$] and similar combination with onium salts [e.g. tetrabutylammonium bromide (TBA-Br) and tetrabutylphosphonium bromide (TBP-Br)]. Phosphazenium salts were effective anion-resources for iron halide and enhanced electric density of iron, and their unique catalytic activities were induced by the bulkiness (ca. 12Å in diameter), the conjugated structure for delocalization of electron, and the remotely separated anion from the central cation due to the dendritic structure.[18] Such unique structure encouraged the author to examine other monomers especially for functional ones, since the deactivation might be prevented.

In this chapter, the author employed the phosphazenium system for other monomers except MMA: a methacrylate carrying poly(ethylene glycol) pendent group (PEGMA), *N*,*N'*-dimethylaminoethyl methacrylate (DMAEMA), and methyl acrylate (MA). A combination of $FeBr_2$/PZN-Br induced living radical polymerization of PEGMA to give high conversion (> 90%) and narrow molecular weight distributions (MWDs), distinguished from comparative counterparts, and the tolerance of PEG side chain was demonstrated with cyclicvoltammetry (CV) analyses. Furthermore, the system allowed control for block copolymerization of MMA and PEGMA, random copolymerization of MMA and DMAEMA, and homopolymerization of MA.

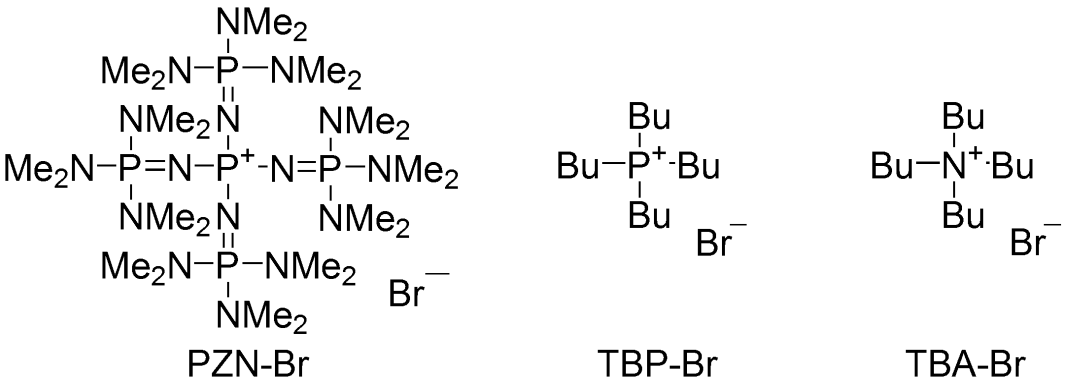

Figure 1. Onium salts for $FeBr_2$

Results and Discussion

1. Polymerization of PEGMA

At first, an equimolar combination of $FeBr_2$ with phosphazenium bromide (PZN-Br) was employed for polymerization of PEGMA in conjunction with bromide initiator [H-$(MMA)_2$-Br] in toluene at 60 °C ($[PEGMA]_0/[H\text{-}(MMA)_2\text{-}Br]_0/[FeBr_2]_0/[PZN\text{-}Br]_0$ = 500/5/5/5 mM). While the conventional iron catalyst [$FeBr_2(PPh_3)_2$] exhibited little catalytic activity, the phosphazenium system induced a smooth polymerization where the monomer-conversion reached over 90% within 48 h without retardation (Figure 2).

The molecular weights of the obtained poly(PEGMA)s linearly increased as the conversion and the SEC curves shifted to higher molecular weight keeping the narrow molecular weight distributions (M_w/M_n < 1.3), indicating a high degree of control over the polymerization (Figure 3). Note that the discussion on the controllability for molecular weight is less essential because the molecular weights were measured under the calibration with standard PMMAs.

The phosphazenium salt was compared with other onium salts such as tetrabutylammonium bromide (TBA-Br) and tetrabutylphosphonium bromide (TBP-Br) in the

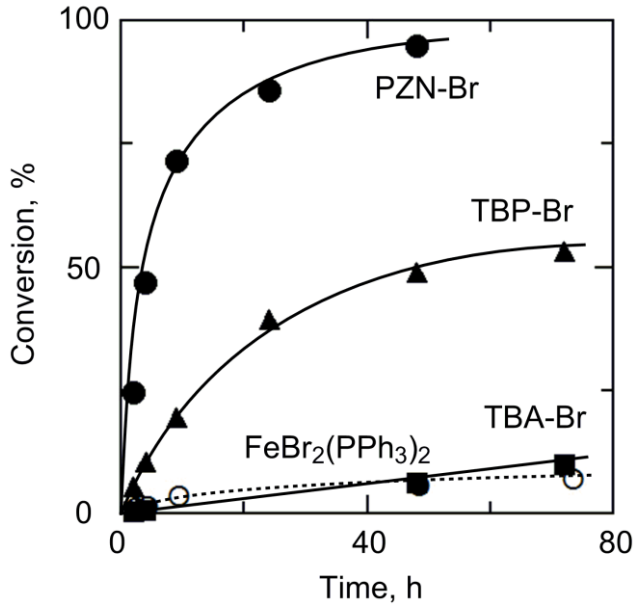

Figure 2. Polymerization of PEGMA with $FeBr_2$/onium salt with H-$(MMA)_2$-Br in toluene at 60 °C: $[PEGMA]_0$ = 500 mM; $[H\text{-}(MMA)_2\text{-}Br]_0$ = 5.0 mM; $[FeBr_2]_0$ = 5.0 mM; $[Onium\ salt]_0$ = 5.0 mM. Onium salt: PZN-Br (●); TBP-Br (▲); TBA-Br (■). Iron catalyst: $FeBr_2(PPh_3)_2$ (5.0 mM) (○).

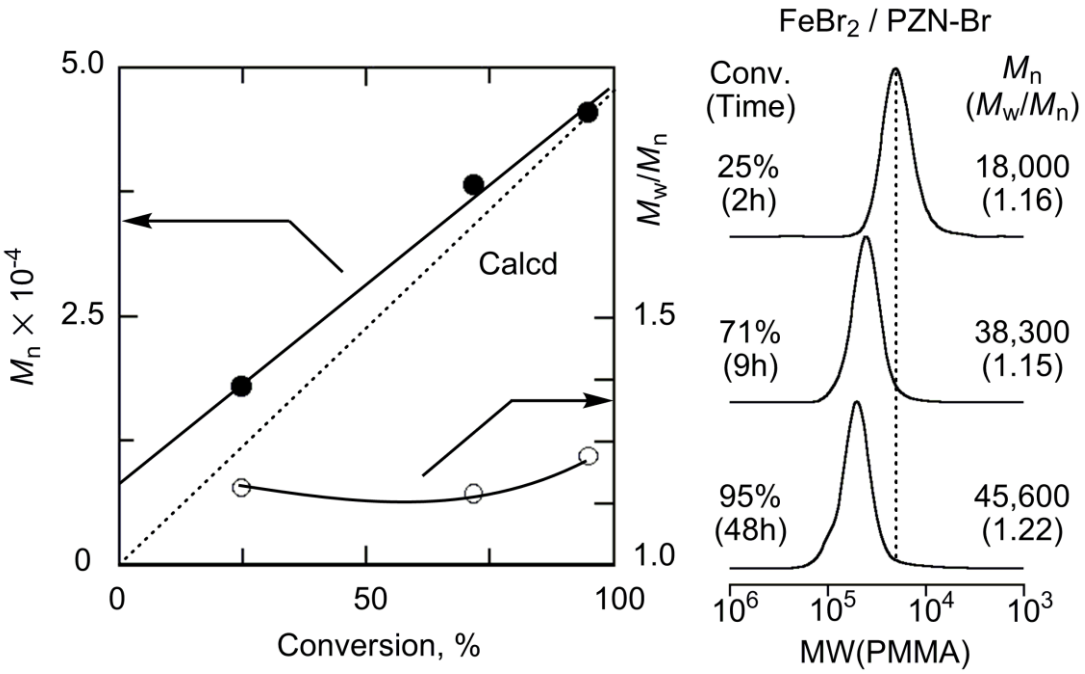

Figure 3. Polymerization of PEGMA with H-$(MMA)_2$-Br/$FeBr_2$/PZN-Br in toluene at 60 °C: $[PEGMA]_0$ = 500 mM; $[H\text{-}(MMA)_2\text{-}Br]_0$ = 5.0 mM; $[FeBr_2]_0$ = 5.0 mM; $[PZN\text{-}Br]_0$ = 5.0 mM.

polymerization of PEGMA, coupled with equimolar $FeBr_2$. A combination with TBA-Br showed little catalytic activity for PEGMA, although it catalyzed MMA polymerization at moderate rate (60%, 72 h).[18] With TBP-Br, the conversion reached ~50%, however the polymerization was gradually retarded. These results suggested that the high catalytic activity for PEGMA was specific to with the phosphazenium salt and the bulky and conjugated structure would be contribute to protect the iron center from an unfavorable interaction with the polar PEG side group.

2. CV analysis: Tolerance to PEG group

The catalysis in metal-catalyzed living radical polymerization is based on the redox behavior ($Mt^n \leftrightarrow Mt^{n+1}$) of the catalyst, and then observation of the redox potential often supports the catalytic activity. Thus, the author measured cyclic voltammetry (CV) for the $FeBr_2$/PZN-Br after heating with PEGMA to see the tolerance of the PEG moiety for the complex. The sample was prepared in $ClCH_2CH_2Cl$ solution with *n*-Bu_4NPF_6 as a supporting electrolyte, followed by heating the toluene solution ($[FeBr_2]_0/[PZN\text{-}Br]_0/[PEGMA]_0$ = 5/5/5 mM) at 60 °C for 3 h and evaporation of the toluene.

As presented in Chapter 1, the $FeBr_2$/PZN-Br complex showed a clear oxidation/reduction wave, derived from one electron redox between Fe^{II} and Fe^{III} at E_{pa} = 0.30

V and E_{pc} = 0.16 V (Figure 4A, dashed line). The other peaks at higher voltage are likely due to the redox of PZN-Br itself. Even after the heating with PEGMA, it showed a similar redox wave (Figure 4A, solid line), and the redox cycle was recurrent after several scan. The result supports that not only the Fe(II) complex but also the Fe(III) species are tolerance of the functional monomer. On the other hand, the redox waves of conventional iron catalyst [$FeBr_2(PPh_3)_2$] were clearly changed via the heating with PEGMA (Figure 4B). Thus, the superior catalysis of the $FeBr_2$/PZN-Br complex for PEGMA was supported even with the CV analyses.

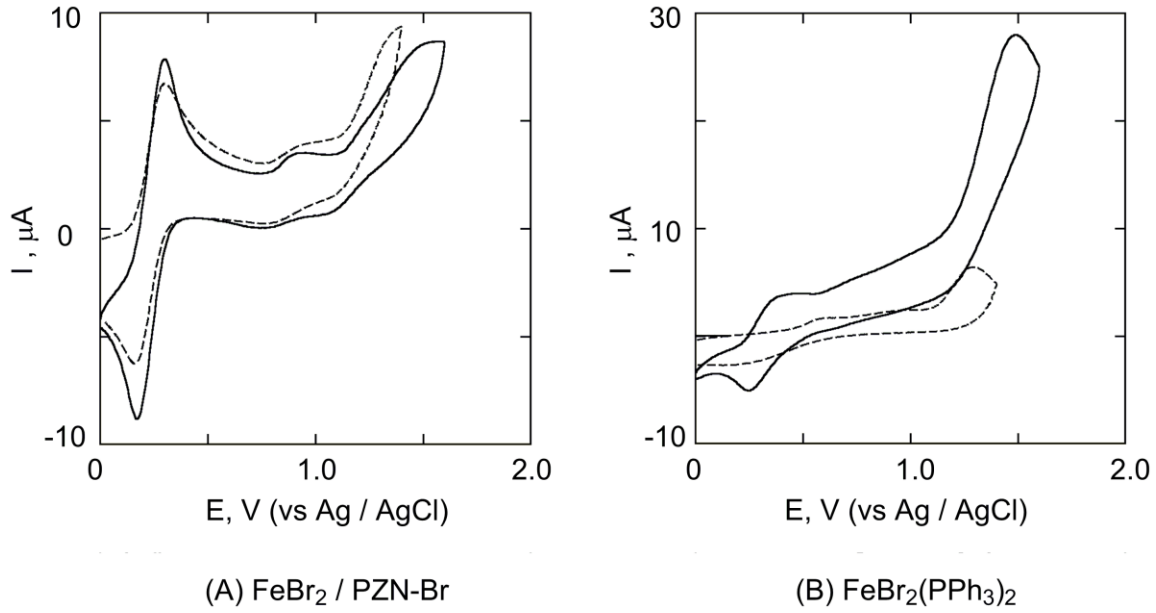

Figure 4. Cyclic voltammograms of iron catalyst/PEGMA (5.0/5.0 mM) in $ClCH_2CH_2Cl$ at 25 °C: $[n\text{-}Bu_4NPF_6]_0$ = 100 mM (supporting electrolyte). Aging in toluene at 60 °C for 3 h before measurement (solid line); fresh catalyst without PEGMA and aging (dashed line). Iron catalyst: $FeBr_2$/PZN-Br (A); $FeBr_2(PPh_3)_2$ (B).

3. Block Copolymerization of MMA and PEGMA

Given the catalytic activity of $FeBr_2$/PZN-Br for both MMA and PEGMA, the author performed a block copolymerization of MMA and PEGMA via sequential monomer-addition. MMA (100 eq to initiator) was first polymerized with the complex and the initiator in THF at 60 °C. When the conversion reached 85% in 100 h, PEGMA (50 eq) was added into the reaction mixture along with fresh $FeBr_2$/PZN-Br (Figure 5). The added PEGMA was smoothly consumed and the conversion reached 85% within 168 h (total 268 h). SEC curves shifted to high molecular weights keeping narrow distributions (M_w/M_n = 1.30), although small shoulders were seen on both sides of the main peak, probably caused by unavoidable

side-reactions.

Figure 6 shows ^{1}H NMR spectra of PMMA prepolymer (Figure 6A) and PMMA-*b*-PPEGMA block copolymer (Figure 6B), obtained in the block copolymerization. For the former, in addition to the characteristic peaks of a PMMA main chain (*a*-*c*), a small peak of methoxy protons in the terminal MMA unit adjacent to the ω-end C-Br bond was observed at 3.7 ppm [*c*(ω), Figure 6A]. For the latter, the small peak was disappeared, and then new peaks of the PEGMA repeat unit (*d*-*h*) were observed. These results suggested that the PEGMA was almost quantitatively polymerized from PMMA terminal to give the block copolymer.

Furthermore, the author synthesized the block copolymer with the reverse order (PEGMA → MMA). Thus, PEGMA (50 eq to the initiator) was first polymerized with the $FeBr_2$/PZN-Br complex in THF at 60 °C, and then MMA was sequentially added when the PEGMA conversion exceeded 90% (Figure 7). The added MMA was smoothly consumed and the conversion finally reached 88% in 72 h (total 102 h). The SEC curves shifted to high molecular weights keeping the narrow distributions (M_w/M_n = 1.16). Thus, the $FeBr_2$/PZN-Br complex was found to exhibit a high catalytic activity for living radical polymerization of PEGMA.

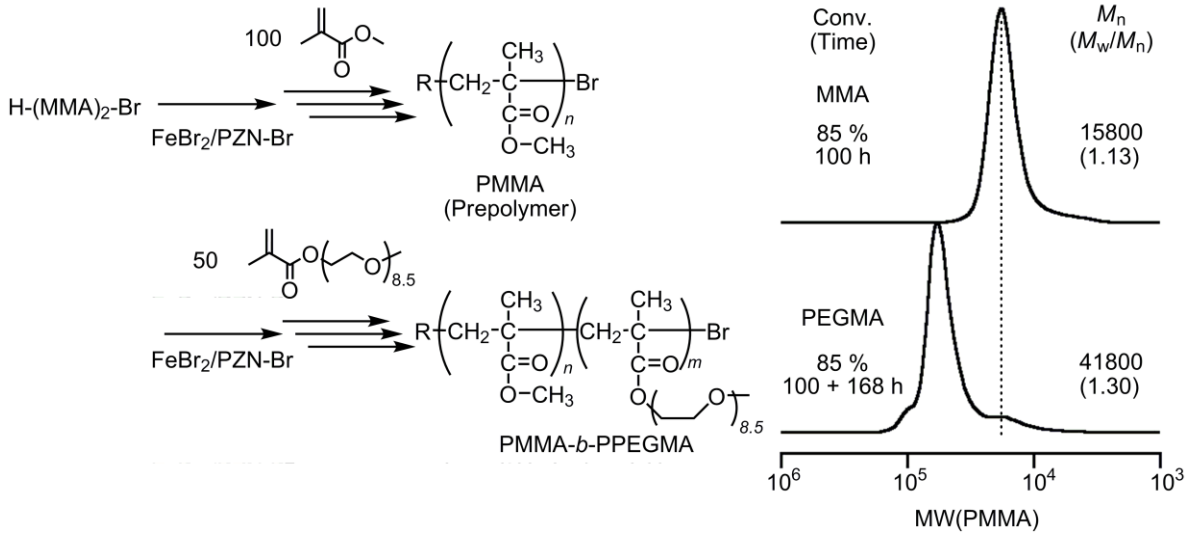

Figure 5. SEC curves of PMMA and PMMA-*b*-PPEGMA obtained with H-$(MMA)_2$-Br/$FeBr_2$/PZN-Br in THF at 60 °C: $[MMA]_0$= 2000 mM; $[H\text{-}(MMA)_2\text{-}Br]_0$ = 20 mM; $[FeBr_2]_0$ = 10 mM; $[PZN\text{-}Br]_0$ =10 mM; $[PEGMA]_{add}$ = 1000 mM; $[FeBr_2]_{add}$ = 10 mM; $[PZN\text{-}Br]_{add}$ = 10 mM.

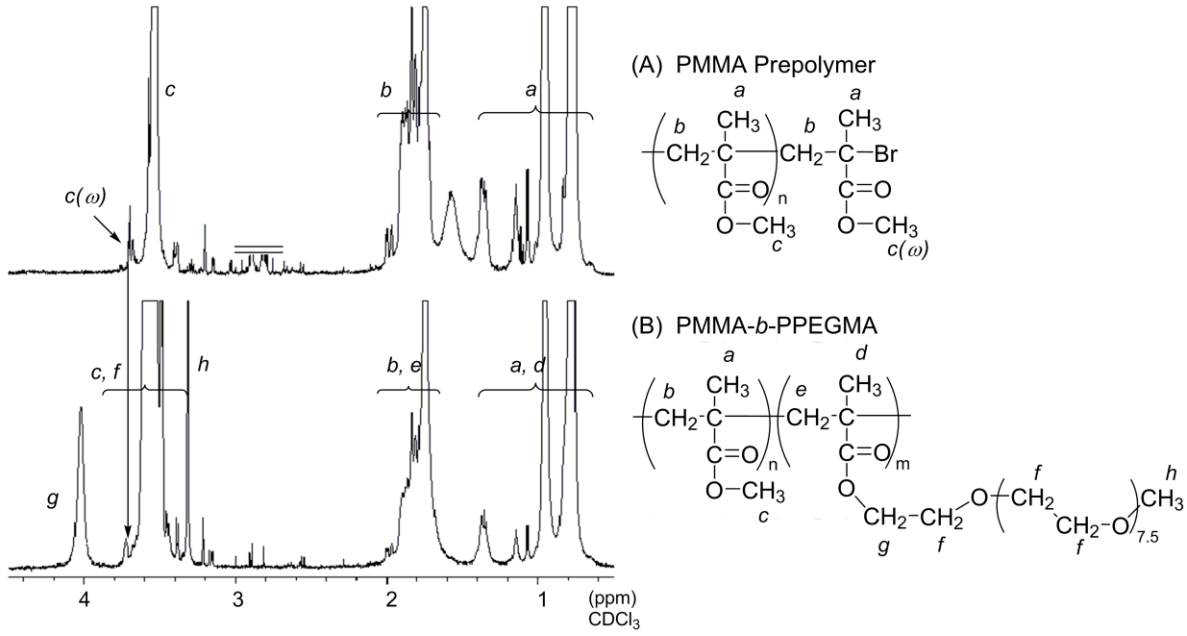

Figure 6. ^{1}H NMR analysis of PMMA and PMMA-*b*-PPEGMA obtained with H-$(MMA)_2$-Br/$FeBr_2$/PZN-Br in THF at 60 °C: $[MMA]_0$= 2000 mM; $[H\text{-}(MMA)_2\text{-}Br]_0$ = 20 mM; $[FeBr_2]_0$ = 10 mM; $[PZN\text{-}Br]_0$ =10 mM; $[PEGMA]_{add}$ = 1000 mM; $[FeBr_2]_{add}$ = 10 mM; $[PZN\text{-}Br]_{add}$ = 10 mM.

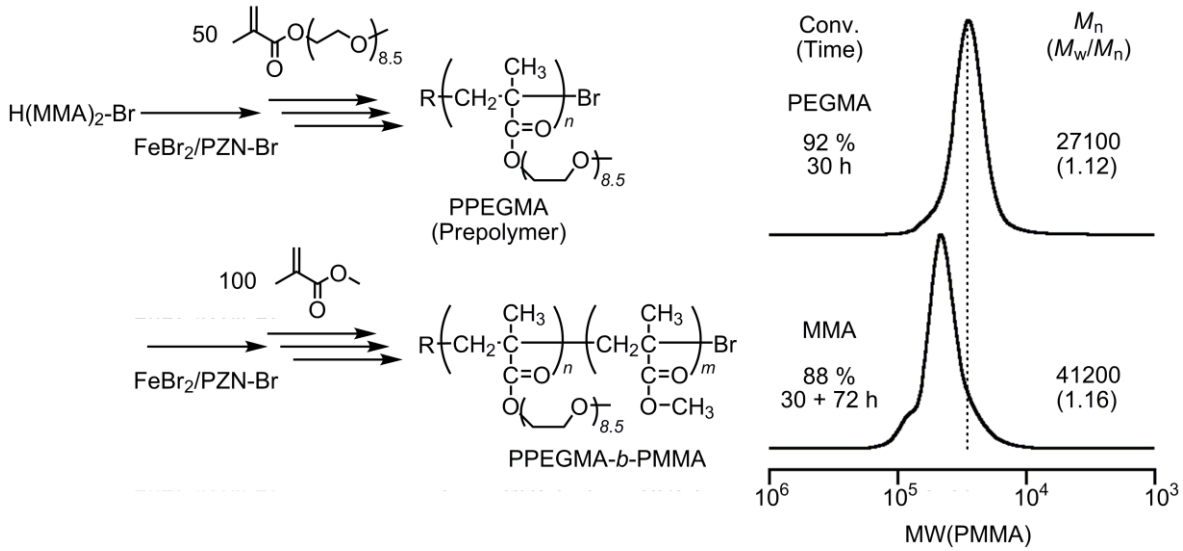

Figure 7. SEC curves of PPEGMA and PPEGMA-*b*-PMMA obtained with H-$(MMA)_2$-Br/$FeBr_2$/PZN-Br in THF at 60 °C: $[PEGMA]_0$= 1000 mM; $[H\text{-}(MMA)_2\text{-}Br]_0$ = 20 mM; $[FeBr_2]_0$ = 10 mM; $[PZN\text{-}Br]_0$ =10 mM; $[MMA]_{add}$ = 2000 mM; $[FeBr_2]_{add}$ = 5.0 mM; $[PZN\text{-}Br]_{add}$ =5.0 mM.

4. (Co)Polymerization of DMAEMA

N,*N*'-Dimethylaminoethyl methacrylate (DMAEMA) is the one of the common functional monomers, however, iron-catalyzed living radical polymerization systems for DMAEMA have never reported, because the pendant amino group likely interacts with the iron to reduce or lose the activity. The high activity of the $FeBr_2$/PZN-Br complex for PEGMA encouraged the author to employ it for polymerization of DMAEMA.

Homopolymerization of DMAEMA was attempted with the $FeBr_2$/PZN-Br complex, in conjunction with H-$(MMA)_2$-Br as an initiator in toluene at 60 °C. The monomer was smoothly and quantitatively polymerized (95%, 48 h), however the polymerization was less controlled to give broad MWDs (Table 1, Entry 1). The amino group would alter the catalytic functions via some interaction. Thus, copolymerizations of DMAEMA and MMA were examined with the fixed total monomer concentration, 2000 mM (Table 1, Entry 2-4). With less or same amount of DMAEMA, they both were consumed at the same rate and the obtained polymers were fairly controlled with reasonable M_ns and narrow MWDs. The controllability, judged from the MWD narrowness, was higher than that with the conventional catalyst [$FeBr_2(PPh_3)_2$] (Table 1, Entry 5-7). Figure 8 shows one example indicating the difference of catalysis between the two catalysts for the copolymerization ($[MMA]_0/[DMAEMA]_0$ = 1600/400 mM). As seen in the time-conversion curves and the

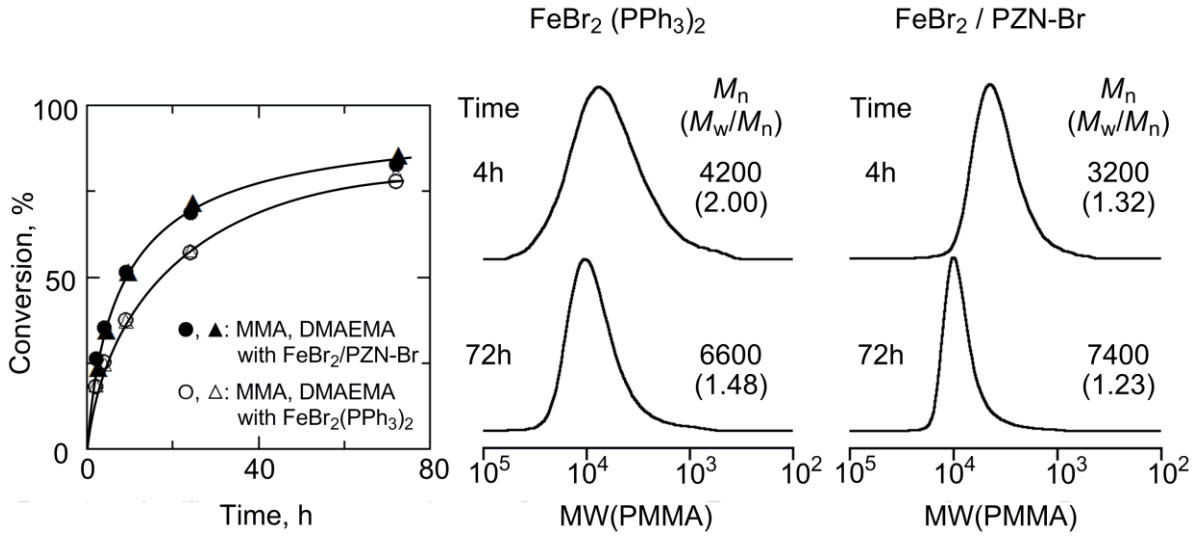

Figure 8. Comparison of $FeBr_2$/PZN-Br and $FeBr_2(PPh_3)_2$ on random copolymerization of MMA and DMAEMA with H-$(MMA)_2$-Br in toluene at 60 °C: $[MMA]_0$ = 1600 mM; $[DMAEMA]_0$ = 400 mM; $[H\text{-}(MMA)_2\text{-}Br]_0$ = 20 mM; $[Iron\ Catalyst]_0$ = 10 mM. Iron catalyst: $FeBr_2$/PZN-Br (●, ▲); $FeBr_2(PPh_3)_2$ (○, △).

SEC traces of the products, the $FeBr_2$/PZN-Br complex gave faster polymerization and narrower MWDs of produced copolymers than $FeBr_2(PPh_3)_2$. Thus, the phosphazenium system found to be effective even for copolymerizations of DMAEMA and MMA.

Table 1. Copolymerization of MMA and DMAEMA with Iron Catalysts[a]

Entry	Catalyst	Monomer (mM) (MMA/DMAEMA)	Time (h)	Conversion (%) (MMA/DMAEMA)	M_n	M_w/M_n
1	$FeBr_2$/PZN-Br	0/2000	48	–/95	21600[b]	5.89[b]
2		1800/200	72	81/86	8300[c]	1.13[c]
3		1600/400	72	83/85	7400[c]	1.23[c]
4		1000/1000	72	81/83	7300[c]	1.27[c]
5	$FeBr_2(PPh_3)_2$	1800/200	168	79/83	8000[c]	1.24[c]
6		1600/400	72	78/80	6600[c]	1.48[c]
7		1000/1000	72	80/82	6900[c]	1.31[c]

[a] $[H\text{-}(MMA)_2\text{-}Br]_0$ = 20 mM; $[Catalyst]_0$ = 10 mM in toluene at 60 °C.
[b] Analyzed by DMF GPC [c] Analyzed by THF GPC

5. Polymerization of MA

Finally, controlled polymerization of MA was attempted with the phosphazenium system. The optimum condition for MMA was first applied for the polymerization ($[MA]_0/[H\text{-}(MMA)_2\text{-}Br]_0/[FeBr_2]_0/[PZN\text{-}Br]_0$ = 2000/20/10/10 mM). In contrast to the MMA polymerization, the polymerization suspended at ~30% conversion and the MWDs of the product were much broader (Figure 9).

Thus, the monomer concentration and the halide of the phosphazenium ion were changed to improve the activity and controllability. As the monomer concentration was increased to 4 M, the conversion reached over 50% (Figure 10A). When the phosphazenium iodide (PZN-I) was employed in place of the bromide (PZN-Br), the MWDs of the produced polymers became narrower (Figure 10B). The iodide anion is more dissociative than the bromide, and then the ionization effect would favorably contribute to the improvement in the catalytic activity. As the monomer concentration was further increased to 6 M with PZN-I,

the conversion finally reached over 70% and the molecular weights and the MWDs were fairly controlled (Figure 10C). The polymerization was performed with the conventional complex [$FeBr_2(PPh_3)_2$] under the same condition to see the catalytic superiority: the MWDs of the products were broader with multimodal peaks, indicating poorer control (Figure 10D). Thus, the phosphazenium system was found to be useful for controlled polymerization of MA, although the activity was still insufficient.

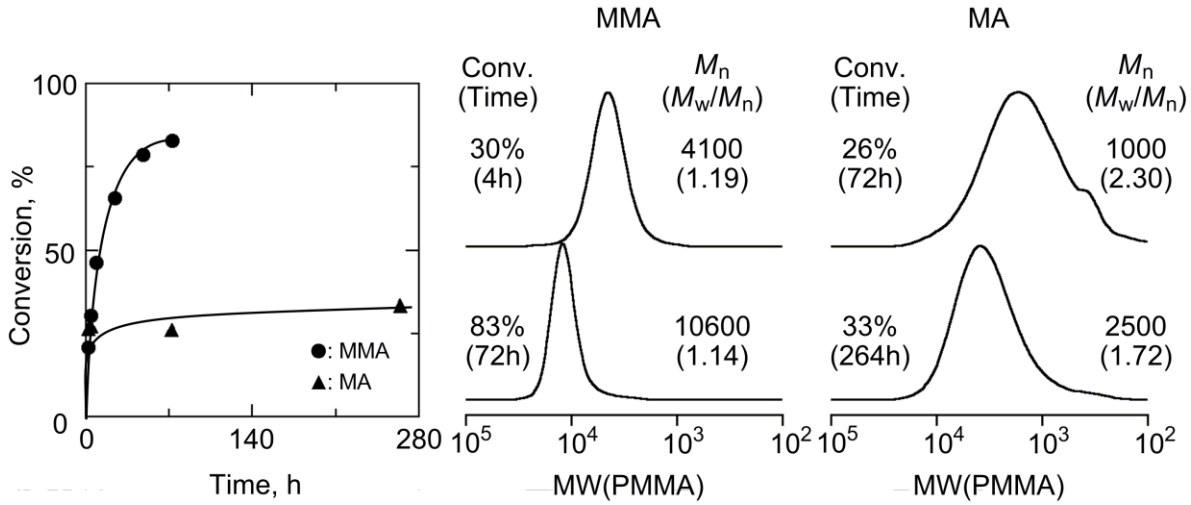

Figure 9. Polymerization of MMA and MA with H-$(MMA)_2$-Br/$FeBr_2$/PZN-Br in THF at 60 °C: $[Monomer]_0$ = 2000 mM; $[H\text{-}(MMA)_2\text{-}Br]_0$ = 20 mM; $[FeBr_2]_0$ = 10 mM; $[PZN\text{-}Br]_0$ = 10 mM.

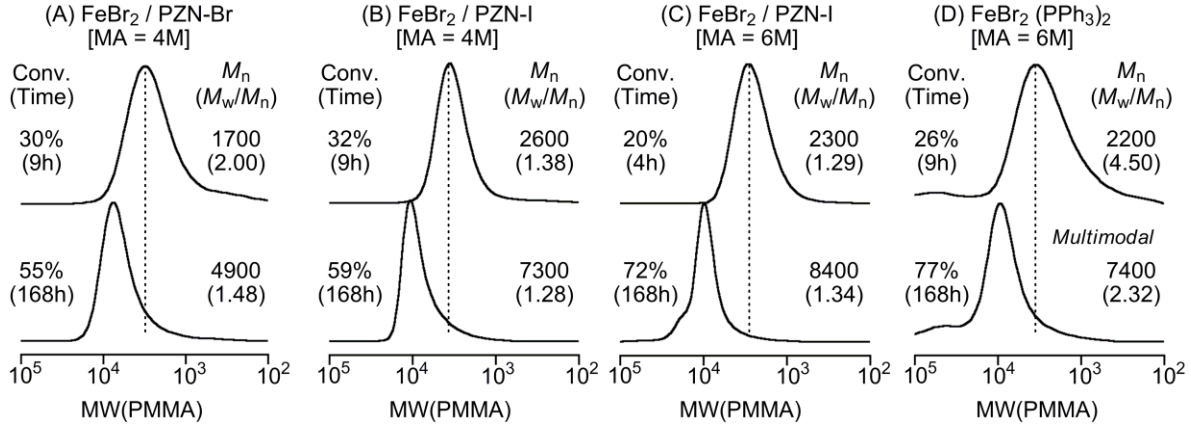

Figure 10. Effects of iron catalysts on polymerization of MA with H-EMA-Br in THF at 80 °C: (A), (B): $[MA]_0$ = 4000 mM; $[H\text{-}EMA\text{-}Br]_0$ = 40 mM; $[FeBr_2]_0$ = 20 mM; $[PZN\text{-}X]_0$ = 20 mM. (C): $[MA]_0$ = 6000 mM; $[H\text{-}EMA\text{-}Br]_0$ = 60 mM; $[FeBr_2]_0$ = 30 mM; $[PZN\text{-}I]_0$ = 30 mM. (D): $[MA]_0$ = 6000 mM; $[H\text{-}EMA\text{-}Br]_0$ = 60 mM; $[FeBr_2(PPh_3)_2]_0$ = 30 mM.

Conclusion

A phosphazenium bromide combined with $FeBr_2$ ($FeBr_2$/PZN-Br) was effective for living radical polymerization of functional methacrylate carrying poly(ethylene glycol) pendent group (PEGMA) to give controlled polymers, with narrow MWDs (M_w/M_n ~ 1.2). This catalytic system exhibited a significant improvement of the catalytic activity, compared with simple onium salts or the conventional iron catalyst [$FeBr_2(PPh_3)_2$]. The phosphazenium system also gave better control for copolymerizations of DMAEMA with MMA and homopolymerization of MA than $FeBr_2(PPh_3)_2$. The bulkiness and conjugated structure of the phosphazenium salts would contribute to such an enhancement of the catalysis for controlled polymerizations of polar or coordinating monomers.

Experimental Section

Materials

MMA (TCI; purity >99%) was dried overnight over calcium chloride and purified by double distillation from calcium hydride before use. MA (TCI; purity >99%) was dried overnight over calcium chloride and purified by distillation from calcium hydride before use. Poly(ethylene glycol) methyl methacrylate [PEGMA; $CH_2=CMeCO_2(CH_2CH_2O)_nMe$; Me = CH_3; n = 8.5 on average] (Aldrich) and *N,N'*-dimethylaminoethyl methacrylate (DMAEMA) (TCI; purity >98 %) were of commercial source and purified by passing through an inhibitor removal column (Aldrich) and degassed by reduced pressure before use. The MMA-dimer bromide [H-$(MMA)_2$-Br; H-$(CH_2CMeCO_2Me)_2$-Br] as an initiator was prepared according to literature.[19] Iron bromide (Aldrich; purity >98%), tetrabutylammonium bromide (TCI; >98%), and tetrabutylphosphonium bromide (TCI; >99%) were used as received and handled in a glove box (M. Braun Labmaster 130) under a moisture- and oxygen-free argon atmosphere (H_2O <1 ppm; O_2 <1 ppm). The phosphazenium salts were received form Mitsui Chemical, Inc. and handled in a glove box.[20] Toluene and THF (Kishida Kagaku; purity >99%) were passed through purification columns (Solvent Dispensing System; Glass Contour) and bubbled with dry nitrogen for more than 15 min immediately before use. *n*-Octane (internal standard for gas chromatography) and 1,2,3,4-tetrahydronaphthalene (tetralin; internal standard for ^{1}H NMR analysis) was dried over calcium chloride and distilled

twice from calcium hydride.

Polymerization Procedures

Polymerization was carried out by the syringe technique under dry argon in baked glass tubes equipped with a three-way stopcock or in sealed glass vials. A typical procedure for PEGMA polymerization with $(MMA)_2$-Br/$FeBr_2$/PZN-Br was as follows. In a 50-mL round-bottom flask, $FeBr_2$ (4.85 mg, 0.0225 mmol), PZN-Br (36.9 mg, 0.0225 mmol) and toluene (3.27 mL) were added under dry argon and stirred at 60 °C in 5 minutes. After cooling to room temperature, tetralin (0.20 mL), PEGMA (0.99 mL, 2.25 mmol), and H-$(MMA)_2$-Br (0.043 mL of 519 mM in toluene, 0.0225 mmol) were added sequentially under dry argon. The total volume of reaction mixture was thus 4.5 mL. Immediately after mixing, aliquots (0.60 mL each) of the solution were injected into glass tubes which were then sealed (except when a stopcock was used) and placed in an oil bath kept at desired temperature. In predetermined intervals, the polymerization was terminated by cooling the reaction mixtures to -78 ºC. Monomer conversion was determined by ^{1}H NMR from the integrated peak area of the olefinic protons of the monomers with tetralin as internal standard. The quenched reaction solutions were diluted with toluene (ca. 20 mL) without washing with water and evaporated to dryness to give the products that were subsequently dried overnight under vacuum at room temperature. For DMAEMA, the same procedures as described above were applied.

For MMA and MA, the same procedures as described above were applied except that monomer conversion was determined from the concentration of residual monomer measured by gas chromatography with *n*-octane as an internal standard and polymer solutions were washed with water three times before evaporation.

Measurements

The molecular weight distribution, M_n, and M_w/M_n values of homopolymers of PEGMA and DMAEMA and block copolymers of MMA and PEGMA were measured by SEC in DMF containing 10 mM LiBr at 40 °C on three polystyrene gel columns [Shodex KF-805L (pore size: 20-1000Å; 8.0 mm i.d.×30 cm) ×3; flow rate 1.0 mL/min] connected to a Jasco PU-980 precision pump and a Jasco 930-RI refractive-index detector, and UV-970 UV/vis detector set at 270 nm. The columns were calibrated against 11 standard PMMA samples (Polymer Laboratories; M_n = 1,000-1,200,000; M_w/M_n = 1.06-1.22) as well as MMA

monomer.

Random copolymers of MMA and DMAEMA were measured by SEC in THF at 40 °C using three polystyrene gel columns [Shodex KF-400RL × 2 and KF-400RH] that were connected to a Shodex DU-H2000 precision pump, a Shodex RI-74 refractive index detector, and a Shodex UV-41 UV/vis detector set at 250 nm. The columns were calibrated against 11 standard PMMA samples (Polymer Laboratories; M_n = 1,000-1,200,000; M_w/M_n = 1.06-1.22).

^{1}H-NMR spectra of the obtained polymers were recorded in $CDCl_3$ at 25 °C on a JEOL JNM-LA500 spectrometer operating at 500.16 MHz. Polymers for ^{1}H-NMR analysis were fractionated by preparative SEC.

Cyclic voltammograms were recorded by using a Hokuto Denko HZ-3000 apparatus. The sample-preparation for PEGMA/$FeBr_2$/PZN-Br catalyst is described. PEGMA (0.6 mL of 50 mM in toluene, 0.030 mmol), $FeBr_2$ (6.5 mg, 0.030 mmol), PZN-Br (24.6 mg, 0.030 mmol) and toluene (6 mL) were added sequentially in a baked glass tube equipped with a three-way stopcock under argon and stirred at 60 °C for 3 h. After heating, solvent was evaporated and a solution of *n*-Bu_4NPF_6 (supporting electrolyte) in CH_2ClCH_2Cl solution (100 mM, 6 mL) was added into the tube under argon. Measurements were carried out at 0.1 Vs^{-1} under argon at 25 °C. A three-electrode cell was used which was equipped with a platinum disk as a working electrode, a platinum wire as a counter electrode, and an Ag/AgCl electrode as a reference.

References and Notes

(1) For recent reviews on transition metal catalyzed living radical polymerization, see: (a) Kamigaito, M.; Ando, T.; Sawamoto, M. *Chem. Rev.* **2001**, *101*, 3689-3745. (b) Kamigaito, M.; Ando, T.; Sawamoto, M. *Chem. Rec.* **2004**, *4*, 159-175. (c) Ouchi, M.; Terashima, T.; Sawamoto, M. *Acc. Chem. Res.* **2008**, *41*, 1120-1132. (d) Matyjaszewski, K.; Xja, J. *Chem. Rev.* **2001**, *101*, 2921-2990. (e) Matyjaszewski K., Ed.; *Controlled/Living Radical Polymerization From Synthesis to Materials*; ACS Symposium Series 944; American Chemical Society: Washington, DC, 2006.Bolm, C.; Legros, J.; Paih, J. L.; Zani, L. *Chem. Rev.* **2004**, *104*, 6217-6254.

(2) (a) Kato, M.; Kamigaito, M.; Sawamoto, M.; Higashimura, T. *Macromolecules* **1995**, *28*, 1721-1723. (b) Ando, T.; Kato, M.; Kamigaito, M.; Sawamoto, M. *Macromolecules* **1996**, *29*, 1070-1072.

(3) Wang, J. S.; Matyjaszewski, K. *J. Am. Chem. Soc.* **1995**, *117*, 5614-5615.

(4) (a) Bolm, C.; Legros, J.; Paih, J. L.; Zani, L. *Chem. Rev.* **2004**, *104*, 6217-6254. (b) Enthaler, S.; Junge, K.; Beller, M. *Angew. Chem. Int. Ed.* **2008**, *47*, 3317-3321.

(5) Ando, T.; Kamigaito, M.; Sawamoto, M. *Macromolecules* **1997**, *30*, 4507-4510.

(6) Matyjaszewski, K.; Wei, M.; Xia, J.; McDermott, N. E. *Macromolecules* **1997**, *30*, 8161-8164.

(7) Kotani, Y.; Kamigaito, M.; Sawamoto, M. *Macromolecules* **1999**, *32*, 6877-6880.

(8) Kotani, Y.; Kamigaito, M.; Sawamoto, M. *Macromolecules* **2000**, *33*, 3543-3549.

(9) Zhu, S.; Yan, D. *Macromolecules* **2000**, *33*, 8233-8238.

(10) Louie, Y.; Grubbs, R. H. *Chem. Commun.* **2000**, 1479-1480.

(11) Gibson, V. C.; O'Reilly, R. K.; Reed, W.; Wass, D. F.; White, A. J. P.; Williams, D. J. *Chem. Commun.* **2002**, 1850-1851.

(12) Göbelt, B.; Matyjaszewski, K. *Macromol. Chem. Phys.* **2000**, *201*, 1619-1624.

(13) O'Reilly, R. K.; Gibson, V. C.; White, A. J. P.; Williams, D. J. *J. Am. Chem. Soc.* **2003**, *125*, 8450-8451.

(14) Xue, Z.; Lee, B. W.; Noh, S. K.; Lyoo, W. S. *Polymer* **2007**, *48*, 4704-4714.

(15) Niibayashi, S.; Hayakawa, H.; Jin, R-H.; Nagashima, H. *Chem. Commun.* **2007**, 1855-1857.

(16) Uchiike, C.; Terashima, T.; Ouchi, M.; Ando, T.; Kamigaito, M.; Sawamoto, M. *Macromolecules* **2007**, *40*, 8658-8662.

(17) Ferro, R.; Milione, S.; Bertolasi, V.; Capacchione, C.; Grassi, A. *Macromolecules* **2007***, 40,* 8544-8546.

(18) Furuyama, R.; Fujita, T.; Funaki, S. F.; Nobori, T.; Nagata, T.; Fujiwara, K. *Catalysis Surveys from Asia* **2004**, *8*, 61-71.

(19) Ando, T.; Kamigaito, M.; Sawamoto, M. *Tetrahedron* **1997**, *53*, 15445-15457.

(20) Nobori, T.; Kouno, M.; Suzuki, T.; Mizutani, K.; Kiyono, S.; Sonobe, Y.; Takaki, U. Phosphazenium salt and preparation process thereof, and process for producing poly(alkylene oxide), U.S. 5,990,352 (1999).

PART II

Design of Half-Metallocene Iron Catalysts

Chapter 3

Carbonyl/Phosphine Hetero-Ligated Cyclopentadienyl Iron Catalysts: Catalytic Activity and Polymerization Mechanism

Abstract

Two neutral ligands, carbonyl and phosphine, were cooperatively incorporated into half metallocene iron(II) complexes [CpFeBr(CO)(L^{phos}); Cp = C_5H_5; L^{phos} = PPh_3, $P(OPh)_3$, $PMePh_2$, PMe_2Ph, P(*n*-Bu)$_3$] for more active and versatile systems in transition metal-catalyzed living radical polymerization. For methyl methacrylate (MMA) with a bromide initiator [$Me_2C(CO_2Me)CH_2C(Me)$-$(CO_2Me)Br$; Me = CH_3] [H-$(MMA)_2$-Br], these hetero-ligated catalysts are superior, in terms of catalytic activity and molecular weight control, to similar homo-ligated half-metallocenes carrying two identical ligands such as $CpFe(CO)_2Br$ and $CpFe(L^{phos})_2Br$. Among the $CpFe(CO)(L^{phos})Br$ complexes examined, $CpFe(CO)(PMePh_2)Br$ showed the highest activity and the best controllability (> 90% conversion within 24 h; M_w/M_n = 1.29), and the "living" character of the polymerizations therewith was proved by sequential monomer-addition experiments. In spite of the high activity, the Fe(II) complex is stable and robust enough to be handled under air, rendering it suitable for practical use. The concomitant high activity and high stability were attributed to the *in-situ* generation of a real active catalyst with a 16-electron configuration via the irreversible release of the carbonyl group from $CpFe(CO)(L^{phos})Br$ upon the activation of a terminal C-Br bond, as confirmed by FT-IR monitoring of model reactions with the initiator as a dormant-end model compound.

Introduction

A key component of transition metal-catalyzed chemical reactions is obviously a metal complex catalyst, which determines and controls critical parameters including rate, efficiency, selectivity, versatility, etc.,[1] and it is particularly true for metal-mediated living radical polymerization (Scheme 1), which the author's and other groups have been pursuing over a decade.[2] In general, a metal complex consists of a transition metal center and a ligand(s), and the two components are connected through coordination and sometimes metal-carbon bonds formed from the vacant d-orbital of the former and the σ-, π-, or n-electrons of the latter. The ligands thereby affect the electronic as well as steric environments of complexes and, in turn, their catalytic performance.

Living radical polymerizations are now powerful tools to synthesize controlled polymeric architectures, because, unlike the ionic counterparts, they are simple and easy to execute, robust and reproducible under varying conditions, and, above all, versatile and applicable to a wide range of monomers including functional derivatives that are often required in biochemistry, materials science, and other disciplines beyond chemistry. "Transition metal-catalyzed" living radical polymerization (Scheme 1) is one of such systems in which metal catalysts are responsible for molecular weight control, reaction rate, and applicable monomers, among other factors.[2]

For example, a catalyst (Mt^n; n = valence number) activates the carbon-halogen bond in an initiator (I-X) or in a dormant polymer terminal (~~~C-X) so as to trigger its homolysis into a carbon-centered growth-active radical (I• or ~~~C•) via one-electron oxidation from

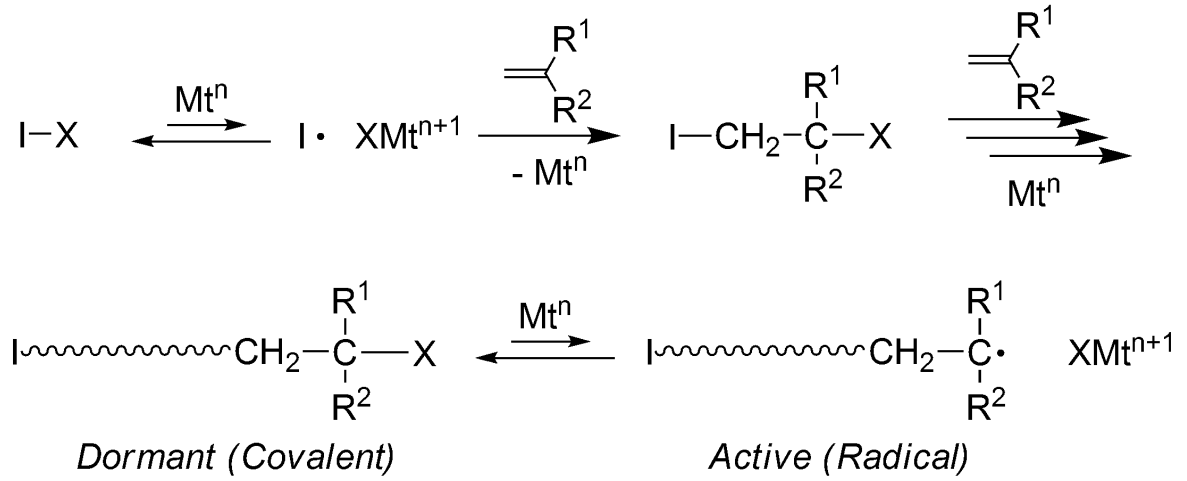

Scheme 1. Transition-Metal Catalyzed Living Radical Polymerization

Mt^n to Mt^{n+1}. These growing species propagate with monomers, and the oxidized catalyst sooner or later donates back its halogen X to the radical, to regenerate the dormant terminal while returning to the original lower valance state via one-electron reduction from Mt^{n+1} to Mt^n. The polymerization thus proceeds by repeating the reversible activation-deactivation process, or a one-electron oxidation-reduction cycle, and with the dormant species thermodynamically much more favored than the radical species, the instantaneous radical concentration is kept so low as to practically suppress undesirable bimolecular terminations and chain-transfer reactions.

For such a unique catalysis, ruthenium[3] and copper[4] catalysts are vanguards, and their catalytic activities are high enough to induce not only living homopolymerizations but also block and random copolymerizations of virtually all radically polymerizable monomers.

Belonging to the group-8 family as with ruthenium, divalent iron (Fe^{II}) also potentially catalyzes living radical polymerization, and since the first successful example with $FeCl_2(PPh_3)_2$,[5] a fairly wide variety of iron catalysts have been developed with use of different ligands, including bipyridine,[6] cyclopentadiene (Cp),[7] pentamethylcyclopentadiene,[8] isophthalic acid,[9] imidazolidene,[10] diimine,[11] diiminopyridine,[12] salicylaldiminato,[13] pyridylphosphine,[14] triazacyclononane,[15] alkyl phosphine,[16] bis(oxazoline),[17] phosphine-nitrogen chelates,[18] and phosphazene.[19] The increasingly extensive development primarily stems from the additional advantages of iron complexes: environmentally benign, safe (or less toxic), biocompatible, and abundant.[20] Nevertheless, in general, iron catalysts are inferior to ruthenium and copper counterparts, especially in terms of versatility in monomers, fine reaction tuning, and tolerance of polar functionality and solvents. Therefore, improvement in iron catalysts is of importance and would promise actual applications of metal-catalyzed living radical polymerization.

In this chapter, the author designed and developed novel iron complexes that were more active and versatile in living radical polymerization, or more specifically, a series of saturated (18-electron) cyclopentadienyl $(Cp)Fe^{II}$ bromides with two neutral ligands (L^1 and L^2): $Fe^{II}(Cp)L^1L^2Br$. As proposed for similar 18-electron ruthenium complexes [e.g., $(Ind)RuCl(PPh_3)_2$[21] and $Cp^*RuCl(PPh_3)_2$[22] ; Ind = C_9H_7; Cp* = η-C_5Me_5], they would turn "unsaturated" in the activation process where acquiring a halogen from an initiator or a dormant polymer terminal via ligand release or slipping from η^5 to η^3 configurations. Thus, the combination of two neutral ligands in $Fe^{II}(Cp)L^1L^2Br$ would be important for the smooth conversion to the unsaturated form upon one-electron oxidation as well as for the one-electron

reduction of the central iron in the reverse step.

Herein, the author targeted "hetero-ligated" complexes, namely, introduction of two different neutral ligands onto the Fe^{II} center, such as for $Fe^{II}(Cp)(CO)(L^{phos})Br$ with triphenyl(alkyl)phosphine (L^{phos}) and carbonyl (CO). In general, the former ligand is a "σ-donor" to increase the electron density of the central metal, whereas the latter is a "π-acceptor" to reduce the electron density due to coordination via back-donation. Such a hetero ligation would be prospective for the facile and fast structural conversion of catalysts from their saturated to unsaturated forms via cooperative adjustment of the electronic states. $Fe^{II}(Cp)(CO)(L^{phos})Br$ can be easily prepared by the reaction of commercially available $Fe^{II}(Cp)(CO)_2Br$ with corresponding phosphine (L^{phos}) on heating (Scheme 2),[23] and thus a variety of phosphines with different properties would allow both electric and steric modulations of the iron complexes into more active, versatile, and functionality-tolerant catalysts. In this chapter, the author employed these catalysts for the possible living radical polymerization of polymerization of methyl methacrylate (MMA). Also, the catalytic activity and the reaction mechanism were examined by cyclic voltammetry (CV) and FT-IR.

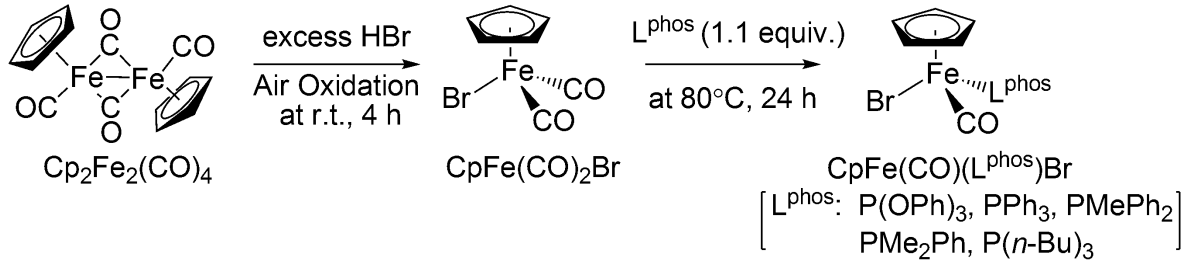

Scheme 2. Synthesis of $CpFe(CO)(L^{phos})Br$

Results and Discussion

1. Living Radical Polymerization of MMA with $CpFe(CO)(L^{phos})Br$

A FeCp complex with triphenylphosphine (PPh_3) and carbonyl (CO) [$CpFe(CO)(PPh_3)Br$] was employed as our first "hetero-ligated" catalyst for polymerization of MMA in conjunction with H-$(MMA)_2$-Br as an initiator without an additive in toluene at 60 °C ($[MMA]_0/[H\text{-}(MMA)_2\text{-}Br]_0/[CpFe(CO)(PPh_3)Br]_0$ = 4000/40/10 mM). As shown in Figure 1, the catalyst induced a smooth polymerization (conversion ~90% in 24 h) and gave controlled PMMAs with fairly narrow molecular weight distributions (MWDs; $M_w/M_n < 1.5$). On the other hand, a homo-ligated dicarbonyl derivative [$CpFe(CO)_2Br$; precursor of

CpFe(CO)(PPh_3)Br] resulted in limited conversion (~20%) and broader MWDs (M_w/M_n > 2.0). These results indicate that the design of neutral ligands for $Fe^{II}(Cp)L^1L^2Br$ is critical to the catalytic activity and that such a hetero ligation is promising for living radical polymerization.

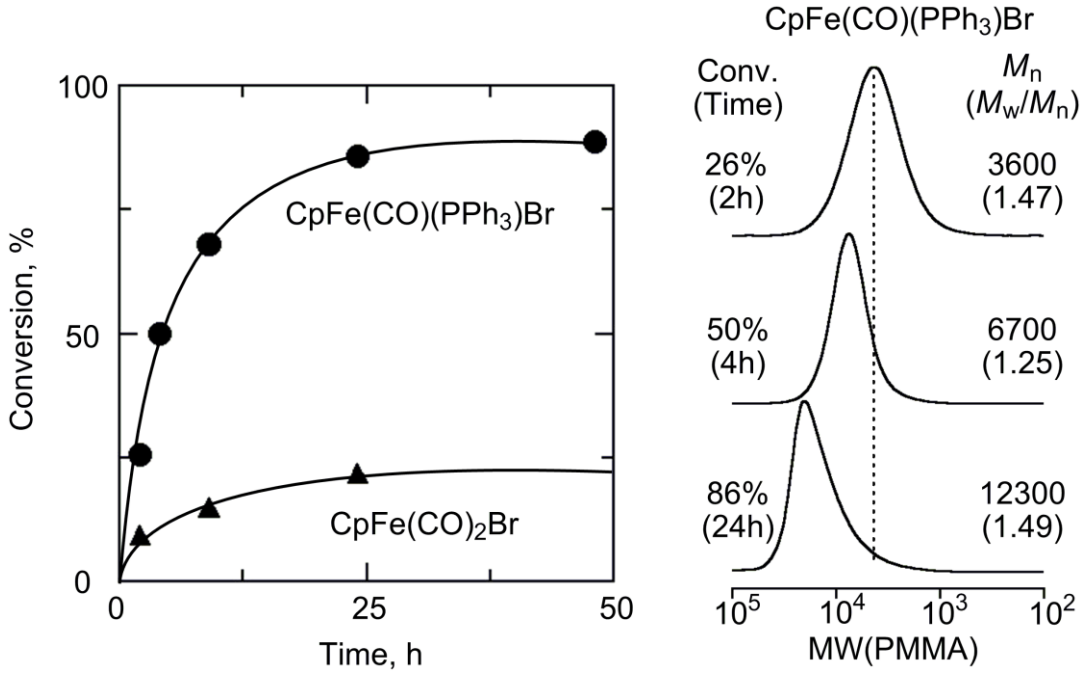

Figure 1. Living radical polymerization of MMA with H-$(MMA)_2$-Br/Fe(II) catalyst in toluene at 60 °C: $[MMA]_0$ = 4000 mM; $[H\text{-}(MMA)_2\text{-}Br]_0$ = 40 mM; $[Fe(II)\ catalyst]_0$ = 10 mM. Fe(II) catalyst: CpFe(CO)(PPh_3)Br (●); $CpFe(CO)_2Br$ (▲).

2. Effects of Phosphine Ligands in CpFe(CO)(L^{phos})Br

Given the possibility of living radical polymerization with CpFe(CO)(PPh_3)Br, the author prepared a series of Cp-based iron catalysts carrying different phosphines [CpFe(CO)(L^{phos})Br; L^{phos} = $P(OPh)_3$, $PMePh_2$, PMe_2Ph, P(*n*-Bu)$_3$] to study effects of the phosphine ligand in MMA polymerization with H-$(MMA)_2$-Br in toluene at 60 °C (Figure 2). The phosphite complex [L^{phos} = $P(OPh)_3$] resulted in lower activity, similar to the dicarbonyl complex [$CpFe(CO)_2Br$], while other four complexes catalyzed smooth and faster polymerizations to give >80% conversion within 24 h. Upon near completion of the reactions, they gave almost controlled polymers (M_w/M_n = 1.25-1.50), however, an endurance of the catalytic activity was dependent on the ligands: polymerization was gradually retarded at ~75% conversion with PPh_3 and P(*n*-Bu)$_3$, whereas such retardation was absent with $PMePh_2$ and PMe_2Ph. Also, MWDs (M_w/M_n values) stayed rather unchanged throughout the polymerizations, but with PMe_2Ph, MWD drastically decreased from an initial broad

distribution (conv. = 33%, M_w/M_n > 3; conv. = 87%, M_w/M_n = 1.38). These differences of the phosphine ligands in catalytic performance were analytically examined in the following sections.

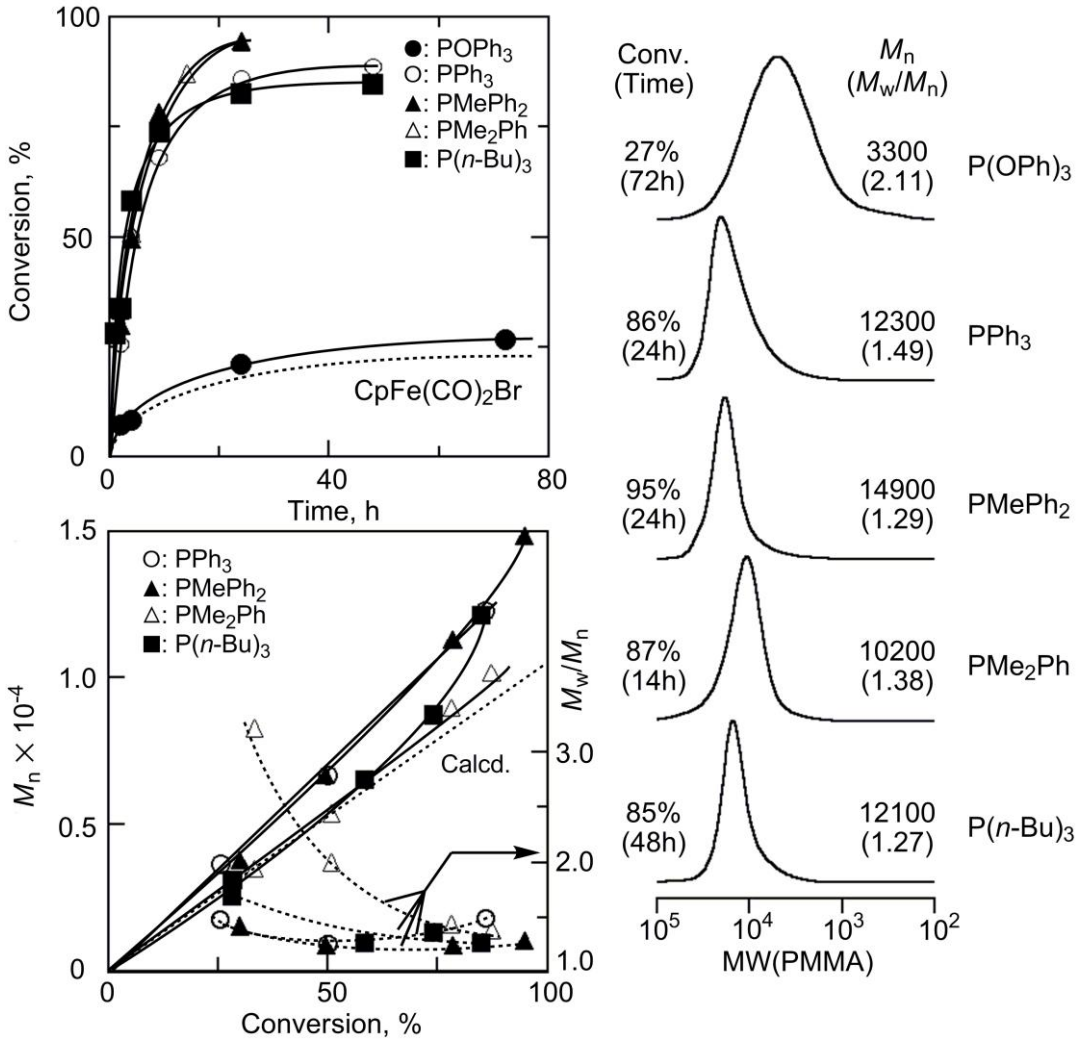

Figure 2. Effects of phosphine ligand on living radical polymerization of MMA with H-$(MMA)_2$-Br/CpFe(CO)(L^{phos})Br in toluene at 60 °C: $[MMA]_0$ = 4000 mM; $[H\text{-}(MMA)_2\text{-}Br]_0$ = 40 mM; $[CpFe(CO)(L^{phos})Br]_0$ = 10 mM. L^{phos}: $P(OPh)_3$ (●); PPh_3 (○); $PMePh_2$ (▲); PMe_2Ph (△); $P(n\text{-}Bu)_3$ (■).

3. Cyclic Voltammetry Analyses

As the catalysis in metal-catalyzed living radical polymerization is based on a one-electron redox cycle of the catalyst, cyclic voltammetry (CV) is helpful to discuss catalytic activities. Thus, CV was run with the iron complexes to determine and compare redox potentials: E_{pa}, oxidation peak; E_{pc}, reduction peak; $E_{1/2} = (E_{pa} + E_{pc})/2$; $\Delta E = E_{pa} - E_{pc}$.

All the complexes showed clear and reversible oxidation/reduction waves in the range of 0 to 1.8 V, most likely assigned to one-electron redox cycle between Fe^{II} and Fe^{III}, and the waves were reproducible in several scans without hysteresis (Figure 3 and Table 1). This indicates the high stability of both oxidized and reduced states, in contrast to a homo-ligated dicarbonyl iodide complex [$CpFe(CO)_2I$] which requires certain metal alkoxide [$Ti(O\textit{i}\text{-}Pr)_4$ or $Al(O\textit{i}\text{-}Pr)_3$] as an additive (cocatalyst) for such a recurrent cycle as well as for catalyzing living radical polymerizations.[8,24]

In addition to ligating mode (homo vs. hetero), the redox potential was obviously dependent on the nature of the ligands: The dicarbonyl (CO/CO) and the phosphite [$CO/P(OPh)_3$] complexes had higher redox potentials and hence low catalytic activities. In these complexes, electron donation from the ligands to iron would be insufficient for facilitating the oxidation process. The other complexes, all active in MMA polymerization, in fact showed lower potentials. Beside these qualitative assessment, no quantitative correlation between *E* value and catalytic performance was indentified for the four $Fe^{II}(Cp)L^1L^2Br$ catalysts.

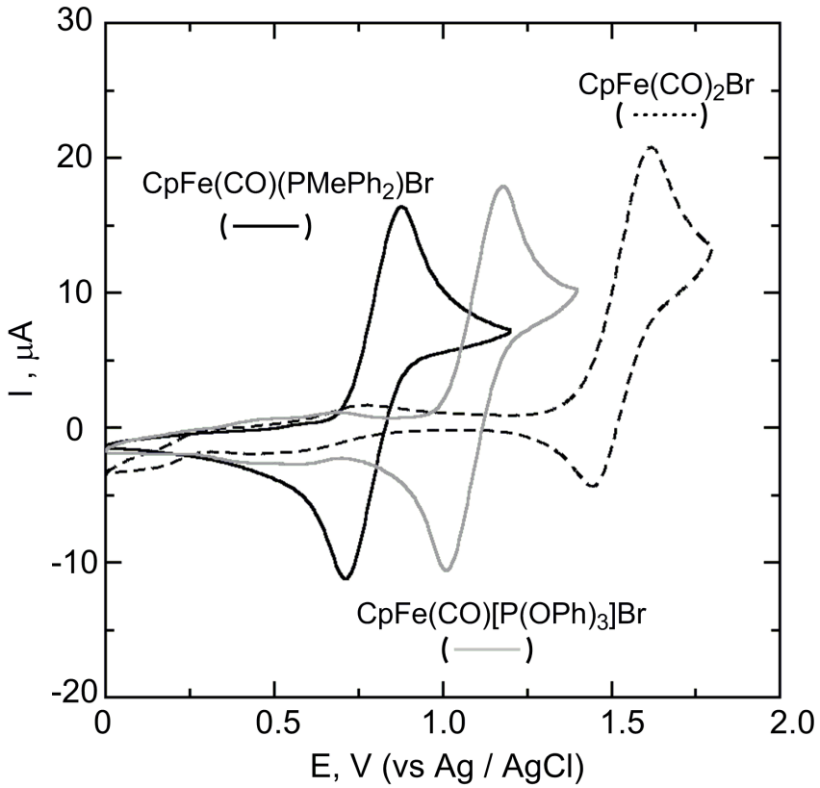

Figure 3. Cyclic voltammograms of Fe(II) catalysts in $ClCH_2CH_2Cl$ at 25 °C: [Fe(II) catalyst]$_0$ = 5.0 mM; [*n*-Bu_4NPF_6]$_0$ = 100 mM. Fe(II) catalyst: $CpFe(CO)(PMePh_2)Br$ (solid line); $CpFe(CO)[P(OPh)_3]Br$ (gray line); $CpFe(CO)_2Br$ (dashed line).

Table 1. Cyclic Voltammetry Analyses of CpFe(CO)(L)Br Catalysts[a]

Ligand	E_{pa} (V)	E_{pc} (V)	$E_{1/2}$ (V)	ΔE (V)
CO	1.63	1.44	1.54	0.18
$P(OPh)_3$	1.18	1.01	1.09	0.17
PPh_3	0.90	0.72	0.81	0.18
$PMePh_2$	0.88	0.71	0.79	0.17
PMe_2Ph	0.84	0.66	0.75	0.18
P(*n*-Bu)$_3$	0.80	0.61	0.71	0.19

[a] $[CpFe(CO)(L)Br]_0$ = 5.0 mM; $[n\text{-}Bu_4NPF_6]_0$ = 100 mM in CH_2ClCH_2Cl at 25 °C. $E_{1/2} = (E_{pa} + E_{pc})/2$; $\Delta E = E_{pa} - E_{pc}$.

4. FT-IR Analysis: Conversion to 16e Complex

The carbonyl ligand on $Fe^{II}(Cp)(CO)(L^{phos})Br$ was analyzed by FT-IR, to see the possible structural conversion of the saturated 18e complex into a 16e form, when it reacted with an initiator [H-$(MMA)_2$-Br] at polymerization temperature (60 °C) (see Experimental Section).

Figure 4 shows FT-IR spectra from 1600 to 2200 cm^{-1} for the mixture with $CpFe(CO)_2Br$ [Figure 4 (A)] and $CpFe(CO)(L^{phos})Br$ [L^{phos} = $P(OPh)_3$, PPh_3, $PMePh_2$, PMe_2Ph, P(*n*-Bu)$_3$; Figure 4 (B)-(F)]. The FT-IR data consist of two spectra for each complex, where the upper spectrum is for "before heating" and the lower for "after heating". Peaks at around 2000 cm^{-1} are derived from the C≡O stretching and those around 1730 cm^{-1} are due to the ester C=O in the initiator. With less active catalysts, $CpFe(CO)_2Br$ and $CpFe(CO)[P(OPh)_3]Br$, the C≡O bands remained unchanged even after the heating, indicating that the carbonyl ligands were still ligated on the complexes [Figure 4 (A) and (B)]. In contrast, with the active catalysts [$CpFe(CO)(L^{phos})Br$; L^{phos} = PPh_3, $PMePh_2$, PMe_2Ph, P(*n*-Bu)$_3$], the same C≡O bands almost disappeared or much weakened [Figure 4 (C)-(F)], which suggests the carbonyl ligand was irreversibly released upon activation of the initiator. Indeed, when allowed to stand for analysis, the solution changed from green (18e complex) to reddish brown (16e complex); the color change thus support CO elimination.

These results demonstrate that a more electron-donating phosphine like P(*n*-Bu)$_3$ promotes the carbonyl elimination to give in situ an active unsaturated 16e-complex. However, with PMe_2Ph, the elimination seemed slower, judged from the clearly remained

peak even after heating. The slow carbonyl release would account for the initial broad MWD with PMe_2Ph (Figure 2). Thus, carbonyl elimination is essential to catalyze living radical polymerization, and it is affected by the neighboring phosphine ligand.

Scheme 3 shows a proposed mechanism based on these analyses. Carbonyl release should be irreversible because of the gaseous character of CO, and hence the polymerization involves 16e and 17e complexes, 16e Fe(II) for the activation of dormant species and 17e Fe(III) for radical deactivation (capping).

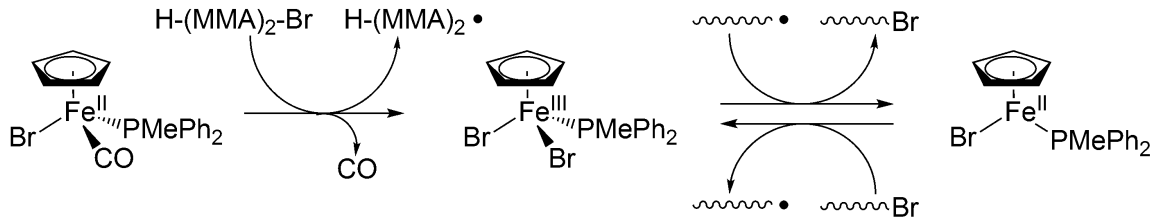

Scheme 3. Proposed Polymerization Mechanism of $CpFe(CO)(PMePh_2)Br$

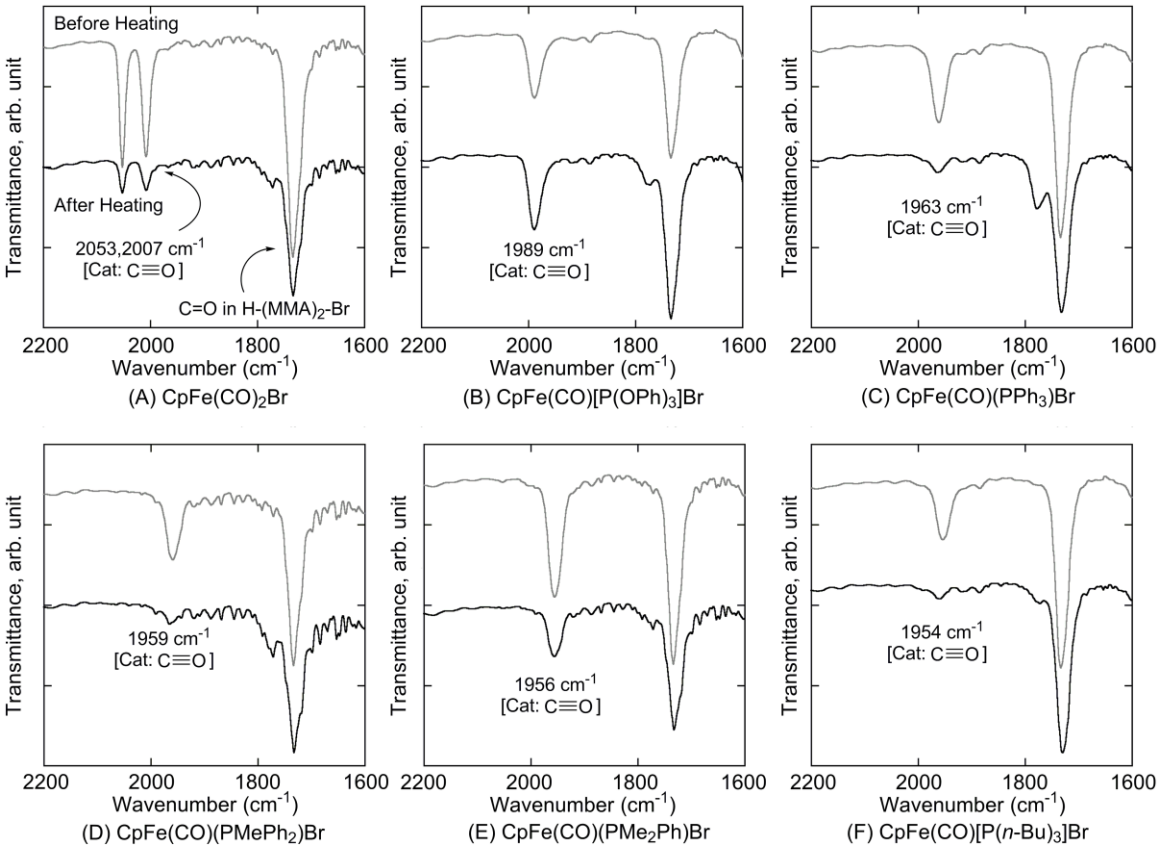

Figure 4. FT-IR analysis of Fe(II) complex/H-$(MMA)_2$-Br in $CHCl_3$ at 25 °C: [Fe(II) complex]$_0$ = 5.0 mM; [H-$(MMA)_2$-Br]$_0$ = 20 mM. Condition: "Before Heating" (gray line); "After Heating", aged at 60 °C for 8 h before measurement (solid line). Fe(II) catalyst: (A) $CpFe(CO)_2Br$; (B) $CpFe(CO)[P(OPh)_3]Br$; (C) $CpFe(CO)(PPh_3)Br$; (D) $CpFe(CO)(PMePh_2)Br$; (E) $CpFe(CO)(PMe_2Ph)Br$; (F) $CpFe(CO)[P(n\text{-}Bu)_3]Br$.

5. CpFe(CO)(PMePh$_2$)Br vs CpFe(PMePh$_2$)$_2$Br

According to the proposed mechanism, the catalytic properties of CpFe(CO)(L^{phos})Br might be similar to those of the corresponding diphosphine analogs [CpFe(L^{phos})$_2$Br]. Thus, with PMePh$_2$ their catalysis in MMA polymerization was examined, to clarify some superiority of the hetero ligation (Figure 5).

CpFe(PMePh$_2$)$_2$Br induced MMA polymerization at almost the same rate as with the carbonyl-phosphine complex [CpFe(CO)(PMePh$_2$)Br] and gave controlled polymers. The SEC curves of the products were fairly narrow, but a slight "tailing" in lower molecular weight region was noticeable, hence the M_w/M_n values a little larger. For diphosphine complexes, a released phosphine (non volatile) remains in the system and might have a chance to re-coordinate the iron, in contrast to the irreversible elimination of the CO ligand in CpFe(CO)(PMePh$_2$)Br. Such a phosphine re-coordination might make the dormant-active species equilibrium slower, resulting in broader MWDs.

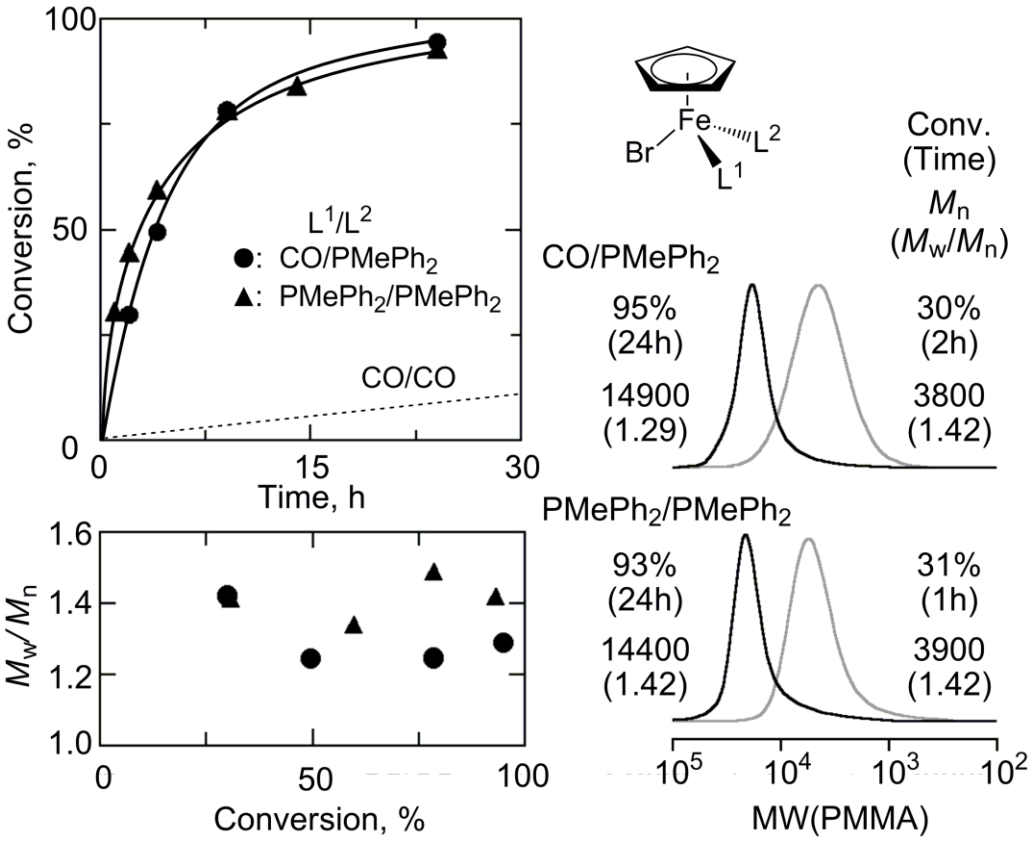

Figure 5. Living radical polymerization of MMA with H-(MMA)$_2$-Br/Fe(II) catalyst in toluene at 60 °C: [MMA]$_0$ = 4000 mM; [H-(MMA)$_2$-Br]$_0$ = 40 mM; [Fe(II) catalyst]$_0$ = 10 mM. Fe(II) catalyst: CpFe(CO)(PMePh$_2$)Br (●); CpFe(PMePh$_2$)$_2$Br (▲).

The carbonyl-phosphine complexes were stable enough to be treated under air. For example, a solution of $CpFe(CO)(PMePh_2)Br$ in toluene was deliberately bubbled with air for 3 minutes before polymerization. The green color of the complex was not changed throughout the procedures, indicating some tolerance of air. After degassing, the catalyst solution was directly employed for MMA polymerization under the same conditions as mentioned above (Figure 6). Even after the air exposure, the iron catalyst turned out as active as an oxygen-free complex. In sharp contrast, the diphosphine complex $CpFe(PMePh_2)_2Br$, similarly exposed to air before use, immediately changed in color, from purple into brown, and an unidentified insoluble complex precipitated. Air exposure also deteriorated catalytic activity and controllability. Thus, the hetero-ligated complexes were tolerant of air and superior in handling, to the diphosphine homo-ligated counterparts.

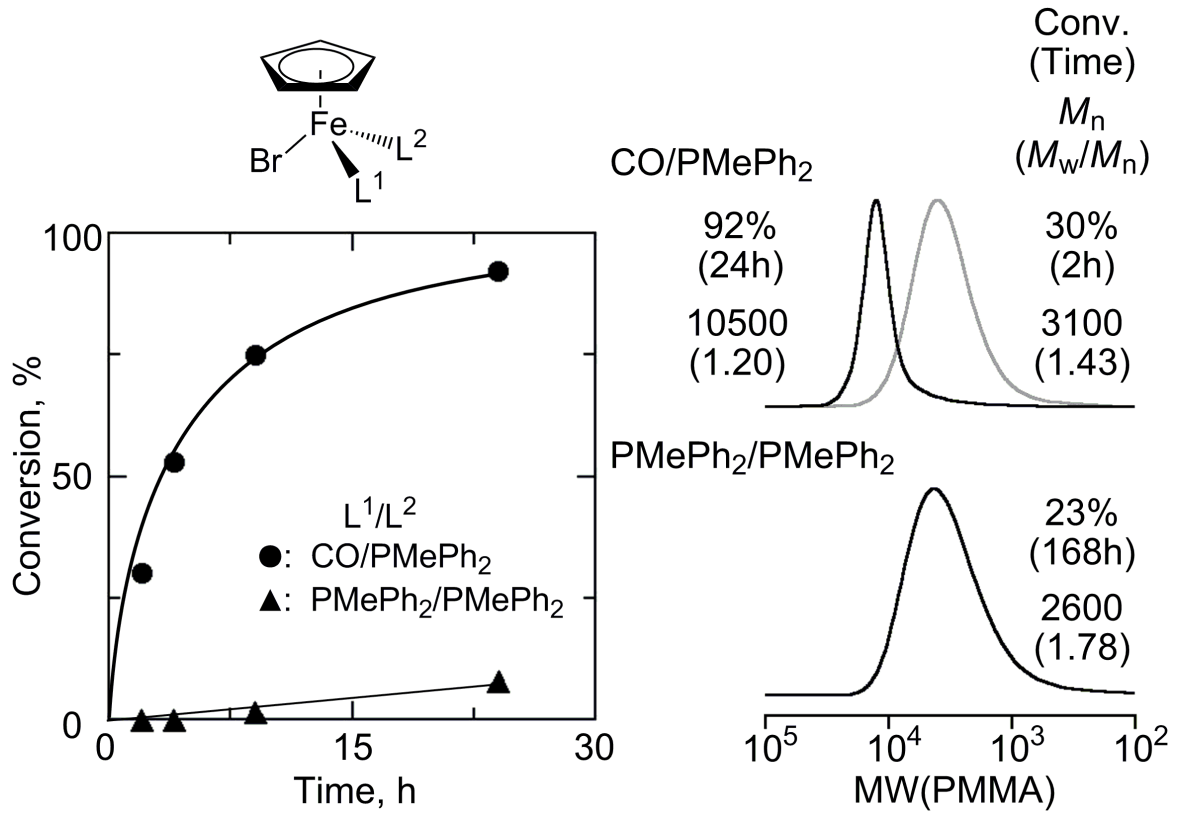

Figure 6. Living radical polymerization of MMA in toluene at 60 °C with $H\text{-}(MMA)_2\text{-}Br$/Fe(II) catalyst, followed by air bubbling to the catalyst at 25 °C for 3 min: $[MMA]_0$ = 4000 mM; $[H\text{-}(MMA)_2\text{-}Br]_0$ = 40 mM; $[Fe(II)\ catalyst]_0$ = 10 mM. Fe(II) catalyst: $CpFe(CO)(PMePh_2)Br$ (●); $CpFe(PMePh_2)_2Br$ (▲).

6. Sequential Monomer Addition

To investigate living nature of the MMA polymerization with $CpFe(CO)(PMePh_2)Br$, monomer-addition experiment was performed (Figure 7). A fresh MMA was added to the polymerization solution when MMA conversion reached over 80% in ca. 22 h. Monomer consumption was smooth in the second stage and gave an additional 83% conversion (totally 168%). Polymer molecular weight was linearly increased even at the second stage, and the SEC curves shifted to higher molecular weight keeping the narrow molecular weight distribution, although just a small peak was left. As a concurrent addition of the catalyst was not required in the second stage, the complex, or its modified active form, retains catalytic activity during the two-step polymerization.

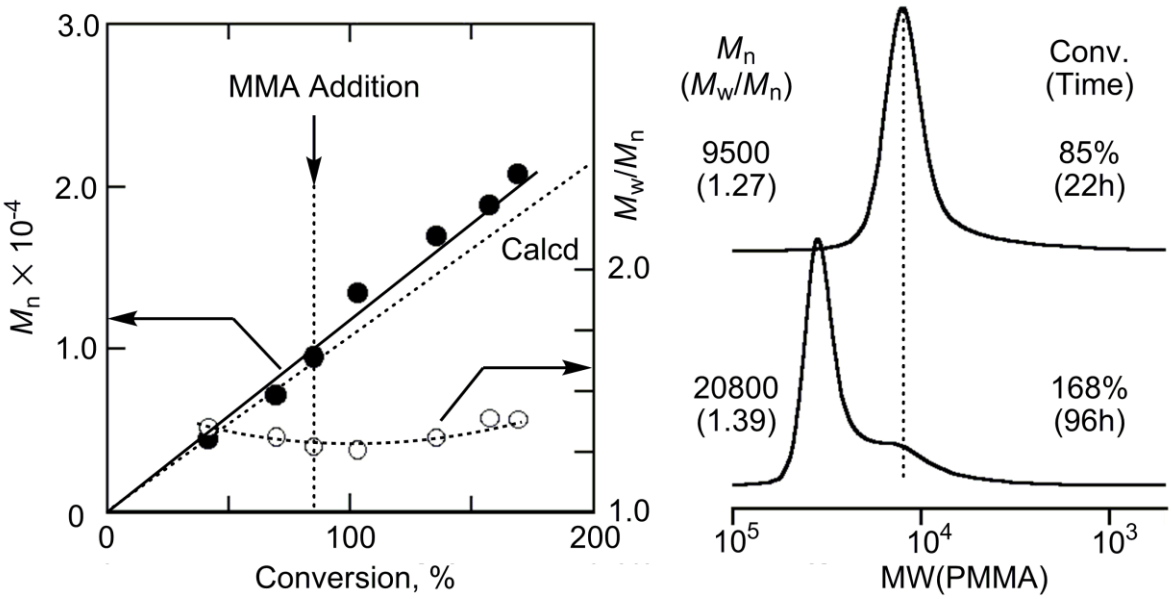

Figure 7. Monomer-addition experiment in the polymerization of MMA with H-$(MMA)_2$-Br/$CpFe(CO)(PMePh_2)Br$ in toluene at 60 °C: $[MMA]_0 = [MMA]_{add} = 4000$ mM; $[H\text{-}(MMA)_2\text{-}Br]_0 = 40$ mM; $[CpFe(CO)(PMePh_2)Br]_0 = 10$ mM.

7. Polymerization of Other Monomers

Most of conventional iron complexes such as $FeBr_2(PPh_3)_2$ tend to be deactivated upon interaction with polar groups (e.g., amino and hydroxyl groups) as well as polar solvents. However, the dicarbonyl Cp iron complexes $[CpFe(CO)_2Br]$ and the related analogs are tolerant enough to catalyze living radical polymerizations of styrene and acrylates even in the presence of a large amount of water.[25] Such backgrounds encouraged the author to employ $CpFe(CO)(PMePh_2)Br$ for various polar monomers: methacrylate with a pendent poly(ethyleneglycol) (PEGMA); *N,N'*-dimethylaminoethyl methacrylate (DMAEMA);

2-hydroxyethyl methacrylate (HEMA); and methyl acrylate (MA) (Table 2). The polymerization of PEGMA was fairly controlled, in which the molecular weights were increased with conversion, but it was decelerated at around 70% conversion. For the other monomers, polymerization control was totally difficult, as suggested by varying colors of polymerization solutions [yellow (PEGMA, DMAEMA, and MA) or white (HEMA)] that were totally different from reddish brown in the living MMA polymerization. As-prepared solutions of $CpFe(CO)(PMePh_2)Br$ with these polar monomers, on the other hand, colored green, as with the catalyst/MMA solution, implying that not the 18e complex but the *in-situ* generated 16e form $[CpFe^{II}(PMePh_2)Br]$ or its oxidized form $[CpFe^{III}(PMePh_2)Br_2]$ would be less tolerance to these monomers.

Table 2. Polymerizations of Various Monomers with $CpFe(CO)(PMePh_2)Br$

Monomer	Time (h)	Conv. (%)	M_n	M_w/M_n
PEGMA[a]	4	35	20500	1.45
PEGMA[a]	24	69	31400	1.51
DMAEMA[b]	24	73	26000	2.90
HEMA[c]	168	51	98200	2.59
MA[d]	168	73	6200	2.70

[a] $[PEGMA]_0$ = 500 mM, $[H\text{-}(MMA)\text{-}Br]_0$ = 5.0 mM, $[CpFe(CO)(PMePh_2)Br]_0$ = 5.0 mM in toluene at 60 °C.
[b] $[DMAEMA]_0$ = 2000 mM, $[H\text{-}(MMA)\text{-}Br]_0$ = 20 mM, $[CpFe(CO)(PMePh_2)Br]_0$ = 10 mM in toluene at 60 °C.
[c] $[HEMA]_0$ = 2000 mM, $[H\text{-}(MMA)\text{-}Br]_0$ = 20 mM, $[CpFe(CO)(PMePh_2)Br]_0$ = 10 mM in methanol at 60 °C.
[d] $[MA]_0$ = 4000 mM, $[H\text{-}(MMA)\text{-}Br]_0$ = 40 mM, $[CpFe(CO)(PMePh_2)Br]_0$ = 10 mM in toluene at 80 °C.

Conclusion

A series of half-metallocene Fe(II) complexes with a carbonyl and an electron-donating phosphine ligand [$CpFe(CO)(L^{phos})Br$; L^{phos} = PPh_3, $PMePh_2$, PMe_2Ph, $P(n\text{-}Bu)_3$] catalyzed living radical polymerization of MMA to give controlled molecular weights and narrow molecular weight distributions. Their high activities were supported by lower redox potentials with CV analysis. FT-IR analyses for reaction of the catalysts with the initiator revealed that the phosphine ligand promoted to an elimination of the carbonyl ligand to *in-situ* give a real active catalyst with 16e. They easily turn into active catalysts under the polymerization conditions; however they are stable enough to be treated under air. These features would be suitable for actual applications, along with the environmental aspects of a central iron.

Experimental Section

Materials

MMA (TCI; purity >99 %) and methyl acrylate (MA) (TCI; purity >99 %) were dried overnight over calcium chloride and purified by double distillation from calcium hydride before use. 2-Hydroxyethyl methacrylate (HEMA) (Aldrich; purity >99 %) was distilled under reduced pressure before use. Poly(ethyleneglycol) methacrylate [PEGMA; $CH_2{=}CMeCO_2(CH_2CH_2O)_nMe$; Me = CH_3; n = 8.5 on average] (Aldrich) and *N*,*N'*-dimethylaminoethyl methacrylate (DMAEMA) (TCI; purity >98 %) were purified by passing through an inhibitor removal column (Aldrich) and was subsequently degassed by three-time vacuum-argon bubbling cycles before use. The MMA dimer bromide [$H\text{-}(MMA)_2\text{-}Br$; $H\text{-}(CH_2CMeCO_2Me)_2\text{-}Br$] as an initiator was prepared according to literature.[26,27] $Cp_2Fe_2(CO)_4$ (Aldrich; purity >99 %) was used as received and handled in a glove box (M. Braun Labmaster 130) under a moisture- and oxygen-free argon atmosphere (H_2O <1 ppm; O_2 <1 ppm). Triphenylphosphine (PPh_3; Ph = C_6H_5) (Aldrich, purity >99 %), methyldiphenylphosphine ($PMePh_2$) (Aldrich; purity >99 %), dimethylphenylphosphine (PMe_2Ph) (Aldrich; purity >97 %), tributylphosphine [$P(n\text{-}Bu)_3$] (Aldrich; purity >97 %), triphenylphosphite [$P(OPh)_3$] (Aldrich; purity >97 %) were used as received. Toluene, dichloromethane (CH_2Cl_2) and *n*-hexane (all Kishida Kagaku; purity >99 %) were dried and

purified by passing through purification columns (Solvent Dispensing System; Glass Contour) and bubbled with dry nitrogen for more than 15 min immediately before use. Chloroform ($CHCl_3$) (Wako Chemicals; anhydrous; purity >99 %) was bubbled with dry nitrogen for more than 15 min immediately before use. *n*-Octane (internal standard for gas chromatography) and 1,2,3,4-tetrahydronaphthalene (tetralin; internal standard for ^{1}H NMR) were dried over calcium chloride and distilled twice from calcium hydride.

Catalyst Syntheses

$CpFe(CO)_2Br$ was prepared by the method of Fisher[28] and Hallam.[29] IR ($CHCl_3$): 2053, 2007 cm $^{-1}$ ν(CO). Anal. Calcd for $C_7H_5BrFeO_2$: C, 32.73; H, 1.96; Br, 31.11. Found: C, 33.17; H, 2.07; Br, 30.83. $CpFe(PMePh_2)_2Br$ was obtained by the method of Lehmkuhl et al.[30]

A series of $CpFe(CO)(L^{phos})Br$ were synthesized by the method of Treichel et al. as follows:[23] A toluene solution of $CpFe(CO)_2Br$ (1.0 g, 3.89 mmol) and 1.1 equivalent of phosphine [L^{phos} = PPh_3, $P(OPh)_3$, $PMePh_2$, PMe_2Ph, or $P(n\text{-}Bu)_3$] was magnetically stirred at 80 °C for 24 h under dry argon. The solutions gradually changed from rust to yellow-green irrespective of phosphine employed. The reaction mixture was then filtered at 25 °C to remove precipitates, and the filtrate was evaporated in vacuo to dryness to remove the solvent. The crude product was washed with *n*-hexane (15 mL × 3), dissolved in CH_2Cl_2 (8.0 mL), and recrystallized by gradual addition of *n*-hexane (40 mL), followed by standing at -30 °C for 72 h. The supernatant solvent were removed by a cannula with filter paper, and the crystal was washed with *n*-hexane (2.0 mL × 2) and dried under vacuum. The complexes were characterized by elemental analysis and 500-MHz ^{1}H-NMR spectroscopy at room temperature in $CDCl_3$ on a Jeol JNM-ECA500 spectrometer.

$CpFe(CO)(PPh_3)Br$: Isolated yield, 14 %. ^{1}H-NMR (ppm): 4.39 (s, 5H, Cp-*H*), 7.3-7.5 (m, 15H, Ar-*H*). IR ($CHCl_3$): 1963 cm^{-1} ν(CO). Anal. Calcd for $C_{24}H_{20}BrFeOP$: C, 58.69; H, 4.10; Br, 16.27. Found: C, 58.51; H, 4.07; Br, 16.49.

$CpFe(CO)[P(OPh)_3]Br$: Isolated yield, 86 %. ^{1}H-NMR (ppm): 4.17 (s, 5H, Cp-*H*), 7.15 (m, 3H, Ar-*H*), 7.38 (m, 12H, Ar-*H*). IR ($CHCl_3$): 1989 cm $^{-1}$ ν(CO). Anal. Calcd for $C_{24}H_{20}BrFeO_4P$: C, 53.47; H, 3.74; Br, 14.82. Found: C, 53.39; H, 3.80; Br, 14.58.

$CpFe(CO)(PMePh_2)Br$: Isolated yield, 32 %. ^{1}H-NMR (ppm): 2.04 (d, 3H, P-C*H*$_3$), 4.44 (s, 5H, Cp-*H*), 7.4-7.5 (m, 8H, Ar-*H*), 7.75-7.80 (m, 2H, Ar-*H*). IR ($CHCl_3$): 1959 cm $^{-1}$ ν(CO). Anal. Calcd for $C_{19}H_{18}BrFeOP$: C, 53.19; H, 4.23; Br, 18.62. Found: C, 53.63; H,

4.42; Br, 17.39.

CpFe(CO)(PMe_2Ph)Br: Isolated yield, 20 %. ^{1}H-NMR (ppm): 1.68 (d, 3H, P-C*H*$_3$), 2.06 (d, 3H, P-C*H*$_3$), 4.38 (s, 5H, Cp-*H*), 7.45 (m, 3H, Ar-*H*), 7.69 (t, 2H, Ar-*H*). IR ($CHCl_3$): 1956 cm $^{-1}$ ν(CO). Anal. Calcd for $C_{14}H_{16}BrFeOP$: C, 45.82; H, 4.39; Br, 21.77. Found: C, 46.35; H, 4.50; Br, 19.79.

CpFe(CO)[P(*n*-Bu)$_3$]Br: Isolated yield, 43 %. ^{1}H-NMR (ppm): 0.86 (t, 9H, C*H*$_3$), 1.3-1.4 (m, 12H, C*H*$_2$), 1.7-1.8 (q, 6H, P-C*H*$_2$), 4.47 (s, 5H, Cp-*H*). IR ($CHCl_3$): 1954 cm $^{-1}$ ν(CO). Anal. Calcd for $C_{18}H_{32}BrFeOP$: C, 50.14; H, 7.48; Br, 18.53. Found: C, 50.07; H, 7.64; Br, 18.35.

Polymerization Procedures

Polymerization was carried out by the syringe technique under dry argon in baked glass tubes equipped with a three-way stopcock or in sealed glass vials. A typical procedure for MMA polymerization with H-(MMA)$_2$-Br/CpFe(CO)($PMePh_2$)Br was as follows: In a 50-mL round-bottom flask were sequentially added CpFe(CO)($PMePh_2$)Br (21.5 mg, 0.05 mmol), toluene (2.23 mL), *n*-octane (0.27 mL), MMA (2.14 mL, 20 mmol), and H-(MMA)$_2$-Br (0.36 mL of 553.4 mM in toluene, 0.20 mmol) under dry argon at room temperature, where the total volume of the reaction mixture was thus 5.0 mL. Immediately after mixing, aliquots (0.80 mL each) of the solution were injected into glass tubes which were then sealed (except when a stopcock was used) and placed in an oil bath kept at desired temperature. In predetermined intervals, the polymerization was terminated by cooling the reaction mixtures to -78 ºC. Monomer conversion was determined from the concentration of residual monomer measured by gas chromatography with *n*-octane as an internal standard. The quenched reaction solutions were diluted with toluene (ca. 20 mL), washed with water three times, and evaporated to dryness to give the products that were subsequently dried overnight under vacuum at room temperature.

For PEGMA, DMAEMA and HEMA, the same procedures as described above were applied except that monomer conversion was determined by ^{1}H NMR from the integrated peak area of the olefinic protons of the monomers with tetralin as internal standard. The products were similarly isolated but without washing with water because of their hydrophilicity.

Model Reactions

Model reactions between the iron complex catalyst and H-$(MMA)_2$-Br as a dormant-end model were followed under an inert atmosphere by FT-IR spectroscopy with a JASCO FT/IR 4200 spectrometer. Typical procedures were as described below for $CpFe(CO)(PMePh_2)Br$: $CpFe(CO)(PMePh_2)Br$ (2.1 mg, 5.0×10^{-3} mmol), H-$(MMA)_2$-Br (5.6 mg, 0.020 mmol), and toluene (1.0 mL) were added under dry argon into a baked glass tube equipped with a three-way stopcock. The mixture was stirred at 60 °C for 8 h, and the solvent was removed by evaporation. The residue was dissolved in degassed $CHCl_3$ (1.0 mL), and the solution was transferred under dry argon into a sealed liquid KBr cell (optical path, 0.1 mm). Spectra were recorded at predetermined intervals.

Measurements

For poly(MMA) and poly(MA), M_n and M_w/M_n were measured by size-exclusion chromatography (SEC) in chloroform at 40 ºC on three polystyrene-gel columns [Shodex K-805L (pore size: 20-1000 Å; 8.0 mm i.d. × 30 cm); flow rate, 1.0 mL/min] connected to a Jasco PU-980 precision pump and a Jasco 930-RI refractive-index detector, and a Jasco 970-UV ultraviolet detector. The columns were calibrated against 13 standard poly(MMA) samples (Polymer Laboratories; M_n = 630–1,200,000; M_w/M_n = 1.06–1.22) as well as the monomer. For poly(PEGMA), poly(DMAEMA), and poly(HEMA), DMF containing 10 mM LiBr was applied as an eluent.

Cyclic voltammograms were recorded on a Hokuto Denko HZ-3000 apparatus. A typical procedure is as follows: $CpFe(CO)(PMePh_2)Br$ (15.0 mg, 0.035 mmol) was dissolved into a 100 mM solution of *n*-Bu_4NPF_6 (supporting electrolyte) in CH_2ClCH_2Cl (7.0 mL) under dry argon in a baked glass tube equipped with a three-way stopcock. Voltammograms were recorded under argon at a scan rate 0.1 Vs^{-1} in a three-electrode cell equipped with a platinum disk as a working electrode, a platinum wire as a counter electrode, and an Ag/AgCl electrode as a reference.

References and Notes

(1) Crabtree, R. H., Ed.; *The Organometallic Chemistry of the Transition Metals*; John Wiley & Sons, Inc.: New York, 2001.

(2) For recent reviews on transition metal catalyzed living radical polymerization, see: (a) Kamigaito, M.; Ando, T.; Sawamoto, M. *Chem. Rev.* **2001**, *101*, 3689-3745. (b) Kamigaito, M.; Ando, T.; Sawamoto, M. *Chem. Rec.* **2004**, *4*, 159-175. (c) Ouchi, M.; Terashima, T.; Sawamoto, M. *Acc. Chem. Res.* **2008**, *41*, 1120-1132. (d) Matyjaszewski, K.; Xja, J. *Chem. Rev.* **2001**, *101*, 2921-2990. (e) Matyjaszewski K., Ed.; *Controlled/Living Radical Polymerization From Synthesis to Materials*; ACS Symposium Series 944; American Chemical Society: Washington, DC, 2006.

(3) (a) Kato, M.; Kamigaito, M.; Sawamoto, M.; Higashimura, T. *Macromolecules* **1995**, *28*, 1721-1723. (b) Ando, T.; Kato, M.; Kamigaito, M.; Sawamoto, M. *Macromolecules* **1996**, *29*, 1070-1072.

(4) Wang, J. S.; Matyjaszewski, K. *J. Am. Chem. Soc.* **1995**, *117*, 5614-5615.

(5) Ando, T.; Kamigaito, M.; Sawamoto, M. *Macromolecules* **1997**, *30*, 4507-4510.

(6) Matyjaszewski, K.; Wei, M.; Xia, J.; McDermott, N. E. *Macromolecules* **1997**, *30*, 8161-8164.

(7) Kotani, Y.; Kamigaito, M.; Sawamoto, M. *Macromolecules* **1999**, *32*, 6877-6880.

(8) Kotani, Y.; Kamigaito, M.; Sawamoto, M. *Macromolecules* **2000**, *33*, 3543-3549.

(9) Zhu, S.; Yan, D. *Macromolecules* **2000**, *33*, 8233-8238.

(10) Louie, Y.; Grubbs, R. H. *Chem. Commun.* **2000**, 1479-1480.

(11) Gibson, V. C.; O'Reilly, R. K.; Reed, W.; Wass, D. F.; White, A. J. P.; Williams, D. J. *Chem. Commun.* **2002**, 1850-1851.

(12) Göbelt, B.; Matyjaszewski, K. *Macromol. Chem. Phys.* **2000**, *201*, 1619-1624.

(13) O'Reilly, R. K.; Gibson, V. C.; White, A. J. P.; Williams, D. J. *J. Am. Chem. Soc.* **2003**, *125*, 8450-8451.

(14) Xue, Z.; Lee, B. W.; Noh, S. K.; Lyoo, W. S. *Polymer* **2007**, *48*, 4704-4714.

(15) Niibayashi, S.; Hayakawa, H.; Jin, R-H.; Nagashima, H. *Chem. Commun.* **2007**, 1855-1857.

(16) Uchiike, C.; Terashima, T.; Ouchi, M.; Ando, T.; Kamigaito, M.; Sawamoto, M. *Macromolecules* **2007**, *40*, 8658-8662.

(17) Ferro, R.; Milione, S.; Bertolasi, V.; Capacchione, C.; Grassi, A. *Macromolecules* **2007***, 40,* 8544-8546.

(18) Uchiike, C.; Ouchi, M.; Ando, T.; Kamigaito, M.; Sawamoto, M. *J. Polym. Sci., Part A: Polym. Chem.* **2008**, *46*, 6819-6827.

(19) Chapter 1 of this thesis.

(20) Bolm, C.; Legros, J.; Paih, J. L.; Zani, L. *Chem. Rev.* **2004**, *104*, 6217-6254.

(21) Takahashi, H.; Ando, T.; Kamigaito, M.; Sawamoto, M. *Macromolecules* **1999**, *32*, 3820-3823.

(22) Watanabe, T.; Ando, T.; Kamigaito, M.; Sawamoto, M. *Macromolecules* **2001**, *34*, 4370-4374.

(23) Treichel, P. H.; Shubkin, R. L.; Barnett, K. W.; Reichard, D. *Inorg. Chem.* **1966**, *5*, 1177-1181.

(24) Ando, T.; Kamigaito, M.; Sawamoto, M. *Macromolecules* **2000**, *33*, 6732-6737.

(25) Fuji, Y.; Ando, T.; Kamigaito, M.; Sawamoto, M. *Macromolecules* **2002**, *35*, 2949-2954.

(26) Holland, K. A.; Rae, I. D. *Aust. J. Chem.* **1987**, *40*, 687-692.

(27) Ando, T.; Kamigaito, M.; Sawamoto, M. *Tetrahedron* **1997**, *53*, 15445-15457.

(28) Fischer, E. O.; Moser, E. *Inorg. Synth.* **1970**, *12*, 35-36.

(29) Hallam, B. F.; Pauson, P. L. *J. Chem. Soc.* **1956**, 3030-3037.

(30) Lehmkuhl, H.; Mehler, G. *Chem. Ber.* **1985**, *118*, 2407-2417.

Chapter 4

Carbonyl/*N*-heterocyclic Carbene (NHC) Hetero-Ligated Cp-Iron Catalyst: High Activity for Methyl Acrylate and Methyl Methacrylate

Abstract

In this chapter, the author employed a half-metallocene iron (II) carbonyl complex carrying *N*-heterocyclic carbene [i.e., 1,3-bis(2,4,6-trimethylphenyl)imidazol-2-ylidene: IMes] for living radical polymerization to see effects of the higher electron donating property on the catalysis. The complex, CpFe(CO)(IMes)Br, allowed "controlled" polymerization of methyl acrylate (MA) in conjunction with an bromide-initiator [H-(MMA)$_2$-Br] to give fairly narrow molecular weight distributions (MWDs: M_w/M_n ~1.3), while the phosphine derivative [CpFe(CO)(PMePh$_2$)Br] resulted in less controlled polymers with much broader MWDs for MA. A clear correlation between an electron donation of the ligand and a redox potential ($Fe^{II} \leftrightarrow Fe^{III}$) of the complex was also confirmed by FT-IR (wavelength of the CO ligand) and cyclic voltammetry (CV) with the series of complexes including the phosphine-based derivatives [CpFe(CO)(L^{phos})Br]: as the electron donation was higher, the redox potential lower; the carbene complex showed lowest redox potential among the examined. The low redox potential would lead to the predominant catalysis for the MA polymerization. The catalyst was active enough to control polymerization of methyl methacrylate (MMA) even for high polymerization degree condition (DP_n = 1000).

Introduction

N-heterocyclic carbene (NHC) is categorized as a singlet carbene bearing an occupied σ-orbital and a vacant p-orbital. Nitrogens in the vicinal position act as π-donors and σ-acceptors to fill the p-orbital of the carbene carbon and stabilize the carbene lone pair by negative inductive effect (Figure 1).[1] Thus, NHC can coordinate on a transition metal by giving the two electrons as a σ-donor ligand, and the electron donating ability is known to be higher than ubiquitous phosphine ligands. As the bulkiness is also tuned by the substituent on the nitrogen, NHC is currently available as a ligand to modify a state of the central metal for various catalytic reactions, similar to the phosphines.

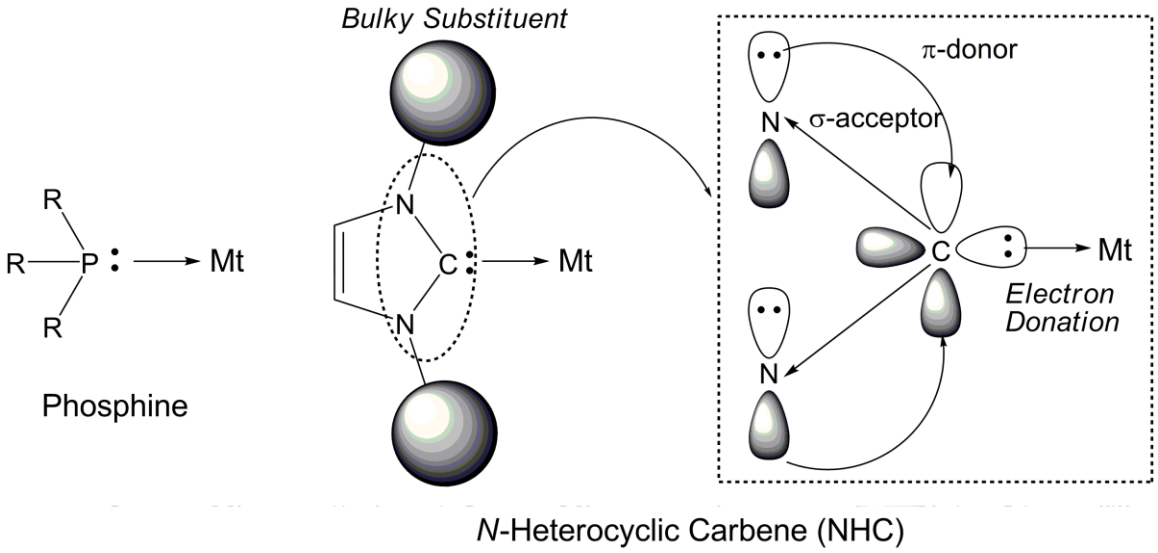

Figure 1. NHCs as electron-donating ligands

In a transition metal-catalyzed living radical polymerization[2,3] (Scheme 1), the transition metal complex serves as a catalyst to control the polymerization. In this system, the complex (Mt^n/L; n = valence number, L = ligands) reversibly activates the carbon-halogen bond in an initiator (R-X; X = halogen) or in a dormant polymer terminal (~~~C-X) to reduce a concentration of the propagating radical species (R• or ~~~C•) via the one-electron redox catalysis. A choice of the transition-metal complex is essential to achieve desired catalysis [e.g., activity/controllability and monomer versatility] and the catalytic activity depends on the ligand as well as the central metal. The author's group has reported that the stronger electron-donation from the ligands decreases the redox potential to enhance the activity.[4] As regarding a higher electron donation, NHC would be one of promising ligands.[5,6]

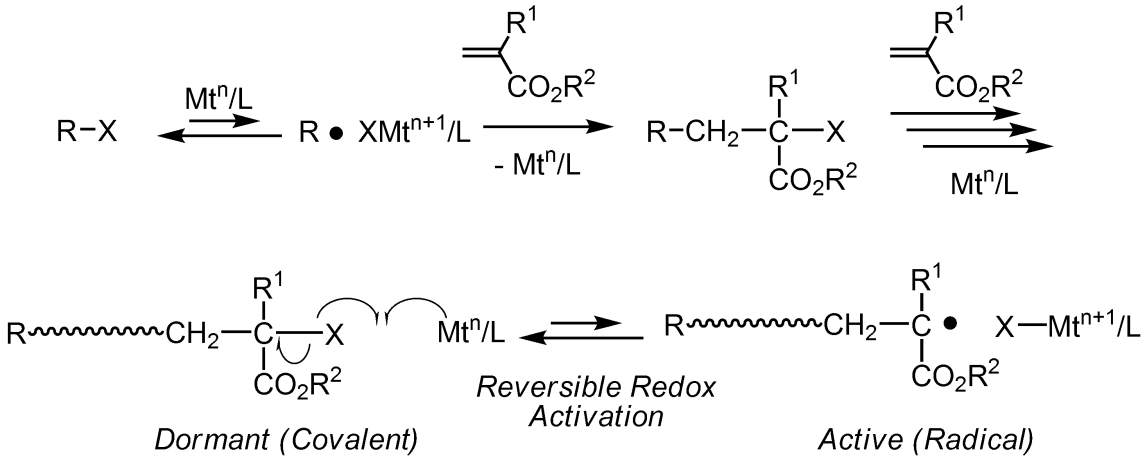

Scheme 1. Transition Metal-Catalyzed Living Radical Polymerization

Development of iron-catalysts for living radical polymerization has been paid attention because of the sustainable characters.[6-20] However, the activity is still inferior to those of the vanguards, such as ruthenium-[2] and copper-based[21] catalysts, and then the evolution has been required. The author has studied the catalyst design of iron complexes to increase the activity for living radical polymerizations. For example, as shown in Chapter 3, "hetero-ligation" of a phosphine ligand (L^{phos}) and carbonyl (CO) was effective to enhance the activity for cyclopentadienyl (Cp; η-C_5H_5) iron complexes [CpFe(CO)(L^{phos})Br; L^{phos} = PPh_3, $PMePh_2$, PMe_2Ph, P(*n*-Bu)$_3$].[22] These iron complexes were active for living radical polymerization of methyl methacrylate (MMA) to give well-controlled polymers and spectroscopic analyses of the model reaction indicated that the complexes irreversibly release the CO ligand to generate real active catalysts [CpFe(L^{phos})Br] via the activation process. The activity and CO-dissociation behavior depended on the phosphine ligand, and the electron donation from the phosphine ligand seemed to be important for the catalysis. Unfortunately, their utility was limited to the MMA polymerization, and they failed to catalyze polymerization of methyl acrylate (MA). To achieve wide application of monomers, another ligand design would be required.

Thus, the author focused on NHC as a high electron donating ligand for the iron complex. In this chapter, 1,3-bis(2,4,6-trimethylphenyl)imidazol-2-ylidene (IMes) was introduced as the NHC ligand on CpFe(CO)(L)Br, and the resultant complex [CpFe(CO)(IMes)Br] was employed for living radical polymerizations of MA and methyl methacrylate (MMA). The catalytic activity and the reaction mechanism were discussed with cyclic voltammetry (CV) and FT-IR analyses.

Results and Discussion

1. Synthesis and Analyses of CpFe(CO)(IMes)Br

The CO/NHC hetero-ligated complex [CpFe(CO)(IMes)Br] was synthesized by mixing a commercially available dicarbonyl CpFe complex [$CpFe(CO)_2Br$] and a NHC chloride (IMes-Cl) under UV-irradiation (Scheme 2).[23]

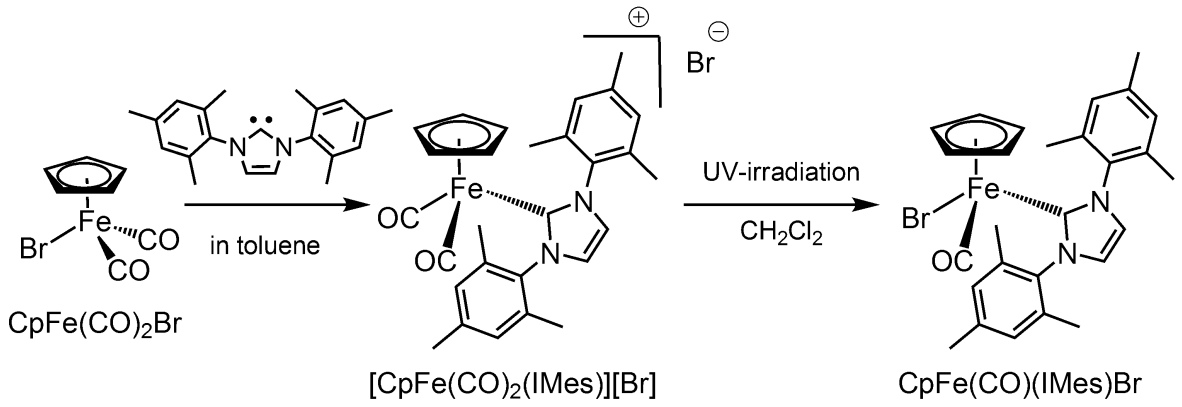

Scheme 2. Synthesis of $CpFe(CO)(L^{phos})Br$

Figure 2 shows the FT-IR spectrum of the isolated product, measured in $CHCl_3$ at 25 °C. For the starting compound [$CpFe(CO)_2Br$], two peaks were observed at 2053 cm^{-1} and 2007 cm^{-1}, attributed to the stretching frequency of C≡O, while they were disappeared and new one peak was appeared at 1950 cm^{-1} for the resulting complex, likely indicating one carbonyl ligand was substituted to the IMes ligand to give CpFe(CO)(IMes)Br. The stretching frequency of C≡O was known to show the electron-donor properties of another neutral ligand on the same metal, called as Tolman Electronic Parameter.[24] Indeed, the wavelength of CO became lower, as the basicity of phosphine ligand was increased for $CpFe(CO)(L^{phos})Br$.[22] The peak of CpFe(CO)(IMes)Br was further lower than every synthesized phosphine-ligated one [$CpFe(CO)(L^{phos})Br$], indicated that the IMes donates the electron to iron center more highly than the phosphine ligand similar to other nickel[25] and iridium[26] complexes.

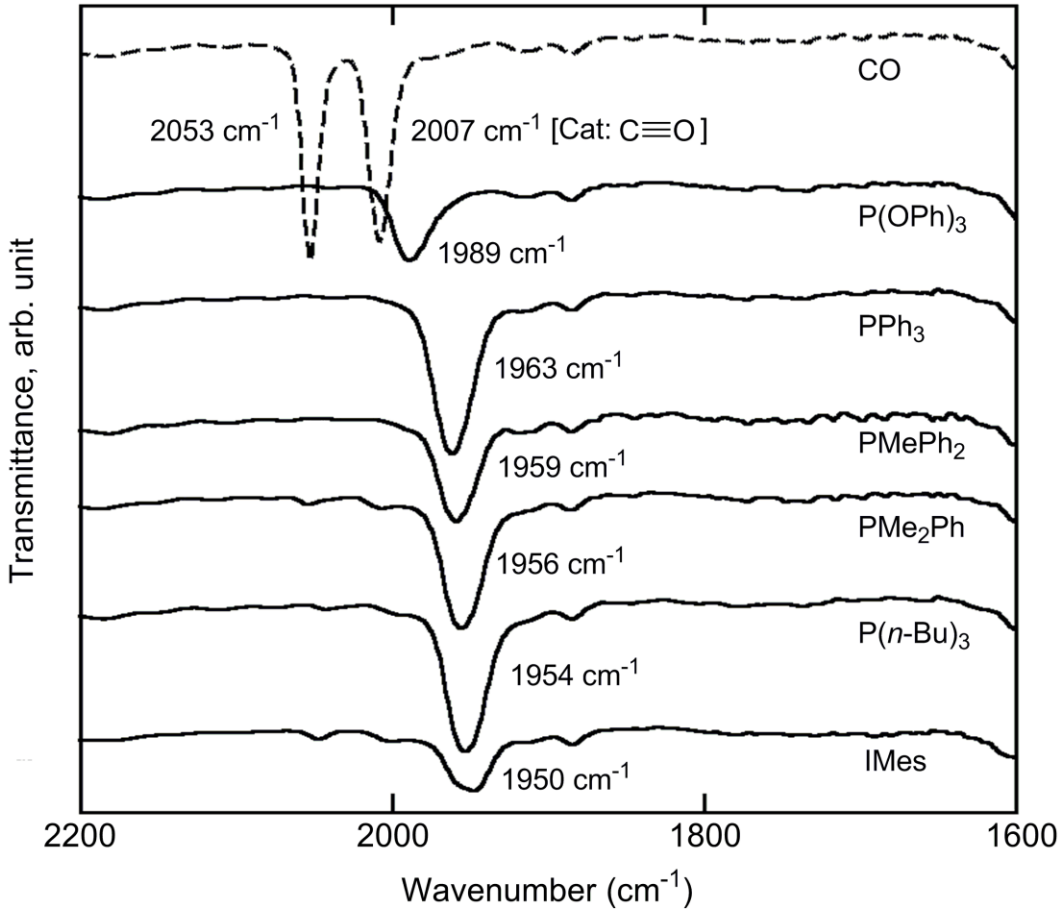

Figure 2. FT-IR spectra of CpFe(CO)(L)Br and $CpFe(CO)_2Br$ in $CHCl_3$ at 25 °C: [Iron complex]$_0$ = 5.0 mM.

Then, the redox potentials of CpFe(CO)(IMes)Br was measured by cyclic voltammetry (CV), since the electron donation from the ligand often contributes to a reduction in the redox potential leading to an enhancement of the catalytic activity for metal-catalyzed living radical polymerization. The solution in 1,2-dichloroethane was measured at 25 °C with *n*-Bu_4NPF_6 as a supporting electrolyte (100 mM, vs Ag/AgCl). The NHC complex showed a clear oxidation/reduction wave, likely assigned by one electron redox interconversion between Fe(II) and Fe(III). The half oxidation-reduction potential ($E_{1/2}$) was 0.52 V [$E_{1/2} = (E_{pa} + E_{pc})/2$; E_{pa}: oxidation potential; E_{pc}: reduction potential] which was clearly lower than the phosphine derivatives [$CpFe(CO)(L^{phos})Br$; $E_{1/2} \sim 0.7$-0.8 V].

Thus, the relationship between the $E_{1/2}$ and the C≡O stretching wavenumber was examined for the series of hetero-ligated CpFe complexes. As shown in Figure 3, there is a nice correlation between the two parameters: as the wavelength of CO is decreased, $E_{1/2}$ of the complex becomes lower; the NHC complex showed lowest redox potential among the

examined complexes. This result indicates that the electron donation from the ligand reduces the redox potential and the NHC complex is promising as a more active catalyst for living radical polymerization than the phosphine derivatives.

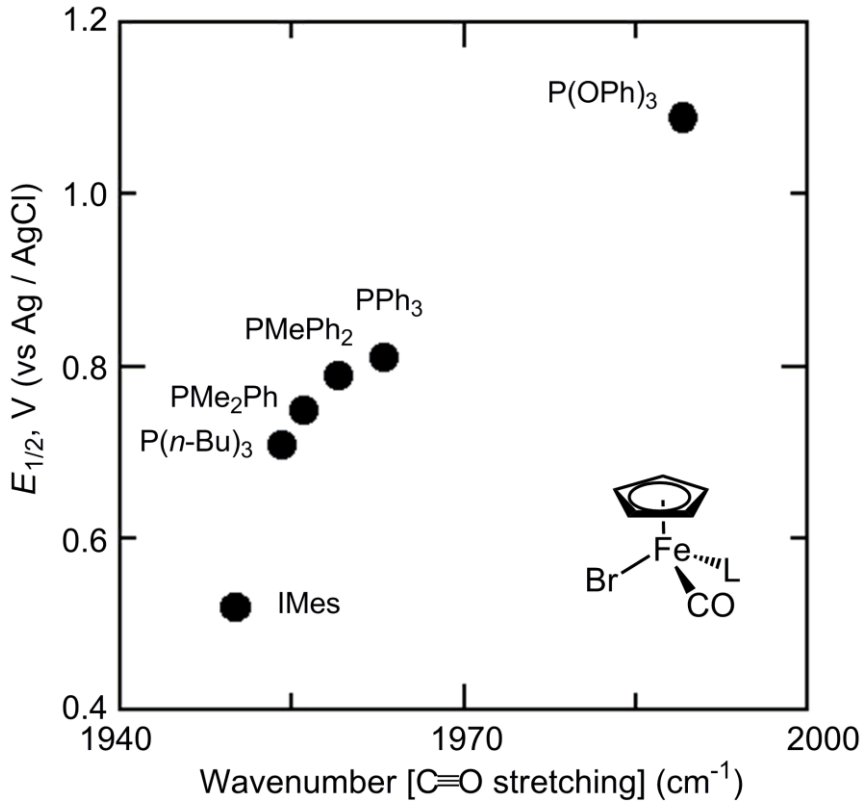

Figure 3. Correlations between half oxidation-reduction potentials measured by CV and CO stretching wavenumber of measured by FT-IR for CpFe(CO)(L)Br: CV: [Iron complex]$_0$ = 5.0 mM; [*n*-Bu_4NPF_6]$_0$ = 100 mM in $ClCH_2CH_2Cl$ at 25 °C. FT-IR: [Iron complex]$_0$ = 5.0 mM in $CHCl_3$ at 25 °C.

2. Polymerization of MA

As shown in Chapter 3, phosphine-ligated complexes [CpFe(CO)(L^{phos})Br] fairly catalyzed living radical polymerization for MMA, however they were less active for methyl acrylate (MA). For the polymerization control with MA, the tighter carbon-halogen bond needs to be activated because of the secondary carbon structure, and the more reactive radical species to be more smoothly capped than the MMA polymerization. From these points of view, a complex with lower redox potential would be suitable for the polymerization control. Thus, the author first employed the CpFe(CO)(IMes)Br with lower redox potential, for polymerization of MA, to compare with an active phosphine ligated complex,

$CpFe(CO)(PMePh_2)Br$. The polymerizations were done without an additive in conjunction with a bromide-initiator [H-$(MMA)_2$-Br] in toluene at 80 °C ($[MA]_0/[H\text{-}(MMA)_2\text{-}Br]_0/[catalyst]_0$ = 4000/40/10 mM) (Figure 4). The *N*-heterocyclic carbene catalyst showed a catalytic activity for the polymerization. Further, the molecular weight distributions of the produced poly(MA)s were narrower (MWDs; $M_w/M_n \sim 1.3$) than those with the phosphine-based catalyst ($M_w/M_n > 2$). These results showed that the IMes ligand improved the catalytic activity for polymerization of MA because of its higher electron donation.

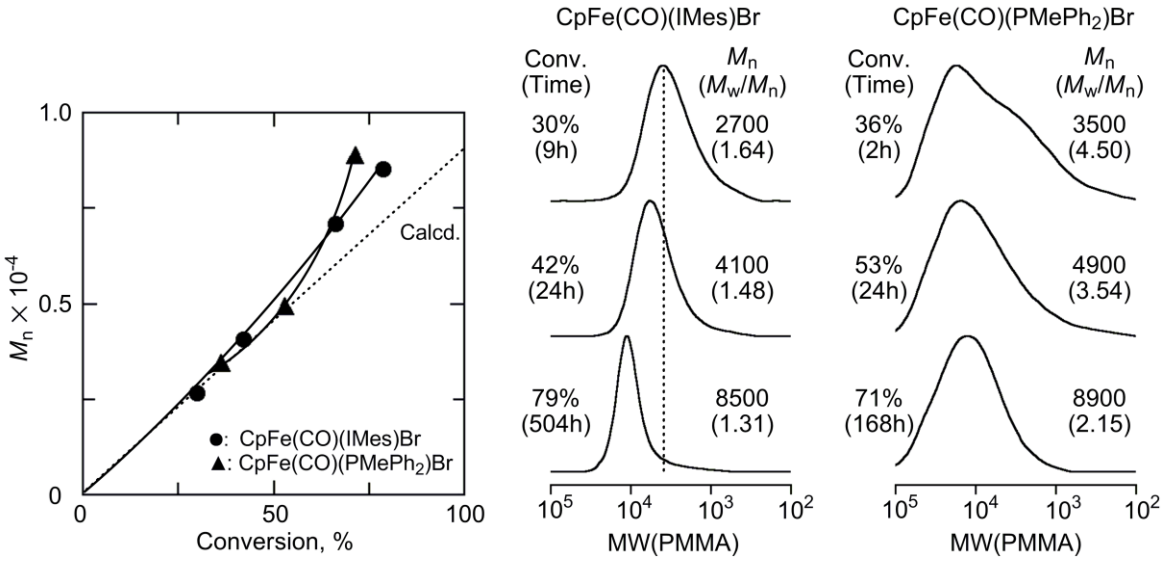

Figure 4. Comparisons between $CpFe(CO)(IMes)Br$ and $CpFe(CO)(PMePh_2)Br$ on living radical polymerization of MA with H-$(MMA)_2$-Br in toluene at 80 °C: $[MA]_0$ = 4000 mM; $[H\text{-}(MMA)_2\text{-}Br]_0$ = 40 mM; $[Iron\ catalyst]_0$ = 10 mM. Iron catalyst: $CpFe(CO)(IMes)Br$ (●); $CpFe(CO)(PMePh_2)Br$ (▲).

3. Polymerization of MMA

Then, the author employed $CpFe(CO)(IMes)Br$ for polymerization of MMA with bromide-initiator [H-$(MMA)_2$-Br] in toluene at 60 °C ($[MMA]_0/[H\text{-}(MMA)_2\text{-}Br]_0/[CpFe(CO)(IMes)Br]_0$ = 4000/40/10 mM) (Figure 5). The polymerization was almost quantitative: the conversion reached over 90% within 3 days. The molecular weights of the obtained polymers were increased in direct proportion to monomer conversion, and the values were close to the ideal ones, calculated from monomer/initiator ratio and the conversion. The controllability for the molecular weights was improved in comparison with the phosphine derivatives $CpFe(CO)(L^{phos})Br$ [$L^{phos} = PPh_3$,

$PMePh_2$, PMe_2Ph, P(*n*-Bu)$_3$] tending to give higher molecular weights,[22] as shown in Figure 5 with CpFe(CO)($PMePh_2$)Br. The MWDs were also controlled to be narrow (M_w/M_n ~ 1.2).

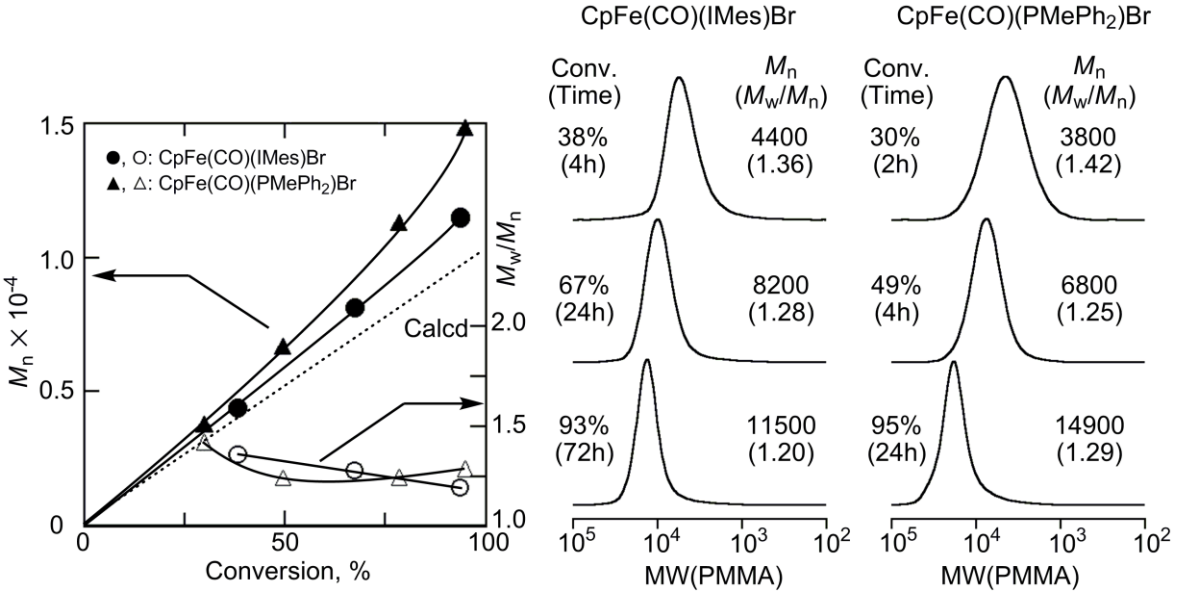

Figure 5. Comparisons between CpFe(CO)(IMes)Br and CpFe(CO)($PMePh_2$)Br on living radical polymerization of MMA with H-(MMA)$_2$-Br in toluene at 60 °C: [MMA]$_0$ = 4000 mM; [H-(MMA)$_2$-Br]$_0$ = 40 mM; [Iron catalyst]$_0$ = 10 mM. Iron catalyst: CpFe(CO)(IMes)Br (●, ○); CpFe(CO)($PMePh_2$)Br (▲, △).

4. Monomer Addition Experiments and Synthesis of High Molecular Weight PMMA

To check the living nature for the CpFe(CO)(IMes)Br catalyzed system, the author examined so called a "monomer-addition experiment". When the MMA-conversion reached around 73%, a fresh MMA was added to the polymerization solution. In the second phase, MMA was smoothly consumed to give additional 102% conversion (totally 175%) (Figure 6). The molecular weights were increased in direct proportion to the conversion, and the SEC curves shifted to higher molecular weight, although a slight tailing was detected. As a concurrent addition of the catalyst was not required, the catalyst was still active as well as the propagating ends.

Furthermore, the system was applied for synthesis of higher molecular weights PMMA targeting 10^5 of M_n for 100% conversion (the monomer/initiator ratio: 1,000). As shown in Figure 7, the conversions reached around 90% within 120 h and the MWDs were fairly narrow (M_w/M_n < 1.5), although a slight tailing was detected in lower molecular weight region. The molecular weights relatively agreed with the theoretical values even for nearly 10^5 of M_n. Such controlled syntheses of high DP_n, requiring frequent catalytic cycle, was

harder with CpFe(CO)($PMePh_2$)Br to give broader MWDs (M_w/M_n > 1.7). These results also indicated that the CO/IMes hetero-ligated complex [CpFe(CO)(IMes)Br] showed higher activity/controllability for living polymerization of MMA than the phosphine counterparts.

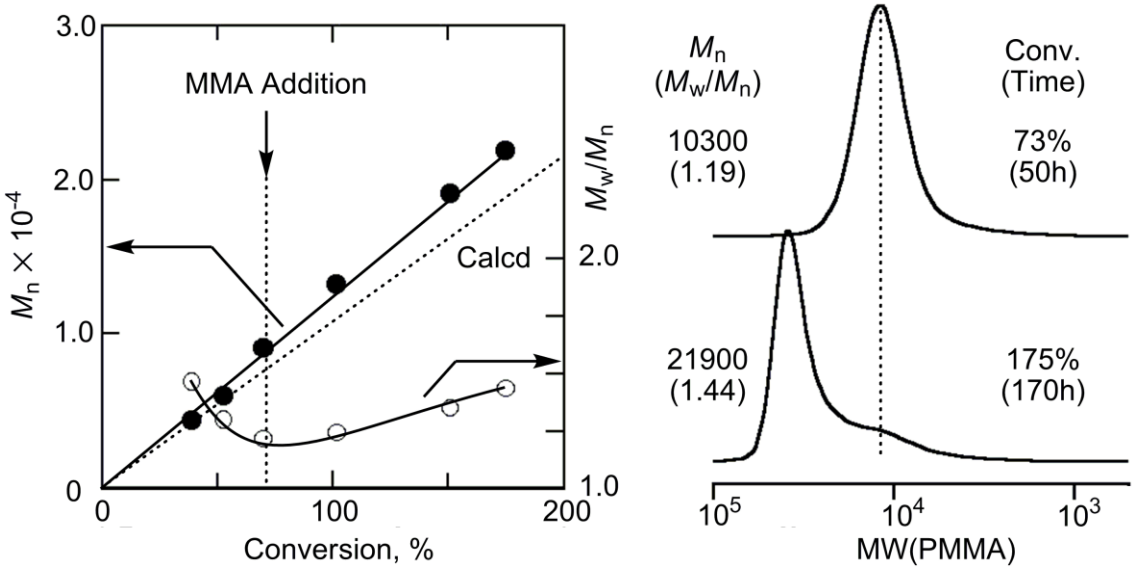

Figure 6. Monomer-addition experiment in the polymerization of MMA with H-$(MMA)_2$-Br/CpFe(CO)(IMes)Br in toluene at 60 °C: $[MMA]_0 = [MMA]_{add}$ = 4000 mM; $[H\text{-}(MMA)_2\text{-}Br]_0$ = 40 mM; $[CpFe(CO)(IMes)Br]_0$ = 10 mM.

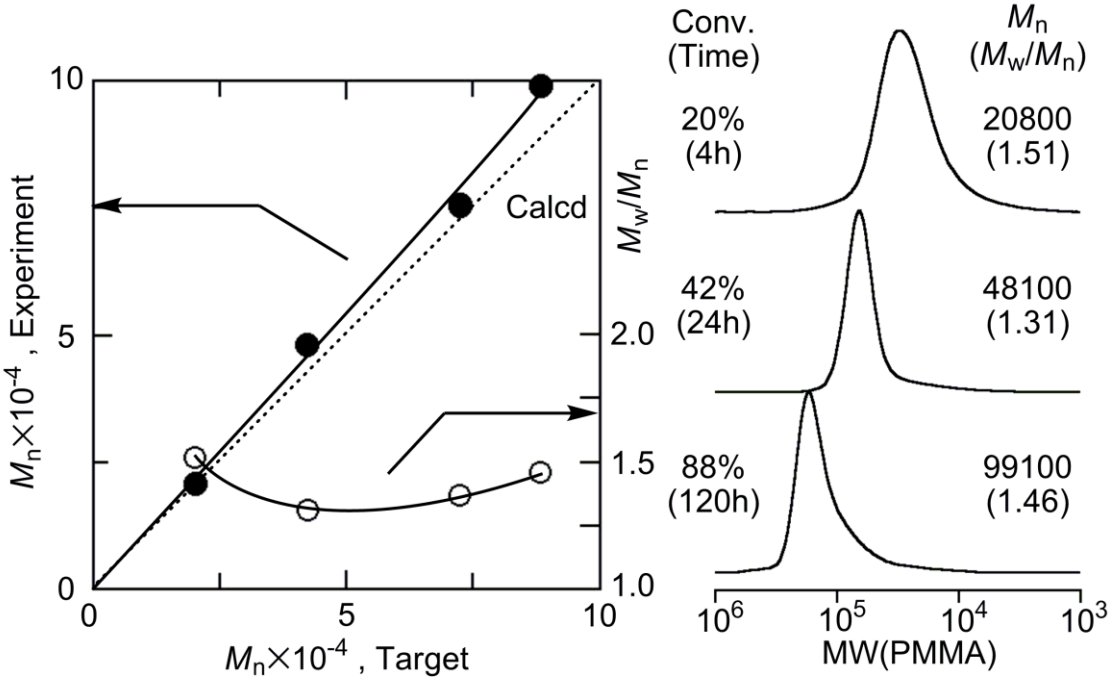

Figure 7. Synthesis of high molecular weight PMMA targeted 1000 mer with H-$(MMA)_2$-Br/CpFe(CO)(IMes)Br in toluene at 60 °C: $[MMA]_0$ = 5000 mM; $[H\text{-}(MMA)_2\text{-}Br]_0$ = 5.0 mM; $[CpFe(CO)(IMes)Br]_0$ = 2.0 mM.

5. FT-IR Analysis: Model Reaction

To examine the polymerization mechanism in this system, CpFe(CO)(IMes)Br was reacted with H-$(MMA)_2$-Br as a model compound for the growing "dormant" polymer in toluene at the polymerization temperature (60 °C), and the resulting mixture was analyzed by FT-IR. Figure 8 shows FT-IR spectra from 1600 to 2200 cm^{-1} of the mixture before (upper; dashed line) and after heating at 60 °C for 8 h (down; solid line) measured in $CHCl_3$, followed by an evaporation of toluene.

The peak at 1950 cm^{-1} is derived from C≡O stretching on CpFe(CO)(IMes)Br and that at around 1730 cm^{-1} is from the ester C=O in the initiator (see the dashed line). After heating, the peak around 1950 cm^{-1} was almost disappeared (see the solid line), indicating that the carbonyl ligand was irreversibly released via the activation of the initiator, same as the case with CpFe(CO)($PMePh_2$).[22] The transformation was also suggested by the color change

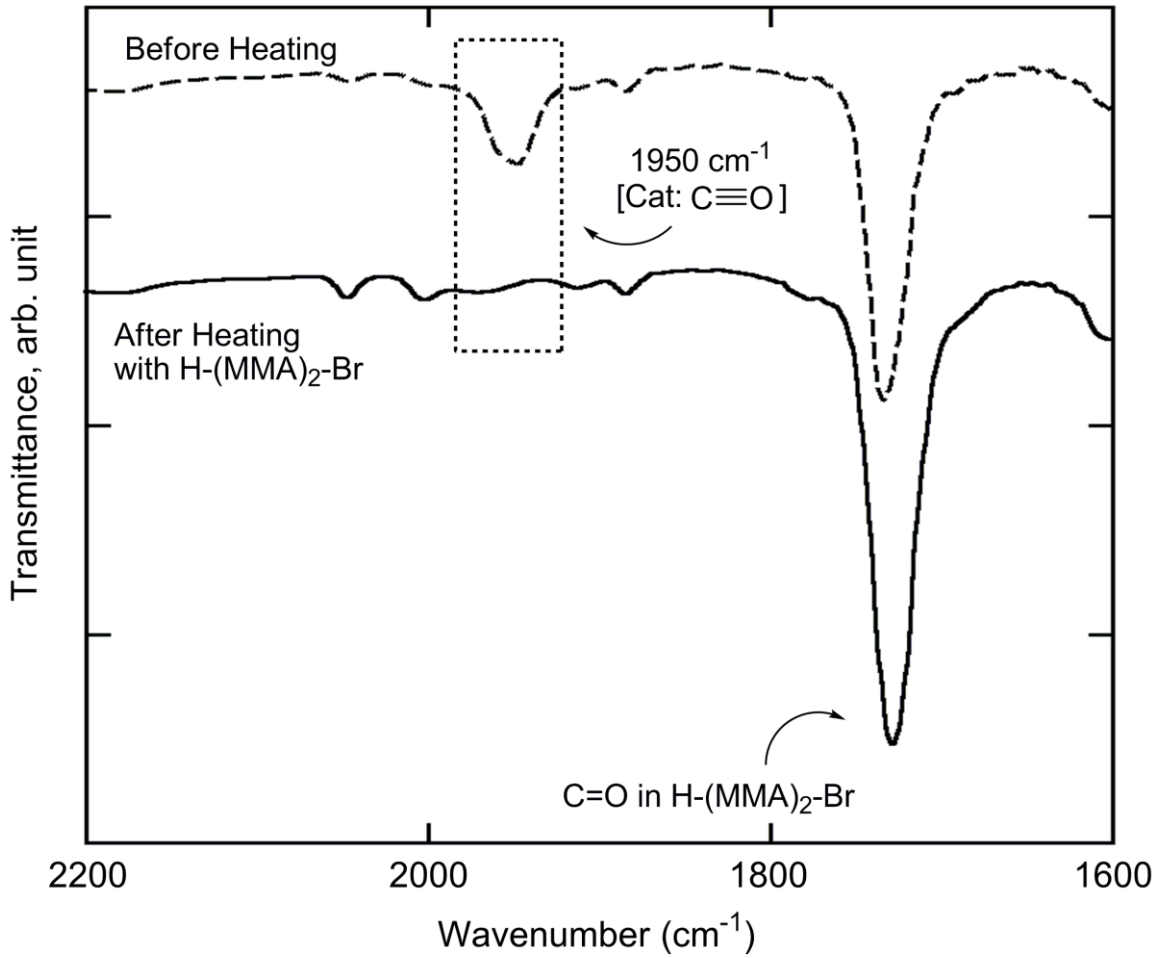

Figure 8. FT-IR analysis of H-$(MMA)_2$-Br/CpFe(CO)(IMes)Br in $CHCl_3$ at 25 °C: $[CpFe(CO)(IMes)Br]_0$ = 5.0 mM; $[H\text{-}(MMA)_2\text{-}Br]_0$ = 20 mM. Condition: "Before Heating" (dashed line); "After Heating", aged at 60 °C for 8 h with H-$(MMA)_2$-Br before measurement (solid line).

from pale green to reddish brown. Thus, the real active catalyst would be CpFe(IMes)Br with 16e, generated after the CO elimination.

On the other hand, two small peaks were newly generated at higher wavenumber (2050, 2005 cm^{-1}) after the model reaction. These peaks were almost same as a dicarbonyl iron complex [$CpFe(CO)_2Br$], and then the complex was possibly generated during the polymerization. However, as it was found that the dicarbonyl complex showed almost no catalytic activity for polymerization of MMA,[22] the complex might be uninvolved for the polymerization control.

Conclusion

The *N*-heterocyclic carbene-ligated iron complex [CpFe(CO)(IMes)Br] was effective as a catalyst for living radical polymerization. The catalytic activity was superior to the phosphine derivatives [$CpFe(CO)(L^{phos})Br$]: it was applicable for MA polymerization control; a finer control was achieved for MMA polymerization. The higher activity was demonstrated by the higher electron donation and the resultant lower redox potential, measured with FT-IR and CV. FT-IR analyses for a model reaction suggested that the original 18e complex turned into 16e one [CpFe(IMes)Br] via an activation of the initiator to work as a real active catalyst.

Experimental Section

Materials

MMA (TCI; purity >99%) was dried overnight over calcium chloride and purified by double distillation from calcium hydride before use. MA (TCI; purity >99%) was dried overnight over calcium chloride and purified by distillation from calcium hydride before use. The MMA dimer bromide [H-$(MMA)_2$-Br; H-$(CH_2CMeCO_2Me)_2$-Br] as an initiator was prepared according to literature.[27] $Cp_2Fe_2(CO)_4$ (Aldrich; purity >99%) and 1,3-bis(2,4,6-trimethylphenyl)imidazolium chloride (IMes-Cl) (Aldrich) were used as received and handled in a glove box (M. Braun Labmaster 130) under a moisture- and oxygen-free argon atmosphere (H_2O <1 ppm; O_2 <1 ppm). *t*-BuOK (Aldrich; 1M in THF)

was used as purchased. Toluene, THF, CH_2Cl_2 and *n*-hexane (Kishida Kagaku; purity >99%) were passed through purification columns (Solvent Dispensing System; Glass Contour) and bubbled with dry nitrogen for more than 15 min immediately before use. $CHCl_3$ (Wako Chemicals, anhydrous; purity >99%) was bubbled with dry nitrogen for more than 15 min immediately before use. *n*-Octane (internal standard for gas chromatography) was dried over calcium chloride and distilled twice from calcium hydride.

Catalyst Syntheses

$CpFe(CO)_2Br$[28] and $CpFe(CO)(PMePh_2)Br$[29] were synthesized according to literatures.

CpFe(CO)(IMes)Br was synthesized by the method of Buchgraber et al. as follows:[23] A mixture of IMes-Cl (1.076 g, 3.156 mmol) and *t*-BuOK (3.79 mL of 1M in THF; 3.790 mmol) in THF (15 mL) was stirred for 10 min at 0 °C and elevated to 25 °C for 1 h. After evaporation of the solvent, the free carbene was extracted in toluene (ca. 20 mL) and filtered with celite. The filtrate was added to $[CpFe(CO)_2Br]$ solution (733.0 mg in 15 mL toluene, 2.854 mmol) and stirred overnight at 25 °C. The yellow precipitate was gradually formed, seemed an ionic complex $[CpFe(CO)_2(IMes)]^+[Br]^-$. The solid was filtered, washed with toluene (5.0 mL × 2) and dried under vacuum.

The yellow solid was dissolved in CH_2Cl_2 (12 mL) and was irradiated under UV (Riko, UVL-400P; 400W) at 25 °C for 4 h. The solution turned to green. After evaporation of the solvent, washed with *n*-hexane (15 mL × 2) and dried under vacuum. The green solid was extracted in toluene (45 mL) and filtrate was evaporated under vacuo. The crude product was dissolved in CH_2Cl_2 (5.0 mL), and recrystallized by gradual addition of *n*-hexane (20 mL), followed by standing at -30 °C for 72 h. The supernatant solvent were removed by a cannula with filter paper, and the crystal was washed with *n*-hexane (2.0 mL × 2) and dried under vacuum. The complexes were characterized by elemental analysis, FT-IR spectroscopy at room temperature in $CHCl_3$ on JASCO FT/IR 4200 and 500-MHz ^{1}H-NMR spectroscopy at room temperature in CD_2Cl_2 on a Jeol JNM-ECA500 spectrometer.

Isolated yield, 26% (400 mg). ^{1}H-NMR (CD_2Cl_2, ppm): 2.06-2.08 (s, 12H, *o*-C*H*$_3$), 2.41 (s, 6H, *p*-C*H*$_3$), 3.95 (s, 5H, Cp-*H*), 7.07-7.11 (t, 6H, mes-C*H* and imidazolium-*H*). IR ($CHCl_3$): 1950 cm $^{-1}$ ν(CO). Anal. Calcd for $C_{27}H_{29}BrN_2FeO$: C, 60.81; H, 5.48; Br, 14.98. Found: C, 59.81; H, 5.61; Br, 16.95.

Polymerization Procedures

Polymerization was carried out by the syringe technique under dry argon in baked glass tubes equipped with a three-way stopcock or in sealed glass vials. A typical procedure for MMA polymerization with H-$(MMA)_2$-Br/CpFe(CO)(IMes)Br was as follows. In a 50-mL round-bottom flask CpFe(CO)(IMes)Br (26.7 mg, 0.05 mmol), toluene (2.23 mL), *n*-octane (0.27 mL), MMA (2.14 mL, 20 mmol), and H-$(MMA)_2$-Br (0.36 mL of 553.4 mM in toluene, 0.20 mmol) were added sequentially under dry argon at room temperature where the total volume of reaction mixture was thus 5.0 mL. Immediately after mixing, aliquots (0.80 mL each) of the solution were injected into glass tubes which were then sealed (except when a stopcock was used) and placed in an oil bath kept at desired temperature. In predetermined intervals, the polymerization was terminated by cooling the reaction mixtures to -78 ºC. Monomer conversion was determined from the concentration of residual monomer measured by gas chromatography with *n*-octane as an internal standard. The quenched reaction solutions were diluted with toluene (ca. 20 mL), washed with water three times, and evaporated to dryness to give the products that were subsequently dried overnight under vacuum at room temperature.

Measurements

For poly(MMA) and poly(MA), M_n and M_w/M_n were measured by size-exclusion chromatography (SEC) in chloroform at 40 ºC on three polystyrene-gel columns [Shodex K-805L (pore size: 20-1000 Å; 8.0 mm i.d. × 30 cm); flow rate, 1.0 mL/min] connected to a Jasco PU-980 precision pump and a Jasco 930-RI refractive-index detector, and a Jasco 970-UV ultraviolet detector. The columns were calibrated against 13 standard poly(MMA) samples (Polymer Laboratories; M_n = 630-1,200,000; M_w/M_n = 1.06-1.22) as well as the monomer.

Cyclic voltammograms were recorded by using a Hokuto Denko HZ-3000 apparatus. A typical procedure is as follows: CpFe(CO)(IMes)Br (13.3 mg, 0.025 mmol) was dissolved into a 100 mM solution of *n*-Bu_4NPF_6 (supporting electrolyte) in CH_2ClCH_2Cl (5.0 mL) under dry argon in a baked glass tube equipped with a three-way stopcock. Voltammograms were recorded under argon at a scan rate 0.1 Vs^{-1} in a three-electrode cell equipped with a platinum disk as a working electrode, a platinum wire as a counter electrode, and an Ag/AgCl electrode as a reference.

FT-IR spectra of the CpFe(CO)(IMes)Br was recorded by using JASCO FT/IR 4200. The sample-was prepared that CpFe(CO)(IMes)Br (2.7 mg, 5.0×10^{-3} mmol), H-$(MMA)_2$-Br (5.6 mg, 0.020 mmol) and toluene (1.0 mL) were added into the baked glass tube equipped with a three-way stopcock under dry argon. After mixing at 60 °C for 8 h, the solvent was evaporated. The residue was dissolved in degassed $CHCl_3$ and purged in the sealed liquid KBr cell where the thickness was 0.1 mm. Measurements were carried out under inert atmosphere.

References and Notes

(1) (a) Herrmann, W. A.; Köcher, C. *Angew. Chem., Int. Ed. Engl.* **1997**. *36*, 2162-2187. (b) Herrmann, W. A. *Angew. Chem., Int. Ed.* **2002**. *41*, 1290-1309. (c) Herrmann, W. A.; Weskamp, T.; Böhm, V. P. W. *Adv. Organomet. Chem.* **2002**, *48*, 1-69.

(2) (a) Kato, M.; Kamigaito, M.; Sawamoto, M.; Higashimura, T. *Macromolecules* **1995**, *28*, 1721-1723. (b) Ando, T.; Kato, M.; Kamigaito, M.; Sawamoto, M. *Macromolecules* **1996**, *29*, 1070-1072.

(3) For recent reviews on transition metal catalyzed living radical polymerization, see: (a) Kamigaito, M.; Ando, T.; Sawamoto, M. *Chem. Rev.* **2001**, *101*, 3689-3745. (b) Kamigaito, M.; Ando, T.; Sawamoto, M. *Chem. Rec.* **2004**, *4*, 159-175. (c) Ouchi, M.; Terashima, T.; Sawamoto, M. *Acc. Chem. Res.* **2008**, *41*, 1120-1132. (d) Ouchi, M.; Terashima, T.; Sawamoto, M. *Chem. Rev.* **2009**, *109*, 4963-5050. (e) Matyjaszewski, K.; Xja, J. *Chem. Rev.* **2001**, *101*, 2921-2990. (f) Controlled/Living Radical Polymerization From Synthesis to Materials; Matyjaszewski K., Ed.; ACS Symposium Series 944; American Chemical Society: Washington, DC, 2006.

(4) (a) Ando, T.; Kamigaito, M.; Sawamoto, M. *Macromolecules* **2000**, *33*, 5825-5829. (b) Watanabe, T.; Ando, T.; Kamigaito, M.; Sawamoto, M. *Macromolecules* **2001**, *34*, 4370-4374. (c) Kamigaito, M.; Watanabe, Y.; Ando, T.; Sawamoto, M. *J. Am. Chem. Soc.* **2002**. *124*, 9914-9915.

(5) NHC ligands for ruthenium complexes in living radical polymerizations, see: (a) Simal, F.; Delfosse, S.; Demonceau, A.; Noels, A. F.; Denk, K.; Kohl, F. J. Weskamp, T.; Herrmann, W.A. *Chem. Eur. J.* **2002**, *8*, 3047-3052. (b) Delaude, L.; Delfosse, S.; Richel, A.; Demonceau, A.; Noels, A. F. *Chem. Commun.* **2003**, 1526-1527.

(6) NHC ligands for iron complexes in living radical polymerizations, see: Louie, Y.; Grubbs, R. H. *Chem. Commun.* **2000**, 1479-1480.

(7) Ando, T., Kamigaito, M.; Sawamoto, M. *Macromolecules* **1997**, *30*, 4507-4510.

(8) Matyjaszewski, K.; Wei, M.; Xia, J.; McDermott, N. E. *Macromolecules* **1997**, *30*, 8161-8164.

(9) Kotani, Y.; Kamigaito, M.; Sawamoto, M. *Macromolecules* **1999**, *32*, 6877-6880.

(10) Kotani, Y.; Kamigaito, M.; Sawamoto, M. *Macromolecules* **2000**, *33*, 3543-3549.

(11) Zhu, S.; Yan, D. *Macromolecules* **2000**, *33*, 8233-8238.

(12) Göbelt, B.; Matyjaszewski, K. *Macromol. Chem. Phys.* **2000**, *201*, 1619-1624.

(13) Gibson, V. C.; O'Reilly, R. K.; Reed, W.; Wass, D. F.; White, A. J. P.; Williams, D. J. *Chem. Commun.* **2002**, 1850-1851.

(14) O'Reilly, R. K.; Gibson, V. C.; White, A. J. P.; Williams, D. J. *J. Am. Chem. Soc.* **2003**, *125*, 8450-8451.

(15) Xue, Z.; Lee, B. W.; Noh, S. K.; Lyoo, W. S. *Polymer* **2007**, *48*, 4704-4714.

(16) Niibayashi, S.; Hayakawa, H.; Jin, R-H.; Nagashima, H. *Chem. Commun.* **2007**, 1855-1857.

(17) Uchiike, C.; Terashima, T.; Ouchi, M.; Ando, T.; Kamigaito, M.; Sawamoto, M. *Macromolecules* **2007**, *40*, 8658-8662.

(18) Ferro, R.; Milione, S.; Bertolasi, V.; Capacchione, C.; Grassi, A. *Macromolecules* **2007**, *40*, 8544-8546.

(19) Uchiike, C.; Ouchi, M.; Ando, T.; Kamigaito, M.; Sawamoto, M. *J. Polym. Sci., Part A: Polym. Chem.* **2008**, *46*, 6819-6827.

(20) Chapter 1 in this thesis.

(21) Wang, J. S.; Matyjaszewski, K. *J. Am. Chem. Soc.* **1995**, *117*, 5614-5615.

(22) Chapter 3 in this thesis.

(23) Buchgraber, P.; Toupet, L.; Guerchais, V. *Organometallics* **2003**, *22*, 5144-5147.

(24) Tolman, C. A. *Chem. Rev.* **1977**, *77*, 313-348.

(25) Dorta, R; Stevens, E. D.; Scott, N. M.; Costabile, C.; Cavallo, L.; Hoff, C. D.; Nolan, S. P. *J. Am. Chem. Soc.* **2005**, *127*, 2485-2495.

(26) Kelly, R. A. III; Clavier, H.; Giudice, S.; Scott, N. M.; Stevens, E. D.; Bordner, J.; Samardjiev, I.; Hoff, C. D.; Cavallo, L.; Nolan, S. P. *Organometallics* **2008**, *27*, 202-210.

(27) Ando, T.; Kamigaito, M.; Sawamoto, M. *Tetrahedron* **1997**, *53*, 15445-15457.

(28) (a) Fischer, E. O.; Moser, E. *Inorg. Synth.* **1970**, *12*, 35-36. (b) Hallam, B. F.; Pauson, P. L. *J. Chem. Soc.* **1956**, 3030-3037.

(29) Treichel, P. H.; Shubkin, R. L.; Barnett, K. W.; Reichard, D. *Inorg. Chem.* **1966**, *5*, 1177-1181.

Chapter 5

Pentamethylcyclopentadienyl (Cp*) Iron Catalysts: High Activity and Versatility for Functional Monomers

Abstract

A series of pentamethylcyclopentadienyl Fe(II) complexes, ligated by one carbonyl (CO) and one phosphine [Cp*Fe(CO)(L^{phos})Br; Cp* = C_5Me_5; L^{phos} = PPh_3, $PMePh_2$, PMe_2Ph, P(*m*-tol)$_3$, and P(*p*-tol)$_3$], were employed for living radical polymerization. In conjunction with a bromide initiator [H-(MMA)$_2$-Br], these Cp*Fe complexes catalyzed living radical polymerization of methyl methacrylate (MMA) better controlled than those with the corresponding cyclopentadienyl (Cp) complexes [CpFe(CO)(L^{phos})Br; Cp = C_5H_5]. The finer control was demonstrated by successful monomer-addition experiments, a wider range of controllable molecular weight (M_n = 10^4-10^5 or DP_n = 100-1000), and narrower molecular weight distributions (M_w/M_n ~ 1.2). FT-IR analysis of initiator-catalyst model reactions showed that an efficient carbonyl release from the original coordinatively saturated 18e complex into the unsaturated 16e form is important in the catalysis to generate a growing radical from the initiator. The higher catalytic activity allowed controlled polymerizations of other monomers that are not available for the Cp catalysts, such as methyl acrylate and a functional methacrylate with poly(ethylene glycol) pendent group.

Introduction

Transition metal-catalyzed living radical polymerization is one of powerful tools to prepare controlled polymeric architectures for a wide variety of commodity as well as functional monomers (Scheme 1).[1] In this system, a metal catalyst is critical in controlling molecular weight and its distribution, polymerization rate, and versatility in terms of monomers and reaction conditions. The catalyst (Mt^n; n = valence number) activates the carbon-halogen bond in an initiator (R-X; X = halogen) or in a dormant polymer terminal (~~~C-X) via homolytic cleavage to generate a carbon-centered growing radical (R・ or ~~~C・), while undergoing one electron-oxidation from Mt^n to Mt^{n+1}. The radical species are capable of initiating radical propagation, and after some growing steps with monomers, they are capped with the halogen in the oxidized catalyst (Mt^{n+1}), thereby to regenerate a dormant species and the original lower valence-state complex (Mt^n). Among transition metals, ruthenium (Ru)[2] and copper (Cu)[3] complexes are highly active and induce not only living homopolymerizations but also random and block copolymerizations of many monomers.

Iron complexes offer another class of transition metal catalysts that are increasingly getting important: environmentally benign, safe, less toxic, biocompatible, and abundant.[4] Since the first successful report with $FeCl_2(PPh_3)_2$,[5] the potency of divalent iron (Fe^{II})

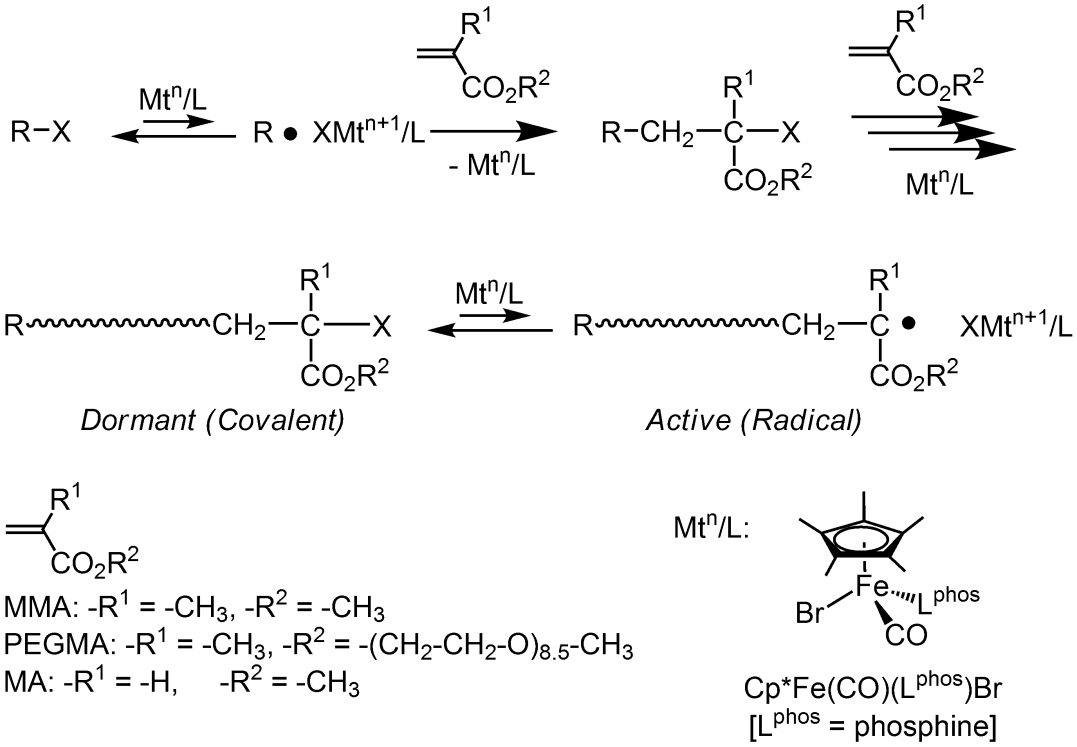

Scheme 1. Transition-Metal Catalyzed Living Radical Polymerization

complexes in living radical polymerization has in fact been demonstrated.[6-19] However, as polymerization catalysts, iron complexes are generally inferior to ruthenium and copper counterparts, especially in terms of versatility and tolerance of polar monomers and solvents.

To overcome these problems, a saturated (18 electron) half-metallocene iron complexes would be promising for active catalysts, if the author follow his research group's previous structural design for active ruthenium-based vanguards [e.g., (Ind)$RuCl(PPh_3)_2$[20] and $Cp^*RuCl(PPh_3)_2$;[21] Ind (indenyl) = C_9H_7; Cp* (pentamethylcyclopentadienyl) = η-C_5Me_5], whose metal belongs to group 8 as with iron. The stronger electron-donation from the multiple ligands would enhance catalytic activity for the living radical polymerization involving one electron redox. Most importantly, it has been proposed that the saturated "18e" complexes need to turn into unsaturated "16e" forms via a ligand release to accept a halogen on the activation process. The transformation should be one of the most essential processes for superior catalysis or polymerization control.[22]

In Chapter 3, the author focused on 18e "hetero-ligated" cyclopentadienyl iron complexes coordinated with a carbonyl (CO) and a phosphine [$CpFe(CO)(L^{phos})Br$; L^{phos} = phosphine] and expected that either ligand would be selectively and smoothly released on the activation. Because of the coordinatively saturated 18e structure and the robust coordination of a CO ligand, these catalysts indeed turned out to be highly active in living radical polymerization of methyl methacrylates (MMA) and, when isolated, to be so stable as to be handled even under air at room temperature. Once they encounter an initiator (R-Br) at 60 °C, however, they immediately and irreversibly release the CO ligand to generate *in-situ* a real active catalyst [$CpFe(L^{phos})Br$] that is active enough to induce living radical polymerization of MMA. However, their catalytic activity is insufficient to polymerize acrylates and polar functional methacrylates.

In this chapter, the author designed pentamethylcyclopentadienyl iron(II) complexes [$Cp^*Fe^{II}(CO)(L^{phos})Br$] with a similar carbonyl-phosphine hetero ligation toward further

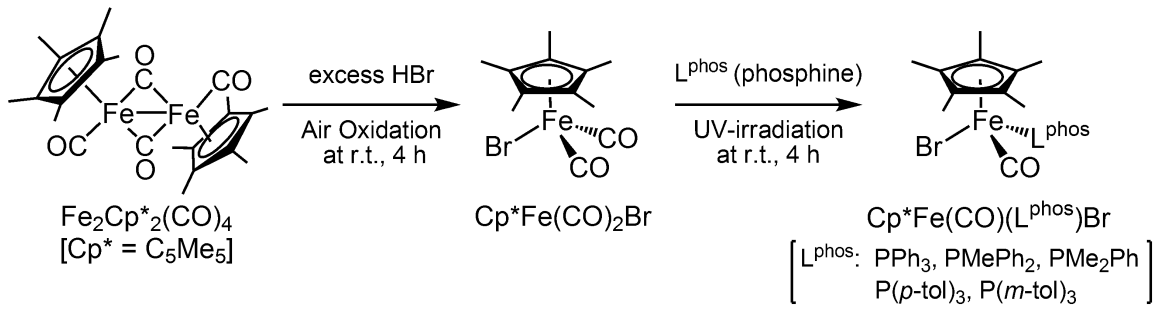

Scheme 2. Synthesis of $Cp^*Fe(CO)(L^{phos})Br$

improvement of the Cp-iron catalyst family, i.e., to be more active, easier to handle, and more versatile and tolerant of functional monomers. The design is in part based on ruthenium complexes that the high electron ability of Cp* ligand enhances catalytic activity.[21,23] Thus, a series of Cp*Fe(CO)(L^{phos})Br were prepared by the reactions of Cp*Fe$(CO)_2$Br with phosphine under UV-irradiation (Scheme 2).[24] They accordingly showed better catalytic performances in MMA polymerization than the CpFe catalysts in terms of molecular weight control and sustained activity (up to >90% conversion). More importantly, some Cp* complexes gave controlled polymers even from methyl acrylate (MA) and a methacrylate (PEGMA) carrying a poly(ethylene glycol) pendent group.

Results and Discussion

1. Ligand Effects on the Catalytic Performance of Cp*Fe(CO)(L^{phos})Br

To investigate the effects of the phosphine ligands in hetero ligation, the author first employed a series of Cp*Fe(CO)(L^{phos})Br [L^{phos} = PPh_3, $PMePh_2$, PMe_2Ph, P(*m*-tol)$_3$, and P(*p*-tol)$_3$] and their common dicarbonyl precursor [Cp*Fe$(CO)_2$Br] for living radical polymerization of MMA in toluene at 60 °C ($[MMA]_0/[H\text{-}(MMA)_2\text{-}Br]_0/[\text{iron complex}]_0$ = 4000/40/10 mM) (Figure 1). All the hetero-ligated complexes induced smooth polymerization, and monomer conversion reached over 90% within 48 h [Figure 1(A)]. The molecular weights of the obtained PMMAs were increased in direct proportion to monomer conversion and were close to the calculated values assuming that one initiator produced one polymer chain [Figure 1(B)]. After the polymerizations, the brown color, derived from the catalyst, was disappeared to be transparent by water-washing, indicating "catalyst removal" possible. On the other hand, the dicarbonyl version resulted in a slower polymerization, a limited conversion (~50%) and poorly controlled molecular weight distributions (MWDs; $M_w/M_n > 2$). In this case, the catalyst color was not disappeared via the water-washing procedure after the polymerization. Thus, the hetero-ligated complexes were more active and better catalysts.

Within the Cp*Fe family, polymerization rate was dependent on the phosphine ligands: P(*p*-tol)$_3$ ≈ P(*m*-tol)$_3$ ≈ $PMePh_2$ > PPh_3 > PMe_2Ph. This would be linked to the structural conversion of the saturated 18e complex into the corresponding unsaturated 16e variant upon the halogen abstraction from the dormant carbon-halogen terminal, as demonstrated for CpFe(CO)(L^{phos})Br.[25]

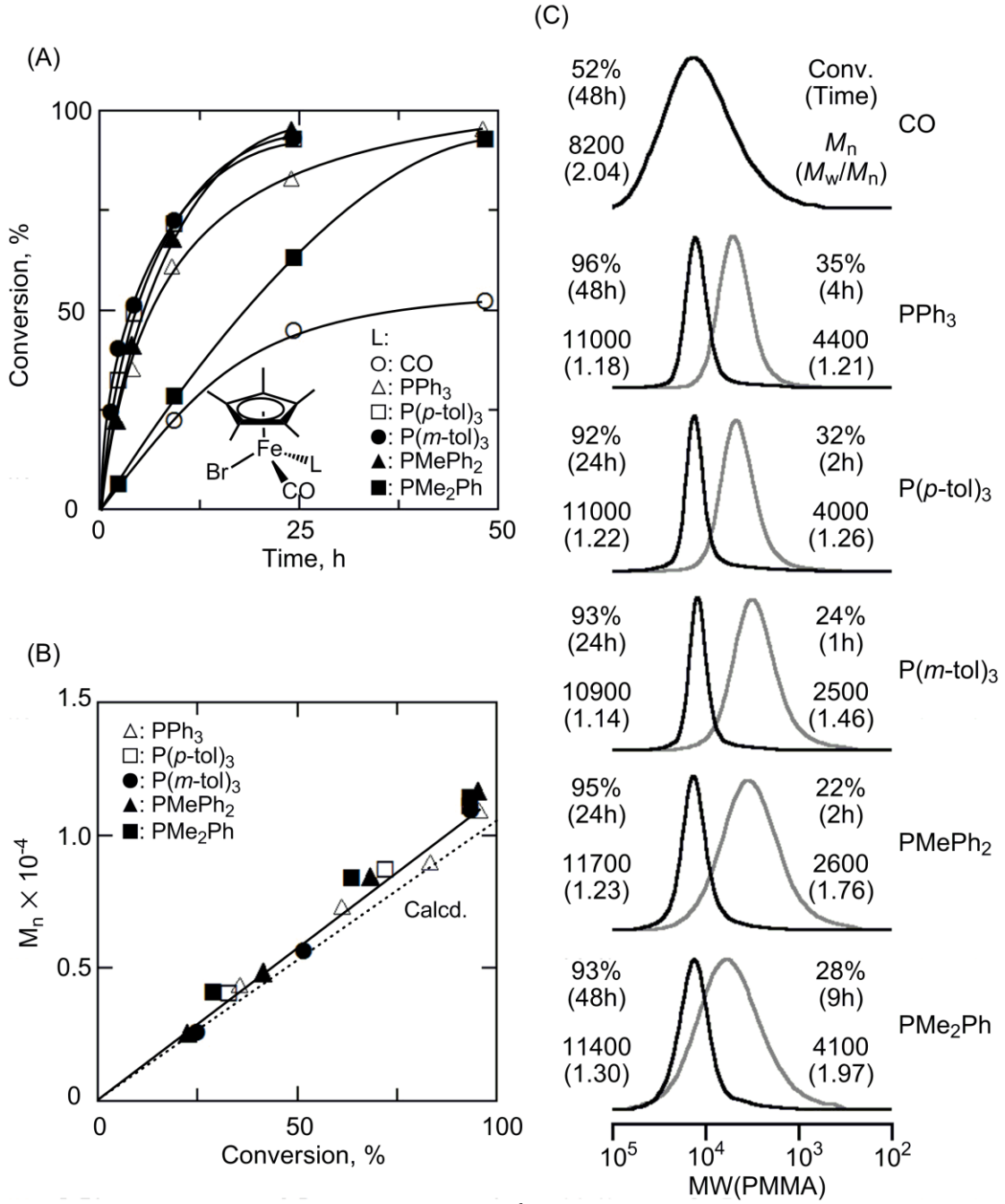

Figure 1. Ligand effects of Cp*Fe(CO)(L^{phos})Br on living radical polymerization of MMA with H-$(MMA)_2$-Br in toluene at 60 °C: $[MMA]_0$ = 4000 mM; $[H\text{-}(MMA)_2\text{-}Br]_0$ = 40 mM; $[Cp^*Fe(CO)(L^{phos})Br]_0$ = 10 mM. Ligand: CO (○); PPh_3 (△); P(*p*-tol)$_3$ (□); P(*m*-tol)$_3$ (●); $PMePh_2$(▲); PMe_2Ph (■). (A) Time-conversion plots; (B) Conversion-M_n plots; (C) SEC curves.

2. Model Reactions with Dormant End Model

Thus, model reactions of the Cp*Fe catalysts with the initiator [H-$(MMA)_2$-Br] at the polymerization temperature (60 °C) were analyzed by monitoring changes in the carbonyl

ligands by FT-IR; H-$(MMA)_2$-Br was considered as the smallest homolog of the dormant PMMA species capped with bromine. Figure 2 shows FT-IR spectra (1600-2200 cm^{-1} region) of a catalyst-initiator equimolar mixture before (upper) and after (down) the reactions. The peaks at around 1900-2000 cm^{-1} are derived from the C≡O stretching of the ligand and those around 1730 cm^{-1} from the ester C=O in the initiator.

Notably, upon mixing with the dormant model, the carbonyl signals of all Cp*Fe(CO)(L^{phos})Br catalysts but the PMe_2Ph derivative almost disappeared [Figure 2(A)-(D)], suggesting conversion of the saturated and hetero-ligated 18e complexes into carbonyl-free unsaturated 16e complexes Cp*Fe(L^{phos})Br.

The same model systems were also analyzed by ^{31}P NMR spectroscopy to see the phosphine coordination status. Even after mixing with the dormant model, the signals of the phosphine ligands remained unchanged regardless of the phosphine structures, and no peaks

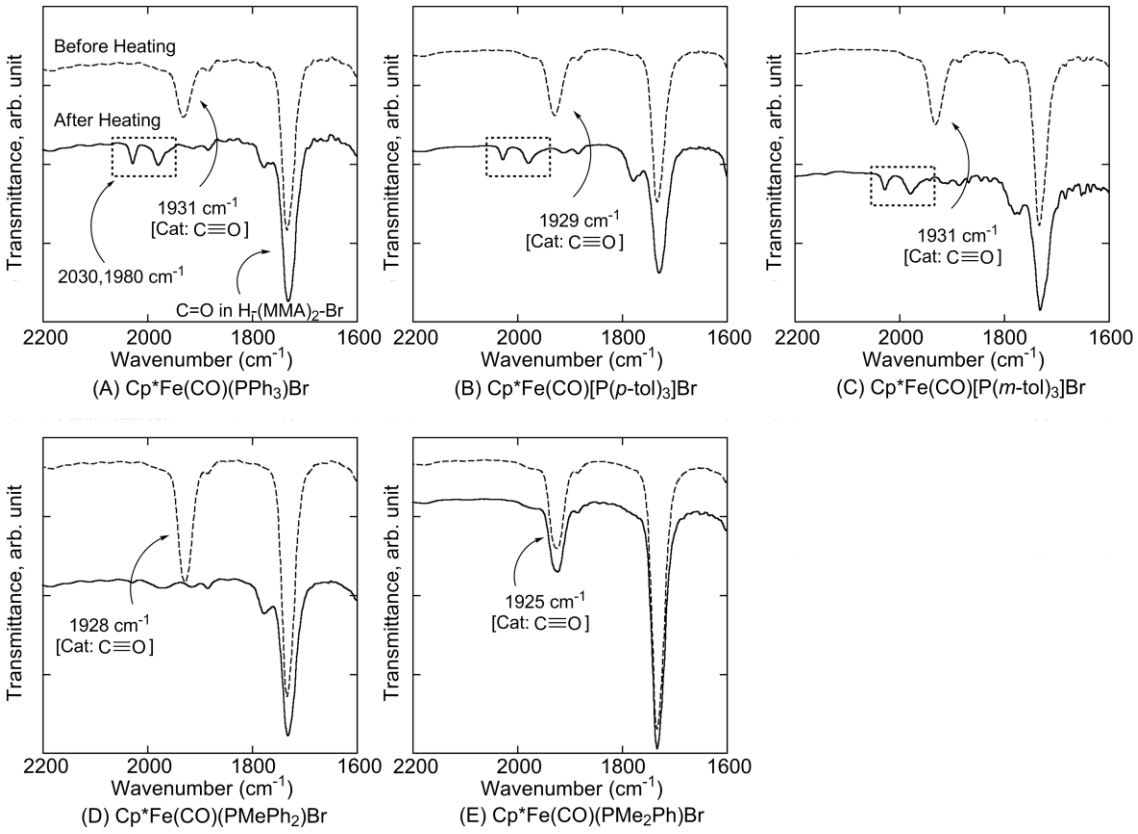

Figure 2. FT-IR analysis of Cp*Fe(CO)(L^{phos})Br/H-$(MMA)_2$-Br in $CHCl_3$ at 25 °C: $[Cp^*Fe(CO)(L^{phos})Br]_0$ = 5.0 mM; $[H\text{-}(MMA)_2\text{-}Br]_0$ = 20 mM. Condition: "Before Heating" (gray line); "After Heating", aged at 60 °C for 8 h before measurement (solid line). Cp*Fe(CO)(L^{phos})Br: (A) Cp*Fe(CO)(PPh_3)Br; (B) Cp*Fe(CO)[P(*p*-tol)$_3$]Br; (C) Cp*Fe(CO)[P(*m*-tol)$_3$]Br; (D) Cp*Fe(CO)($PMePh_2$)Br; (E) Cp*Fe(CO)(PMe_2Ph)Br.

indicative of free phosphines were observed, either, all excluding the possible phosphine, rather than carbonyl elimination.

With a vacant site for halogen extraction from the dormant end (~~~C-Br) now available, the 16e complexes would be real "active" catalysts for living radical polymerization, as observed with CpFe(CO)(L^{phos})Br catalysts.[25] Comparison with similar model reactions for the CpFe family indicates that the 18e-16e conversion apparently occurs faster with the Cp*Fe derivatives, which accounts for the faster polymerizations and the narrower MWDs with these catalysts.

In contrast, the C≡O peak for the PMe_2Ph complex obviously remained intact after the reaction [Figure 2(E)], suggesting a slow carbonyl release and thereby a slow transformation into the 16e complex. This is consistent with the slower polymerization and the broader MWDs (especially at the initial stage) observed with this catalyst [Figure 1, (A) and (C)].

Specifically for the triphenylphosphine-based complexes [L^{phos} = PPh_3, P(*p*-tol)$_3$, P(*m*-tol)$_3$], two minor peaks newly emerged at higher wave numbers (1980 and 2030 cm^{-1}) upon the disappearance of the carbonyl 1900-2000 cm^{-1} bands, and the positions of the new signals were exactly the same as for the dicarbonyl complex [Cp*Fe(CO)$_2$Br] [Figure 2(A)-(C)]. Such by-products did not form from similar CpFe complexes nor from Cp*Fe(CO)($PMePh_2$)Br. Given the poor catalytic performance of the dicarbonyl complex (see above and Figure 1), however, the real active catalysts should be the *in-situ* formed carbonyl-free 16e complexes [Cp*Fe(L^{phos})Br]. The role of the dicarbonyl complex is under investigation, but it might contribute to the deactivation process (radical-halogen coupling), because the polymer MWDs at the final conversions were obviously narrower than that with Cp*Fe(CO)($PMePh_2$)Br, which did not give the dicarbonyl complex.

3. Comparison with Cp-Based Complexes

Thus, the author focused on the difference between the Cp- and the Cp*-based complexes [(Z)Fe(CO)(L^{phos})Br; Z = Cp, Cp*] in the catalysis for MMA polymerization. Figure 3 shows conversion-M_n plots and SEC curves at around 90% conversion for the polymerizations with both catalyst series carrying PPh_3, P(*m*-tol)$_3$, and $PMePh_2$. There was little difference in overall polymerization rate (i.e., time to reach ~90% conversion) between the two categories with the same phosphine ligand. On the other hand, polymer MWDs were obviously narrower, and molecular weights better controlled (closer to the calculated), for the Cp* complexes, especially with PPh_3 and P(*m*-tol)$_3$. From these results, the Cp*

complexes catalyzed a faster reversible activation between dormant and active species with a higher initiating efficiency

Shown in Table 1, the contribution of Cp* as a conjugated electron-donating group was indeed supported by the lower redox potentials measured by cyclic voltammetry (CV). The half-wave oxidation potentials ($E_{1/2}$) are invariably lower for Cp* by >0.2 V for three phosphine ligands.

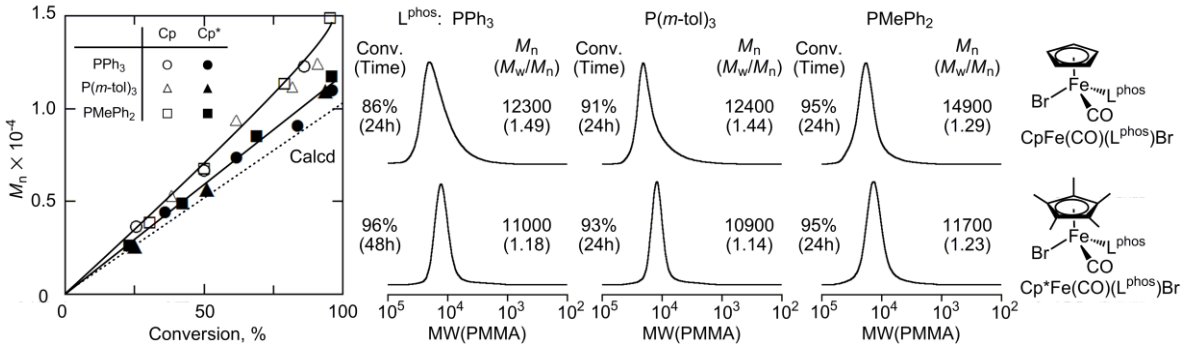

Figure 3. Comparisons between CpFe(CO)(L^{phos})Br and Cp*FeBr(CO)(L^{phos})Br on living radical polymerization of MMA with H-$(MMA)_2$-Br in toluene at 60 °C: $[MMA]_0$ = 4000 mM; $[H\text{-}(MMA)_2\text{-}Br]_0$ = 40 mM; [Iron Catalyst]$_0$ = 10 mM. Iron catalyst: CpFe(CO)(PPh_3)Br (○); CpFe(CO)[P(*m*-tol)$_3$]Br (△); CpFe(CO)($PMePh_2$)Br (□); Cp*Fe(CO)(PPh_3)Br (●); Cp*Fe(CO)[P(*m*-tol)$_3$]Br (▲); Cp*Fe(CO)($PMePh_2$)Br (■).

Table 1. Cyclic Voltammetry Analyses of CpFe(CO)(L^{phos})Br and Cp*Fe(CO)(L^{phos})Br[a]

Ligand		E_{pa} (V)	E_{pc} (V)	$E_{1/2}$ (V)	ΔE (V)
PPh_3	Cp	0.90	0.72	0.81	0.18
	Cp*	0.63	0.46	0.55	0.18
P(*m*-tol)$_3$	Cp	0.83	0.65	0.74	0.18
	Cp*	0.62	0.40	0.51	0.22
$PMePh_2$	Cp	0.88	0.71	0.79	0.17
	Cp*	0.63	0.44	0.53	0.19

[a] [Iron complex]$_0$ = 5 mM; $[n\text{-}Bu_4NPF_6]_0$ = 100 mM in CH_2ClCH_2Cl at 25 °C.

$E_{1/2} = (E_{pa} + E_{pc})/2$; $\Delta E = E_{pa} - E_{pc}$.

Within the Cp or Cp* families, the oxidation potential also depended on the phosphine ligands, and the observed order PPh_3 > $PMePh_2$ > P(*m*-tol)$_3$, though not very significant, agrees with the rate order in MMA polymerization (see above and Figure 1).

4. High Catalytic Activity and Controllability

To demonstrate the high catalytic activity and controllability of Cp*Fe(CO)(L^{phos})Br, we performed a monomer-addition experiment with the *meta*-tolyl phosphine complex [L^{phos} = P(*m*-tol)$_3$]. When a conversion reached around 90% in the polymerization of MMA, a fresh MMA was added to the polymerization solution. Even in the second phase, MMA was smoothly consumed to give an additional 85% conversion (total 175% relative to the first feed) (Figure 4). Beyond the second monomer addition, molecular weight increased in direct proportion with conversion, and the SEC (MWD) curves shifted to higher molecular weight keeping narrow distributions (M_w/M_n = 1.16), although a slight tailing was detected. As a concurrent addition of the catalyst was not required, the catalytic activity seemed to be kept during the second-stage polymerization.

The high catalytic activity of Cp*Fe(CO)[P(*m*-tol)$_3$]Br encouraged the author to synthesize higher molecular weight polymers with narrow MWDs. Thus, the author varied the monomer/initiator feed ratio from 100 through 400 to 1000, targeting M_n up to 10^5 at

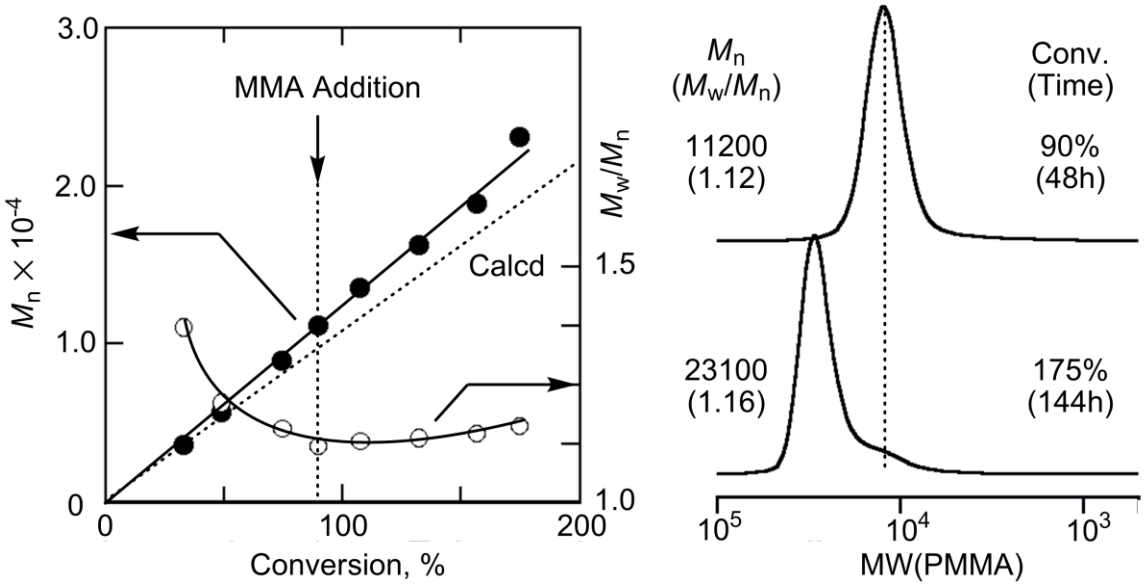

Figure 4. Monomer-addition experiment in the polymerization of MMA with H-(MMA)$_2$-Br/Cp*Fe(CO)[P(*m*-tol)$_3$]Br in toluene at 60 °C: $[MMA]_0 = [MMA]_{add}$ = 4000 mM; $[H\text{-}(MMA)_2\text{-}Br]_0$ = 40 mM; $[Cp^*Fe(CO)[P(m\text{-tol})_3]Br]_0$ = 4.0 mM.

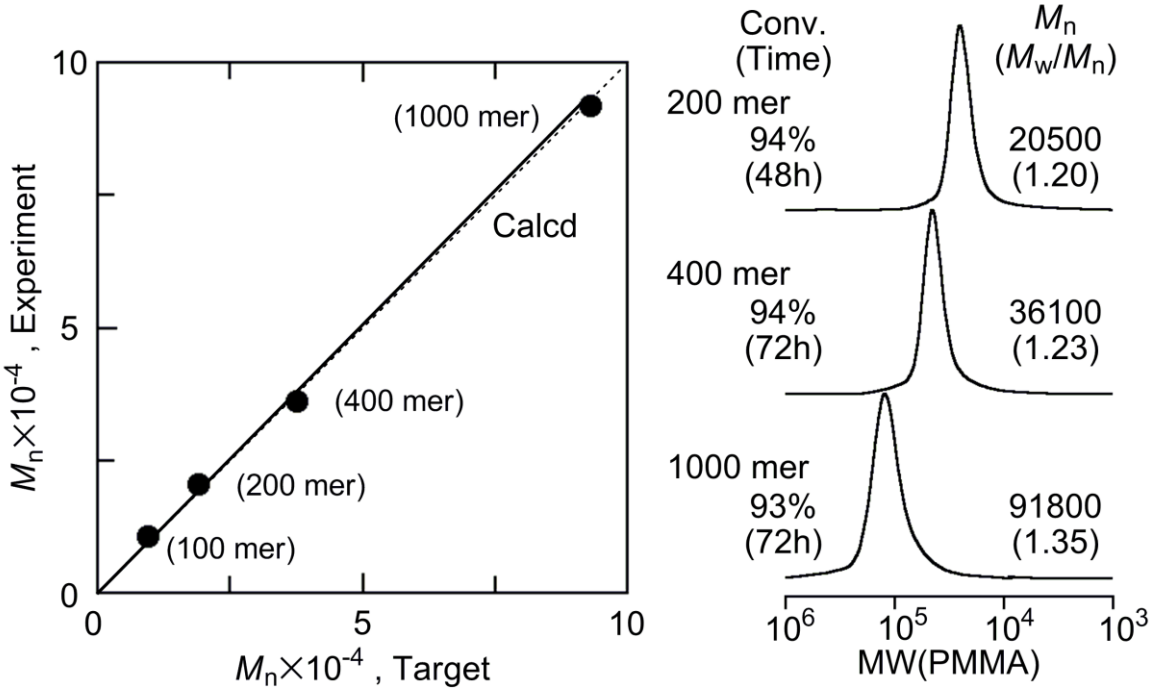

Figure 5. Synthesis of high molecular weight PMMA targeted 100 (A), 200 (B), 400 (C), 1000 mer (D) with H-(MMA)$_2$-Br/Cp*Fe(CO)[P(*m*-tol)$_3$]Br in toluene at 60 °C: [MMA]$_0$/[H-(MMA)$_2$-Br]$_0$/[Cp*Fe(CO)[P(*m*-tol)$_3$]Br]$_0$ = 4000/40/10 mM (A); 4000/20/4.0 mM (B); 4000/10/2.0 mM (C); 5000/5.0/1.0 mM (D).

100% conversion (Figure 5). Under all these conditions, conversion reached over 90%, and the molecular weights invariably agreed well with the calculated values based on the feed ratio and conversion, keeping fairly narrow MWDs (M_w/M_n < 1.4). These results demonstrate a high catalytic activity or a high turn-over frequency of the Cp*Fe catalyst.

5. Polymerization of Functional Monomers

The higher catalytic activity of the Cp* catalysts also promised application for other monomers, especially functional monomers. We then addressed a polymerization of a methacrylate (PEGMA) carrying a poly(ethylene glycol) pendant, one of the popular functional monomers. Figure 6 shows a comparison of the PEGMA polymerizations with Cp*Fe(CO)(PMePh$_2$)Br and CpFe(CO)(PMePh$_2$)Br. The Cp catalyst gave a decelerated polymerization with a limited conversion (~70%), whereas the Cp* derivative induced an almost quantitative polymerization (conversion >90%). Moreover, the latter produced better-controlled polymers with narrower MWDs [M_w/M_n = 1.29 (Cp*) vs 1.51 (Cp)]. Thus, the enhancement of electron density by the Cp* ligand was found to improve catalytic activity for a functional monomer.

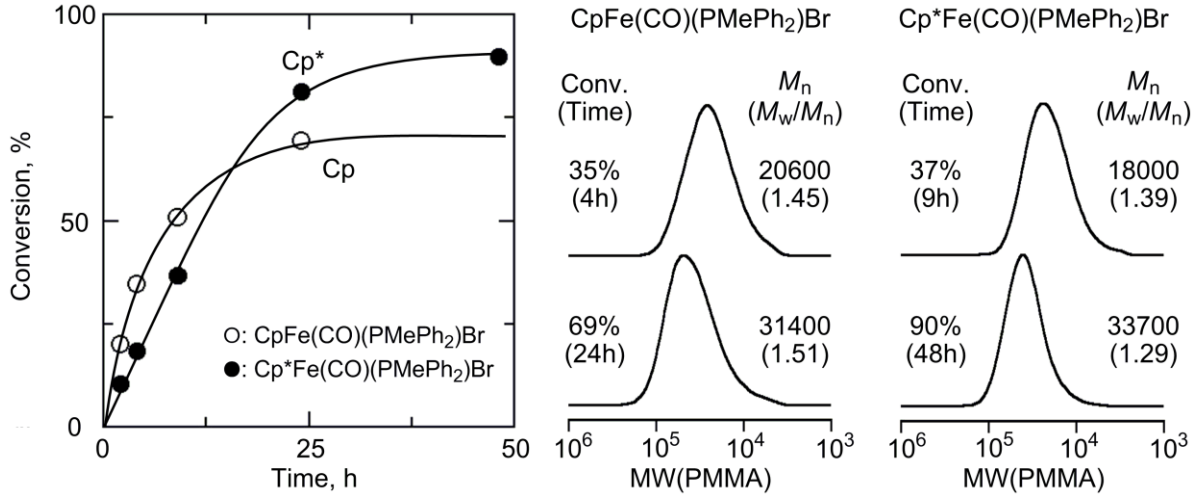

Figure 6. Comparisons between CpFe(CO)($PMePh_2$)Br and Cp*Fe(CO)($PMePh_2$)Br on living radical polymerization of PEGMA with H-$(MMA)_2$-Br in toluene at 60 °C: $[PEGMA]_0$ = 500 mM; $[H\text{-}(MMA)_2\text{-}Br]_0$ = 5.0 mM; $[Iron\ catalyst]_0$ = 5.0 mM. Iron catalyst: CpFe(CO)($PMePh_2$)Br (○); Cp*Fe(CO)($PMePh_2$)Br (●).

However, this catalyst was still insufficient for an amine-containing monomer, *N,N'*-dimethylaminoethyl methacrylate (DMAEMA), for which polymer MWD was much broader, though conversion reached high (>90%) in 25 h. The interaction of the amino moiety with the catalyst would disrupt the equilibrium balance between dormant and active species. Further ligand-design is required for such functional monomers with higher polarity and coordinating nature.

Given the catalytic activity of Cp*Fe(CO)($PMePh_2$)Br for PEGMA, a sequential block copolymerization of MMA and PEGMA was performed with H-$(MMA)_2$-Br (Figure 7). MMA (100 eq to initiator) was first polymerized in conjunction in toluene at 60 °C. When MMA conversion reached 80% in 25 h, PEGMA (50 eq) and an additional feed of the catalyst (2.0 mM) were added into the reaction mixture. The added PEGMA was smoothly consumed, and its conversion reached around 80% within 48 h (total 72 h). SEC curves shifted to higher molecular weight, indicative of long-lived growing species, but small shoulders were seen on both sides of the main peak, probably due to dead and coupling polymers.

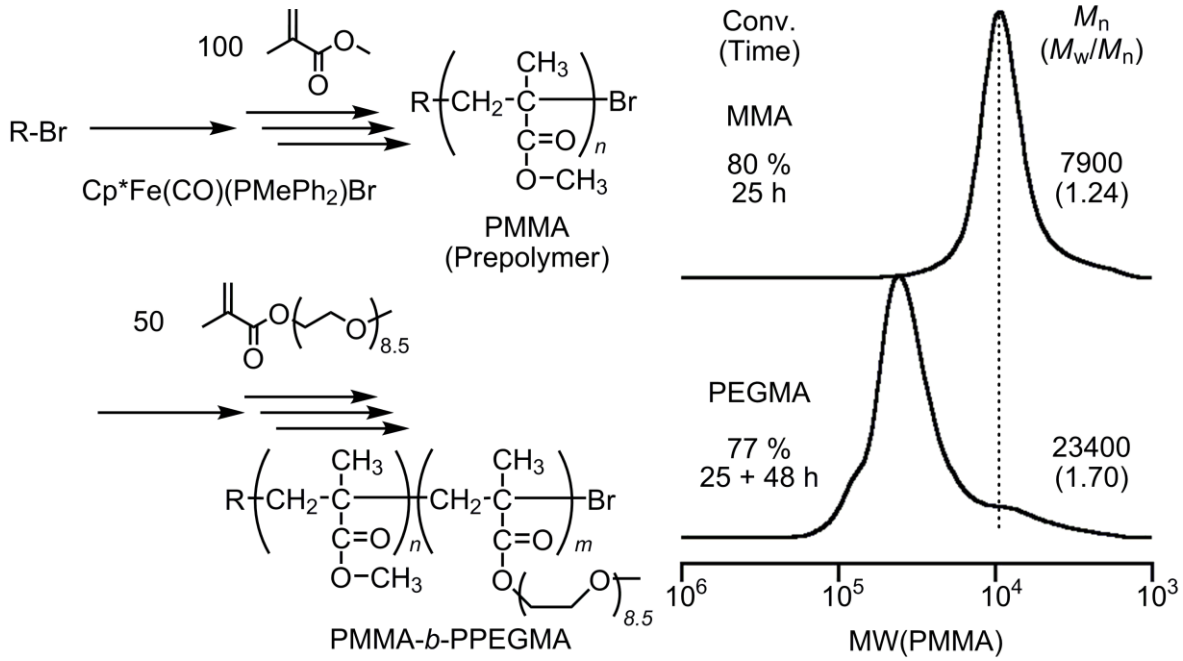

Figure 7. SEC curves of PMMA and PMMA-*b*-PPEGMA obtained with H-$(MMA)_2$-Br/Cp*Fe(CO)($PMePh_2$)Br in toluene at 60 °C: $[MMA]_0$ = 2000 mM; $[H\text{-}(MMA)_2\text{-}Br]_0$ = 20 mM; $[Cp^*Fe(CO)(PMePh_2)Br]_0$ = 5.0 mM; $[PEGMA]_{add}$ = 1000 mM; $[Cp^*Fe(CO)(PMePh_2)Br]_{add}$ = 2.0 mM.

6. Polymerization of MA

As reported in Chapter 3, a hetero-ligated Cp-based complex [CpFe(CO)($PMePh_2$)Br] that is effective for MMA ($M_w/M_n \sim 1.3$) is less active and cannot control polymerization of MA ($M_w/M_n > 2$). For MA, the growing radical is inherently reactive, and thus a faster halogen-capping (deactivation) would be particularly significant. Additionally, the less bulky monomer possibly interacts with the catalyst and thereby disrupts the ligand configuration to interfere catalytic performance. From these viewpoints, the Cp*Fe derivatives were promising, relative to the CpFe, because of their lower redox potential and the more bulky structure.

Thus, MA was polymerized with four Cp*Fe(CO)(L^{phos})Br catalysts [L^{phos} = PPh_3, $PMePh_2$, P(*m*-tol)$_3$, P(*p*-tol)$_3$] in conjunction with H-$(MMA)_2$-Br in toluene at 80 °C ($[MA]_0/[initiator]_0/[catalyst]_0$ = 4000/40/10 mM) (Figure 8). With P(*m*-tol)$_3$ and P(*p*-tol)$_3$ ligands, fairly narrow MWDs and molecular weight increase were observed, although the polymerizations markedly slowed down at a limited conversion (~60%) [Figure 8, (a) and (b)]. On the other hand, the PPh_3 or $PMePh_2$ complexes gave uncontrolled polymers [Figure 8, (c)

and (d)]. These results show that, with bulkier and more electron-donating Cp* and phosphine ligands, Cp*Fe(CO)(L)Br is relatively effective for MA polymerization, but that further ligand design might improve its catalytic performance for acrylates.

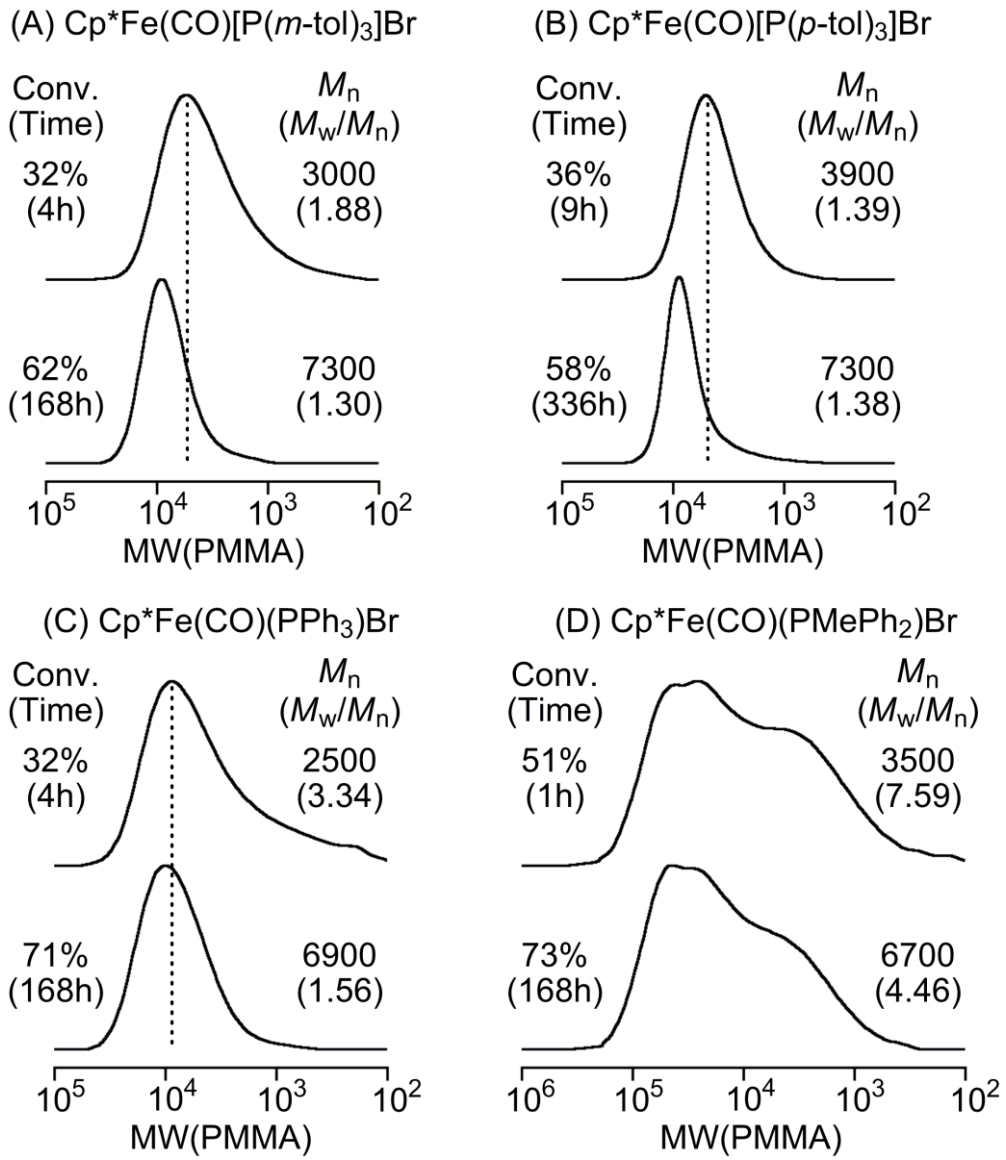

Figure 8. Polymerization of MA with H-$(MMA)_2$-Br/Cp*Fe(CO)(L^{phos})Br in toluene at 80 °C: $[MA]_0$ = 4000 mM; $[H\text{-}(MMA)_2\text{-}Br]_0$ = 40 mM; $[Cp^*Fe(CO)(L^{phos})Br]_0$ = 10 mM. Cp*Fe(CO)(L^{phos})Br: (A) Cp*Fe(CO)[P(*m*-tol)$_3$]Br; (B) Cp*Fe(CO)[P(*p*-tol)$_3$]Br; (C) Cp*Fe(CO)(PPh_3)Br; (D) Cp*Fe(CO)($PMePh_2$)Br.

Conclusion

A series of hetero-ligated Cp*Fe(II) complexes with carbonyl and phosphine ligands [Cp*Fe(CO)(L^{phos})Br; L^{phos} = PPh_3, $PMePh_2$, PMe_2Ph, P(*m*-tol)$_3$, P(*p*-tol)$_3$] were active catalysts for living radical polymerizations of MMA, MA, and a PEG-functionalized methacrylate (PEGMA). Importantly, the introduction of the Cp* ligand, relative to Cp, allowed a better polymerization control for a functional methacrylate (PEGMA) and acrylate (MA). FT-IR analysis on model reactions revealed a fast carbonyl release that transforms the original 18e complex [Cp*Fe(CO)(L^{phos})Br] into an unsaturated 16e form [Cp*Fe(L^{phos})Br], most probably acting a true "active" catalyst with a high turn-over frequency in the dormant-active equilibrium.

Such an *in-situ* transformation of a stable precursor into a true "active" catalyst would be useful for actual applications. We have also tried to prepare the 18e diphosphine Cp* complexes [Cp*Fe(L^{phos})$_2$Br], which likely turn into the same 16e intermediate [Cp*Fe(L^{phos})Br] during the polymerization. However, they were rather impractical because the starting complexes are too unstable to be isolated. As another way for such an *in-situ* generation of the intermediate catalyst, we have found that a direct usage of 18e dicarbonyl iron complex with pentaphenylcyclopentadienyl ligand [(η-C_5Ph_5)Fe(CO)$_2$] in the presence of a phosphine ligand was also available for the living radical polymerization [This catalyst was discussed in the next chapter (Chapter 6)].

Experimental Section

Materials

MMA (TCI; purity >99%) was dried overnight over calcium chloride and purified by double distillation from calcium hydride before use. MA (TCI; purity >99%) was dried overnight over calcium chloride and purified by distillation from calcium hydride before use. Poly(ethylene glycol) methyl methacrylate [PEGMA; CH_2=$CMeCO_2(CH_2CH_2O)_n$Me; Me = CH_3; n = 8.5 on average] (Aldrich) and *N,N'*-dimethylaminoethyl methacrylate (DMAEMA) (TCI; purity >98 %) were of commercial source and purified by passing through an inhibitor removal column (Aldrich) and degassed by reduced pressure before use. The MMA dimer bromide [H-(MMA)$_2$-Br; H-(CH_2CMeCO_2Me)$_2$-Br] as an initiator was prepared according to

literature.[26] $Cp_2Fe_2(CO)_4$ (Aldrich; purity >99%) and $Cp^*_2Fe_2(CO)_4$ (Azmax; purity >98%) were used as received and handled in a glove box (M. Braun Labmaster 130) under a moisture- and oxygen-free argon atmosphere (H_2O <1 ppm; O_2 <1 ppm). Triphenylphosphine (PPh_3: Aldrich, purity >99%), methyldiphenylphosphine ($PMePh_2$: Aldrich, purity >99%), dimethylphenylphosphine (PMe_2Ph: Aldrich, purity >97%), tri-*p*-tolylphosphine [P(*p*-tol)$_3$: Wako, purity >98%], tri-*m*-tolylphosphine [P(*m*-tol)$_3$: Aldrich, purity >97%] were used as received. Toluene, THF, CH_2Cl_2 and *n*-hexane (Kishida Kagaku; purity >99%) were passed through purification columns (Solvent Dispensing System; Glass Contour) and bubbled with dry nitrogen for more than 15 min immediately before use. $CHCl_3$ (Wako Chemicals, anhydrous; purity >99%) was bubbled with dry nitrogen for more than 15 min immediately before use. Cyclohexane (Wako, anhydrous) was used as received. *n*-Octane (internal standard for gas chromatography) and 1,2,3,4-tetrahydronaphthalene (tetralin; internal standard for ^{1}H NMR analysis) was dried over calcium chloride and distilled twice from calcium hydride.

Catalyst Syntheses

$CpFe(CO)_2Br$[27] and $CpFe(CO)(PMePh_2)Br$[28] were synthesized according to literatures. $Cp^*Fe(CO)_2Br$ was synthesized by the method of King et al.[29] IR ($CHCl_3$): 2028, 1979 cm^{-1} ν(CO). Anal. Calcd for $C_{12}H_{15}BrFeO_2$: C, 44.08; H, 4.62; Br, 24.44. Found: C, 44.31; H, 4.45; Br, 24.65.

A series of $Cp^*Fe(CO)(L^{phos})Br$ were synthesized by the method of Barras et al. as follows:[24] A cyclohexane (100 mL) and THF (7.0 mL) mixed solution of $Cp^*Fe(CO)_2Br$ (1.0 g, 3.06 mmol) and 1.5 equivalent of phosphine [L^{phos} = PPh_3, $PMePh_2$, PMe_2Ph, P(*m*-tol)$_3$ or P(*p*-tol)$_3$] was magnetically stirred and was irradiated under UV (Riko, UVL-400P; 400W) at 25 °C for 4 h under dry argon. The solutions changed from rust to green irrespective of phosphine employed. The reaction mixture was evaporated and then the residue was washed with *n*-hexane (15 mL × 2). The residue was extracted in toluene (60 mL) and filtered at 25 °C to remove precipitates, and the filtrate was evaporated in vacuo to dryness to remove the solvent. The crude product was dissolved in CH_2Cl_2 (7.0 mL), and recrystallized by gradual addition of *n*-hexane (60 mL), followed by standing at -30 °C for 72 h. The supernatant solvent were removed by a cannula with filter paper, and the crystal was washed with *n*-hexane (2.0 mL × 2) and dried under vacuum. The complexes were characterized by elemental analysis, FT-IR spectroscopy at room temperature in $CHCl_3$ on JASCO FT/IR 4200

and 500-MHz ^{1}H-NMR spectroscopy at room temperature in $CDCl_3$ on a Jeol JNM-ECA500 spectrometer.

Cp*Fe(CO)(PPh_3)Br; Isolated yield, 75%. ^{1}H-NMR (ppm): 1.3-1.5 (m, 15H, Cp-C*H*$_3$), 7.3-7.6 (m, 15H, Ar-*H*). IR ($CHCl_3$): 1931 cm^{-1} ν(CO). Anal. Calcd for $C_{29}H_{30}BrFeOP$: C, 62.06; H, 5.39; Br, 14.24. Found: C, 62.04; H, 5.32; Br, 14.31.

Cp*Fe(CO)($PMePh_2$)Br; Isolated yield, 35%. ^{1}H-NMR (ppm): 1.4-1.6 (m, 15H, Cp-C*H*$_3$), 2.00 (d, 3H, P-C*H*$_3$), 7.4-7.8 (m, 10H, Ar-*H*). IR ($CHCl_3$): 1928 cm^{-1} ν(CO). Anal. Calcd for $C_{24}H_{28}BrFeOP$: C, 57.74; H, 5.65; Br, 16.01. Found: C, 57.74; H, 5.54; Br, 16.14.

Cp*Fe(CO)(PMe_2Ph)Br: Isolated yield, 72%. ^{1}H-NMR (ppm): 1.4-1.5 (m, 15H, Cp-C*H*$_3$), 1.60 (d, 3H, P-C*H*$_3$), 1.86 (d, 3H, P-C*H*$_3$), 7.4-7.7 (m, 5H, Ar-*H*). IR ($CHCl_3$): 1925 cm^{-1} ν(CO). Anal. Calcd for $C_{19}H_{26}BrFeOP$: C, 52.20; H, 6.00; Br, 18.28. Found: C, 52.01; H, 5.93; Br, 18.03.

Cp*Fe(CO)[P(*m*-tol)$_3$]Br: Isolated yield, 70%. ^{1}H-NMR (ppm): 1.3-1.5 (m, 15H, Cp-C*H*$_3$), 2.29 (m, 9H, Ph-C*H*$_3$), 7.1-7.3 (m, 12H, Ar-*H*). IR ($CHCl_3$): 1931 cm^{-1} ν(CO). Anal. Calcd for $C_{32}H_{36}BrFeOP$: C, 63.70; H, 6.01; Br, 13.24. Found: C, 64.56; H, 5.95; Br, 12.58.

Cp*Fe(CO)[P(*p*-tol)$_3$]Br: Isolated yield, 67%. ^{1}H-NMR (ppm): 1.2-1.3 (m, 15H, Cp-C*H*$_3$), 2.31 (m, 9H, Ph-C*H*$_3$), 7.1-7.4 (m, 12H, Ar-*H*). IR ($CHCl_3$): 1930 cm^{-1} ν(CO). Anal. Calcd for $C_{32}H_{36}BrFeOP$: C, 63.70; H, 6.01; Br, 13.24. Found: C, 62.57; H, 5.84; Br, 16.11.

Polymerization Procedures

Polymerization was carried out by the syringe technique under dry argon in baked glass tubes equipped with a three-way stopcock or in sealed glass vials. A typical procedure for MMA polymerization with H-(MMA)$_2$-Br/Cp*Fe(CO)($PMePh_2$)Br was as follows. In a 50-mL round-bottom flask Cp*Fe(CO)($PMePh_2$)Br (25.0 mg, 0.05 mmol), toluene (2.23 mL), *n*-octane (0.27 mL), MMA (2.14 mL, 20 mmol), and H-(MMA)$_2$-Br (0.36 mL of 553.4 mM in toluene, 0.20 mmol) were added sequentially under dry argon at room temperature where the total volume of reaction mixture was thus 5.0 mL. Immediately after mixing, aliquots (0.80 mL each) of the solution were injected into glass tubes which were then sealed (except when a stopcock was used) and placed in an oil bath kept at desired temperature. In predetermined intervals, the polymerization was terminated by cooling the reaction mixtures to -78 ºC. Monomer conversion was determined from the concentration of residual monomer measured

by gas chromatography with *n*-octane as an internal standard. The quenched reaction solutions were diluted with toluene (ca. 20 mL), washed with water three times, and evaporated to dryness to give the products that were subsequently dried overnight under vacuum at room temperature.

For MA, the same procedures as descried above were applied and for PEGMA, the same procedures as described above were applied except that monomer conversion was determined by ^{1}H NMR from the integrated peak area of the olefinic protons of the monomers with tetralin as internal standard. The products were similarly isolated but without washing with water because of their hydrophilicity.

Measurements

For poly(MMA) and poly(MA), M_n and M_w/M_n were measured by size-exclusion chromatography (SEC) in chloroform at 40 °C on three polystyrene-gel columns [Shodex K-805L (pore size: 20-1000 Å; 8.0 mm i.d. × 30 cm); flow rate, 1.0 mL/min] connected to a Jasco PU-980 precision pump and a Jasco 930-RI refractive-index detector, and a Jasco 970-UV ultraviolet detector. The columns were calibrated against 13 standard poly(MMA) samples (Polymer Laboratories; M_n = 630-1,200,000; M_w/M_n = 1.06-1.22) as well as the monomer. For poly(PEGMA), DMF containing 10 mM LiBr was applied as an eluent.

Cyclic voltammograms were recorded by using a Hokuto Denko HZ-3000 apparatus. A typical procedure is as follows: Cp*Fe(CO)(PMePh$_2$)Br (17.5 mg, 0.035 mmol) was dissolved into a 100 mM solution of *n*-Bu$_4$NPF$_6$ (supporting electrolyte) in CH_2ClCH_2Cl (7.0 mL) under dry argon in a baked glass tube equipped with a three-way stopcock. Voltammograms were recorded under argon at a scan rate 0.1 Vs^{-1} in a three-electrode cell equipped with a platinum disk as a working electrode, a platinum wire as a counter electrode, and an Ag/AgCl electrode as a reference.

FT-IR spectra of the Cp*Fe complexes were recorded by using JASCO FT/IR 4200. The sample was prepared that Cp*Fe(CO)(PMePh$_2$)Br (2.5 mg, 5.0 × 10^{-3} mmol), H-(MMA)$_2$-Br (5.6 mg, 0.020 mmol) and toluene (1.0 mL) were added into the baked glass tube equipped with a three-way stopcock under dry argon. After mixing at 60 °C for 8 h, the solvent was evaporated. The residue was dissolved in degassed $CHCl_3$ and purged in the sealed liquid KBr cell where the thickness was 0.1 mm. Measurements were carried out under inert atmosphere.

References and Notes

(1) For recent reviews on transition metal catalyzed living radical polymerization, see: (a) Kamigaito, M.; Ando, T.; Sawamoto, M. *Chem. Rev.* **2001**, *101*, 3689-3745. (b) Kamigaito, M.; Ando, T.; Sawamoto, M. *Chem. Rec.* **2004**, *4*, 159-175. (c) Ouchi, M.; Terashima, T.; Sawamoto, M. *Acc. Chem. Res.* **2008**, *41*, 1120-1132. (d) Matyjaszewski, K.; Xja, J. *Chem. Rev.* **2001**, *101*, 2921-2990. (e) Controlled/Living Radical Polymerization From Synthesis to Materials; Matyjaszewski K., Ed.; ACS Symposium Series 944; American Chemical Society: Washington, DC, 2006.

(2) (a) Kato, M.; Kamigaito, M.; Sawamoto, M.; Higashimura, T. *Macromolecules* **1995**, *28*, 1721-1723. (b) Ando, T.; Kato, M.; Kamigaito, M.; Sawamoto, M. *Macromolecules* **1996**, *29*, 1070-1072.

(3) Wang, J. S.; Matyjaszewski, K. *J. Am. Chem. Soc.* **1995**. *117*, 5614-5615.

(4) (a) Bolm, C.; Legros, J.; Paih, J. L.; Zani, L. *Chem. Rev.* **2004**, *104*, 6217-6254. (b) Enthaler, S.; Junge, K.; Beller, M. *Angew. Chem. Int. Ed.* **2008**, *47*, 3317-3321.

(5) Ando, T.; Kamigaito, M.; Sawamoto, M. *Macromolecules* **1997**, *30*, 4507-4510.

(6) Matyjaszewski, K.; Wei, M.; Xia, J.; McDermott, N. E. *Macromolecules* **1997**, *30*, 8161-8164.

(7) Kotani, Y.; Kamigaito, M.; Sawamoto, M. *Macromolecules* **1999**, *32*, 6877-6880.

(8) Kotani, Y.; Kamigaito, M.; Sawamoto, M. *Macromolecules* **2000**, *33*, 3543-3549.

(9) Zhu, S.; Yan, D. *Macromolecules* **2000**, *33*, 8233-8238.

(10) Louie, Y.; Grubbs, R. H. *Chem. Commun.* **2000**, 1479-1480.

(11) Göbelt, B.; Matyjaszewski, K. *Macromol. Chem. Phys.* **2000**, *201*, 1619-1624.

(12) Gibson, V. C.; O'Reilly, R. K.; Reed, W.; Wass, D. F.; White, A. J. P.; Williams, D. J. *Chem. Commun.* **2002**, 1850-1851.

(13) O'Reilly, R. K.; Gibson, V. C.; White, A. J. P.; Williams, D. J. *J. Am. Chem. Soc.* **2003**, *125*, 8450-8451.

(14) Xue, Z.; Lee, B. W.; Noh, S. K.; Lyoo, W. S. *Polymer* **2007**, *48*, 4704-4714.

(15) Niibayashi, S.; Hayakawa, H.; Jin, R-H.; Nagashima, H. *Chem. Commun.* **2007**, 1855-1857.

(16) Uchiike, C.; Terashima, T.; Ouchi, M.; Ando, T.; Kamigaito, M.; Sawamoto, M. *Macromolecules* **2007**, *40*, 8658-8662.

(17) Ferro, R.; Milione, S.; Bertolasi, V.; Capacchione, C.; Grassi, A. *Macromolecules* **2007**, *40*, 8544-8546.

(18) Uchiike, C.; Ouchi, M.; Ando, T.; Kamigaito, M.; Sawamoto, M. *J. Polym. Sci., Part A: Polym. Chem.* **2008**, *46*, 6819-6827.

(19) Chapter 1 of this thesis.

(20) Takahashi, H.; Ando, T.; Kamigaito, M.; Sawamoto, M. *Macromolecules* **1999**, *32*, 3820-3823.

(21) Watanabe, T.; Ando, T.; Kamigaito, M.; Sawamoto, M. *Macromolecules* **2001**, *34*, 4370-4374.

(22) Ouchi, M.; Ito, M.; Kamemoto, S.; Sawamoto, M. *Chem. Asian. J.* **2008**, *3*, 1358-1364.

(23) Ando, T.; Kamigaito, M.; Sawamoto, M. *Macromolecules* **2000**, *33*, 5825-5829.

(24) Barras, J-P.; Davis, S. G.; Metzler, M. R.; Edwards, A. J.; Humphreys, V. M.; Prout, K. *J. Organomet. Chem.* **1993**, *461*, 157-165.

(25) Chapter 3 of this thesis.

(26) Ando, T.; Kamigaito, M.; Sawamoto, M. *Tetrahedron* **1997**, *53*, 15445-15457.

(27) (a) Fischer, E. O.; Moser, E. *Inorg. Synth.* **1970**, *12*, 35-36. (b) Hallam, B. F.; Pauson, P. L. *J. Chem. Soc.* **1956**, 3030-3037.

(28) Treichel, P. H.; Shubkin, R. L.; Barnett, K. W.; Reichard, D. *Inorg. Chem.* **1966**, *5*, 1177-1181.

(29) King, R. B.; Stone, F. G. *Inorg. Synth.* **1963**, *7*, 99-115.

Chapter 6

Pentaphenylcyclopentadienyl Iron Catalyst: Fast Transformation into Active Catalyst

Abstract

Iron dicarbonyl complex bearing a pentaphenylcyclopentadiene (η-C_5Ph_5: Cp^{Ph}), $(Cp^{Ph})Fe(CO)_2Br$, was employed for living radical polymerization of methyl methacrylate (MMA) in conjunction with a bromide initiator [H-$(MMA)_2$-Br]. The complex itself was stable and inactive for the polymerization of MMA, however, in the presence of triphenylphosphine (PPh_3), it smoothly polymerized MMA to give controlled polymers with narrow molecular weight distributions (~ 90% conversion within 24 h; M_w/M_n = 1.2). Analyses of the model reaction with FT-IR and ^{31}P-NMR clarified that the carbonyl ligands were efficiently exchanged with the phosphine for the complex to transform into real active catalyst. The ligand exchange was much faster than with other cyclopentadiene-based family [i.e., $CpFe(CO)_2Br$, Cp = η-C_5H_5; $Cp^*Fe(CO)_2Br$, Cp* = η-C_5Me_5], which was reflected in the superiority in the catalytic activity, i.e., faster polymerization and narrower molecular weight distributions. The high catalytic activity was also proved by the monomer addition experiment, fine control even for higher molecular weight polymer (M_w/M_n < 1.2 under 1000 mer condition), and control for methyl acrylate. Such an *in-situ* transformation from a stable complex to an active catalyst would be advantageous to practical applications.

Introduction

For organic reactions and polymerizations, transition metal-catalyzed systems have contributed a great deal to the development because of the versatile and tunable property of the catalyst with the diverse combination of ligands and the central metal.[1] Transition-metal catalyzed living radical polymerization[2] is one of such catalytic systems where the complex contributes to control of the radical propagation in addition polymerization of vinyl monomers (Scheme 1).[3] Here, the catalysis is a reversible activation for carbon-halogen bond (C-X: X = halogen) at the growing end involving one-electron redox ($Mt^n \leftrightarrow XMt^{n+1}$) to generate carbon-centered radical (C•) by "halogen abstraction" and to cap (deactivate) the radical species by "halogen return". Such a temporal activation allows lower concentration of the radical species, leading to a controlled polymerization free from undesirable side reactions. Thanks to the feasible procedures and diversity of the applicable monomers including functional ones, this is now a powerful tool to construct novel functional polymeric materials with well-defined structures.

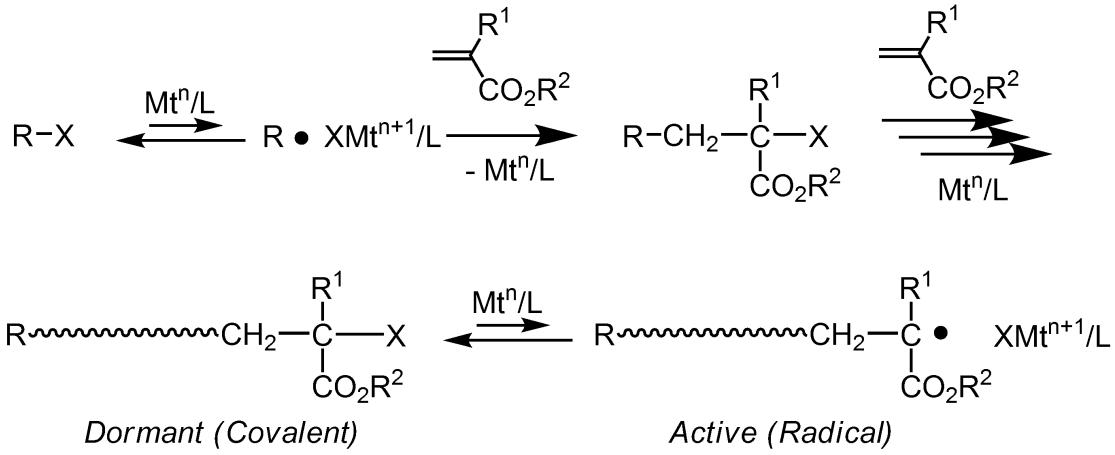

Scheme 1. Transition Metal-Catalyzed Living Radical Polymerization

For the catalyst evolution in transition-metal catalyzed living radical polymerization, the main efforts have been directed for and improvement of the catalytic activity toward syntheses of higher molecular weight polymers with narrow molecular weight distributions (MWDs), a wide applicability for various monomers including high polar ones, and a reduction in the catalytic amount. On the other hand, as the systems have been utilized for curious applications, the practical utilities are also required in addition to those catalytic functions. For example, the rare or precious metals for the catalysts should be replaced with

ubiquitous ones to suppress a depletion of natural resources. Also, too active or poisonous catalysts might be hard to be handled for industrial processes. From these practical viewpoints, iron should be one of the most ideal central metals for the complex.[4] Since the first discovery with $FeCl_2(PPh_3)_2$ by the author's group,[5] a variety of iron complexes have been developed for the catalysts,[6-24] however there are few examples to satisfy both of catalytic activity for variety of monomers and practical utilities with convenience in handling.

In Chapter 3 and 5, the author have found that carbonyl-phosphine hetero-ligated cyclopentadienyl complexes [Cp'Fe(CO)(L^{phos})Br; Cp' = η-C_5H_5 (Cp)[23] or η-$C_5(CH_3)_5$ (Cp*)[24]: L^{phos} = phosphine], prepared via the ligand exchange for Cp'Fe$(CO)_2$Br in the presence of phosphine ligand on heating or under UV irradiation, are active to catalyze living radical polymerization (Scheme 2). Although they are stable even under oxygen, once they encounter an initiator for the metal-catalyzed living radical polymerization at the polymerization temperature (>60 °C), they turned into unsaturated active species [Cp'Fe(L^{phos})Br] via the carbonyl release to catalyze the polymerization. Such a transformation was confirmed by FT-IR and ^{31}P NMR for the model reaction with the initiator [H-$(MMA)_2$-Br]. Thus, in these polymerizations, stable complexes with convenience in handling are *in-situ* transformed into "real" active ones to trigger the controlled radical propagation. As for the difference between the Cp and Cp* complexes, the latter apparently shows higher catalytic activity to give narrower MWDs for wide range of monomers. Same as the ruthenium analogues,[25] the five methyl-substitutions with electron donating ability

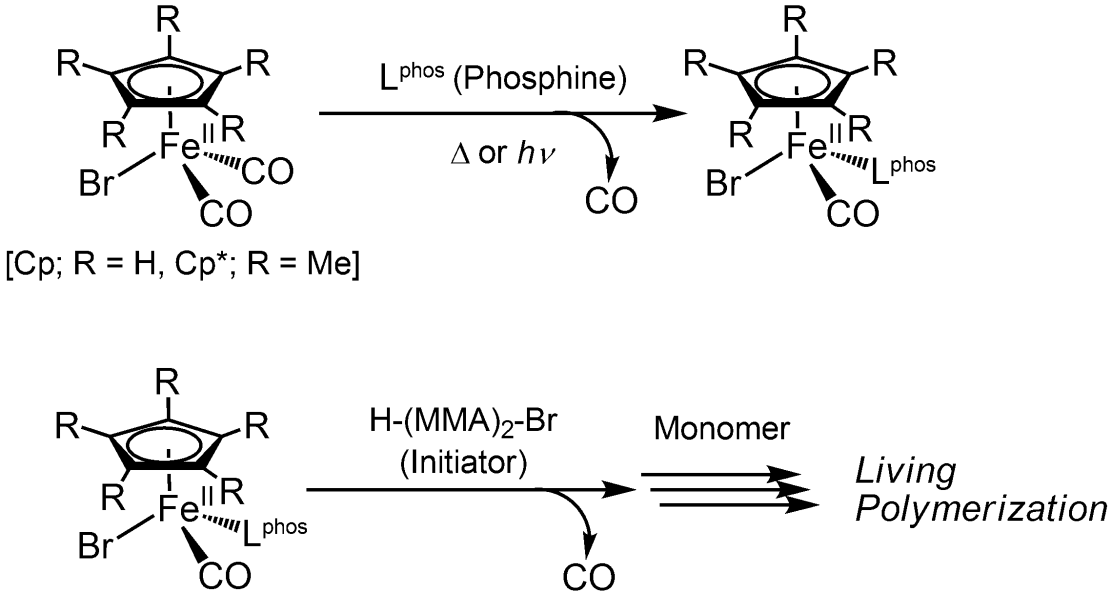

Scheme 2. Living Radical Polymerization with (Cp')Fe(CO)(L^{phos})Br

reduces the redox potential to enhance the catalytic activity. Thus, properties of the Cp-based anionic ligand can affect the catalytic activity as well as the neutral ligands (i.e., phosphine and carbonyl).

From these backgrounds, the author embarked on a further modification of the half-metallocene iron complex toward a more useful catalyst for the living radical polymerization, focusing on another class of cyclopentadiene-based ligand, pentaphenylcyclopentadiene (η-C_5Ph_5; Cp^{Ph}).[26-29] The Cp^{Ph} is apparently different from the methyl substituted (η-C_5Me_5; Cp*) in terms of bulkiness and electronic property, and indeed some examples have been reported on the Cp^{Ph}-complexes exhibiting unique ligand exchange,[27] redox behavior,[28] and catalysis.[29] For example, it was shown that a carbonyl replacement reaction with a phosphorous donor ligand for $(Cp^{Ph})Ru(CO)_2Br$ occurs via a dissociative mechanism much faster than other cyclopentadiene-family due to the bulkier structure of the η-C_5Ph_5.[27] The similar iron complex $[(Cp^{Ph})Fe(CO)_2Br]$ is also one of the given Cp^{Ph}-based derivatives, however according to the literature, the carbonyl ligand is not exchanged with phosphine by thermolysis or UV photolysis unlike the Cp and Cp* counterparts.[30,31] With the author's findings that carbonyl ligand is specifically released under the condition for living radical polymerization with carbonyl-phosphine hetero-ligated cyclopentadienyl complexes $[Cp'Fe(CO)(L^{phos})Br]$, the author expected that even for the dicarbonyl Cp^{Ph}-complex $[(Cp^{Ph})Fe(CO)_2Br]$ the CO ligands are replaced with phosphine ligand under the condition to give a real active catalyst $[(Cp^{Ph})Fe(L^{phos})Br]$ similar to with $Cp'Fe(CO)(L^{phos})Br$ (Scheme 3).

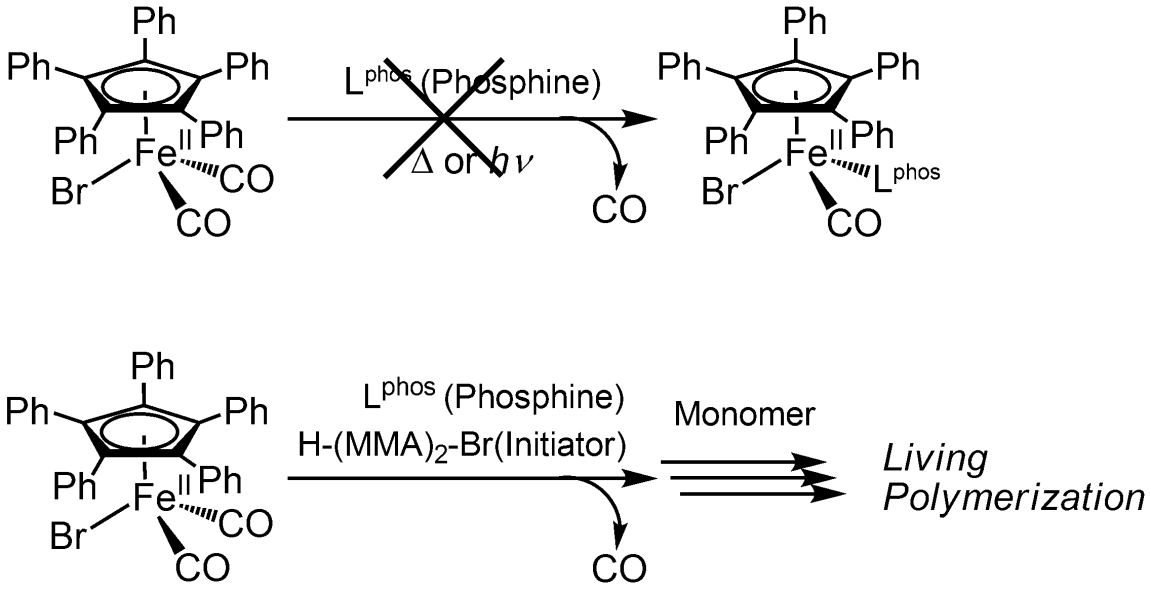

Scheme 3. Living Radical Polymerization with $(Cp^{Ph})Fe(CO)(L^{phos})Br$

Thus, the author used the dicarbonyl complex [$(Cp^{Ph})Fe(CO)_2Br$] for metal-catalyzed living radical polymerization of methyl methacrylate (MMA), coupled with a bromide initiator [H-$(MMA)_2$-Br]. The polymerization did not occur in the absence of phosphine, whereas just an addition of catalytic amount of phosphine induced smooth and quantitative polymerizations to give controlled polymers with predictable molecular weights and narrow molecular weight distributions. Analysis of the model reaction with the initiator with FT-IR and ^{31}P NMR revealed that phosphorus complexes are *in-situ* generated free from the carbonyl. This system is active enough to produce high molecular weight polymers keeping the controllability and to control for other monomers, such as a functional methacrylate and methyl acrylate (MA).

Results and Discussion

1. Living Radical Polymerization of MMA with $(Cp^{Ph})Fe(CO)_2Br$ in the Presence of PPh_3

The author first employed the dicarbonyl complex [$(Cp^{Ph})Fe(CO)_2Br$] for MMA polymerization in toluene at 60 °C, coupled with H-$(MMA)_2$-Br as an initiator ($[MMA]_0/[H\text{-}(MMA)_2\text{-}Br]_0/[(Cp^{Ph})Fe(CO)_2Br]_0$ = 4000/40/4.0 mM). The complex showed no catalytic activity for MMA polymerization, similar to other dicarbonyl cyclopentadienyl derivatives [$CpFe(CO)_2Br$[23] and $Cp^*Fe(CO)_2Br$[24]]. Such dicarbonyl cyclopentadienyl complexes seem to be less active for MMA, although the two vanguards show catalytic activity for styrenes and acrylates in the presence of larger amount of metal alkoxide [i.e., $Ti(O\textit{i}\text{-}Pr)_4$ or $Al(O\textit{i}\text{-}Pr)_3$] as a cocatalyst.[8] Rather surprisingly, once just same amount of PPh_3 was added as the catalyst ($[PPh_3]_0$ = 4.0 mM), MMA was smoothly consumed and the conversion reached around 90% within a few days. With 2 equivalence of PPh_3 was added, the polymerization was further accelerated (90% in 24 h) and further increase (4 eq) was less effective on the polymerization rate. Regardless of the phosphine amount, molecular weights of the produced PMMAs were linearly increased in proportion to the conversion in accordance with the calculated values, and the distributions were fairly narrow (M_w/M_n = 1.2 for ~ 90% conversion). Thus, just the catalytic amount of phosphine ligand dramatically changed the catalytic activity of the complex for living radical polymerization.

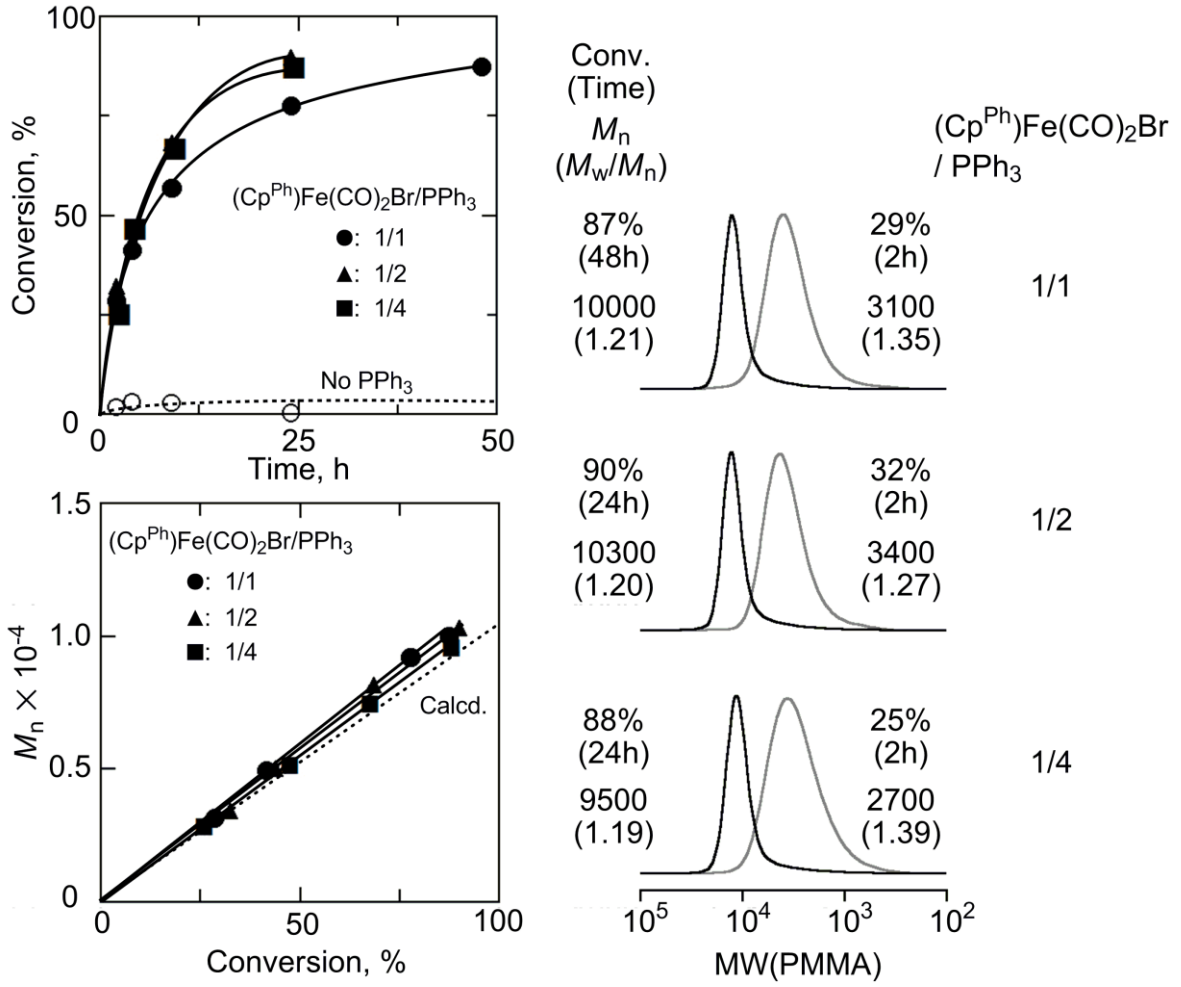

Figure 1. Polymerization of MMA with H-(MMA)$_2$-Br/(Cp^{Ph})Fe(CO)$_2$Br/PPh$_3$ in toluene at 60 °C: [MMA]$_0$ = 4000 mM; [H-(MMA)$_2$-Br]$_0$ = 40 mM; [(Cp^{Ph})Fe(CO)$_2$Br]$_0$ = 4.0 mM; [PPh$_3$]$_0$ = 0 (○), 4.0 (●), 8.0 (▲), 16 (■) mM.

2. FT-IR and ^{31}P NMR Analyses for Model Reaction

The starting complex [(Cp^{Ph})Fe(CO)$_2$Br] is electronically saturated with 18e, and then some ligand-related reaction should occur to trigger the living radical polymerization. The author thus analyzed FT-IR and ^{31}P NMR for the model reaction with the initiator [H-(MMA)$_2$-Br] in the presence of PPh$_3$ to examine the catalyst transformation during the polymerization.

For FT-IR analysis, the three components were mixed in toluene at 60 °C under dry argon for 8 hours ([H-(MMA)$_2$-Br]$_0$/[(Cp^{Ph})Fe(CO)$_2$Br]$_0$/[PPh$_3$]$_0$ = 20/5.0/10 mM), as the model reaction of the polymerization. After an evaporation of the toluene, the residue was dissolved in CHCl$_3$ for the measurement. As a result, the peaks derived from C≡O stretching

on the complex at 2038 and 1999 cm^{-1} of wavenumber were perfectly disappeared [Figure 2(B)], although they were observed for the sample before the heating procedure [Figure 2 (A)]. This result would indicate an irreversible dissociation of the CO via the model reaction. As the peaks were not disappeared just for heating with PPh_3 [Figure 2(C)], the carbonyl ligands would be dissociated only for the reaction with the initiator or the one-electron activation of carbon halogen bond.

The same reaction was analyzed with ^{31}P-NMR to see the coordination behavior of the added phosphine (Figure 3). Before heating the mixture, only one peak was observed at around 0 ppm, derived from the "free" triphenylphosphine, meaning that the added phosphine was not coordinated into the iron at the ambient temperature (Figure 3A). After heating it at 60 °C, this peak was totally disappeared, and new three peaks were instead appeared at 18, 32,

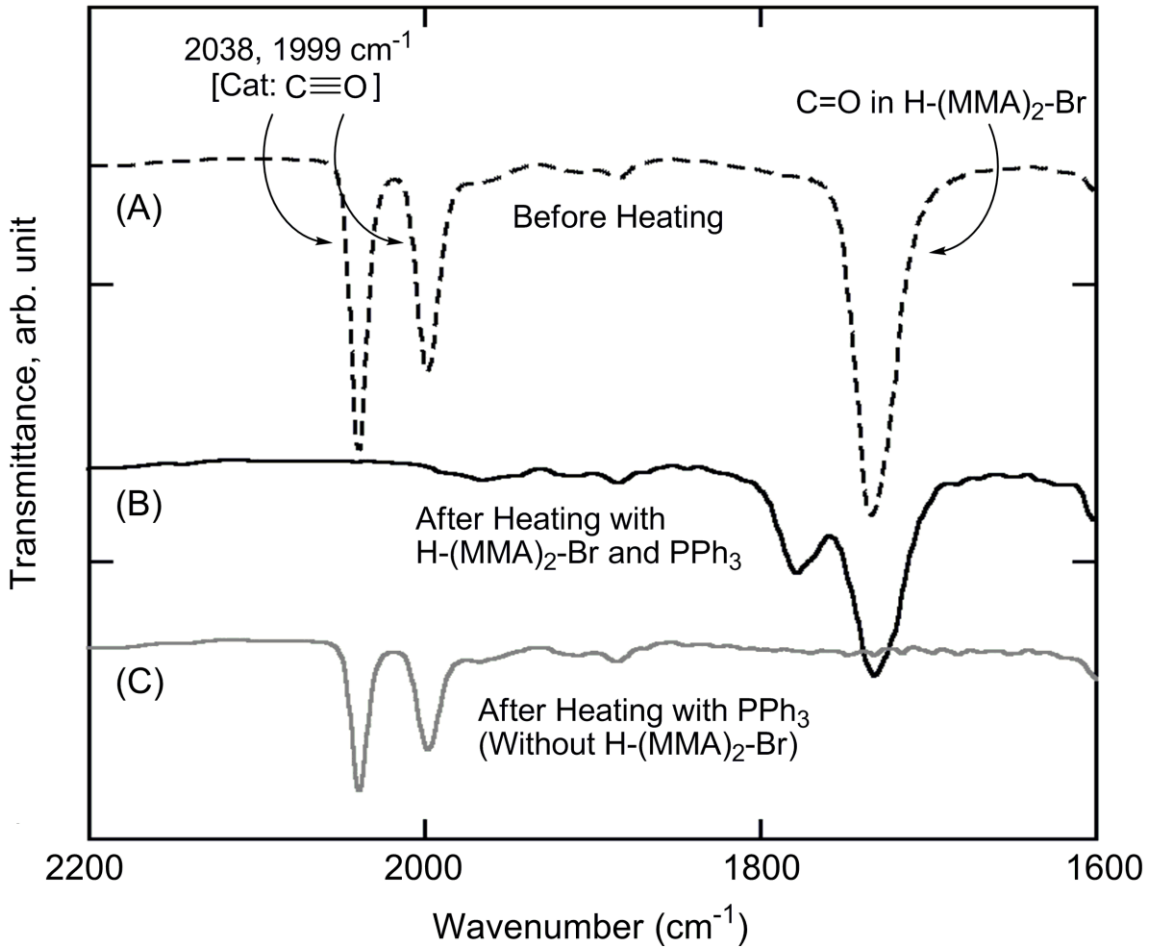

Figure 2. FT-IR analysis of H-$(MMA)_2$-Br/$(Cp^{Ph})Fe(CO)_2Br$/PPh_3 in $CHCl_3$ at 25 °C: $[(Cp^{Ph})Fe(CO)_2Br]_0$ = 5.0 mM; $[PPh_3]_0$ = 10 mM; $[H\text{-}(MMA)_2\text{-}Br]_0$ = 20 mM. Condition: (A) "Before Heating" (dashed line); (B) "After Heating", aged at 60 °C for 8 h with H-$(MMA)_2$-Br and PPh_3 before measurement (solid line); (C) "After Heating", aged at 60 °C for 8 h with PPh_3 before measurement (gray line).

and 44 ppm (Figure 3B). Although the accurate attributions for these peaks were still unknown, some phosphine bearing complexes are most likely generated through the model reaction. As the FT-IR analyses indicated the formation of carbonyl free complexes, they would be the divalent [(Cp^{Ph})Fe(PPh_3)Br] and [(Cp^{Ph})Fe(PPh_3)$_2$Br], or the trivalent [(Cp^{Ph})Fe(PPh_3)Br_2].

Given these analyses for the model reaction, the author proposes the catalyst transformation in the living radical polymerization as shown in Scheme 4. The starting 18e complex [(Cp^{Ph})Fe(CO)$_2$Br] is too stable to induce ligand exchange with phosphine by thermolysis or UV photolysis, however once it encounters the halide initiator for living

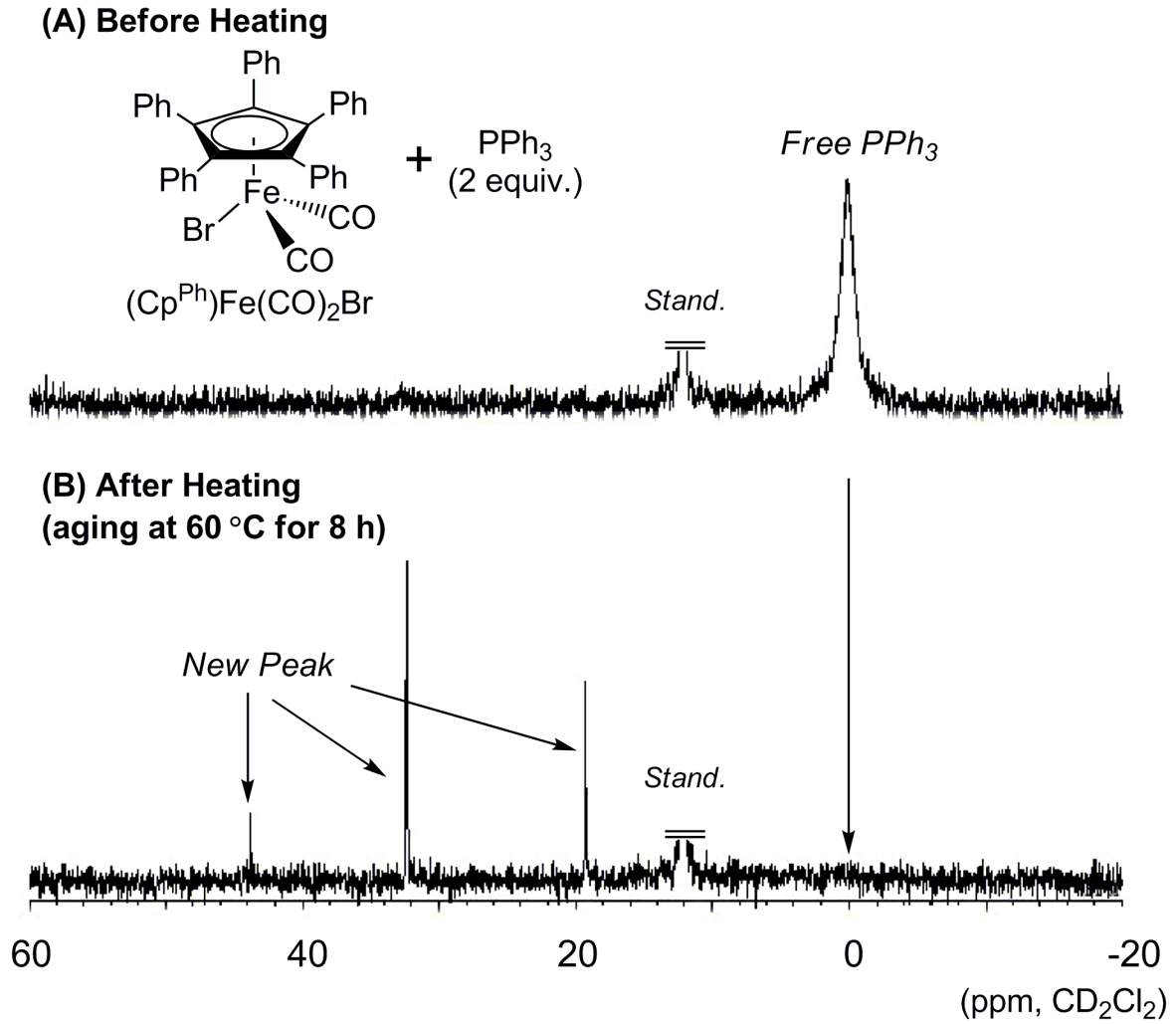

Figure 3. ^{31}P NMR analysis of H-(MMA)$_2$-Br/(Cp^{Ph})Fe(CO)$_2$Br/PPh_3 in CD_2Cl_2 at 25 °C: [(Cp^{Ph})Fe(CO)$_2$Br]$_0$ = 10 mM; [PPh_3]$_0$ = 20 mM; [H-(MMA)$_2$-Br]$_0$ = 40 mM. Condition: (A) "Before Heating"; (B) "After Heating", aged at 60 °C for 8 h in toluene before measurement.

radical polymerization [i.e., H-(MMA)$_2$-Br], it releases the carbonyl ligand to accept the bromine from the initiator to give the radical species [H-(MMA)$_2$•] and the trivalent complex [(Cp^{Ph})Fe(CO)Br$_2$]. In the presence of triphenylphosphine, it would coordinate into the trivalent Fe(III) via the ligand exchange with the remained CO ligand to give the PPh$_3$-coordinated Fe(III) complex [(Cp^{Ph})Fe(PPh$_3$)Br$_2$]. This Fe(III) complex would efficiently return the bromine to the radical species to turn into the corresponding Fe(II) complex [(Cp^{Ph})Fe(PPh$_3$)Br], which work as a "real" active catalyst afterward. In the absence of PPh$_3$, the generating carbonyl Fe(III) complex [(Cp^{Ph})Fe(CO)Br$_2$] would be too unstable to return the bromine, leading to no polymerization due to some decomposition.[32]

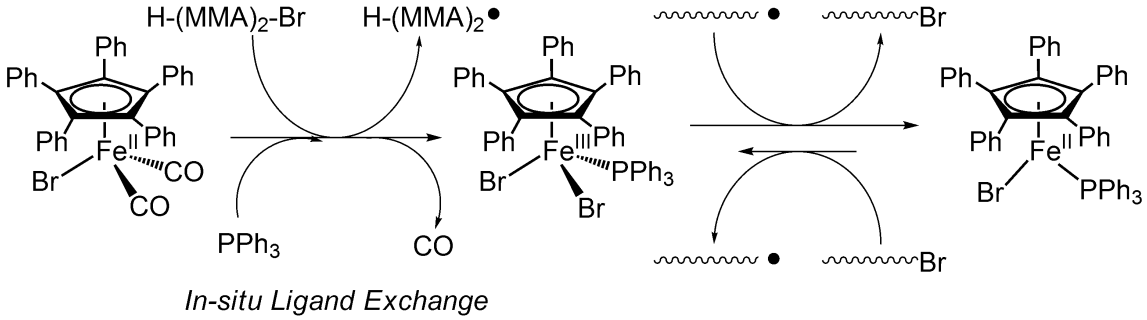

Scheme 4. Proposed Polymerization Mechanism of (Cp^{Ph})Fe(CO)$_2$Br/PPh$_3$

3. Comparison with Other Cyclopetadienyl Ligands: Effects of the Phenyl Group

To examine effects of the pentaphenylcyclopentadiene ligand, the catalysis for the MMA polymerization was compared with the other dicarbonyl cyclopentadiene-based iron complexes [CpFe(CO)$_2$Br and Cp*Fe(CO)$_2$Br] under the same condition using 2 equivalent of PPh$_3$. As shown in Figure 4, both of them also induced the polymerization in the presence of PPh$_3$, but the polymerizations were slower than (Cp^{Ph})Fe(CO)$_2$Br. At the early stage with low conversion, the molecular weight distributions of the polymers with the two complexes were much broader than with (Cp^{Ph})Fe(CO)$_2$Br [M_w/M_n > 2 vs < 1.3 with (Cp^{Ph})Fe(CO)$_2$Br], although final distribution indexes at the high conversion were similar to those with the Cp^{Ph} complex.

To examine the causes of these differences in the polymerization behaviors, the author followed the time course of the model reaction with FT-IR for the three complexes [CpFe(CO)$_2$Br, Cp*Fe(CO)$_2$Br, and (Cp^{Ph})Fe(CO)$_2$Br]. The reaction condition was same as above: the initiator, the complex, and PPh$_3$ were mixed in toluene at 60 °C under dry argon ([H-(MMA)$_2$-Br]$_0$/[iron complex]$_0$/[PPh$_3$]$_0$ = 20/5.0/10 mM). Figure 5 shows FT-IR spectra

with the range of 1600-2200 cm^{-1} of wavenumber for $CpFe(CO)_2Br$ (A), $Cp^*Fe(CO)_2Br$ (B) and $(Cp^{Ph})Fe(CO)_2Br$ (C). The top spectrum is for "before heating" (0 h), and the lower are for "after heating" in predetermined times (2, 4, and 8 h). For the every complex, there were two peaks at around 2000 cm^{-1} from the stretching of C≡O ligands, and one peak at around 1730 cm^{-1} from C=O in the initiator before the heating procedure. As shown above, in the case of $(Cp^{Ph})Fe(CO)_2Br$, the peaks from carbonyl ligands were disappeared, indicating an irreversible elimination of the ligands to give "real" active catalysts. The transformation seemed to be very fast: the peaks were almost vanished in 2 h. On the other hand, with the other two complexes, the carbonyl peaks were not disappeared, although their intensity was gradually weakened. Thus, it was found that $(Cp^{Ph})Fe(CO)_2Br$ more smoothly releases the carbonyl for the activation of the radical initiator than the other cyclopentadienyl complexes,

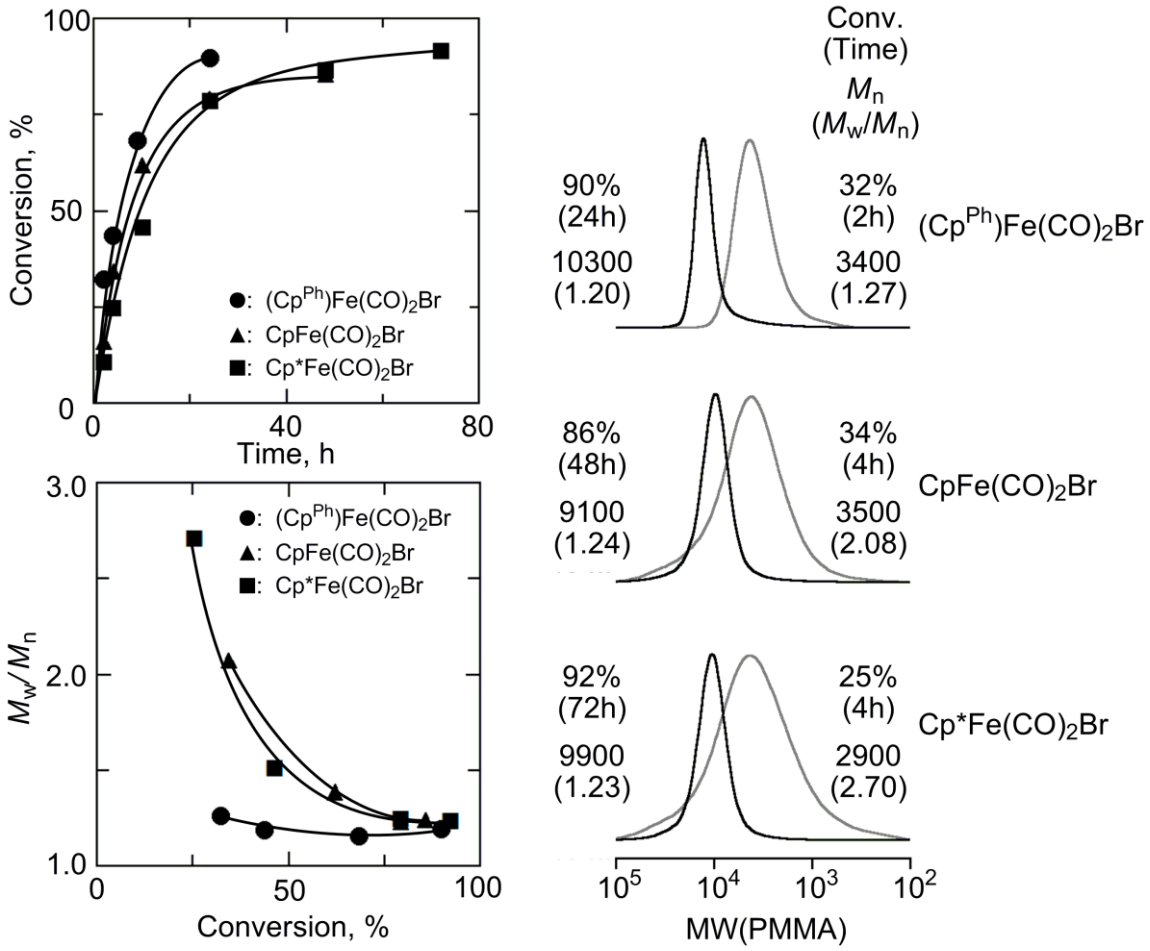

Figure 4. Effects of iron catalyst on living radical polymerization of MMA with H-$(MMA)_2$-Br/PPh_3 in toluene at 60 °C: $[MMA]_0$ = 4000 mM; $[H\text{-}(MMA)_2\text{-}Br]_0$ = 40 mM; $[Iron\ Catalyst]_0$ = 4.0 mM; $[PPh_3]_0$ = 8.0 mM. Iron Catalyst: $(Cp^{Ph})Fe(CO)_2Br$ (●), $CpFe(CO)_2Br$ (▲), $Cp^*Fe(CO)_2Br$ (■).

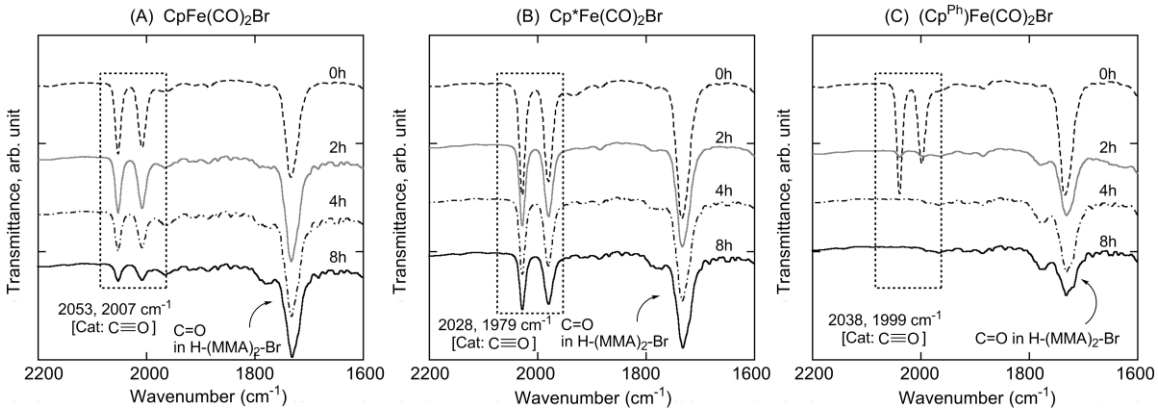

Figure 5. FT-IR analysis of dicarbonyl half-metallocene iron complex combined with H-$(MMA)_2$-Br and PPh_3 in $CHCl_3$ at 25 °C aged at 60 °C before measurement: [Iron Complex]$_0$ = 5.0 mM; [PPh_3]$_0$ = 10 mM; [H-$(MMA)_2$-Br]$_0$ = 20 mM. Reaction Time: 0 h (dashed line); 2 h (gray line); 4 h (broken line); 8 h (solid line). Iron Complex: $CpFe(CO)_2Br$ (A); $Cp^*Fe(CO)_2Br$ (B); $(Cp^{Ph})Fe(CO)_2Br$ (C).

and this would contribute to better control of the polymerization, especially at the early polymerization stage.

4. Effects of Phosphine Additives

Taking advantage of the *in-situ* introduction of the added PPh_3, the author examined effects of the phosphine ligand to modify the activity toward more useful catalytic system. Thus, five kinds of phosphines [L^{phos} = PPh_3, P(*m*-tol)$_3$, $PMePh_2$, PMe_2Ph, P(*n*-Bu)$_3$] were compared as additives for the MMA polymerization with [$(Cp^{Ph})Fe(CO)_2Br$] as a starting catalyst in conjunction with H-$(MMA)_2$-Br in toluene at 60 °C (Figure 6). All the phosphines induced smooth polymerizations and the MMA conversion reached over 90% within 50 h. Addition of PPh_3, P(*m*-tol)$_3$ and $PMePh_2$ gave controlled molecular weights and narrow MWDs (M_w/M_n < 1.3), while PMe_2Ph and P(*n*-Bu)$_3$ resulted in less controlled polymers with broad MWDs (M_w/M_n > 2.0). Such higher basic phosphine would enhance the catalytic activity too much, leading to less ideal equilibrium balance for the control with higher concentration of active species.

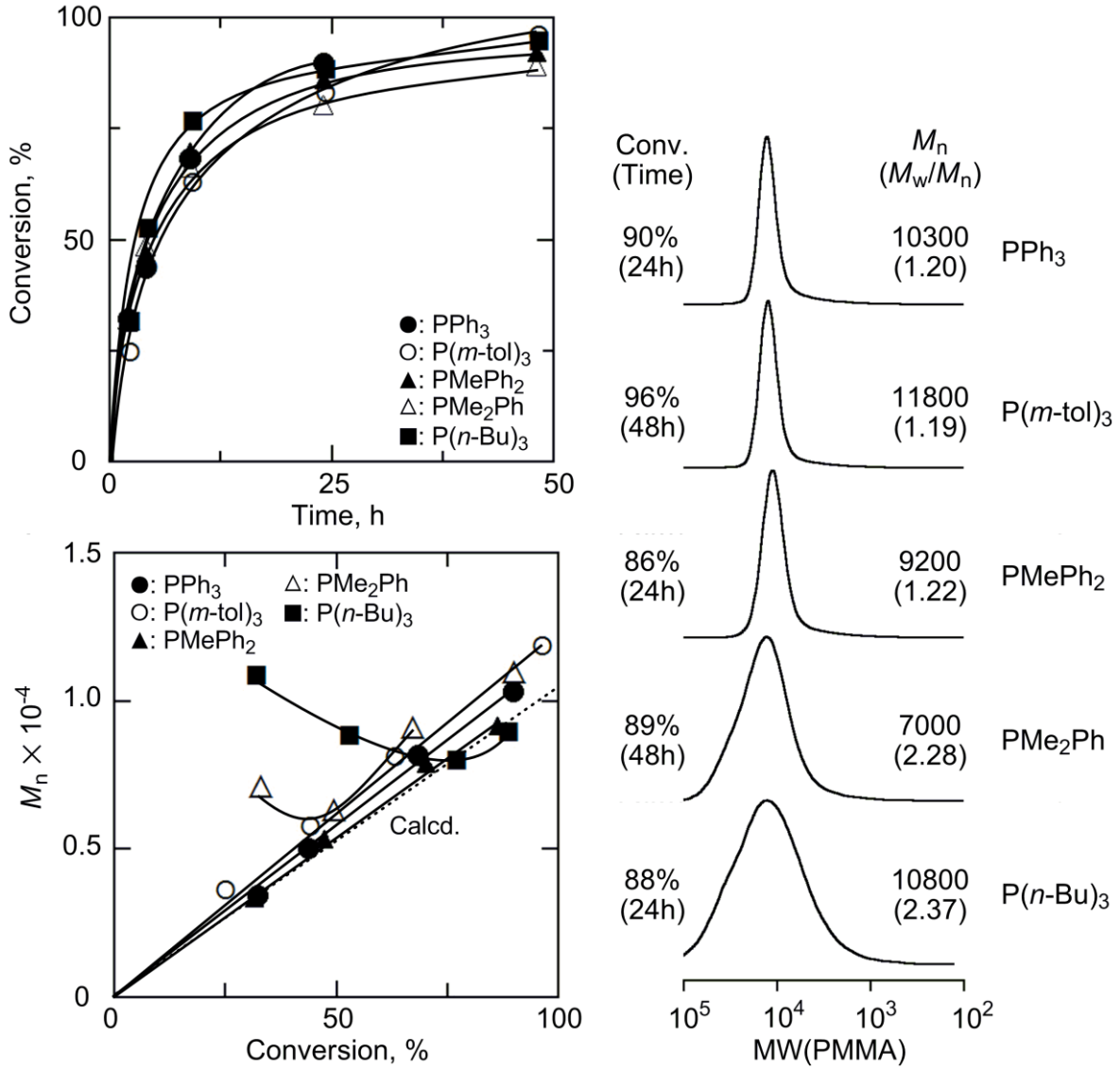

Figure 6. Effects of phosphine for $(Cp^{Ph})Fe(CO)_2Br$/phosphine catalytic systems on living radical polymerization of MMA with H-$(MMA)_2$-Br in toluene at 60 °C: $[MMA]_0$ = 4000 mM; $[H\text{-}(MMA)_2\text{-}Br]_0$ = 40 mM; $[(Cp^{Ph})Fe(CO)_2Br]_0$ = 4.0 mM; $[phosphine]_0$ = 8.0 mM. Phosphine: PPh_3 (●); P(*m*-tol)$_3$ (○); $PMePh_2$ (▲); PMe_2Ph (△); P(*n*-Bu)$_3$ (■).

5. High Catalytic Activity of $(Cp^{Ph})Fe(CO)_2Br$: Monomer Addition Experiments and Synthesis of High Molecular Weight Polymers

To check the catalytic activity of $(Cp^{Ph})Fe(CO)_2Br$ in conjunction with PPh_3, the author carried out so called "monomer-addition" experiment. When the MMA-conversion reached 87% in the polymerization with $(Cp^{Ph})Fe(CO)_2Br/PPh_3$, a fresh MMA was added. Even in the second phase, MMA was smoothly consumed to give additional 74% conversion (totally 161%, for 120 h) (Figure 7). The molecular weights increased in direct proportion

with the conversion and the SEC curves shifted to higher molecular weight keeping the unimodal shape and narrow MWD (M_w/M_n = 1.25), although just a slight tailing was detected. As a concurrent addition of the catalyst was not required, the catalyst was still active at the latter stage as well as the terminal carbon-bromine bond.

The high controllability encouraged the author to synthesize higher molecular weight polymers with narrow MWDs. The author thus performed the polymerization for the monomer/initiator ratio to be 1,000, targeting 100,000 of M_n for 100% conversion (Figure 8). The conversions reached about 90% within 96 h and the MWDs of the obtained PMMAs were quite narrow (M_w/M_n < 1.2). The molecular weights agreed well with the theoretical values calculated values based on assumption that one molecule of bromide initiator generated one living chain even for nearly 100,000 of M_n. From these results, it was found that $(Cp^{Ph})Fe(CO)_2Br$ shows high activity and controllability for living radical polymerization of MMA in the presence of PPh_3.

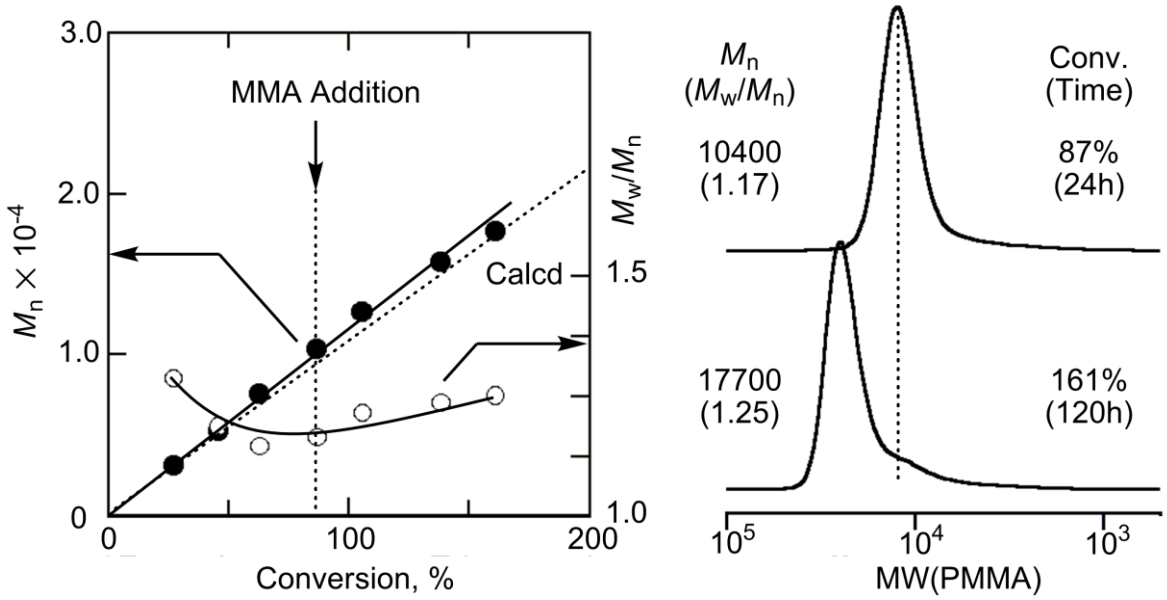

Figure 7. Monomer-addition experiment in the polymerization of MMA with H-$(MMA)_2$-Br/$(Cp^{Ph})Fe(CO)_2Br$/PPh_3 in toluene at 60 °C: $[MMA]_0$ = $[MMA]_{add}$ = 4000 mM; $[H\text{-}(MMA)_2\text{-}Br]_0$ = 40 mM; $[(Cp^{Ph})Fe(CO)_2Br]_0$ = 4.0 mM; $[PPh_3]_0$ = 8.0 mM.

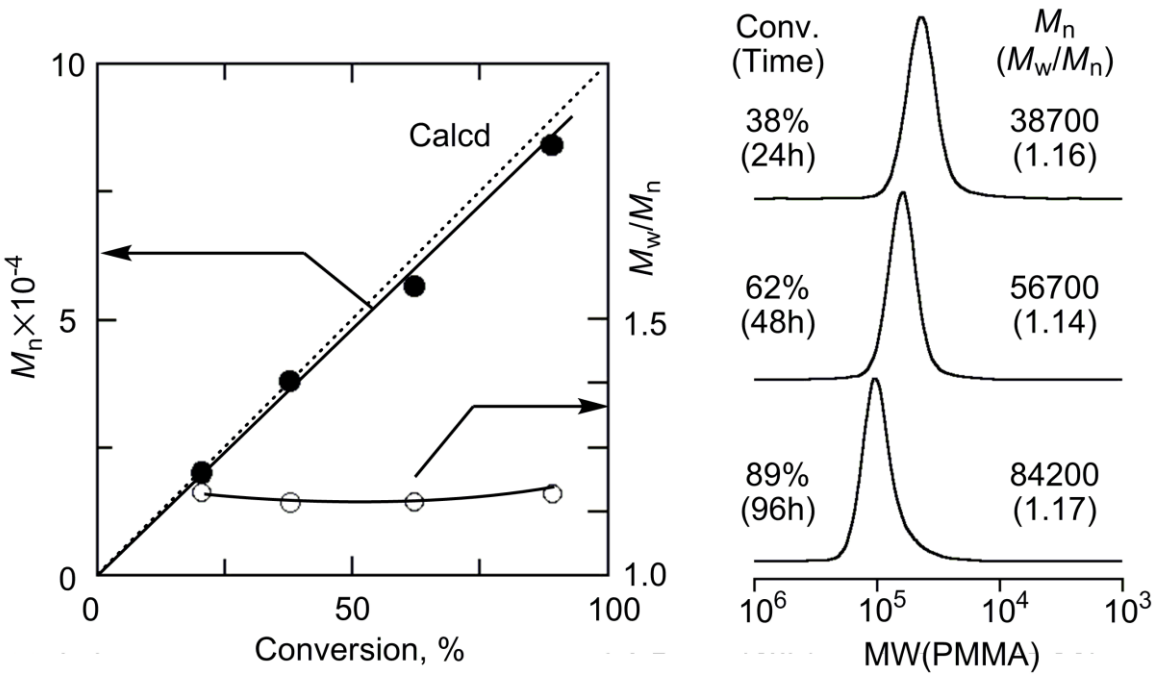

Figure 8. Synthesis of high molecular weight PMMA targeted 1000 mer with H-$(MMA)_2$-Br/$(Cp^{Ph})Fe(CO)_2Br/PPh_3$ in toluene at 60 °C: $[MMA]_0$ = 5000 mM; $[H\text{-}(MMA)_2\text{-}Br]_0$ = 5.0 mM; $[(Cp^{Ph})Fe(CO)_2Br]_0$ = 1.0 mM; $[PPh_3]_0$ = 2.0 mM.

6. Polymerization of Methyl Acrylate

The author then examined the polymerization of MA with the same systems. In the MA polymerization, the carbon-halogen bond in the dormant species is tighter and the growing radical species is more reactive than with MMA, and hence both of activation and deactivation need to be further promoted to control the polymerization: more sophisticated catalysis is required. As for the analog complexes [(Cp')Fe(CO)(L^{phos})Br; Cp' = Cp, Cp*], the Cp* derivatives give a glimpse of the controllability (M_w/M_n ~ 1.3-1.4), but the conversion was limited (< 60%),[24] while the Cp cannot control the polymerization.[23]

Figure 9 shows the time-conversion curves and SEC profiles of the produced poly(MA)s with $(Cp^{Ph})Fe(CO)_2Br$, coupled with three kinds of phosphine: PPh_3, P(*m*-tol)$_3$, and $PMePh_2$. Although there was little difference in the catalysis for the MMA polymerizations among the three ligands (Figure 9), the polymerization behaviors were dependent on the phosphine ligand. An addition of $PMePh_2$ gave faster polymerization, however the MWDs were obviously broader. With PPh_3 and P(*m*-tol)$_3$, the conversion reached over 80%, and the molecular weights are increased with the conversions, finally to give narrower MWDs (M_w/M_n ~ 1.3-1.4). Thus, the combination of $(Cp^{Ph})Fe(CO)_2Br$ and phosphine found to be effective even for control of MA polymerization.

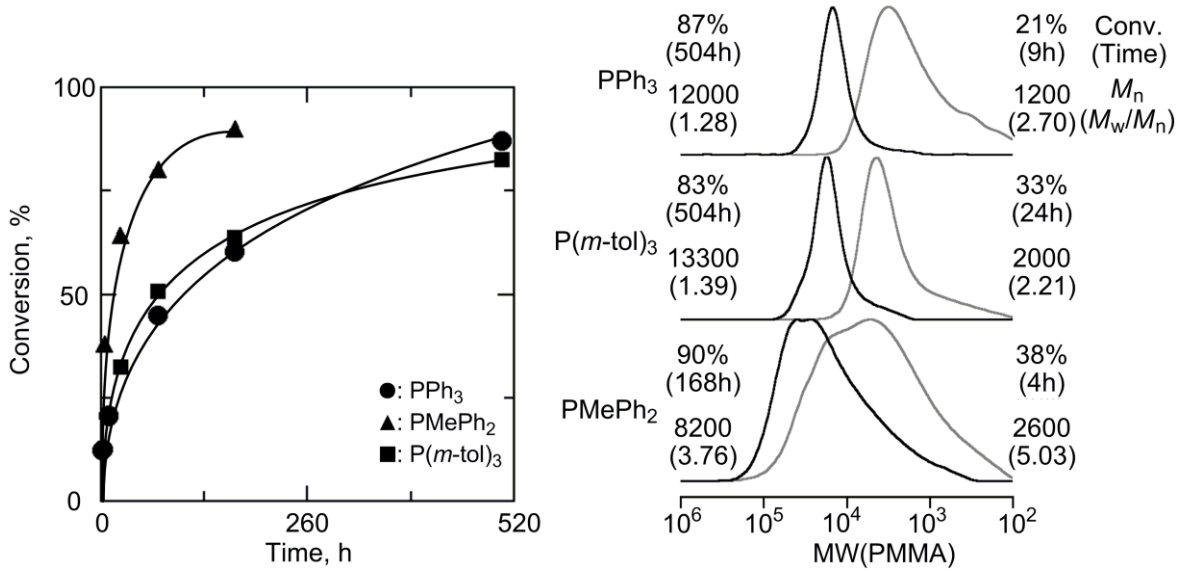

Figure 9. Polymerization of MA with H-$(MMA)_2$-Br/$(Cp^{Ph})Fe(CO)_2Br$/phosphine in toluene at 80 °C: $[MA]_0$ = 4000 mM; $[H\text{-}(MMA)_2\text{-}Br]_0$ = 40 mM; $[(Cp^{Ph})Fe(CO)_2Br]_0$ = 10 mM; $[phosphine]_0$ = 20 mM. Phosphine: PPh_3 (●); $PMePh_2$ (▲); P(*m*-tol)$_3$ (■).

7. Polymerization of Functional Methacrylates

The bulkiness of pentaphenylcycelopentadiene (Cp^{Ph}) was expected to contribute to some protection from the interaction of the central iron with functional groups or the poisoning. Thus, the author attempted the polymerization of some methacrylates carrying functional side groups, such as poly(ethyleneglycol) (PEGMA), dimethylamino group (DMAEMA), and hydroxyl group (HEMA). However, these polymerizations were less controlled. These functional groups would likely interact with the iron when vacant coordination sites were generated via the CO release in competition with the phosphine, resulting in a deactivation for the catalysis.

Conclusion

The iron dicarbonyl complex bearing pentaphenylcyclopentadiene [(Cp^{Ph})$Fe(CO)_2Br$] is too stable for the carbonyl ligand to be exchanged with phosphine ligands under thermal or UV irradiation stimulus, however, on heating with an initiator of living radical polymerization in the presence of a catalytic amount of a phosphine ligand, the carbonyl ligands were smoothly exchanged with it to give "real" active catalyst, which were supported by FT-IR and ^{31}P-NMR analyses for the model reaction. Thanks to the smooth transformation, the complex effectively catalyzed living radical polymerization in the presence of a phosphine ligand and the initiator to give controlled molecular weights and narrow molecular weight distributions. Such *in-situ* transformation from the stable complex to the real active catalyst would be ideal toward practical applications of living radical polymerizations.

Experimental Section

Materials

MMA (TCI; purity >99%) was dried overnight over calcium chloride and purified by double distillation from calcium hydride before use. MA (TCI; purity >99%) was dried overnight over calcium chloride and purified by distillation from calcium hydride before use. Poly(ethylene glycol) methyl methacrylate [PEGMA; CH_2=$CMeCO_2(CH_2CH_2O)_nMe$; Me = CH_3; n = 8.5 on average] (Aldrich) and *N,N'*-dimethylaminoethyl methacrylate (DMAEMA) (TCI; purity >98 %) were of commercial source and purified by passing through an inhibitor removal column (Aldrich) and degassed by reduced pressure before use. The MMA dimer bromide [H-$(MMA)_2$-Br; H-$(CH_2CMeCO_2Me)_2$-Br] as an initiator was prepared according to literature.[33] Iron pentacarbonyl [$Fe(CO)_5$] (Kanto Kagaku, purity >95%) was used as received. Pentaphenyl-2,4-cyclopentadienylbromide [(Cp^{Ph})Br] (Aldrich, purity >90%) was used as received and handled in a glove box (M. Braun Labmaster 130) under a moisture- and oxygen-free argon atmosphere (H_2O <1 ppm; O_2 <1 ppm). Triphenylphosphine (PPh_3: Aldrich, purity >99%), methyldiphenylphosphine ($PMePh_2$: Aldrich, purity >99%), dimethylphenylphosphine (PMe_2Ph: Aldrich, purity >97%), tri-*n*-butylphosphine [P(n-Bu)$_3$: Aldrich, purity >97%], tri-*m*-tolylphosphine [P(m-tol)$_3$: Aldrich, purity >97%] were used as received. Toluene, CH_2Cl_2 and *n*-hexane (Kishida Kagaku; purity >99%) were passed

through purification columns (Solvent Dispensing System; Glass Contour) and bubbled with dry nitrogen for more than 15 min immediately before use. $CHCl_3$ (Wako Chemicals, anhydrous; purity >99%) was bubbled with dry nitrogen for more than 15 min immediately before use. *n*-Octane (internal standard for gas chromatography) and 1,2,3,4-tetrahydronaphthalene (tetralin; internal standard for ^1H NMR analysis) was dried over calcium chloride and distilled twice from calcium hydride.

Catalyst Syntheses

$CpFe(CO)_2Br$[34] and $Cp^*Fe(CO)_2Br$[35] were synthesized according to literatures.

$(Cp^{Ph})Fe(CO)_2Br$ was synthesized by the method of Field et al. as follows:[36] A toluene (65 mL) solution of $(Cp^{Ph})Br$ (1.08 g, 2.05 mmol) and $Fe(CO)_5$ (0.486 g, 2.46 mmol) was magnetically stirred at 25 °C for 24 h under dry argon and the solution gradually turned to red. The reaction mixture was evaporated and then the residue was extracted into CH_2Cl_2 (20 mL) and added *n*-hexane (15 mL). After stirring, the suspension was filtered at 25 °C to remove precipitates, and *n*-hexane (15 mL) was added to the filtrate. The mixture was stand at -30 °C for 72 h to yield dark red purple crystals. The supernatant solvent were removed by a cannula with filter paper, and the crystal was washed with *n*-hexane (2.0 mL × 2) and dried under vacuum. The complexes were characterized by elemental analysis, FT-IR spectroscopy at room temperature in $CHCl_3$ on JASCO FT/IR 4200.

Isolated yield, 49% (0.64 g). IR ($CHCl_3$): 2038, 1999 cm $^{-1}$ ν(C≡O). Anal. Calcd for $C_{37}H_{25}BrFeO_2$: C, 69.73; H, 3.95; Br, 12.54. Found: C, 69.50; H, 4.02; Br, 13.73.

Polymerization Procedures

Polymerization was carried out by the syringe technique under dry argon in baked glass tubes equipped with a three-way stopcock or in sealed glass vials. A typical procedure for MMA polymerization with $H\text{-}(MMA)_2\text{-}Br/(Cp^{Ph})Fe(CO)_2Br/PPh_3$ was as follows. In a 50-mL round-bottom flask $(Cp^{Ph})Fe(CO)_2Br$ (10.2 mg, 0.016 mmol), PPh_3 (8.4 mg, 0.032 mmol), toluene (1.82 mL), *n*-octane (0.21 mL), MMA (1.71 mL, 16 mmol), and $H\text{-}(MMA)_2\text{-}Br$ (0.26 mL of 609.14 mM in toluene, 0.16 mmol) were added sequentially under dry argon at room temperature where the total volume of reaction mixture was thus 4.0 mL. Immediately after mixing, aliquots (0.60 mL each) of the solution were injected into glass tubes which were then sealed (except when a stopcock was used) and placed in an oil bath kept at desired temperature. In predetermined intervals, the polymerization was terminated

by cooling the reaction mixtures to -78 °C. Monomer conversion was determined from the concentration of residual monomer measured by gas chromatography with *n*-octane as an internal standard. The quenched reaction solutions were diluted with toluene (ca. 20 mL), washed with water three times, and evaporated to dryness to give the products that were subsequently dried overnight under vacuum at room temperature.

For MA, the same procedures as descried above were applied. For PEGMA, DMAEMA and HEMA, the same procedures as described above were applied except that monomer conversion was determined by ^{1}H NMR from the integrated peak area of the olefinic protons of the monomers with tetralin as internal standard. The products were similarly isolated but without washing with water because of their hydrophilicity.

Measurements

For poly(MMA) and poly(MA), M_n and M_w/M_n were measured by size-exclusion chromatography (SEC) in chloroform at 40 ºC on three polystyrene-gel columns [Shodex K-805L (pore size: 20-1000 Å; 8.0 mm i.d. × 30 cm); flow rate, 1.0 mL/min] connected to a Jasco PU-980 precision pump and a Jasco 930-RI refractive-index detector, and a Jasco 970-UV ultraviolet detector. The columns were calibrated against 13 standard poly(MMA) samples (Polymer Laboratories; M_n = 630-1,200,000; M_w/M_n = 1.06-1.22) as well as the monomer. For poly(PEGMA), poly(DMAEMA) and poly(HEMA), DMF containing 10 mM LiBr was applied as an eluent.

FT-IR spectra of the $(Cp^{Ph})Fe(CO)_2Br/PPh_3/H\text{-}(MMA)_2\text{-}Br$ catalytic system were recorded by using JASCO FT/IR 4200. The sample-was prepared that $(Cp^{Ph})Fe(CO)_2Br$ (3.2 mg, 5.0×10^{-3} mmol), PPh_3 (2.6 mg, 0.010 mmol), $H\text{-}(MMA)_2\text{-}Br$ (5.6 mg, 0.020 mmol) and toluene (1.0 mL) were added into the baked glass tube equipped with a three-way stopcock under dry argon. After mixing at 60 °C for predetermined time, the solvent was evaporated. The residue was dissolved in degassed $CHCl_3$ and purged in the sealed liquid KBr cell where the thickness was 0.1 mm. Measurements were carried out under inert atmosphere.

^{31}P-NMR spectra of $(Cp^{Ph})Fe(CO)_2Br/PPh_3/H\text{-}(MMA)_2\text{-}Br$ catalytic system were recorded by 500-MHz spectroscopy at room temperature in CD_2Cl_2 on a Jeol JNM-ECA500 spectrometer using H_3PO_4 as a standard. The sample-was prepared that $(Cp^{Ph})Fe(CO)_2Br$ (6.4 mg, 0.010 mmol), PPh_3 (5.2 mg, 0.020 mmol), $H\text{-}(MMA)_2\text{-}Br$ (11.2 mg, 0.040 mmol) and toluene (1.0 mL) were added into the baked glass tube equipped with a three-way stopcock under dry argon. After mixing at 60 °C for 8 h, the solvent was evaporated. The

residue was dissolved in CD_2Cl_2 and purged in the sealed NMR-tube with a H_3PO_4 toluene-d^8 solution sealed in a capillary under inert atmosphere.

References and Notes

(1) Crabtree, R. H., Ed.; *The Organometallic Chemistry of the Transition Metals*; John Wiley & Sons, Inc.: New York, 2001.

(2) (a) Kato, M.; Kamigaito, M.; Sawamoto, M.; Higashimura, T. *Macromolecules* **1995**, *28*, 1721-1723. (b) Ando, T.; Kato, M.; Kamigaito, M.; Sawamoto, M. *Macromolecules* **1996**, *29*, 1070-1072.

(3) For recent reviews on transition metal catalyzed living radical polymerization, see: (a) Kamigaito, M.; Ando, T.; Sawamoto, M. *Chem. Rev.* **2001**, *101*, 3689-3745. (b) Kamigaito, M.; Ando, T.; Sawamoto, M. *Chem. Rec.* **2004**, *4*, 159-175. (c) Ouchi, M.; Terashima, T.; Sawamoto, M. *Acc. Chem. Res.* **2008**, *41*, 1120-1132. (d) Ouchi, M.; Terashima, T.; Sawamoto, M. *Chem. Rev.* **2009**, *109*, 4963-5050. (e) Matyjaszewski, K.; Xja, J. *Chem. Rev.* **2001**, *101*, 2921-2990. (f) Matyjaszewski K., Ed.; *Controlled/Living Radical Polymerization From Synthesis to Materials*; ACS Symposium Series 944; American Chemical Society: Washington, DC, 2006.

(4) (a) Bolm, C.; Legros, J.; Paih, J. L.; Zani, L. *Chem. Rev.* **2004**, *104*, 6217-6254. (b) Enthaler, S.; Junge, K.; Beller, M. *Angew. Chem. Int. Ed.* **2008**, *47*, 3317-3321.

(5) Ando, T., Kamigaito, M.; Sawamoto, M. *Macromolecules* **1997**, *30*, 4507-4510.

(6) Matyjaszewski, K.; Wei, M.; Xia, J.; McDermott, N. E. *Macromolecules* **1997**, *30*, 8161-8164.

(7) Kotani, Y.; Kamigaito, M.; Sawamoto, M. *Macromolecules* **1999**, *32*, 6877-6880.

(8) Kotani, Y.; Kamigaito, M.; Sawamoto, M. *Macromolecules* **2000**, *33*, 3543-3549.

(9) Zhu, S.; Yan, D. *Macromolecules* **2000**, *33*, 8233-8238.

(10) Louie, Y.; Grubbs, R. H. *Chem. Commun.* **2000**, 1479-1480.

(11) Göbelt, B.; Matyjaszewski, K. *Macromol. Chem. Phys.* **2000**, *201*, 1619-1624.

(12) Gibson, V. C.; O'Reilly, R. K.; Reed, W.; Wass, D. F.; White, A. J. P.; Williams, D. J. *Chem. Commun.* **2002**, 1850-1851.

(13) O'Reilly, R. K.; Gibson, V. C.; White, A. J. P.; Williams, D. J. *J. Am. Chem. Soc.* **2003**, *125*, 8450-8451.

(14) Xue, Z.; Lee, B. W.; Noh, S. K.; Lyoo, W. S. *Polymer* **2007**, *48*, 4704-4714.

(15) Niibayashi, S.; Hayakawa, H.; Jin, R-H.; Nagashima, H. *Chem. Commun.* **2007**, 1855-1857.

(16) Uchiike, C.; Terashima, T.; Ouchi, M.; Ando, T.; Kamigaito, M.; Sawamoto, M. *Macromolecules* **2007**, *40*, 8658-8662.

(17) Ferro, R.; Milione, S.; Bertolasi, V.; Capacchione, C.; Grassi, A. *Macromolecules* **2007**, *40*, 8544-8546.

(18) Uchiike, C.; Ouchi, M.; Ando, T.; Kamigaito, M.; Sawamoto, M. *J. Polym. Sci., Part A: Polym. Chem.* **2008**, *46*, 6819-6827.

(19) Chapter 1 of this thesis.

(20) Takahashi, H.; Ando, T.; Kamigaito, M.; Sawamoto, M. *Macromolecules* **1999**, *32*, 3820-3823.

(21) Watanabe, T.; Ando, T.; Kamigaito, M.; Sawamoto, M. *Macromolecules* **2001**, *34*, 4370-4374.

(22) Ouchi, M.; Ito, M.; Kamemoto, S.; Sawamoto, M. *Chem. Asian. J.* **2008**, *3*, 1358-1364.

(23) Chapter 3 of this thesis.

(24) Chapter 5 of this thesis.

(25) Ando, T.; Kamigaito, M.; Sawamoto, M. *Macromolecules* **2000**, *33*, 5825-5829.

(26) Janiak, C.; Schumann, H. *Adv. Organomet. Chem.* **1991**, *33*, 291-393.

(27) Adams, H.; Bailey, N. A.; Browning, A. F.; Ramsden, J. A.; White, C. *J. Organomet. Chem.* **1990**, *387*, 305-314.

(28) Broadley, K.; Lane, G. A.; Connelly, N. G.; Geiger, W. E. *J. Am. Chem. Soc.* **1983**, *105*, 2486-2487.

(29) Fu, G. *Acc. Chem. Res.* **2000**, *33*, 412-420.

(30) McVey, S.; Pauson, P. L. *J. Chem. Soc.* **1965**, 4312-4318.

(31) Manners, I; Connelly, N. G. *J. Chem. Soc. Dalton. Trans.* **1989**. 283-288.

(32) Even in the absence of PPh_3, the carbonyl peaks were disappeared in the model reaction for FT-IR, indicating the possibility that the dicarbonyl complex can activate the initiator. However, since MMA was not polymerized at all as shown in Figure 1, the author conclude that the resultant trivalent complex $[(Cp^{Ph})Fe(CO)Br_2]$ would be too unstable to generate some divalent species for further catalysis.

(33) Ando, T.; Kamigaito, M.; Sawamoto, M. *Tetrahedron* **1997**, *53*, 15445-15457.

(34) Fischer, E. O.; Moser, E. *Inorg. Synth.* **1970**, *12*, 35-36.

(35) King, R. B.; Stone, F. G. *Inorg. Synth.* **1963**, *7*, 99-115.

(36) Field, L. D.; Hambley, T. W.; Lindall, C. M.; Masters, A. F. *Polyhedron* **1989**, *8*, 2425-2430.

LIST OF PUBLICATIONS

Chapter 1

"Active, Versatile, and Removable Iron Catalysts with Phosphazenium Salts for Living Radical Polymerization of Methacrylates"

Muneki Ishio, Masao Katsube, Makoto Ouchi, Mitsuo Sawamoto, and Yoshihisa Inoue

Macromolecules, **2009**, *42*, 188-193.

Chapter 2

"Phosphazenium Salts as Ligand of Iron Catalysts for Living Radical Polymerization: High Tolerance to Functional Monomers"

Muneki Ishio, Takaya Terashima, Makoto Ouchi, Mitsuo Sawamoto, and Yoshihisa Inoue

J. Polym. Sci., Part A: Polym. Chem., *to be submitted.*

Chapter 3

"Carbonyl-Phosphine Hetero-Ligated Halfmetallocene Iron(II) Catalysts for Living Radical Polymerization: Concomitant Activity and Stability"

Muneki Ishio, Takaya Terashima, Makoto Ouchi, and Mitsuo Sawamoto

Polym. J., **2010**, *42*, 17-24.

Chapter 4

"*N*-Heterocyclic Carbene Ligand for Halfmetallocene Iron(II) Complexes: High Catalytic Activity and Versatility for Living Radical Polymerization"

Muneki Ishio, Makoto Ouchi, and Mitsuo Sawamoto

J. Polym. Sci., Part A: Polym. Chem., *to be submitted.*

Chapter 5

"Carbonyl-Phosphine Heteroligation for Pentamethylcyclopentadienyl (Cp*)-Iron Complexes: Highly Active and Versatile Catalysts for Living Radical Polymerization"

Muneki Ishio, Takaya Terashima, Makoto Ouchi, and Mitsuo Sawamoto

Macromolecules, **2010**, *43*, 920-926.

Chapter 6

"Pentaphenylcyclopentadienyl Iron Dicarbonyl Catalysts for Living Radical Polymerization: Smooth Generation of Real Active Catalysts"

Muneki Ishio, Makoto Ouchi, and Mitsuo Sawamoto

J. Polym. Sci., Part A: Polym. Chem., *to be submitted.*

ACKNOWLEDGEMENTS

This thesis presents the studies which the author carried out from 2005 to 2010 at the Department of Polymer Chemistry, Graduate School of Engineering, Kyoto University under the direction of Professor Mitsuo Sawamoto.

First of all, the author would like to express his sincere gratitude to Professor Mitsuo Sawamoto for his continuous guidance and encouragement through the course work. He is also grateful to Dr. Makoto Ouchi and Dr. Takaya Terashima for their helpful and convincing suggestions, and stimulating discussions.

The author wished to express his thanks to all members of Sawamoto laboratory for useful suggestion and their friendship during the course of research. Especially he thanks sincerely to Mr. Masao Katsube for his discussion and kind guidance in experimental technique in the early phase of this research. The author is also obliged to Ms. Miro Takayama for her assistance during the author's school life.

The author acknowledges Dr. Yoshihisa Inoue (Mitsui Chemical, Inc) for support of phosphazenium salts in Chapter 1-2 and also Dr. Takeshi Niitani (Nippon Soda Co., Ltd) for the measurements of Inductively Coupled Plasma Atomic Emission Spectroscopy (ICP-AES) in Chapter 1.

The author wishes to thank for all "ORION" members, especially to Prof. Yoshio Okamoto (Harbin Engineering University), Prof. Sadahito Aoshima (Osaka University), Prof. Eiji Yashima (Nagoya University), Prof. Masami Kamiagito (Nagoya University), and Associate Prof. Tsuyoshi Ando (Nara Institute of Science and Technology) for their meaningful discussion and kind encouragement.

The author would like to express his appreciation to Prof. Shiro Kobayashi (Kyoto Institute of Technology), and Dr. Tokuma Fukuoka (Advanced Industrial Science and Technology), for introducing him to polymer and organometallic chemistry and kind encouragement.

Acknowledgements

The author is very grateful to Japan Society for Grant-in-Aid for research assistant of the Global COE Program, "International Center for Integrated Research and Advanced Education in Materials Science" of Kyoto University (2007-2010) and Kuraray Co., Ltd for “Ohara Scholarship” (2009-2010).

Finally, the author wishes to express his deep appreciation to his parents, Mr. Takanobu Ishio and Mrs. Mariko Ishio, his brother Mr. Naoki Ishio, his sister Ms. Megumi Ishio and his all family for their constant care and affectionate encouragement.

Muneki Ishio

Department of Polymer Chemistry
Graduate School of Engineering
Kyoto University
2010